Elucidating the Role of miR-617 in Oral Squamous Cell Carcinoma Pathogenesis

A thesis submitted for the degree of

Doctor of Philosophy

in the Faculty of Science

by

NEELANJANA SARKAR

Department of Developmental Biology and Genetics

Indian Institute of Science

Bengaluru-560012, India

November 2023

“I have become my own version of an optimist. If I can't make it through one door, I'll go through another door- or I'll make a door. Something terrific would come no matter how dark the present.”

— Rabindranath Tagore

To my parents…

DECLARATION

I hereby declare that the results of my research work presented in this thesis were carried out in the Department of Developmental Biology and Genetics, Indian Institute of Science, Bengaluru, Karnataka, under the supervision of Prof. Arun Kumar since August 2017. I further declare that no degree, diploma, or fellowship has been awarded based on these results in any institution and I authorize the Indian Institute of Science to make this thesis available to any other institution for research purposes.

Neelanjana Sarkar

Serial no. 03-07-00-10-11-17-1-14897

Acknowledgements

Pursuing research not only depends on one's passion for the field but also takes an incredibly supportive group of people that makes it easier to sustain and thrive in the journey of a Ph.D. In this regard, I would earnestly like to thank my Ph.D. supervisor, Prof. Arun Kumar for believing in my convictions, even in inclement times. He has set a benchmark of relentlessness dedication and hard work for all of us in the laboratory. I have walked up to him with bizarre experimental problems and ideas every now and then but he has been nothing but patient and hopeful with me. He has always encouraged me to explore new directions when the old set ways did not work, this eventually helped me develop myself as an independent researcher. His constant guidance and critical scientific inputs immensely helped me in completing this thesis. Along with his research inputs, his keen intuition in managing and allocating funds to procure lab resources provided me with a holistic skill set to successfully run a laboratory. I will be forever indebted to him for his support and mentorship.

I would also like to thank all the other faculties of the Department of Developmental Biology and Genetics (DBG) for their valuable suggestions and comments during my annual work presentations, especially Prof. Ramray Bhat for his insights on the nude mice experiment. I would like to thank all my course instructors for enlightening me with the toil and consistency that goes into making seminal scientific discoveries. I am deeply grateful to my comprehensive examiners comprising Prof. Sandhya Visweswariah, Prof. P.N. Rangarajan, Prof. Dipankar Nandi, Dr. Srimonta Gayen, and Prof. Arun Kumar for instilling the value of being articulative and inquisitive in me, while analysing data. I would like to thank the DBG office staff, Bharthi ma'am, Amey, Rupa, Kavya, and Monika for their administrative support and Bilal for his help in the RT-PCR facility.

I would like to thank all the members of the Central Animal Facility (CAF) for providing and maintaining the animals during my experiment. I am grateful to Dr. G. Champaka (Kidwai Memorial Institute of Oncology, Bengaluru) for her advice and cooperation in providing the oral cancer patient samples along with the patient records. I sincerely thank all the patients who voluntarily consented to provide their precious samples, without whom this study would have remained incomplete. I gratefully acknowledge the research scholarship provided by the Department of Biotechnology, Ministry of Science & Technology, Government of India from 2017-2022, and the financial assistance provided by the Indian institute of Science (IISc) from 2022-2023.

I would like to thank all the past and present members of the AK lab for providing me with a conducive learning environment. I am forever grateful to Dr. Karthik Mallela for training me with all the necessary lab techniques and participating in insightful scientific discussions that helped me take the solo flight. I appreciate the scientific suggestions that I have received from Dr. Naresh Mahajan and Dr. Dhanashree Anil More from time to time. Dr. Wendy D'Souza has been my guardian angel, and I cherish the time and rapport we shared in the laboratory. I am fortunate to have an army of amazing juniors, Harsha, Mukund, Sakshi, and Soumi, from whom I have learnt the most while discussing experiments and training them during their course of Ph.D. I would also like to thank Dr. Pankhuri Kaushik, Shraddha, Harshi, and Shreyas for all their help and support. I would also like to thank Mr. H.S. Srivatsa for all his assistance in laboratory-associated paperwork. This lab has been my haven for all these years and will continue to hold a special place in my heart forever.

I am also deeply inspired by the contagious scientific zeal of Prof. Chandana Barat and Prof. Uma Siddhanta who have always motivated me to look out of the box and shaped my overall development since college. I am also thankful to Prof. Aniruddha Banerji for boosting my confidence during Ph.D. interviews in 2017.

I am also thankful to my batchmates Debolina, Purba, Dr. Tamasa De, Devendra, Dr. Urbi Roy, Dr. Pooja Chaukimath, Shyamili, Shweta, and Mani for being hospitable enough to share their chemicals and equipment, whenever in need. I would also like to thank the past and present secretaries of Genesis, especially Dr. Tamasa De for being a cooperative co-secretary during my tenure as a secretary of Genesis.

Friends can make or break your life, quite literally so for me. I am indebted to Ushashi and Debolina for being my timeless constants in a sea of variables during my Ph.D. life. I am blessed to have Rishav and his parents, Sanjay uncle and Karabi kakima by my side who have empowered me with their genuine care, love, and support in my pursuit of Ph.D. I am lucky to have Anwesha, Debopriya, Sunetra, Sayan and, Debasmita with me even when I have not managed to meet them for years. I am in awe of the empathy with which Vikramjit patiently listens to me while I discuss my experiments, atheism, and more, across time zones. Last but not the least, I am glad that I have a compassionate friend in Harsha, someone a little younger than me but always manages to ground me with her reality checks. Please continue to be the mirror that never lies.

How can I stop without acknowledging my silent cheerleaders? My parents have been

my strongest pillar of strength and faith ever since. My father is the most calm and upright person that I have ever met and I sincerely hope to have acquired or imbibed a fraction of his resolve and dedication towards all his endeavours. My mother is the reason why I have always aspired to go beyond the conservative societal norms, her bravery and kindness never cease to amaze me. I am extremely grateful to my parents and elder brother for introducing me to the songs and poetry of the literary genius Gurudev Rabindranath Tagore. He has been my friend, guide, and philosopher all along, someone so far away yet so tangible through his thought-provoking creations. I am forever indebted to my parents for their tireless efforts and for being the wind beneath my wings.

I want to thank the Indian Institute of Science for providing me with the opportunity to work here. The countless trees on the campus made me realize the power of resilience. Just as they lose a branch or two in a storm and yet recover in no time, we shall too, no matter how difficult our lives get. Lastly, I express my gratitude to all those people who were not mentioned here but have directly or indirectly helped me in countless ways.

Thank you all.

ABBREVIATIONS

ºC	Degree centigrade
µg	Microgram
µL	Microliter
µM	Micromolar
aa	Amino acid
AKT	AKT serine/threonine kinase
APC	Adenomatous polyposis coli protein
APS	Ammonium persulphate
ASR	Age standardized rate
AZA	5-Azacytidine
BAX	BCL2 associated X, apoptosis regulator
bp	Base pair
BCL2	B-cell lymphoma 2
BCL6	B-cell lymphoma 6
BSA	Bovine serum albumin
B-CLL	B cell chronic lymphocytic leukemia
BLAST	Basic local alignment search tool
CCAT2	Colon cancer associated transcript 1
CCND1	Cyclin D1
CDK6	Cyclin dependent kinase 6
CDKN2B	Cyclin dependent kinase inhibitor 2B
cDNA	Complementary DNA
CDKN2A	Cyclin dependent kinase inhibitor 2A
CDS	Coding sequence
CircRNA	Circular RNA
cm	Centimetre
CNOT6L	CCR4-NOT transcription complex subunit 6 like

COX	Cytochrome C oxidase
CTNNB1	Catenin beta 1
DADA	Divisive amplicon denoising algorithm
DAPK	Death associated protein kinase
DBTSS	Database of transcriptional start sites
DEPC	Diethyl pyrocarbonate
DGCR8	DiGeorge syndrome critical region gene 8
DMEM	Dulbecco's modified Eagle's medium
DMSO	Dimethyl sulphoxide
DNA	Deoxyribonucleic acid
DNase	Deoxyribonuclease
dNTP	Deoxyribonucleotide triphosphate
DNMT	DNA methyltransferase
DPBS	Dulbecco's phosphate buffered saline
EGFR	Epidermal growth factor receptor
EIF3E	Eukaryotic translation initiation factor 3 subunit E
FBS	Fetal bovine serum
FDA	The United States food and drug administration
FOXCUT	FOXC1 upstream transcript
FTH1P3	Ferritin heavy chain 1 pseudogene 3
G	Gram
GAPDH	Glyceraldehyde 3-phosphate dehydrogenase
GBD	Global burden of disease
GFP	Green fluorescent protein
GSTM1	Glutathione S-transferase M1
Hr	Hour
H19	H19 imprinted maternally expressed transcript
HCC	Hepatocellular carcinoma
HCV	Hepatitis C virus
HPV	Human papillomavirus
HNSCC	Head and neck squamous cell carcinoma

HRAS	Harvey rat sarcoma viral oncogene homolog
HRP	Horse radish peroxidase
IARC	International agency for research on cancer
IPTG	Isopropyl-β-D-thio-galactopyranoside
IQGAP1	IQ motif containing GTPase activating protein 1
Kb	Kilobase
kDa	Kilodalton
L	Liter
LINE	Long interspersed nucleotide element
LOH	Loss of heterozygosity
LncRNA	Long non-coding RNA
KIT	KIT proto-oncogene, receptor tyrosine kinase
M	Molar
MALAT1	Metastasis associated lung adenocarcinoma transcript 1
MAPK	Mitogen-activated protein kinase
MCPH1	Microcephalin 1
Mg	Milligram
MGMT	O-6-methylguanine-DNA methyltransferase
MET	MET proto-oncogene, receptor tyrosine kinase
Min	Minute
miRNA	MicroRNA
mL	Millilitre
MLH1	MutL homolog 1
Mm	Millimetre
mM	Millimolar
mRNA	Messenger RNA
MRI	Magnetic resonance imaging
MTOR	Mammalian target of rapamycin
MYC	MYC proto-oncogene, bHLH transcription factor
Nm	Nanometre
nM	Nanomolar
ncRNA	Noncoding RNA

NFKB1	Nuclear factor kappa B subunit 1
NRAS	NRAS proto-oncogene, GTPase
Nt	Nucleotide
OD	Optical density
OMPD	Oral potentially malignant disorder
OPL	Oral leukoplakia
OSCC	Oral squamous cell carcinoma
OSF	Oral submucous fibrosis
OS	Overall survival
PAGE	Polyacrylamide gel electrophoresis
PBS	Phosphate buffered saline
PBST	Phosphate buffered saline with 0.1% Tween®20
PCR	Polymerase chain reaction
PI3K	Phosphoinositide 3-kinase
PTEN	Phosphatase and Tensin homolog
PVDF	Polyvinylidene fluoride or polyvinylidene difluoride
PVL	Proliferative verrucous leukoplakia
RAF	Raf proto-oncogene, serine/threonine kinase
RASSF1A	Ras association domain family member 1
RB1	Retinoblastoma 1
RET	Ret proto-oncogene
RISC	RNA-induced silencing complex
RLU	Relative light unit
RNA	Ribonucleic acid
RNase	Ribonuclease
ROS	Reactive oxygen species
Rpm	Rotation per minute
RR	Relative risk
RTK	Receptor tyrosine kinase
RT-PCR	Reverse transcription-PCR
RUNX3	RUNX family transcription factor 3
qRT-PCR	Quantitative real time PCR

S	Svedberg unit
Sec	Second
SCC	Squamous cell carcinoma
ST	Smokeless tobacco
STAT3	Signal transducer and activator of transcription 3
TE	Tris-EDTA
TEMED	Tetramethylethylenediamine
TGF-α	Transforming growth factor-α
TGF- β	Transforming growth factor-β
TSS	Transcription start site
TNM	Tumour-node-metastasis
TP53	Tumour protein P53
TUG1	Taurine up-regulated 1
UCA1	Urothelial cancer associated 1
UTR	Untranslated region
UICC	Union for international cancer control
UV light	Ultraviolet light
V	Voltage
VAPA	VAMP associated protein A
VAV2	Vav guanine nucleotide exchange factor 2
VEGF	Vascular endothelial growth factor
WIF1	WNT inhibitory factor 1
WHO	World health organization
X-gal	5-bromo-4-chloro-3-indolyl-β-D-galactopyranoside

TABLE OF CONTENTS

SECTION		PAGE NUMBER
	Declaration	**iv**
	Acknowledgements	**v-vii**
	Abbreviations	**viii-xii**
1.	**Introduction**	**1**
2.	**Rationale and Objectives of the study**	**47**
3.	**Materials and Methods**	**56**
4.	**Results**	**90**
5.	**Discussion**	**135**
6.	**Conclusions**	**149**
7.	**References**	**156**
8.	**Appendices**	**216**
9.	**Publications**	**223**
10.	**Abstract submitted/meeting attended**	**223**

INTRODUCTION

1. INTRODUCTION

1.1. Oral squamous cell carcinoma

Oral squamous cell carcinoma (OSCC) or oral cancer is the most common malignant epithelial neoplasm of the head and neck region. According to the international classification of diseases (ICD), 10th revision (ICD10 codes-C00-C06), the following sites of occurrence are included under OSCC: lower and upper lip vermilion, labial mucosa, anterior two-third of the tongue, buccal mucosa, the floor of the mouth, gingiva/alveolar ridge, hard palate, and the retromolar trigone (https://www.icd10data.com/ICD10CM/Codes/C00-D49/C00-C14). OSCC accounts for 84-97% of all oral malignancies (Ajay et al., 2018). According to the GLOBOCAN 2020 (http://gco.iarc.fr/) database, it is the 17th most common cancer in the world, with an annual incidence of 3,77,713 cases and a worldwide age-standardized rate (ASR) of 6 and 2.3 per 1,00,000 males and females, respectively. According to the global cancer observatory (GCO), by 2040, the overall incidence of OSCC is predicted to rise by up to 40% with a corresponding increase in mortality (Ali, 2022).

A higher burden of lip and oral cavity cancer is reported (10.2 per 1,00,000) in countries that scored lower on the human development index (HDI) such as India (Sung et al., 2021). In India, OSCC is the 2nd most common cancer having an annual incidence of 1,35,929 cases, preceded by the breast cancer. It is the most common cancer in males and the fourth most common cancer in females of India, with an ASR of 14.8 and 4.6 per 1,00,000 males and females, respectively (GLOBOCAN, 2020; Sung et al., 2021). OSCC tends to cluster in certain high-risk regions, especially South Asia (India and Sri Lanka) and the Pacific Islands (Papua New Guinea accounts for the highest incidence rate worldwide in both sexes), and it is also the leading cause of cancer-associated mortality among men in India and Sri Lanka (Bray et al., 2018).

In India, the lower gingivobuccal complex, comprising the buccal mucosa, gingivobuccal sulcus, lower gingiva and retromolar trigone, is the most common site for oral cancer due to the tobacco chewing habit in contrast to the cancer of the floor-of-mouth and tongue in western countries (Misra et al., 2008). As compared to the west, cancer of the oral cavity is significantly higher in India as about 70% of the cases are reported in the advanced stages [union for international cancer control (UICC), Stage III-IV]. As a result, the chances of a cure are very low, almost negative, with a five-year survival rate of around 20% for locally

advanced disease (Veluthattil et al., 2019). In India, epidemiologically, Kerala and West Bengal report the lowest and highest incidence of oral cancer, respectively. The causative agents are excessive use of smokeless tobacco in the forms of nass, naswar, khaini, pan masala, gutkha, and betel quid (betel leaf coated with slaked lime and wrapped around areca nut and catechu) or tobacco smoking in the form of cigarette, bidi, chutta, reverse type of smoking and hooka in this part of the world (Niaz et al., 2017).

The neoplasia in oral cavity begins with a normal epithelium and successively progresses through hyperplasia, dysplasia, carcinoma *in situ* to invasive carcinoma (Nagpal and Das, 2003). These progressive changes from slightly deregulated proliferation of cells to malignancy occur due to the accumulation of mutations in a limited set of genes. Oncogenes and tumour suppressor genes play a major role in triggering and promoting carcinogenesis in this regard (Hanahan and Weinberg, 2000). Genesis of oral cancer is a sequential process of genetic and epigenetic events leading to the disruption of the normal cellular functions such as cell differentiation, signal transduction, and cell death (Williams, 2000).

1.2. Five-year survival rates of OSCC

OSCC is an aggressive disease, and its poor prognosis is attributed to its late detection and metastasis at an advanced stage (Goertzen et al., 2018). The 5-year survival rate for lower lip lesions is 90%, and metastases are rare. But the carcinoma of the upper lip tends to be more aggressive and metastatic. A retrospective, international, multicentre, and pooled study has focused on the five-year survival of OSCC patients who underwent surgery alone or surgery with adjuvant radiotherapy (Amit et al., 2013). From 1990 to 2011, the five-year overall survival increased from 59% to 70% (Amit et al., 2013). The survival rate can vary due to anatomical location of various subsites, stage, grade of the OSCC, age at diagnosis, treatment, and comorbidity (Chinn and Myers, 2015). While the 5-year relative survival rate for localized disease (no lymph node involvement) is 75%-84%, it is only 20% for floor-of-mouth carcinoma and 36% for tongue carcinoma at an advanced metastatic stage (Chinn and Myers, 2015). Lymph node metastasis decreases survival rate by about half. Metastases reach the regional lymph nodes first and later the lungs. Apart from metastasis, field cancerization-associated local recurrence and drug resistance also contribute to the dismal survival rates of OSCC. The percentage of diagnosed cases and mortality also varies according to the geographical location. Asia accounts for the highest percentage of both diagnosed OSCC cases (64.2%) and mortality (73.3%). Conversely, Oceania has the least percentage of both OSCC diagnosed patients (1.3%)

and disease mortality (0.56%) (Sung et al., 2021). In South America, Central, Eastern and Northern Europe, human papillomavirus (HPV) infections are responsible for a growing percentage of OSCC among young people (Bruni et al., 2016).

Thus, the primary emphasis is on screening for abnormal lesions and understanding the course of OSCC pathogenesis. This will facilitate the early detection of OSCC and thereby enhance patient survival and decrease morbidity. The available treatment options include surgery, radiation therapy, chemotherapy, and immunotherapy. However, despite considerable development in oral cancer treatment regimens in the past three decades, this stark disparity in the global condition versus that in India calls for a serious consideration to combine improved treatment regimens with oral cancer awareness programs to alleviate the situation in India.

1.3. Field cancerization and sites of occurrence of OSCC

Development of OSCC is a multi-step process and field cancerization is a hallmark of OSCC. Based on the analysis of serial sections of OSCC tumours (1 cm or less in diameter), the phenomenon called field cancerization (FC) was first described by Slaughter, Southwick, and Smejkal in 1953 who found separate foci of *in situ* cancer or isolated islands in invasive squamous cell carcinoma (Slaughter et al., 1953). Oral field cancerization implies that oral cancer does not arise as an isolated cellular phenomenon, but rather as an anaplastic tendency of many cells at once that results in a multifocal development process of cancer at various rates within the entire field in response to a carcinogen, particularly tobacco. Such foci grow independently and eventually coalesce to form a single ulcerating tumour. It has been demonstrated that the majority of OSCC cases have a much larger linear extent than infiltration in depth, including the advanced cases (Mohan and Jagannathan, 2014). This suggests that lateral cancerization leads to tumour growth and can be explained by the concept of multiple contiguous foci of carcinogenesis (Slaughter, 1944). The term field cancerization is often used to describe the development of abnormal tissues around a tumorigenic area that create atypical areas, even after complete surgical removal. This may explain the cause of developing secondary primary tumours (SPTs) and the high rate of local recurrences in OSCC. The development of recurrences and SPTs, even when surgical margins are histopathologically tumour-free, corroborates the concept of field cancerization (Mohan and Jagannathan, 2014).

1.4. Steps of carcinogenesis associated with OSCC

Oral carcinogenesis is a complex, multistep process in which genetic and epigenetic changes occur in the genes of excitatory and inhibitory signal transduction pathways that

regulate the normal cellular physiology (Jurel et al, 2014). The cell then becomes functionally independent from the surrounding normal oral epithelium (oral keratinocyte neighbours) upon accumulation of these alterations or mutations (Jurel et al., 2014). Moreover, the signal transduction pathways regulating normal cell physiology are undermined in the tumour cell, allowing it to divide more rapidly, sequester blood vessels to feed that growth, delete or amplify signals to produce abnormal structural or functional changes, and invade normal tissue at local or distant sites (Jurel et al., 2014). The histologic progression of oral carcinogenesis from hyperplasia to invasion and metastasis is believed to reflect the accumulation of these changes (Todd et al., 1997).

In OSCC, the stepwise transition from normal epithelium to invasive cancer through a progressively worsening premalignant state (at the molecular, microscopic, and clinical levels) holds true, but this should not be construed as a straightforward sequence of events (Georgaki et al., 2021). Specifically, at the microscopic level, it is not necessary to go through all grades of dysplasia (i.e., from mild to moderate to severe to carcinoma *in situ*) before development of cancer cell invasion of and through the basement membrane zone; it is possible to encounter invasive cancer cells in the underlying connective tissue without severe or full-thickness dysplastic changes in the overlying epithelium (Georgaki et al., 2021). Indeed, acquisition of invasive properties by epithelial cells is a complex process that involves their interaction with connective tissue elements and the immune system, and it is not solely dependent on a simplistic linear or quantitative expansion of dysplastic features (Santosh and Jones, 2014).

The general idea is that oral carcinogenesis can occur as a two-step process involving the initial presence of oral potentially malignant disorders (OPMDs) that subsequently develop into cancer. The majority (~80%) of oral cancer cases originate from OPMDs (Kramer et al., 1978; Gupta et al., 1989). Oral epithelial dysplasia (OED) is marked as an intermediate stage determining the malignancy potential of varied premalignant precursors in oral cancer development (Warnakulasuriya et al., 2007; Thomas et al., 2012). Thus, OED is used as an indication for malignant transformation of OPMDs. The overall malignant transformation rate of OPMDs is 7.9%, indicating the significance of the problem (Iocca et al., 2020).

1.5. Oral potentially malignant disorders

Oral potentially malignant disorders (OPMDs) are defined as “any oral mucosal abnormality that is associated with a statistically increased risk of developing oral cancer” (Warnakulasuriya et al., 2020). Characteristically, OPMDs present with diverse clinical

attributes, such as colour variations (white, red, and a mix of white and red), morphological changes (plaque/plateau, smooth, grooved, wrinkled, granular, and atrophic), and different sizes, involving different anatomical sites in the oral cavity (Williams et al., 2008; Farah et al., 2014). Examples of OPMDs include oral leukoplakia, oral erythroplakia, oral lichen planus, and oral submucous fibrosis,

1.5.1. Oral leukoplakia

Oral leukoplakia (OL) is a common and potentially malignant condition of the oral mucosa, defined as "A white plaque of questionable risk having excluded (other) known diseases or disorders that carry no increased risk for cancer" (van der Waal, 2009). OL is more frequent in men, and the associated risk factors are consumption of tobacco, areca nut, and alcohol, and HPV infection. Clinically, OL can be divided into two subtypes: homogeneous and non-homogeneous. Homogenous lesions appear as superficial and flat while the non-homogenous ones are more irregular, verrucous or exophytic. Non-homogenous OL presents a higher risk of malignant transformation. In this regard, biopsy is useful to confirm the diagnosis with high specificity and accuracy. Prevention and treatment of OL include clinical surveillance and risk factors elimination as the first step. However, the initial treatment can be made with bleomycin or retinoids. The complete response ratio is not high (10–27%), and the recurrence of OL is almost 50% after treatment with topical retinoic acid (Gorsky and Epstein, 2002). The most common treatment options are surgical excision or CO_2 laser therapy, together with cryotherapy and photodynamic therapy, especially in those cases that show moderate and severe epithelial dysplasia. Efficacy of these treatments is high (70–90% complete response ratio), but the recurrence ratio is about 25–30% of patients (Mogedas-Vegara et al., 2015; Mogedas-Vegara et al., 2016).

Proliferative verrucous leucoplakia (PVL) represents an uncommon type of multifocal OL with aggressive behaviour and resistance to therapies. It clinically shows an asymptomatic white and verrucous plaque and is more frequent in women above 60 years of age. Morphologically, these lesions often present different grades of dysplasia and progress to OSCC, thus a close follow-up is compulsory (Capella et al., 2017).

1.5.2. Oral erythroplakia

Oral erythroplakia **(**OE) represents a single erythematous oral mucosal lesion with a high rate of malignant transformation (Warnakulasuriya, 2018). It is associated with tobacco, alcohol abuse, and high-risk HPV. Its prevalence is between 0.02% and 0.83%, mostly affecting

middle-aged adults (van der Waal, 2010). Its clinical appearance is characterized by a solitary erythematous flat lesion within the oral cavity. Due to the high rate of malignant transformation, early diagnosis and treatment are mandatory. Surgical excision or ablation by CO_2 laser therapy is the recommended therapy with low associated morbidity (Yang et al., 2015).

Erythroleukoplakia has a mixed red and white appearance. Unlike erythroplakia, which is well demarcated, erythroleukoplakia often has a blended or ill-defined margin. Clinically, erythroleukoplakia, previously termed as speckled leukoplakia (non-homogenous leukoplakia), presents in two general patterns: either numerous small and irregular leukoplakic areas within a red patch, or as an erythroplakia adjacent to a leukoplakia. Unlike leukoplakia and erythroplakia, patients with erythroleukoplakia often present with symptoms such as pain or soreness. Age, gender, and commonly affected sites for erythroleukoplakia are the same as erythroplakia (Wetzel and Wollenberg, 2020).

1.5.3. Oral lichen planus

Oral lichen planus (OLP) is a chronic autoimmune, inflammatory disease which may affect different organs, such as skin, oral or genital mucosa. Several factors have been held responsible for this kind of lesion, but the aetiology remains unclear. OLP is more frequent in middle aged women with a low rate of malignant transformation (<1–6%) (Kurago, 2016).

Typically, lesions are usually asymptomatic and bilaterally localized in the buccal mucosa. Clinical aspect presents different types of OLPs, such as reticular, plaque-like, bullous, atrophic, or erosive. The most common OLP is the reticular type characterized by thin white plaques called “Wickham’s striae”. Atrophic and erosive patterns are associated with significant pain; bullous pattern is the least common type of OLP, characterized by bullae formation. Plaque-like type is frequently observed in smokers whose lesions may have a combination of characteristics (Alrashdan et al., 2016). The diagnosis of OLP is typically made clinically and confirmed histologically. Treatment of OLP is generally palliative and not curative. The principal goal of management is to reduce inflammation and alleviate symptoms with topical steroids (Al-Hashimi et al., 2007; Garcia-Pola et al., 2017).

1.5.4. Oral submucous fibrosis

Oral submucous fibrosis (OSF) is a chronic disorder of the oral cavity characterized by collagen deposition and strong fibrosis, with high potential of malignant transformation rate (7–30%) (Arakeri and Brennan, 2013). It is frequent in the Asian population, particularly

associated with betel nuts chewing; however, the aetiology seems to be multifactorial. Patients present symptoms, such as pain, xerostomia, a burning sensation, taste disorders and limitation in buccal motility. Biopsy is important to lead the correct diagnosis. Four histopathological stages are described based on the increase of fibrosis and chronic inflammation of oral submucosa, progressive atrophy of epithelium, and degeneration of muscle fibres (Bhatt et al., 2019). Recent evidences show that the malignant transformation could be caused by the alkaloids of areca nut that are capable of stimulating growth of fibroblasts, production of cytokines (especially involving the TGF-β signalling) and activation of immune cells (Shakunthala et al., 2015; Shen et al., 2020). These mechanisms provoke microenvironment alteration and cellular dysregulation of proliferation, survival, differentiation, DNA repair function and tumour transformation (Shakunthala et al., 2015; Shen et al., 2020). The current therapy options aim to reduce symptoms and improve the quality of patient's life. They include anti-inflammatory and anti-fibrosis drugs (steroids, interferon-γ, collagenase, etc.), physical treatment (mouth exercising devices) and surgery in severe OSF. However, there are no established treatment guidelines for clinicians (Shen et al., 2020).

1.6. Oral epithelial dysplasia

While the above mentioned OPMDs are attributed to clinical presentations, oral epithelial dysplasia (OED) is histomorphologically defined as a spectrum of epithelial changes associated with an increased risk of transformation to carcinoma. The criteria used for diagnosing dysplasia include architectural changes (disordered tissue organization) and cytological changes (individual cell abnormality) (Gupta et al., 2020). The WHO three-tier grading of oral dysplasia is traditionally used by pathologists, in which OED is graded as mild, moderate, and severe (Muller, 2018). Grading of dysplasia is essential to inform subsequent management of any given OPMD. The overall evidence indicates a positive correlation between the likelihood and time to malignant transformation with increasing degrees of dysplasia.

There is an increasing recognition of HPV-associated oral epithelial dysplasia. A subset of OED is characterized by distinct histomorphological features which are ascribed to high-risk types of HPV, mainly HPV-16 (McCord et al., 2013; Lerman et al., 2017; Khanal et al., 2017; Hendawi et al., 2020; de la Cour et al., 2021). Clinically, this is distinguished from conventional OED by the presence of karryorhexis, isolated suprabasal apoptotic keratinocytes, occasional nuclear moulding, and variable koilocyte-like cells in the superficial zone (Lerman

et al., 2017). There is strong and diffuse immunoreactivity for p16, but the defining diagnostic criterion is the demonstration of transcriptionally active high-risk HPV, usually by RNA *in situ* hybridization (Lerman et al., 2017; Hendawi et al., 2020). Progression to carcinoma has been reported, but the overall malignant transformation rates currently remain unknown due to reports limited only to small case series. No accepted grading system is established; therefore, HPV-associated OED should, for the present, be graded and clinically managed according to conventional criteria until the significance of these specific cumulative histological changes become known (Odell et al., 2021).

1.7. Aetiological factors

OSCC is a multifactorial disease wherein tobacco and alcohol consumption are the two major aetiological factors associated with it.

1.7.1. Tobacco

Tobacco as an important risk factor can induce OSCC by causing epigenetic alterations of oral epithelial cells and inhibiting multiple systemic immune functions of the host, and its toxic metabolites can cause oxidative stress on tissues (Jiang et al., 2019; Tenore et al., 2020). Tobacco both in smokeless and smoked forms has been shown to induce OSCC (Jiang et al., 2019). South-East Asia accounts for an estimated 90% of the global smokeless tobacco (SLT) use burden, and SLT is considered as one of the major risk factors associated with the high prevalence of OSCC in this region (Gupta and Ray, 2003). SLT is used in many forms varying from chewing tobacco not mixed with any other ingredient to a mixture of tobacco with other ingredients in the form of the pan (betel quid, areca nut with tobacco), naswar, pan-masala or gutkha (chewable tobacco-containing areca nut, slaked lime, and catechu), khaini (chewable tobacco-containing slaked lime) and mishri (powdered tobacco rubbed on the gums as toothpaste) (Gupta, 2013; Khan et al., 2014). A report by the global adult tobacco survey India (GATS-India) indicated that more than one–third (34.6%) of Indians use tobacco in some form: smoking, chewing, application to teeth and gums or sniffing (Gupta, 2013). Among these tobacco users, 20.6% consumed only smokeless tobacco, 8.7% smoked tobacco only, and 5.3% used both smoked as well as smokeless tobacco (Gupta, 2013). SLT is reported to contain 28 known carcinogens of which the non-volatile alkaloid-derived tobacco-specific N-nitrosamines (TSNA) and N-nitrosoamino acids form the major and most abundant group of carcinogens while other carcinogens reportedly present in SLT include volatile N-nitrosamines, certain volatile aldehydes, traces of some polynuclear aromatic hydrocarbons such as benzo[a]pyrene,

certain lactones, urethane, metals, polonium-210 and uranium-235 and -238 (IARC working group on the evaluation of carcinogenic risks to humans, 2007). Khan et al. (2014) performed a random-effects meta-analysis to estimate the risk of oral cancer with the usage of different forms of SLT. The pooled odds ratio (OR) to develop oral cancer for chewing tobacco was 4.7 (range 3.1–7.1) and for pan with tobacco was 7.1 (range 4.5–11.1) (Khan et al., 2014). Another meta-analysis of studies from the South-East Asian region found a significant positive association of SLT use with oral cancer with OR ranging from 1.48 to 27.4 (Gupta et al., 2018). Franceschi et al. (1990) reported an adjusted OR of 11.1 for oral cancer among current smokers of cigarettes and this risk was found to increase significantly with an increasing number of cigarettes smoked per day and the duration of the smoking habit. In comparison to people who have never smoked, the OR of oral cancer was 5.3 for people smoking <15 cigarettes per day and 14.3 for people who smoked >25 cigarettes per day (Franceschi et al., 1990). In India, the prevalence of smokeless tobacco use (26%) is significantly more than that of smoking tobacco (14%) (Gupta, 2013). The commonly smoked tobacco product is bidi (9%) followed by cigarette (6%), hookah (1%), and less than 1% smoke cigars and cheroots (Gupta, 2013).

1.7.2. Alcohol consumption

Alcohol consumption directly accounts for 4.2% of cancer deaths worldwide and is linked to 26.4% of all lips and oral cavity cancers worldwide (WHO, 2018; Marziliano et al., 2020). Alcoholic beverages and acetaldehyde, the main metabolite of ethanol, are classified as class I carcinogens (Dhull et al., 2018). Acetaldehyde causes DNA damage and thus the prolonged and excessive consumption of alcoholic beverages increases the risk of oral squamous cell carcinoma (Feller et al., 2013). Chronic use of alcohol alone may lead to OSCC via several mechanisms, including DNA adduct formation, generation of ethanol-related reactive oxygen metabolites, and interference with the DNA-repair mechanisms (Liu B et al., 2015). A comprehensive meta-analysis of published case-control and cohort studies to investigate the relation between alcohol and cancer risk obtained a pooled OR of 1.75, 2.85, and 6.01 for oral and pharyngeal cancer associated with consumption of 25, 50, and 100 g/day of pure alcohol, respectively (Bagnardi et al., 2001). Tobacco and alcohol work in synergy, with alcohol promoting the carcinogenic effects of tobacco, leading to a multifold increase in the risk of oral cancer (More and D'Cruz, 2013). The synergistic effect of alcohol consumption and tobacco smoke increases the risk of OSCC by making the oral epithelium more permeable, dissolving tobacco, and promoting its penetration (Feller et al., 2013). A recent case-control retrospective study by Tenore et al. (2020) also reinforced the role of tobacco and alcohol as

major risk factors for OSCC as they reported that a high rate of tobacco consumption was associated with an OR of 1.035 (95% CI 1.001–1.070; p = 0.041), while drinker patients showed an OR of 1.035 (95% CI 1.010–1.061; p = 0.05), suggesting a significant risk of developing OSCC.

1.7.3. Areca nut chewing

Areca nut is a primary ingredient of betel quid and is considered as another primary cause of oral cancer in parts of Asia and the Pacific (Warnakulasuriya et al., 2002; Zini et al., 2010; Zhong et al., 2021). Areca nut is chewed by 10%-20% of the world's population with the highest prevalence of use in the Indian subcontinent, large parts of South Asia, and Melanesia (Gupta and Warnakulasuriya, 2002; Zhong et al., 2021). Oral carcinomas of the tongue and buccal mucosa are correlated with areca nut chewing (Li YC et al., 2019). Chewing areca nut is the major cause of the premalignant disease oral submucous fibrosis (OMSF). Tobacco smoking and alcohol consumption have been shown to exert a synergistic effect with areca nut chewing in increasing the risk of malignant transformation of oral submucous fibrosis (Lee et al., 2003; Liu B et al., 2015). Areca cut chewing has also been correlated with reduced cisplatin sensitivity in OSCC patients (Xu et al., 2017).

1.7.4. Human papillomaviruses

Human papillomavirus is a small, nonenveloped, double-stranded, circular DNA virus with a tropism towards epithelial squamous cells (Gupta and Gupta, 2015). High-risk human papillomaviruses (HPVs) (subtypes 16, 18, 31, and 33) are associated with an increased risk of OSCC (Snow and Laudadio, 2010; Kim KS et al., 2014). Low-risk HPVs mainly HPV-6 and 11 appear to be closely associated with a range of oral benign papillomatous lesions, whereas high-risk HPV, HPV-16 and 18 have been found to be associated with OSCC and HPV-16 is associated with OPMDs like oral leukoplakia (OL) including proliferative verrucous leukoplakia (PVL) (Campisi et al., 2007; Prabhu and Wilson, 2013). The frequency of HPV in OSCC varies from 0% to 80%. The prevalence of HPV in OSCC varies depending on several parameters such as geographic differences in population, type of specimen, selection of preparation method, and use of HPV detection method (Miller and Johnstone, 2001). HPV-associated OSCC is characterized by p53 degradation, Rb inactivation, and upregulation of p16 and is more responsive to chemotherapy and radiation compared to HPV-negative OSCC (Marur et al., 2010). No correlation between HPV-positive OSCC and tobacco or alcohol consumption has been found. A strong association has been found between sexual behaviour

and risk of HPV infection (D'Souza et al., 2007). Patients with HPV-positive OSCC are usually younger and present at an advanced stage with large metastatic lymph nodes (Goldenberg et al., 2008).

In China, research has indicated that HPV infection may increase the risk of OSCC carcinogenesis (Zhou et al., 2015). High-risk HPV serotypes, especially HPV16, is positively correlated with OSCC tumorigenesis in young patients (Kaminagakura et al., 2012). Oral tongue squamous cell carcinoma (SCC) is also closely linked with HPV infection (Elango et al., 2011). In contrast, research in Japan and southern Germany have not found a relationship between HPV infection and OSCC patients (Reuschenbach et al., 2013; Rushatamukayanunt et al., 2014). Interestingly, some research found that by increasing the expression of miR-20a, a miRNA involved in cancer development and carcinogenesis, HPV-16 E7 protein may inhibit the development of OSCC (Hu et al., 2016).

In India, there is sparse literature describing HPV infection of the oral cavity in the general population, and the two existing studies are highly discordant (Kulkarni et al., 2011; Pattanshetty et al., 2014). In one study, the saliva rinse of 396 normal individuals from various parts of North Karnataka was collected and polymerase chain reaction (PCR) based high-risk (HR) HPV genotyping was carried out, which reported 2.75% and 22% individuals as positive for HPV16 and HPV18, respectively (Kulkarni et al., 2011). In another study, oral mucosal smears were prepared from 60 healthy individuals and PCR-based HR-HPV genotyping was carried out, which reported 65% of the individuals to be positive for HPV16/18 (Pattanshetty et al., 2014). On the other hand, Western literature reports a low prevalence of HPV infection (<10%) in normal oral mucosa (González-Losa Mdel et al., 2008; Dodson, 2010; Kristoffersen et al., 2012; Gillison et al., 2012; Migaldi et al., 2012). There is not enough evidence to clearly establish the role of latent HPV infection of the oral cavity in normal individuals in the development of cancer. Western literature indicated an association between HR sexual behaviour (oral sex and number of sexual partners) and HNSCC (Farsi et al., 2015). Indian data are sparse in this respect as producing detailed sexual history is usually uncomfortable for the patients as well as the clinicians. Further investigations are required to define a clear relationship between HPV infection and OSCC occurrence.

1.7.5. Diet and oral microbiome

Worldwide, 10-15% of oral cancer burden is attributed to micronutrient deficiency caused by lack of fruits, non-starchy vegetables, and food containing carotenoids in the diet

(Petti, 2009). Foods such as fruits, vegetables, curcumin, and green tea can reduce the risk of oral cancer, while the so-called pro-inflammatory diet, rich in red meat and fried foods, can enhance the risk of occurrence. Dietary factors with a protective effect show different mechanisms that complement and overlap with antioxidant, anti-inflammatory, anti-angiogenic, and anti-proliferative effects (Rodríguez-Molinero et al., 2021).

A case-control study in Southern India observed that the lack of oral hygiene accounted for 32% and 64% of oral cancer cases in men and women respectively (Balaram et al., 2002). The importance of maintaining a normal oral microbiome for prevention of dysbiosis, a microbial shift towards a disease, for example, periodontitis or dental caries, has become more apparent in recent times. Several studies indicate that dysbiosis of the oral microbiome may dictate the progression of OSCC (Wang and Ganly, 2014; Guerrero-Preston et al., 2016; Su et al., 2019). In a recent study, Gopinath et al. (2021) analysed the compositional and metabolic profile of the bacteriome from the swab, saliva, and tissue biopsies in oral cancer patients along with controls using 16S rRNA sequencing on Illumina Miseq (USA) and DADA2 software and found major differences between patients and control subjects. They reported that tumour surfaces carried elevated abundances of taxa belonging to genera Porphyromonas, Enterobacteriae, Neisseria, Streptococcus, and Fusobacteria, whereas Prevotella, Treponema, Sphingomonas, Meiothermus, and Mycoplasma genera were significantly more abundant in deep tissue. Analysis of the metabolic profile of the bacteriome revealed that there is a shift to a pro-inflammatory profile in oral cancer patients compared to the control subjects which is consistent with other studies (Gopinath et al., 2021). Moraes et al. (2016) conducted a case-control study to assess the association between the extent and severity of chronic periodontitis and oral cancer and/or oropharyngeal cancer to conclude that the extent and severity of periodontitis remained as risk indicators for oral cavity and/or oropharyngeal cancer even after the adjustments for traditional confound factors, i.e., smoking and alcohol consumption. There have also been several cases of chronic mechanical irritation (CMI) in an oral site succeeding to OSCC development. CMI of the oral mucosa could be attributed to repeated, low-intense action of three types of CMI factors: dental (malpositions, sharp/broken teeth, and/or rough or defective restorations), prosthetic (ill-fitting dentures, rough/sharp/overextended flanges, and lack of retention/stability), and functional (swallowing, occlusal, and other dysfunctional disorders) (Piemonte et al., 2010; Gupta et al., 2021). The chronic inflammation induced by these intra-oral factors could be associated with an increased risk of oral cancer. Recently, Gupta et al. (2021) performed a systematic review and meta-analysis to explore the association

between chronic mechanical irritation and OSCC. They observed a significant association ($p < 0.00001$) between the chronic oral mucosal irritation and OSCC with an overall risk ratio of 2.56 at a confidence interval of 1.96-3.35. They concluded that chronic oral mucosa irritation has a significant association with OSCC, and the nature of association could be that of a potential co-factor (dependent risk factor) rather than an independent risk factor (Gupta et al., 2021).

1.7.6. Genetic predisposition

Genetic predisposition can also contribute towards an increased risk for oral cancer (Jefferies et al., 1999). A study from India observed a familial aggregation, following an autosomal dominant inheritance pattern and site-specificity in 0.94% of the total oral cancer cases (Ankathil et al., 1996). Another study on the Israeli Jewish population reported that the Ashkenazi group had twice the risk of developing oral cancer compared to the other two ethnic groups that were investigated (Gorsky et al., 1994). Increased incidence of oral cancer is also observed in several inherited cancer syndromes such as xeroderma pigmentosum, ataxia telangiectasia, Bloom syndrome, and Fanconi's anaemia (Prime et al., 2001). A recent systematic review and meta-analysis by Ramos-Garcia et al. (2021) observed that patients with diabetes mellitus have a higher prevalence and greater chance of oral cancer and OPMD development in comparison to non-diabetic patients. They also observed that patients with oral cancer suffering from diabetes mellitus have higher mortality compared to non-diabetic patients with oral cancer. Four members of a family (including the index case and her 3 children) with no history of tobacco usage succumbed to tongue OSCC, and the mutations in the proto-oncogenes *VAV2* and *IQGAP1* were identified as the primary factors responsible for oral cancer in the family (Huang et al., 2019). These genes are involved in the regulation of cell adherence and angiogenesis (Huang et al., 2019).

1.8. Signs and symptoms

Pain is a common symptom in oral cancer patients, representing 30–40% of their main complaints. There are 12 different descriptions of pain, related to TNM (tumour-node-metastasis) staging in the tongue and the tongue/mouth floor (Cuffari et al., 2006). Although pain is the main symptom, it usually arises only when the lesions have reached a remarkable size; this is the time when the patient requests medical assistance. Thus, early carcinomas often go unnoticed because they are asymptomatic (Scully and Bagan, 2009). In later and larger lesions, symptoms may vary from mild discomfort to severe pain, especially on the tongue.

Other symptoms include ear pain, bleeding, mobility of teeth, problems in breathing, difficulty in speech, dysphagia and problems using prosthesis, trismus, and paraesthesia (Haya-Fernández et al., 2004). In some locations, such as the tongue or the floor of the mouth, pain can arise early on. In the case of tongue OSCC, the tongue's movement against the teeth causes more discomfort and pain. In contrast, carcinomas of the lip and buccal mucosa only show intense pain at advanced stages (Barnes et al., 2005). Occasionally patients may present with cervical lymphadenopathy without any other symptoms. In terminal stages, patients may develop skin fistulas, bleeding, severe anaemia, and cachexia (Milian et al., 1993).

Jainkittivong et al. (2009) found that swelling and/or pain were the first signs or symptoms in 180/342 (52.6%) OSCC patients studied. Other authors reported that the main symptoms were ulceration and swelling, followed by pain, bleeding, decreased mobility of the tongue, dysphagia and paraesthesia (Al-Rawi and Talabani, 2008). Gorsky et al. (2004) reported a series of patients with OSCC of the tongue, where the main symptom was pain on the tongue (66.5%), while 29% had a lump on the tongue. Symptoms such as ear pain, voice changes, dysphagia, and cervical tumours were more common in tumours at the tongue base (Gorsky et al., 2004).

1.9. Diagnosis

Diagnosis of oral cancer at an early stage is a crucial factor to improve the prognosis and survival rate of patients. While screening of oral precancer and cancer is done by conventional oral exploration (visual and palpation examination), exfoliative cytology and biopsies (incisional or excisional) are majorly performed for detection of oral cancer in patients who have presented with an identified lesion (Seoane Lestón and Diz Dios, 2010). A surgical biopsy is used to confirm the diagnosis as exfoliative cytological studies are based on microscopic examinations. Imaging techniques like dental panoramic tomography (DPT), computed tomography (CT), and magnetic resonance imaging (MRI) are also used frequently to supplement the clinical evaluation and staging of the primary tumour and regional lymph nodes (Seoane Lestón and Diz Dios, 2010). Further, OSCC lesions are described using the TNM classification, which is recommended by the UICC (union for international cancer control) and describes the anatomical extent and stage of the cancer (Sobin and Fleming, 1997). The TNM based classification provides a basis for the choice of initial treatment, prediction of survival, stratification of patients in clinical trials, accurate communications among healthcare

providers, and uniform reporting of outcomes (van der Schroffe and Baatenburg de Jong, 2009).

Tissue biopsy and histopathological examination will always remain the gold standard for oral cancer diagnosis. On the other hand, with oral cytology, single cells can be analyzed using sophisticated techniques such as cytomorphometry and molecular analysis or using simpler techniques such as Toluidine Blue (dye most used) or Rose Bengal staining (which has proved more promising) yielding very interesting results. Also, optical and diagnostic techniques for imaging have proved particularly useful, but with little clinical relevance as of now (Carreras-Torras and Gay-Escoda et al., 2015).

Recently, there has been an emphasis on finding less invasive and cost-effective methods that provide a more comprehensive view of the cancer profile and help in monitoring its evolution and therapeutics (Cristaldi et al., 2019). Liquid biopsy has emerged as a non-invasive technique that can serve as supportive tools for diagnosis, prognosis, and follow-up of OSCC (Cristaldi et al., 2019). Of special interest is the use of different salivary biomarkers in liquid biopsy for OSCC management. Cristaldi et al. (2019) have recently reviewed data on salivary biomarkers used for detection in saliva liquid biopsy from OSCC patients, particularly circulating tumour DNA (ctDNA), extracellular vesicles (EVs), and microRNAs (miRNAs). It has been suggested by various researchers that a specific group of protein biomarkers are increased in saliva of individuals with OSCC (Franzmann et al., 2005; Nagler et al., 2006; Elashoff et al., 2012). For example, Franzmann et al. (2005) reported CD44 as a probable biomarker of head and neck cancer, whereas Nagler et al. (2006) described Cyfra-21-1 and cancer antigen-25 to be potential biomarkers for oral cancer. In a subsequent study with 64 individuals including patients diagnosed with OSCC, pre-malignant conditions, and healthy controls, an increase in salivary levels of Cyfra-21-1, lactate dehydrogenase, and total protein concentration were shown in OSCC patients compared to other groups (Awasthi, 2017). An increase in the levels of interleukin 8 and subcutaneous adipose tissue was also reported in saliva, exhibiting maximum levels of sensitivity and specificity to diagnose OSCC (Hoffman et al., 2007). Similarly, Arellano-Garcia et al. (2008) described that interleukin 8 and interleukin 1β (IL-8 and IL-1β) levels were increased in saliva of patients with OSCC as compared with the control patients. Gleber-Netto et al. (2016) performed a study involving 180 patients and reported that among the proteomic markers, IL-8 and IL-1β levels were greater in OSCC patients when compared with control and dysplasia patients.

An optical biopsy is another promising non-invasive technique for diagnosing OSCC. It involves light-tissue interactions and different types of spectroscopies like fluorescence spectroscopy, Raman spectroscopy, elastic scattering spectroscopy (ESS), and optical coherence tomography (OCT) (Omar, 2015). A systematic review to examine the validity of using non-invasive methods of diagnosing OSCC, including oral brush biopsy, optical biopsy, and saliva-based oral cancer diagnosis indicated that both saliva-based oral cancer diagnosis and optical biopsy are promising non-invasive methods for diagnosing OSCC with high sensitivity and reliable specificity that are easy for primary care practitioners to perform clinically (Omar, 2015).

1.10. Treatment

The preferred primary treatment regimen for most of the early oral cancers relies on the surgical removal of the tumour section with a recommended adequate margin of more than 5 mm from the tumour front. Radiotherapy, which comprises brachytherapy ± external beam radiotherapy (EBRT), is another alternative to surgery for treating early-stage oral cancers (D'Cruz et al., 2018). A recent analysis of over 20,000 early oral cancers from the national cancer database showed that surgery was the primary modality of choice in approximately 95% of the patients and showed overall survival (OS) benefit compared to radiotherapy (Ellis et al., 2018). Surgery types include maxillectomy, mandibulectomy, glossectomy, radical neck-dissection Mohs surgery, and a combination of glossectomy and laryngectomy (Ozaki et al., 2016; Murphy et al., 2016; Jacobson et al., 2015; Lin et al., 2015). Additional reconstructive surgery such as bone grafting and surgical flaps from the forearm may be required to rebuild the structures removed during the excision of cancer. Adjuvant therapy is often needed to improve outcomes in patients who present oral cancer at an advanced stage. Systemic chemotherapy administered either before (induction or neoadjuvant chemotherapy) or during (concomitant chemotherapy) radiotherapy is increasingly becoming part of the treatment plan for advanced head and neck cancers (Bhide and Nutting, 2010). Platinum-based induction chemotherapy (e.g., cisplatin) and taxanes (e.g., docetaxel and paclitaxel) are the options in the treatment of locally advanced cancer. Cisplatin/infusional 5-fluorouracil/docetaxel forms the standard regimen for chemotherapy. Concomitant chemotherapy during radiotherapy has shown to improve loco-regional control rates, survival, and rates of organ conservation (Bhide and Nutting, 2010).

A recent study found that patients with early-stage I and II OSCCs with close (1–5 mm) and positive (< 1 mm) margins showed a lower 5-year OS rate compared to patients with a clear margin, and close margins were also found to be associated with a >2-fold increased risk of recurrence (Fridman et al., 2018). However, adjuvant therapy was found to significantly improve the outcomes in the case of patients with closed/positive margins (Fridman et al., 2018). The location of the tumour also plays a critical role in the disease prognosis. Jehn et al. (2019) reported that oral and oropharyngeal squamous cell carcinoma patients with tumours located at the base of the tongue, oropharynx, and maxilla exhibit a significantly inferior disease-specific and lower 5-year survival rates, which could be due to higher tumour stage and incomplete resection status. They also observed that cervical lymph node metastasis and distant metastatic spread were more frequently observed with base of the tongue and oropharynx lesions (Jehn et al., 2019). The rate of recurrence is high in oral cancer and occurs in up to two-third of the patients (D'Cruz et al., 2018). Salvage surgery must be considered as the first choice of treatment of recurrent tumours as it gives the best chance at control and survival (Ho et al., 2014; D'Cruz et al., 2018). Re-irradiation has been beneficial in patients unsuitable for salvage surgery, while palliative chemotherapy is the mainstay of treatment for recurrent/metastatic tumours unsuitable for salvage surgery/re-irradiation (Spencer et al., 2008; D'Cruz et al., 2018).

Epidermal growth factor receptor (EGFR) is overexpressed in a wide variety of cancers including OSCC and is associated with poor prognosis (Ang et al., 2002). In recent times, targeted therapy against EGFR, using the monoclonal antibody Cetuximab, has a significant success rate. Bonner et al. (2006, 2010) observed significantly improved disease-free survival (DFS), loco-regional control rates, and OS in patients of head and neck cancer treated with a combination of Cetuximab with radiotherapy compared to radiotherapy alone. Vermorken et al. (2008) also reported improved OS when Cetuximab was used in combination with platinum-based chemotherapy and 5-fluorouracil as first-line treatment in recurrent or metastatic head and neck SCC. Recently, the use of Nivolumab and Pembrolizumab, which are immunotherapy drugs against programmed death-ligand 1 (PD-L1), as a second-line treatment of recurrent head and neck cancers, has gained interest as they improved OS in these settings (Ferris et al., 2016; Seiwert et al., 2016; Ferris et al., 2018).

In OSCC, mean levels of *COX-2* mRNA are increased by 150-fold compared to the normal mucosa (Chan et al., 1999). Over expression of COX-2 is seen in 58 out of 75 patient samples of OSCC and it has a significant association with the lymph node involvement,

histological grade, local recurrence of tumour and patient survival (Byatnal et al., 2015). Antimetastatic effects of certain COX-2 inhibitors (e.g., Nimeluside, NS398, and JTE-22) suggest that these molecules have critical utility in the management of oral cancers (Nishimura et al., 1999; Shiotani et al., 2001; Minter et al., 2003). *In vivo* studies have proven that selective COX-2 inhibition suppresses tumour cell growth (Perkins and Shklar, 1982; Tanaka et al., 1989). Studies in animal models show that COX-2 inhibition can prevent carcinogenesis (Perkins and Shklar, 1982; Tanaka et al., 1989; Eling et al., 1990; Nishimura et al., 1999; Shiotani et al., 2001). The combined use of chemoradiotherapy with a COX-2-targeted approach has shown efficacy due to its synergistic effect (Li et al., 2020).

1.11. Molecular basis and biology of OSCC

Oral cancer is epithelial neoplasia that generally begins with a focal clonal overgrowth of altered stem cells near the basement membrane, that expands upward and laterally, replacing the normal epithelium and later progresses through hyperplasia to dysplasia to carcinoma *in situ* and invasive carcinoma (Nagpal and Das, 2003). A majority of these clinically diagnosed oral potentially malignant disorders which develop into OSCC have been shown to carry genetic alterations like gains in 3q (36.5%), 5p (23%), 7p (21%), 8q (47%), 11q (45%), 20q (31%) and losses in 3p (37%), 8p (18%), 9p (10%), and 18q (11%) (Salahshourifar et al., 2014). As the disease progresses from precancerous lesions to invasive tumours, there is an accumulation of these genetic changes in terms of frequency, type, and size of the abnormalities, even on different regions of the same chromosome (Salahshourifar et al., 2014). Chromosomal segregation, aneuploidy, loss of heterozygosity (LOH), telomere instability, mutations in cell-cycle checkpoints and DNA damage repair genes are well known genetic abnormalities involved in tumorigenesis (Chen et al., 2015). Chen et al. (2015) observed that the loss of heterozygosity in 3p, 9p, 11q and 17p is consistent with the above report and has a significant role in OSCC pathogenesis.

Activation of oncogenes and downregulation of tumour suppressor genes are essential for cancer progression. Significant advances have been made during the last few decades to understand cancer at the molecular level, its application for early and sensitive diagnosis, effective treatment, and improved prognosis. Various oncogenes like *EGFR, TGF-α, CCND1, MYC, BCL2,* and *STAT3* have been reported to be involved in oral cancer pathogenesis (Gkouveris and Nikitakis, 2017; Lakshminarayana et al., 2018). Mutations in signalling pathway genes like *EGFR, FGFR, MET, RET, NOTCH1-4, NFKB 1-2, APC, AXIN1,* and

CTNNB1 cause their downstream signalling mechanisms to remain constitutively triggered, resulting in cell proliferation and metastasis (Xia et al., 2018; Jung and Park, 2020; Majumder et al., 2021). Pathway assessment of 47 tumour samples revealed somatic aberrations within the OSCC genome involved in major pathways, including cell cycle and RTK-MAPK-PI3K pathways (Nakagaki et al., 2017). EGFR, a tyrosine kinase receptor, levels showed an increase of 42% to 58% in OSCC cases with dominant malignancy (Laimer et al., 2007). Mutations in the EGFR gene is prevalent and activate several pathways like RAS/RAF/MEK/ERK and RAS/PI3K/PTEN/AKT/MTOR inducing transformation, proliferation, differentiation, migration, and angiogenesis resulting in advanced oral tumours (Bernardes et al., 2010). The *EGFR* gene has been reported to be amplified in 10% to 30% of oral cancer patients (Leemans et al., 2011). Matta and Ralhan (2009) have reported the presence of *EGFR* variant III (EGFRvIII), a truncated *EGFR* mutant, in OSCC, which is responsible for constitutive activation of downstream signalling and thus in acquiring resistance to EGFR inhibition by monoclonal antibodies. Amplification of *CCND1* was reported in 25-70% of oral cancers, while amplification of *MYC* and *MYCN* and their increased levels were observed in 20-40% of oral cancers (Nagpal and Das, 2003). Xie et al. (1999) reported that overexpression of BCL2 and loss of BAX expression are significantly associated with poor prognosis in oral cancer patients. Grandis et al. (2000) and Nagpal et al. (2002) proposed that constitutive activation of STAT3 is an early event in oral carcinogenesis. Nagpal et al. (2002) reported that 82.2% of oral tumours showed STAT3 expression and activation, whereas STAT3 was not found to be expressed in normal epithelium and premalignant lesions. However, the role of mutated *RAS* genes in human oral carcinogenesis is presently not clear. A report from India demonstrated that 35% of oral squamous cell carcinoma contains *HRAS* mutations (Saranath et al., 1991). However, studies form the western world have shown that the *HRAS* mutations are found in fewer than 5% of head and neck cancers (Gilardi et al., 2020; Coleman et al., 2023). Research over the past several years indicates *HRAS* as one of the most deregulated oncogenes in comparison to *KRAS* and *NRAS* in oral cancer (Murugan et al., 2012). The mutations in *HRAS* are reported in betel quid chewers and smokers (Krishna et al., 2018). Alongside, amplification of the 8q22-q23 (*EIF3E*) and 8q24.21 (*MYC*) occurs in mild dysplasia; the gain of the 8q arm is detected in the invasive OSCC (Chamoli et al., 2021).

Inactivating mutations in tumour suppressor genes involved in oral carcinogenesis have also been reported. *ATM* (ataxia-telangiectasia mutated), a member of the PI3K family, enables p53 and regulates apoptosis. *ATM* mRNA harbours the single nucleotide variation rs189037

(G > A) in its 5'UTR, which is one of the critical polymorphisms that is associated with the occurrence of different cancers and tumour diffusing capacity (Wang et al., 2011; Liu J et al., 2014; Song et al., 2015; Yan Z et al., 2017; Lopez Guerr et al., 2018). Bau et al. (2010) showed that the *ATM* rs189037 A allele is correlated with oral cancer susceptibility, and this polymorphism may be a useful marker for oral cancer prevention and early detection. Mutations in *TP53* are the most frequent genetic errors in OSCC, which promote cell proliferation by inhibiting cell cycle inhibitors such as p16 and p52 (Hou et al., 2015; Ghanghoria et al., 2015). About 40-70% of oral cancers have reported mutations in *TP53,* which lead to the formation of a non-functional protein (Usman et al., 2021). Mutation hot spots in *TP53* include R175, G245, R248, R249, R273, and R282 in the DNA binding domain (Chiang et al., 2021). A report observed that both disruptive and non-disruptive *TP53* mutations are linked to the development of resistance to anticancer drugs such as cisplatin, EGFR-inhibitors, alkylating agents, antiestrogens, anthracyclines, and antimetabolites (Hientz et al., 2017). *TP53* mutations connects with the clinical seriousness of the disease and is prevalent in HPV positive tumour (Hou et al., 2015; Ghanghoria et al., 2015). *TP53* mutations were less commonly found in Asian patients in comparison with Caucasians (Zanaruddin et al., 2013). Mutations in *TP53* have been reported in 25-69% of the oral cancer patients (Das and Nagpal, 2002). Also, mutant forms of TP53 are found to be associated with poor outcomes and an increased likelihood of early recurrence and/or second primary tumours in several cases (Shin et al., 1996). The *CDKN2A* tumour suppressor gene located on chromosome 9p21 codes for p16 protein that is involved in the inhibition of cell cycle G1/S transition. *CDKN2A* is reported to be inactivated in several cancers including OSCC due to somatic mutations, homozygous deletions, LOH, and DNA hypermethylation (Das and Nagpal, 2002). The *CDKN2B* tumour suppressor gene that codes for p15 has been reported to be deleted or downregulated in 10-50% of oral cancers (Gonzalez-Zulueta et al., 1995; Roesler et al., 1998). p27KIP1 protein encoded by the *CDKN1B* gene was observed to be significantly decreased in oral dysplasia and carcinomas compared to the normal epithelium and this decrease was speculated to be an early event in oral carcinogenesis (Jordan et al., 1998). *PTEN*, the negative regulator of the PI3K/AKT pathway, is one of the commonly deregulated genes resulting in the constitutive activation of cell survival signalling correlated with early stage of OSCC (Miyahara et al., 2018). Interestingly, in case of an intact *RB1* gene, loss of p16 expression and/or increased cyclin D1 expression leads to hyperphosphorylation of pRb, resulting in high pRb levels (Chatterjee et al., 2004). This upregulation of pRb is correlated with OSCC development especially in smokers (Thomas et al., 2015).

1.12. Epigenetic alterations in OSCC

Global DNA hypomethylation and locus-specific hypermethylation of CpG islands (CGIs) are the epigenetic hallmarks of cancer. Hypomethylation is mostly caused by the loss of methylation at the repeat elements that are normally heavily methylated, such as satellite DNA (e.g., Sat II) and retrotransposons (e.g., ALUs and LINEs). This loss triggers genomic instability and activation of oncogenes (Nishiyama and Nakanishi, 2021). Locus-specific hypermethylation is typically found in promoter CGIs of diverse genes; it leads to transcriptional silencing which can be inherited. Hypermethylation and consequent silencing of several tumour suppressor genes involved in a wide range of cellular processes, including cell cycle control (e.g., *CDKN2A* and *CDKN2B*), apoptosis (*DAPK, TP73*, and *RASSF1A*), Wnt signalling (*APC, WIF1*, and *RUNX3*), cell-cell adhesion (*CDH1*), and DNA repair (*MGMT* and *MLH1*), have been reported in OSCC (Mascolo et al., 2012). In OSCC, 69 tumour suppressor protein-coding genes are hypermethylated, providing relevance to its staging and grading (Flausino et al., 2022). In another mechanism, hypermethylation itself may physically block the process of binding of transcriptional regulators and genes (Nishiyama and Nakanishi, 2021). Significant effects are also associated with the methylated DNA's role in chromatin condensation due to interactions with various other epigenetic modifications, such as the histone code, polycomb complexes, nucleosome positioning, noncoding RNA, and ATP-dependent chromatin remodelling proteins (Suzuki and Bird, 2008).

Apart from epigenetic changes which involve DNA methylation, histone modifications and non-coding RNAs have also been linked to OSCC initiation and progression (Mascolo et al., 2012). CAF-1, a protein complex formed by three subunits (p48, p60 and p150) with different molecular weights delivers histones H3 and H4 on newly synthesized DNA during DNA replication and DNA repair. CAF-1 facilitates the incorporation and assembly into chromatin of H3K56 acetylated histones in response to oxidative stress and DNA damage; moreover, it contributes to resolve the mismatch-containing strands, restoring chromatin structure on the completion of double-strand break repair. CAF-1/p60 has been found to be overexpressed in a series of human malignancies, including breast, prostate, melanocytic, salivary gland, cervical, endometrial, and renal cell cancers, in close association with their biological aggressiveness. The role of CAF-1/p60 as a new prognostic marker in oral tongue SCC has also been investigated. CAF-1/p60 expression has been found significantly higher in OSCC with a poor prognosis. Sakuma et al. (2006) found a higher expression of deacetylase 6 in OSCC cell lines and OSCC tissue samples in comparison to normal oral tissue and nine

OSCC cell lines. Chang et al. (2009) evaluated the expression of histone deacetylase 2 protein on 20 cases of oral epithelial dysplasia and 93 cases of OSCC. They observed that the overexpression of the HDAC protein is a frequent event in OSCC, and suggested that histone deacetylase 2 protein could be used as a prognostic factor in oral SCC. Recently, long non-coding RNA named HOX transcript antisense RNA (*HOTAIR*) and Ferritin heavy chain 1 pseudogene 3 (*FTH1P3*) have been shown to cause metastasis and poor survival in OSCC (Ghafouri-Fard et al., 2020). Besides *FOXCUT, MALAT1, UCA1, TUG1, CCAT2, FTH1P3, H19,* and *HIFCAR/MIRHG* are known to be downregulated in OSCC (Ghafouri-Fard et al., 2020).

MicroRNAs are another critical mediator of epigenetic gene regulation and the interest in investigating their functional roles in OSCC pathogenesis is rapidly growing (D'Souza and Kumar, 2020). It is also the topic of interest in the present study, substantially described in the subsequent sections.

Significant advances have been made during the last few decades in understanding cancer at the molecular level in order to apply such findings in early and sensitive diagnosis, effective treatment, and improved prognosis. However, a clear understanding of the molecular signals triggering the onset of oral cancer is still not known because of which the 5-year survival rate is the lowest among all major cancers and has not shown any significant improvement in the past two decades (Rivera, 2015). Thus, the current scenario requires the identification of new therapeutic targets and molecular markers to aid in better prognosis and treatment. In this context microRNAs (miRNAs/miRs)) have gained importance as emerging therapeutic targets in cancers. Studies have shown that microRNA-based therapeutics hold a promising potential for cancer management and hence there is a growing need to further explore their roles in various cancers with the aim to develop miRNA-based therapeutics (D'Souza and Kumar, 2020).

1.13. MicroRNAs

1.13.1. Paradigm shift: discovery of microRNAs

Regulation of gene expression has always been one of the most enticing areas of research. Previously it was conceived that the sequence-specific RNA-binding domains of regulatory proteins target noncoding regions of mRNAs to regulate their expression in response to certain cues, but the discovery of a small noncoding RNA that targets an mRNA to regulate its expression is paradigm shifting (Wickens and Takayama, 1994). In a commentary entitled

"Deviants or emissaries", Wickens and Takayama (1994) highlighted the work of Ambros and Ruvkun who discovered the first microRNA (miRNA) *lin-4* and its mechanism of action. While investigating the early development in *Caenorhabditis elegans*, genetic screens revealed that the expression of *lin-14*, a heterochronic gene, was post-transcriptionally regulated by another heterochronic gene *lin-4*. The gene *lin-4* is transcribed to form a short, 21-nt-long RNA species and regulates *lin-14* by imperfectly base-pairing with the untranslated region of its mRNA (Lee et al., 1993; Wightman et al., 1993). The small regulatory RNA (miRNA) discovered by Ambros and Ruvkun (Lee et al., 1993; Wightman et al., 1993) did not turn out to be a deviant rather it was adding complexity to the regulation of mRNA stability and translation, which was earlier conceived as an exclusive function of proteins. Since then, miRNAs have been detected in all animal model systems and some were shown to be highly conserved across species (Pasquinelli et al., 2000; Davis-Dusenbery and Hata, 2010; Li et al., 2010; Friedlander et al., 2014). New miRNAs are still being discovered and consequentially widespread, pervasive, and important regulatory roles of miRNAs are getting recognized (de Rie et al., 2017).

MicroRNAs (miRNAs) comprise a group of small, endogenous noncoding RNAs whose length range from 18-25 nt (nucleotides) and most of the human miRNAs fall within the 20-23 nucleotides range. This variation in length of miRNAs is either attributed to miRNA length heterogeneity (single miRNA precursor giving rise to mature miRNAs of different lengths) or miRNA length diversity (different miRNA precursors giving rise to mature miRNAs of varying lengths) (Starega-Roslan et al., 2009). The common notion is that the miRNAs have evolved independently in plants and animals as their sequences and biogenesis pathways differ substantially. However, recent evidence from non-bilaterian metazoans, plants, as well as various algae raises the possibility that the last common ancestor of these lineages presumably had a miRNA pathway for post-transcriptional regulation of crucial genes (Bråte et al., 2018). A recent study demonstrates that the core of animal miRNA biogenesis, the Microprocessor, is not an animal innovation but originated among their unicellular sister lineages. Several unicellular species harbouring the Microprocessor also express bona fide miRNAs (Bråte et al., 2018). The miRBase database (http://www.mirbase.org/) accounts for 38,589 precursors and 48,860 mature miRNAs across 271 organisms, of which 1,917 precursors and 2,654 mature miRNAs are documented in humans. In addition to that, 3,707 new miRNAs have been identified (Londin et al., 2015), resulting in a total of 6,361 miRNA sequences whose functions are only partially known (Londin et al., 2015). Total number of miRNA genes in humans is 6,904 as per the GeneCards database (Updated in May, 2023; https://www.genecards.org).

Many of these miRNAs are phylogenetically conserved, for example, ~55% of *C. elegans* miRNAs have homologs in humans (Ibanez-Ventoso et al., 2008). These conserved miRNAs have preferentially conserved interactions with most human mRNAs.

Computational and experimental approaches indicate that, on an average, a miRNA may repress more than a hundred mRNAs; over 60% of human protein-coding genes are predicted to contain miRNA-binding sites within their 3′UTRs (Friedman et al., 2009). Furthermore, diverse distinct phenotypes have been observed in loss-of-function studies which involve disruption of miRNA genes in mice encompassing a spectrum of developmental, physiological, and behavioural defects (DeVeale et al., 2021). This suggests that miRNAs influence essentially all developmental processes and diseases, therefore a tight regulation in miRNA expression, half-life, and decay is necessary.

The function of miRNAs was solely considered to be cytoplasmic for a long time. However, the emerging roles of miRNA in the nucleus and other subcellular compartments (viz., mitochondria, endoplasmic reticulum, endosomes and in the membrane-less compartments) to maintain cellular homeostasis led to further probing into the mechanisms of miRNA localization and its subsequent functions in these subcellular compartments (Jie et al., 2021). Of these, nuclear localization of miRNAs and its mechanisms are most well studied, owing to the rise in reports demonstrating the range of transcriptional and post-transcriptional functions that the miRNAs perform in the nucleus.

1.13.2. Genomic location of miRNA genes

MiRNA genes are found across all chromosomes and may be located in the intergenic or intragenic regions of protein-coding or non-coding genes. Human miRNAs are frequently located at fragile sites and cancer-associated genomic regions, indicating a non-random distribution of microRNA genes (Calin et al., 2004). Human chromosome 19 has the highest microRNA density in comparison to the other human chromosomes. The 14q32 and 19q13 are the most microRNA-rich human chromosomal bands, with 4.11 and 3.59 microRNAs per mega-base pair (Mbp) DNA (Boroumand et al., 2019). Moreover, some miRNAs exist as discrete units while some exist in clusters. According to the miRbase database, a cluster is a group of miRNAs that are located within 10 kb of each other. miRNAs belonging to the same cluster may either be co-transcribed or transcribed independently.

Evolutionarily, miRNAs are much younger than protein coding genes (on an average 169 Myr vs. 1195 Myr) such that most of them have only recently arisen after the diversification

of different phylogenetic groups (Patel and Capra, 2017). An estimated 46% of human miRNAs are primate-specific, while about 14% are strictly human-specific (Patel and Capra, 2017). Evolution of miRNA genes involves *de novo* generation from hairpin-structures that are located within the introns or intergenic regions. Most likely, they originate through one of three proposed models: (i) inverted gene duplication of a gene that subsequently becomes the target of the miRNA, (ii) transposon-insertion followed by derivatization, and (iii) spontaneous evolution out of random sequences (Patel and Capra, 2017). However, most of the functionally important miRNAs arose from duplications of existing miRNAs. Many miRNAs have multiple paralogues as an outcome of gene duplications. In these isoforms, the sequence and genomic loci of the primary miRNA (pri-miRNA) vary but identical mature miRNAs are generated. Thus, they eventually target identical mRNAs (Olena and Patton, 2010).

1.13.3. Canonical biogenesis

The biogenesis of miRNA begins in the nucleus where miRNA genes are transcribed into long primary transcripts (pri-miRNAs) that are always capped at the 5'end and usually polyadenylated at the 3'end. Intronic miRNAs are transcribed by polymerase II (Pol II) (Ha and Kim, 2014). All other canonical and nearly all other non-canonical miRNA loci are also under Pol II transcriptional control, which is indistinguishable from that of protein coding genes. Interestingly, miRNAs with upstream Alu elements located in the human chromosome 19 miRNA cluster (C19MC) are transcribed by RNA polymerase III. There are additional human miRNAs which are predicted to be strong candidates of RNA polymerase III-mediated transcription (Borchert et al., 2006).

Pri-miRNAs contain stem loop structures which are cleaved by a cellular RNase class II endonuclease III enzyme called Drosha along with DGCR8/Pasha at the stem of the hairpin structure (Denli et al., 2004). This gives rise to hairpin structures called precursor miRNAs (pre-miRNAs) which are approximately 70-120-nt long. The pre-miRNA harbours a 5'phosphate and a 2-nt overhang at the 3'end, a characteristic feature of endonuclease III cleavage (Han et al., 2004). Pre-miRNA is then transported with the help of Exportin-5 along with Ran-GTP to the cytoplasm and is then processed by the cytoplasmic endonuclease III Dicer (Denli et al., 2004; Okada et al., 2009) to remove the terminal loop, resulting in a mature miRNA duplex (Zhang et al., 2004). The directionality of the miRNA strand determines the name of the mature miRNA form: 5p strand arises from the 5′ end of the pre-miRNA hairpin while the 3p strand originates from the 3′ end. Both 5p and 3p strands derived from the mature miRNA duplex can be loaded onto the Argonaute (AGO) family of proteins (AGO1-4 in

humans) in an ATP-dependent manner (Yoda et al., 2010). For any given miRNA, the proportion of AGO-loaded 5p or 3p strand varies greatly based on the cell type or cellular environment, ranging from near equal proportions to predominantly one or the other (Meijer et al., 2014). The selection of the 5p or 3p strand is dependent in part on the thermodynamic stability at the 5′ ends of the miRNA duplex or a 5′U at nucleotide position 1 (Khvorova et al., 2003). Generally, the strand with lower 5′ stability or 5′ uracil is preferentially loaded onto AGO, and is considered as the guide strand. The passenger strand otherwise known as the unloaded strand is unwound from the guide strand through various mechanisms based on the degree of complementarity. The passenger strands of miRNA that do not contain mismatches are cleaved by AGO2 and degraded by cellular machinery which can produce a strong strand bias. Whereas, miRNA duplexes with central mismatches or non-AGO2 loaded miRNA are passively unwound and degraded (Ha and Kim, 2014).

1.13.4. Non-canonical biogenesis

Multiple non-canonical miRNA biogenesis pathways have been elucidated till date. Non-canonical miRNAs originate from diverse genetic origins and distinct maturation pathways of miRNA biogenesis, bypassing one or more steps of the canonical biogenesis pathway of miRNA which in turn augments the complexity of miRNA functions in the maintenance of physiological functions of the cell (Abdelfattah et al., 2014). These pathways make use of the proteins involved in the canonical pathway, mainly Drosha, Dicer, Exportin-5, and AGO2 in different combinations (O'Brien et al., 2018).

The non-canonical miRNA biogenesis can be broadly grouped into Drosha/DGCR8-independent and Dicer-independent pathways. Pre-miRNAs produced by the Drosha/DGCR8-independent pathway resemble Dicer substrates for example mirtrons, which are produced from the introns of mRNA during splicing (Ruby et al., 2007; Babiarz et al., 2008). Another example is the 7-methylguanosine (m7G)-capped pre miRNAs. These nascent RNAs are directly exported to the cytoplasm through exportin-1 and there is a strong 3p strand bias most likely due to the m7G cap preventing 5p strand loading into Argonaute (Xie et al., 2013). Conversely, Dicer-independent miRNAs are processed by Drosha from endogenous short hairpin RNA (shRNA) transcripts (Yang et al., 2010). These pre-miRNAs require AGO2 to complete their maturation within the cytoplasm because they are of insufficient length to be Dicer-substrates; this promotes loading of the entire pre-miRNA into AGO2 and AGO2-dependent slicing of the 3p strand (Yang et al., 2010). Their maturation takes place via 3′-5′ trimming of the 5p strand (Cheloufi et al., 2010).

The mammalian non-canonical miRNA with the most clearly established function is miR-451. It is one of the most highly expressed miRNAs in the erythrocytes of vertebrates, and mice lacking it have defects in erythroblast maturation (Patrick et al., 2010; Rasmussen et al., 2010).

1.13.5 Mechanism of action

The minimal miRNA-induced silencing complex (miRISC) consists of the guide strand and AGO proteins (Kawamata and Tomari, 2010). The target specificity of miRISC is by virtue of its interaction with complementary sequences on target mRNA, called miRNA response elements (MREs). miRNA-mRNA interactions cause both direct and indirect effects on translation. In the direct effects, initiation of translation or post-initiation of translation is inhibited by preventing the association of ribosomes with target mRNAs. Indirect effects are characterised by premature ribosome fall-off, reduced/stalled elongation, or co-translational protein degradation. Indirect effects of miRNA-mRNA interaction involve deadenylation, resulting in degradation or increased turnover. These effects occur in the cytoplasm, predominantly in the processing bodies (P-bodies), which are enriched for factors involved in mRNA degradation. P-bodies may sequester the mRNAs whose protein formation is prevented (by direct or indirect effects), which can be used later for translation or can be degraded (Krishnan and Damaraju, 2018).

This miRNA-mRNA interaction can also occur via binding of the miRNA seed region (SD) to its target site (TS) in the 3'UTRs/5'UTRs/coding sequences of the target mRNAs, promoters of target genes, other miRNAs, lncRNAs and introns to regulate gene expression (Bartel et al., 2018).

1.13.5.1. Canonical miRNA action

The conventional mode of miRNA function involves the direct interaction of miRNA loaded RISC (miRISC) with the reverse complementary sequences within the 3′-untranslated region (UTR) of target mRNAs (O'Brien et al., 2018). All AGOs silence their target mRNAs by recruiting downstream factors which are proteins from the Glycine-Tryptophan protein of 182 kDa (GW182) family such as trinucleotide repeat-containing gene 6A–6C (TNRC6A–TNRC6C) and the carbon catabolite repressor 4–negative on TATA (CCR4-NOT) complex, that mediate translational repression, deadenylation or decapping of target transcripts (Fabian and Sonenberg, 2012; Stavast and Erkeland, 2019). The miRNA-mediated RNA silencing

processes are mainly localized in processing-bodies (P-bodies) in the cytoplasm (Krishnan and Damaraju, 2018).

1.13.5.2. Non-canonical miRNA action

The plethora of unconventional functions offered by miRNAs include pri-miRNAs coding for peptides, miRNAs interacting with non-AGO proteins, miRNAs activating Toll-like receptors, miRNAs upregulating protein expression, miRNAs targeting mitochondrial transcripts, miRNAs targeting nuclear non-coding RNAs and the last but the most studied one among these wherein miRNAs directly activate gene transcription called the transcriptional gene activation (TGA) (Dragomir et al., 2018).

Since some miRNAs show a higher abundance in the nucleus in comparison to the cytoplasm, it suggests a correlation between nuclear localization/trafficking of miRNAs and its nuclear functions. Some sequence motifs have been demonstrated to facilitate miRNA translocation to the nucleus, but other factors may also direct miRNA localization patterns (Hwang et al., 2007; Jeffries et al., 2011). For example, Hwang et al. (2007) first reported that a 6-nt sequence AGUGUU at the 3' end of human miR-29b is responsible for its preferential nuclear localization (71%) compared to that of miR-29a (42%), which lacks the sequence but is otherwise almost identical. Furthermore, addition of AGUGUU to the 3' ends of other small single-stranded RNAs (ssRNAs) was sufficient to cause their nuclear accumulation. Seven additional sequence motifs promoting the same have been described in a patent by the same group (Mendell et al., 2007). Nuclear localization of miRNAs involves three mechanisms which may not be mutually exclusive (Stavast and Erkeland, 2019).

1. Nuclear localization signal sequences within a subset of miRNAs.
2. Full processing of a subset of miRNAs in the nucleus.
3. Continuous shuttling of miRNAs of which a subset of miRNAs is enriched in the nucleus by virtue of their interaction with the targets.

Consequentially, miRNA-mediated transcriptional regulation has gained importance as functional studies in human cells provide strong evidence that miRNAs regulate the transcription of target genes by binding to reverse complementary sequences in promoter regions. Transcriptional gene activation (TGA) and transcriptional gene silencing (TGS) are the two recognized functions of nuclear miRNAs.

1.13.6. Dysregulated miRNAs in cancer

miRNAs provide a unique perspective into the mechanism of cancer onset, progression, and metastasis (Sarkar and Kumar, 2021). Calin et al. (2004) first demonstrated the role of miRNAs in chronic lymphocytic leukemia (CLL) and concluded that miR-15a and miR-16-1 are downregulated or deleted in a majority of the CLL patients, implicating these miRNAs as tumour suppressors.

The study of miRNAs in cancer focuses on the significant alteration of miRNA levels in malignant cells in comparison to their normal counterparts. A study has shown that tumours exhibit a specific miRNA signature, termed the miRNome, which is characteristic to the malignant state and defines some of their clinicopathological properties (Lu et al., 2005). miRNA expression pattern can also trace back to the developmental origin of the tumour and even aid in understanding the subgroups of different cancers. For examples, tumours of epithelial origin presented a different miRNA expression pattern from haematopoietic malignancies; miRNA profiles can also distinguish acute lymphoblastic leukaemia (ALL) specimens into three major groups: one containing all t (9;22) BCR/ABL- and t (12;21) TEL/AML1-positive samples, a second group containing T-cell ALL samples, and a third group containing the Lysine Methyltransferase 2A (*KMT2A*; previously known as *MLL*) gene rearrangement (Di Leva et al., 2014).

A profiling study of 217 mammalian miRNAs showed that miRNA expression is globally suppressed in tumour cells compared to normal cells (Lu et al., 2005). Nevertheless, more specific alterations of individual miRNA expression are also apparent in tumours (Volinia et al., 2006). In agreement with this observation, global depletion of miRNAs by genetic deletion of the miRNA-processing machinery favours cell transformation and tumorigenesis *in vivo* (Jang and Lee, 2021). This highlights that global decrease in miRNA levels is not simply an effect of tumorigenesis, but it has a causative role in cancer development. Despite the general reduction of miRNAs in cancers, several miRNAs are upregulated, some of which undoubtedly play oncogenic roles.

In comparison to their normal counterparts, miRNAs in malignant tissues are either upregulated or downregulated and are considered as oncogenic or tumour suppressor miRNAs, respectively, in a tissue or cell type specific manner. For instance, in erythroblastic cells, miR-221 and miR-222 act as tumour suppressors by targeting the oncogene *KIT* and inhibiting the growth of erythroblastic leukemia (Felli et al., 2005). On the contrary, they function as

oncogenic miRNAs (oncomiRs) in various human solid tumours by targeting at least four important tumour suppressors—*PTEN* (phosphatase and tensin homolog), *p27*, *p57*, and *TIMP3* (tissue inhibitor of metalloproteinases 3) (Garofalo et al., 2012). Metastamirs are a subset of oncomirs involved in metastasis, which may not catalyse the initial steps of cancer but have pro-metastatic (e.g., miR-10b) or anti-metastatic effects (e.g., miR-146 family) in the later stages of cancer progression (Hurst et al., 2009). The upregulation of oncomirs occurs through one or more of the following mechanisms: loss of repressive epigenetic marks, microRNA gene amplification, induction in miRNA expression by the presence of activators and loss of inhibitors of transcription, and anomaly in post-transcriptional regulation. Similarly, downregulation of tumour suppressor miRNAs occurs via one or more of the following mechanisms: acquisition of repressive epigenetic marks, genomic loss of miRNA gene, inhibition of miRNA expression by the loss of transcription activators and gain of oncogenic transcription repressors, and post-transcriptional dysregulation. Recent evidence indicates that post-transcriptional maturation, rather than transcription of miRNAs, is often perturbed in cancer (Suzuki et al., 2009; Jiang et al., 2015; Garibaldi et al., 2016; Gurtner et al., 2016). Accumulation of pri-microRNAs and corresponding depletion of mature microRNAs (miR-206, miR-26a, miR-105 etc.) occur in human cancers compared to normal tissues, strongly indicating an impairment of crucial steps in microRNA biogenesis (Suzuki et al., 2009; Jiang et al., 2015; Garibaldi et al., 2016). In agreement, inhibition of microRNA biogenesis by depletion of Dicer1 and Drosha tends to enhance tumorigenesis *in vivo* (Gurtner et al., 2016).

All the hallmarks of cancer are affected by miRNA dysregulation, including self-sufficiency in growth signals (e.g., let-7 family and miR-21), insensitivity to growth inhibitory signals (e.g., miR-17-92 cluster and miR-195), limitless replicative potential (e.g., miR-372/373 cluster and miR221/222), evasion from apoptosis (e.g., miR-34a, miR-185, and miR-15/miR-16), angiogenesis (e.g., miR-210, miR-26, miR-15b, and miR-155), invasion and metastasis (e.g., miR-10b, miR-31, miR-200 family, miR-21, and miR-15b), evading immune destruction (e.g., miR-124, miR-155, and miR-17-92), reprogramming energy metabolism (e.g., miR-23a/b, miR-378, miR-143, and miR-15b), tumour-promoting inflammation (miR-23b, miR-155, and let-7d), and genomic instability (miR-21, miR-155, and miR15b) (Di Leva et al., 2014; Berindan-Neagoe et al., 2014; Shah et al., 2016).

As mentioned earlier, redundancy is an important aspect of miRNA targeting. Each miRNA can repress the expression of 100s of mRNAs, and in turn, each mRNA can be targeted by many miRNAs upon binding to its 3'UTR. In malignant tissues, 3′UTRs are frequently

shortened by alternative polyadenylation site choice which leads to an extensive loss of miRNA inhibitory activity; this increases the heterogeneity and plasticity of the tumour cell population (Sandberg et al., 2008; Mayr and Bartel, 2009). A ubiquitous feature of miRNA action in cancer is their participation in feed-forward feedback loops. For example, the NF-κB pathway transcriptionally activates miR-146a, which in turn suppresses the signalling by inhibiting the expression of two upstream regulators of the pathway, TRAF6 and IRAK1 (Taganov et al., 2006).

The ceRNA (competing endogenous RNA) hypothesis states that mRNAs, transcribed pseudogenes, long non-coding RNAs (lncRNAs), and circular RNAs (circRNAs) often share common miRNA response elements (MREs) with the target mRNAs of a miRNA and hence compete with the target mRNAs for that miRNA through MREs in a particular cell or tissue type (Dai et al., 2015). These act as natural miRNA decoys to sequester miRNAs to inhibit their interaction with the target mRNAs (Seitz, 2009; Poliseno et al., 2010; Cesana et al., 2011; Karreth et al., 2011; Tay et al., 2011). A study has demonstrated that *VAPA* and *CNOT6L*, two ceRNAs, have the similar expression profiles as that of *PTEN* and are regulated by the same set of miRNAs, and the knockdown of these ceRNAs led to reduced levels of *PTEN* (Tay et al., 2011). The link between *PTEN*, *VAPA*, and *CNOT6L* was abolished in cells with defective miRNA processing, indicating that the establishment of this regulatory network is dependent on the abundance of miRNAs that can bind to a specific set of mRNAs (Tay et al., 2011). Therefore, it is of utmost need to experimentally identify the functional link between the tumour and the dysregulated miRNAs.

1.13.7. Causes of miRNA dysregulation in cancer

Much like protein coding genes, miRNA genes are dysregulated by chromosomal rearrangements, genomic amplifications, deletions, or mutations. In 2004, Calin and coworkers showed that 98/186 (52.5%) miRNA genes are in genomic regions that are frequently altered in cancer (Calin et al., 2004). While 65 miRNA genes map to the loss of heterozygosity (LOH) regions (e.g., miR-15a/16-1), where a majority of the tumour suppressor genes are located, 15 miRNA genes are situated in the amplified regions (e.g., miR-17-92 cluster, miR-155), which harbour most oncogenes. The breakpoint regions and fragile sites (FRAs), common for sister-chromatid exchange, translocation, deletion, and tumour-associated viral integration, also harbour 61 miRNA genes (e.g., let-7 family members). A clear example of genetic aberration in cancer is represented by the cluster miR-15a/16-1 located on chromosome 13q14.3, the most

frequently deleted region in human CLL (Calin et al., 2002). MiR-15a and miR-16-1 were significantly downregulated in CLL patients that showed the 13q14.3 deletion, demonstrating their tumour suppressive role. The miR-15a/16-1 locus is also affected by mutations: 15% of analysed CLL patients presented a germline mutation in the primary precursor of miR-15a and miR-16-1 that reduces their accumulation (Calin et al., 2005); another point mutation, associated with low levels of both miRNAs, was identified in the 3′ flanking region of miR-16-1 in the New Zealand black mice that spontaneously develops CLL (Raveche et al., 2007). Interestingly, miR-15/16-1 cluster is duplicated and located on a different chromosome 3q25.33 (miR-15b/16-2); this redundancy could represent a safeguard mechanism against loss of the expression of the two miRNAs (Yue and Tigyi, 2010). Another genomic mechanism responsible for miRNA alteration in cancer is the altered levels or presence of mutations in the main enzymes of the miRNA biogenesis machinery, such as Dicer or Drosha. For instance, a decrease of 60% and 51% in the levels of Dicer and Drosha mRNAs, respectively, have been identified in 39% of the patients with ovarian cancer (Merritt et al., 2008). Moreover, the Dicer gene is frequently single-copy deleted in cancer, suggesting that it is a haplo-insufficient tumour suppressor (Kumar et al., 2009; Lambertz et al., 2010). In contrast to this view, another study reported the presence of somatic missense mutations in *DICER1*, affecting its RNase IIIb domain in nonepithelial ovarian tumours (Heravi-Moussavi et al., 2012). The recurrent and focal nature of these mutations and their restriction to nonepithelial ovarian tumours suggested a common oncogenic mechanism associated with a specific altered DICER1 function that is selected during tumour development in these cell types. In this way, a mutated *DICER1* may modify its specificity for the recognition of miRNA precursors and generate a preferential miRNA processing that will create a new miRNome in cancer (Heravi-Moussavi et al., 2012).

Cancer cells are characterised by aberrant epigenetic changes such as promoter DNA hypermethylation of tumour suppressor genes, extensive genomic DNA hypomethylation and alteration of histone modification patterns (Esteller, 2008). In fact, epigenetic modifications represent another common mechanism related to the alteration of miRNA expression in cancer (Lopez-Serra and Esteller, 2012; Fabbri et al., 2013). A majority of the reports showed silencing of tumour suppressor miRNAs by promoter DNA hypermethylation, which in turn allows overexpression of their oncogenic targets (Saito et al., 2006; Lujambio et al., 2007). For example, epigenetically silenced miR-127 is upregulated following DNA methylation and histone acetylation inhibitors treatment (Saito et al., 2006). Activation of miR-127, epigenetically repressed in 75% of primary prostate and bladder tumours, inhibits the

expression of its gene target, proto-oncogene *BCL6*, suggesting that miR-127 is a tumour suppressor (Saito et al., 2006). Similarly, the promoter hypermethylation of miR-124a in colon cancer leads to the upregulation of its oncogenic target *CDK6* (Lujambio et al., 2007).

miRNAs cannot be modulated epigenetically but, in turn, they can modify the epigenetic landmarks of the entire genome by targeting the main enzymes responsible for the epigenetic control. For example, miR-29 family represses the *de novo* DNA methyltransferase genes *DNMT3A* and *DNMT3B* in lung (Fabbri et al., 2007) and AML (Garzon et al., 2009) cancer cells, inducing a general DNA demethylation and reactivation of epigenetically silenced tumour suppressor genes with further loss of tumorigenicity. In addition, genetic deletion of one of the two loci harbouring the miR-101 gene was identified in 37.5% of clinically localized prostate cancer cells and 66.7% of metastatic disease cells (Iliopoulos et al., 2010)). Loss of the miR-101 expression during cancer progression induces an increase in histone methyltransferase EZH2 level, which contributes to the epigenetic silencing of target genes and regulates the survival and metastasis of cancer cells (Varambally et al., 2008). EZH2 is the catalytic subunit of the polycomb repressor complex 2 (PRC2), and SUZ12 is another component of this complex. The *SUZ12* gene is targeted by the miR-200 family (Iliopoulos et al., 2010). This appears to be important in the formation of cancer stem cells where loss of miR-200 increases SUZ12 levels, which epigenetically mediates a polycomb-mediated repression of the E-cadherin (*CDH1*) gene. In conclusion, epigenetic alterations of miRNA genes complemented by genetic inactivation due to mutation or deletion can partially account for the microRNA dysregulation in cancer.

Most of the miRNA genes are transcribed by the RNA polymerase II, and a myriad of Pol II-associated factors are involved in this process, allowing an elaborate transcriptional regulation of miRNA genes in cells (Lee et al., 2004). One of the first examples of cancer-associated transcriptional regulation of miRNA genes is the transcriptional activation of miR-17/92 cluster mediated by the *MYC* oncogene (O'Donnell et al., 2005). O'Donnell and collaborators (2005) showed that MYC induces the expression of the polycistronic miR-17/92 cluster, which counterbalances the apoptotic activity of E2F1, allowing MYC mediated-proliferation (O'Donnell et al., 2005). Another important transcriptional program involves miR-34 family members and the tumour suppressor protein p53 (He et al., 2007). Transcriptionally induced by p53, miR-34 recapitulates the biological effects of p53 activation including apoptosis or cellular senescence, induction of G1 arrest and loss of migration (He et al., 2007). Deletion or loss of function mutations in *TP53* gene is one of the most frequent

genetic abnormalities in cancer; ovarian cancer accounts for 60–80% of both sporadic and familial cases (Bast et al., 2009). In accordance with the loss of p53, miR-34 paralogues (viz., miR-34a, b, and c) are repressed; miR-34a expression is decreased in 100% and miR-34b*/c in 72% of epithelial ovarian cancer with *TP53* mutations (Corney et al., 2007). However, miR-34a is also downregulated in 93% of tumours with wild-type p53, indicating the presence of other mechanisms implicated in the suppression of miR-34a gene (Corney et al., 2007). It is observed that methylation and reduced copy number at the *MIR34A* gene occur in 27% and 39% of ovarian cancer tissues, respectively (Corney et al., 2007).

As described above, miRNA biogenesis is a complex multistep process that integrates several enzymes and regulatory proteins to allow a correct maturation of the primary miRNA precursors. Many components of the miRNA biogenesis machinery could either be dysregulated in tumours or mutated, contributing to a dysregulation in the miRNA expression. The cropping step operated by Drosha is an important point of regulation of miRNA levels. Doxorubicin-induction of p53 increases the expression of several mature miRNAs (e.g., miR-15, miR-16 and miR-145) that have growth-suppressive functions and are downregulated in cancer (Suzuki et al., 2009). In fact, upon treatment, p53 associates with Drosha, promoting a Drosha-mediated processing of certain tumour suppressor miRNAs in response to DNA damage. Thus, the loss of p53 in cancer reduces the levels of miRNAs that are either transcriptionally regulated by p53 or regulated by p53-induced Drosha processing (Suzuki et al., 2009). As previously discussed, processing of pre-miRNAs occurs in the cytoplasm and they need to transit from the nucleus into the cytoplasm, a process that requires the nuclear export receptor XPO5. In cancers with microsatellite instability, which account for 15% of total colon cancer, mutation of *XPO5* generates a truncated version of the protein that is unable to associate with its pre-miRNA cargo and exit the nucleus (Melo et al., 2010). Reduction in the cytoplasmic pre-miRNA pools reduced the rate of the dicing step, resulting in decreased mature miRNA levels. Interestingly, although the heterozygous *XPO5* mutation decreased accumulation of a large fraction (<20%) of detectable miRNAs, many others remained unaffected. It thus appears possible that XPO5 does not bind to pre-miRNAs indiscriminately but has certain substrate preferences, perhaps mediated by sequence or structure. Downregulated miRNAs might then be those that bind poorly to XPO5 and thus cannot compete well for export by limiting amounts of XPO5 (Melo et al., 2010). An important post-transcriptional mechanism of miRNA regulation is represented by the control of let-7 family members maturation mediated by LIN28. Despite the almost ubiquitous expression of let-7

primary precursor in normal and cancer cells, the mature miRNAs are abundantly produced exclusively in normal cells (Thomson et al., 2006). Several laboratories have identified the RNA binding protein LIN28, which interacts in the cytoplasm with pre-let-7 in order to induce terminal uridylation of miRNA precursor through the recruitment of the terminal uridyl transferase (TUTase) Zcchc11 (Heo et al., 2008; Balzeau et al., 2017). The U tail (~14 nt) that is added to the 3' end of pre-let-7 blocks Dicer processing and facilitates the decay of pre-let-7 (Heo et al., 2008). In fact, levels of LIN28 inversely correlate with mature let-7 expression during development (Wu and Belasco, 2005). Given the proto-oncogenic activity of LIN28, this pathway may restrict the expression of the tumour suppressor let-7 and contribute to its repression in cancer (Thorton and Gregory, 2012).

1.13.8. miRNAs as diagnostic markers and therapeutic targets

miRNA repertoire expressed in each cell type/ tissues/ disease condition/ is highly specific. The membrane-enclosed or lipid-bound extracellular miRNAs are remarkably stable and can be detected in virtually all body fluids, including blood, saliva, bronchial secretions, urine, liquor, and breast milk. Therefore, miRNAs can be good biomarkers. For example, several studies have shown that miR-31 is upregulated in OSCC samples and thus can be exploited as a clinical biomarker for OSCC (Liu et al., 2010; Liu et al., 2012), and methylation of miR-9 can be used as a specific and sensitive biomarker for OSCC (Minor et al., 2012). A recent study has also explored the potential of four circulating miRNAs (i.e., miR-92a-3p, miR-92b-3p, miR-320c and miR-629-5p) as non-invasive predictors for diagnosing and monitoring the progression of patients with OSCC (Piao et al., 2023). These four miRNAs were found to be significantly upregulated in the serum of OSCC patients (Piao et al., 2023).

Moreover, due to broad regulative capabilities, miRNAs also bear a high potential as therapeutic targets, at least in diseases in which a clear causal link between the pathologic state and the altered expression of specific miRNAs has been found (Kreth et al., 2018). More importantly, many miRNAs have shown promise in pre-clinical studies as prospective therapeutic targets. In this regard, miRNA mimics exploit the main advantage of endogenous miRNAs being able to target multiple mRNAs at once. miRNA mimics have the same sequence as an endogenous miRNA while the passenger strand carries a few mismatches to prevent RISC loading and potential action as an anti-microRNA (antimiR) (van Rooij and Kauppinen, 2014). Two miRNA mimics have been tested in clinical trials for cancer treatment: the miR-34 mimic MRX34 (Beg et al.,2017; Hong et al., 2020) and the miR-16 mimic MesomiR-1 (van Zandwijk

et al., 2017). AntimiRs are essentially ASOs (Antisense oligonucleotides) designed to be fully or partially complementary to an endogenous miRNA to prevent the interaction with its target genes. AntimiRs may also be referred to as 'antagomiRs' if they are conjugated to cholesterol to improve intracellular delivery (Krützfeldt et al., 2005). Two miR-122 antimiRs have been clinically tested as novel hepatitis C virus (HCV) therapeutic agents: RG-101 (N-acetylgalactosamine-conjugated ASO) and miravirsen (SPC3649; β-D-oxy-LNA) (Gebert et al., 2014). Moreover, anti-miR-92a (MRG-110) was tested for its capability to induce angiogenesis and improve wound healing (ClinicalTrials.gov Identifier: NCT03603431; https://classic.clinicaltrials.gov; Table 1), and anti-miR-21 (RG-012) was tested for its ability to prevent kidney fibrosis in patients with Alport syndrome (ClinicalTrials.gov Identifier: NCT03373786; https://classic.clinicaltrials.gov; Table 1).

MiRNA sponges are artificial transcripts that contain multiple miRNA binding sites to trap and sequester it (Ebert and Sharp, 2010). miRNA sponges may target one specific or multiple different miRNAs (Kluiver et al., 2012; Chang, 2018), for instance, to simultaneously inhibit miR-21, miR-155 and miR-221/miR-222 in tumour cells (Jung et al., 2015), or they may target a whole miRNA seed family, for instance, to sequester miR-181a, miR-181b and miR-181c (Das et al., 2017). Although this strategy has shown great utility as an experimental tool (Bernardo et al., 2018), miRNA sponges have not yet been applied in the clinic. MiRNA-masking ASOs represent an inverted approach that masks the binding site of a miRNA within the target gene (Wang, 2011) and offers a gene-specific and safe therapeutic strategy in cases where seed-family members have dual effects. Tiny 8–10-nt LNAs (Locked nucleic acids) may also be used to mask seed sequences (Murakami and Miyagishi, 2014). The 16-nt oligonucleotide-mediated masking of miR-16 binding sites in *TYRP1*, the mRNA of which acts as a miRNA sponge via three non-canonical miR-16 binding sites in its 3′UTR, resulted in the restoration of the tumour suppressive function of miR-16 in melanoma cells (Gilot et al., 2017). Despite these promising developments, miRNA-masking ASOs have not yet been used in clinics. Different miRNAs in clinical trials are tabulated in Table 1.

Many other similar studies have also emphasized on the role of miRNA in therapeutic interventions, but none of them have gone into clinical trials yet for OSCC treatment. These studies include formulations of Agomirs and Antagomirs which target specific pathology-driving genes by mimicking or binding to their upstream regulating miRNA and are assessed in pre-clinical xenograft studies. In our laboratory, xenograft studies in nude mice have shown that antagomir-155 binds to miR-155 and restores the CDC73 levels which in turn reduces cell

viability, increases apoptosis, and causes marked regression of xenografts, thus may have an important role in therapeutic intervention in OSCC (Rather et al., 2013). We have also observed a similar therapeutic potential of miR-130a antagomir in OSCC which regulates TSC1 levels (Mallela et al., 2021).

As of now, these highly interesting approaches are still preliminary and need extensive improvement. All these studies regarding the prospective role of miRNA as a therapeutic target in OSCC provided us with the impetus to study the role of miRNAs in OSCC in the present study.

1.13.9. MiRNA delivery systems

There are different ways to deliver miRNA mimics and analogues either in the local or systemic system for restorative purposes. Nonviral vectors, such as cationic polymers (Gomes et al., 2013; Hu et al., 2013), dendrimers (Conde et al., 2016), liposomes (Karlsen et al., 2013; Endo-Takahashi et al., 2014), and inorganic particles (Hao et al., 2011; Ghosh et al., 2013) as well as miRNA-inhibitors in the form of ASO/miRNA mimics, have been successfully explored in the field of miRNA therapeutics. Of late, nanoparticle-based conveyance of miRNAs has been proposed as a promising methodology in the treatment of squamous cell carcinoma of the oral cavity (Piao et al., 2012). Tumour suppressor miR-107 delivery using cationic lipid nanoparticles demonstrated decreased cell proliferation *in vitro* and retarded tumour growth *in vivo* (Piao et al., 2012). Liposomal delivery of miR-138 in OSCC successfully inhibited proliferation, migration, and invasion of OSCC cell lines *in vitro* (Zhang et al., 2017). However, poor stability in serum and high toxicity restrict its use *in vivo* (Xue et al., 2015). Exosome-mediated miRNA delivery is protected from enzymatic degradation and found to stably exist in the circulation (Li Y et al., 2015). Recently, miR-138-rich-γδ T cell-derived extracellular vesicles (γδTDEs) demonstrated an antiproliferative effect *in vitro* and *in vivo* with synergistic anti-tumoral and immunostimulatory effects on T cells (Li et al., 2019). Further, lentivirus-mediated delivery of miR-9 and miR-381-3p demonstrated anti-tumour effects in OSCC cell lines as well as *in vivo* mouse models (Yu et al., 2014; Yang et al., 2017). In addition to delivery vehicles, miRNA inhibitors like anti-sense oligonucleotides, miRNA sponges or miRNA mimics have gained interest as therapeutic approaches. miR-21 inhibition using ASO or restoration of miR-99a using miRNA-mimic has been shown to have an anti-tumorigenic effect in OSCC cells (Li et al., 2009; Kawakita et al., 2014). A recent preclinical study using LNA-miR-361-3p demonstrated growth inhibition *in vitro* and tumour growth retardation *in vivo* of

human OSCC cells (Ogawa et al., 2020). Exogenous miR-31 contributed to immortalization of normal oral keratinocytes, indicating its role in early-stage oral carcinogenesis, which on treatment with LNA-miR-31 demonstrated an anti-proliferative effect on immortalized normal oral keratinocytes *in vitro* (Hung et al., 2014). Another mode of delivery is using circRNAs which act like sponges. CircRNA is a type of noncoding RNA, having a covalently closed loop, without a 5′cap or a 3′poly (A) tail, which account for its stability and resistance to RNA exonucleases (Chen and Yang, 2015). In a recent study, hsa_circRNA_100533 was found to act as a sponge of miR-933 and inhibit tumour growth of OSCC cells by targeting *GNAS* (Zhu et al., 2019). Similarly, circPVT1/miR–125b/*STAT3* and lncRNA-*CASC2*/miR-21/*PDCD4* axes were found to regulate oral cancer tumorigenesis (He et al., 2019).

The principal hindrance in the systemic delivery of miRNA is the activation of the immune system, leading to potential endonuclease degradation of miRNAs. At present, viral and non-viral vectors are utilized for miRNA delivery (Bakhshandeh et al., 2012). The utilization of viral vectors is constrained in view of triggering immunogenicity and restricted viral packaging capacity, thereby redirecting the focal point of investigation to non-viral vectors (Hossehnahli et al., 2018). Different non-viral vector systems have been designed, including the direct transfer using sonoporation, gene gun, magnetofection, and hydrodynamic delivery or indirect transfer using synthetic vectors like liposomes, and inorganic nanoparticles (NPs) (Yin et al., 2014). Among these techniques, the entrapment of miRNAs in nanoparticles seems to be practical in terms of protection from endonucleases, non-specific interactions, and immune detection. Furthermore, the use of chemical modification of oligonucleotides remains ill-defined since it is not cost effective and the impact on the immune response and systemic toxicity is unclear. Chemical modifications have proved to enhance the stability and activity of siRNAs and ASOs, and thus might be useful to augment the stability and effectiveness of miRNA mimics and anti-miRs (Bader et al., 2011). Exosomes are cell-derived membrane-bound vesicles discharged from cells, which effectively enter different cells (Kowal et al., 2014). Unlike other engineered nanoparticles, exosomes have transmembrane and membrane-bound proteins which advance endocytosis, and thus improving the delivery of their internal content (e.g., miRNAs) (Vader et al., 2016). Further, despite the preclinical success of ASO/miRNA mimics as therapeutic agents, they still warrant further validation to understand the toxic effects on cells, specificity, and stability of the hybridization between the oligonucleotide sequence and the target mRNA.

1.13.10. Role of dysregulated miRNAs in OSCC pathogenesis

1.13.10.1. Oncomirs

Several miRNAs have been identified to be upregulated in OSCC. One of the well-studied miRNAs is miR-21, which is found to be significantly overexpressed in oral tumours and correlates with poor survival in patients (Wang et al., 2015). Premalignant lesions with a high risk of MT (malignant transformation) can be identified by a concordant increase in miR-181b, miR-345, and miR-21 levels. The upregulation of these miRNAs is associated with lesion severity from progressive dysplasia to OSCC (Singh et al., 2018; Cervigne et al., 2009; Mehdipour et al., 2018). Additionally, lncRNAs *CASC2* and *GAS5* regulate cell proliferation and EMT by sponging miR-21 and thereby relieving the inhibition of its downstream targets *PDCD4* and *PTEN* respectively (Pan et al., 2019; Zeng et al., 2019). miR-21 drives cisplatin-resistance in OSCC cells via inhibiting *PTEN*, *PDCD4* and *MYCN* (Ren et al., 2014; Zheng et al., 2016; Liu et al., 2017). STAT3 is a transcriptional activator of miR-21 and following treatment with STAT3 inhibitors, WP1066 and HJC0152, anti-tumour effects are exerted in OSCC cells due to reduced miR-21 levels (Zhou et al., 2014; Wang et al., 2017). Anti-sense (AS)-miR-21 has also shown therapeutic potential in OSCC cells by inhibiting proliferation and promoting apoptosis *in vitro* and *in vivo* (Wang et al., 2015).

miR-27a plays an oncogenic role in several cancers including OSCC (Venkatesh et al., 2013). It downregulates the tumour suppressor microcephalin 1 (*MCPH1*) by targeting its 3′UTR to promote carcinogenesis (Venkatesh et al., 2013). Apart from its role in tumorigenesis, miR-27a affects drug response and patient prognosis (Li X et al., 2019).

Another miRNA that is markedly up-regulated in oral cancer tissues and plasma is miR-31 relative to oral premalignant lesions and normal tissue (Mehdipour et al., 2018). It regulates *FIH*, *ACOX1*, *SIRT3*, the lipid metabolome, *EP1-ERK-MMP9* signalling, prostaglandin E2, induction of ROS and disruption of mitochondrial activity to promote carcinogenesis (Liu et al., 2010; Kao et al., 2016; Mehdipour et al., 2018; Lai et al., 2018; Kao et al., 2019). miR-31 is associated with poor prognosis in HNSCC patients (Dioguardi et al., 2022). In addition, circular RNA (circRNA) circ_0000140 was found to exert tumour suppressive effect *in vitro* and *in vivo* via miR-31/*LATS2* axis, by inhibiting Hippo signalling pathway (Peng et al., 2020). Further, miR-93-5p upregulation enhanced EMT in OSCC cells and was associated with poor prognosis and post-radiation treatment response in patients (Li G et al., 2015; Greither et al., 2017; Zhang et al., 2020). MiR-134 upregulation in OSCC was reflected in cellular

transformation, E-cadherin downregulation, and poor survival in OSCC patients (Liu et al., 2014; Peng et al., 2018).

Another well studied miRNA, miR-155 was up-regulated in OSCC and is known to target the 3′UTRs of *p27kip1* (*CDKN1B*), a cyclin-dependent kinase inhibitor (*CDKI*), AT-Rich Interaction Domain 2 (*ARID2*), and cell division cycle 73 (*CDC73*) (Rather et al., 2013; Fu et al., 2017; Wu et al., 2020). Overexpression of miR-155 was associated with tobacco chewing habit, and positively correlated with tumour size, TNM stage, histological grade, and lymph node metastasis in OSCC (Wu et al., 2020). miR-155 promotes cancer invasion through EMT by inhibiting the tumour suppressor *SOCS1*, a negative feedback regulator of the JAK/STAT3 pathway (Baba et al., 2016). Additionally, exosome-mediated miR-155 shuttling was observed in cisplatin-resistant oral cancer cells and acquisition of EMT phenotype in cisplatin-sensitive cells (Kirave et al., 2020). In contradiction, Bersani et al. (2018) showed decreased miR-155 expression in three subgroups of tonsillar squamous cell carcinoma (TSCC) and base of tongue cancer (BOTSCC), HPV^{+} TSCC/BOTSCC and HPV^{-} TSCC/ BOTSCC compared to control tissue, suggesting positive correlation with patient survival. miR-196a and miR-196b were up-regulated in oral premalignant lesions (5.9- and 14.8-fold, respectively) and OSCC (9.3- and 17.0-fold, respectively) as compared to controls, indicating their utility as potential biomarkers to discriminate between normal tissue and oral premalignant lesion (Lu et al., 2015). Oncomir miR-211 targets *TGFβRII* and *TCF12* to promote proliferation and invasion in OSCC (Chu et al., 2013). In addition, a negative correlation was observed between lncRNA-*KCNQ1OT1* and miR-211-5p in context of oncogenic transformation and cisplatin resistance in tongue cancer mediated by Ezrin/Fak/Src signalling (Zhang S et al., 2018). The Wnt signalling pathway dysregulation has also been associated with chemoresistance in oral cancer cells (Aminuddin et al., 2016; Javed et al., 2019). miR-218 downregulates *PPP2R5A*, a repressor of Wnt signalling pathway, thereby hyperactivating it to confer cisplatin resistance in OSCC cells (Zhuang et al., 2017). Another study demonstrated chemosensitivity to cisplatin (CDDP) in OSCC cells with low expression of miR-222, further suggesting a combinatorial approach with antisense-miR-222 and cisplatin to be more efficacious (Jiang et al., 2014).

miR-371, miR-372, and miR-373 (miR-371–373 gene cluster) located on chromosome 19q13.4 are specifically expressed in human embryonic stem cells (ESCs) and involved in maintenance of the stemness, possibly via modulation of the Wnt/β- catenin signalling pathway (Zhou et al., 2012). miR-372 and miR-373 were found to be upregulated in several cancers in response to hypoxia through HIF1α and TWIST1 (Loayza et al., 2010). Further, miR-

372/*PCNA* and miR-373/*SPOP* axes were found to promote proliferation and invasion in OSCC (Wang et al., 2019; Zhang et al., 2019). In clinical studies, miR-372 and miR-373 overexpression were found to be associated with nodal metastasis, lymphovascular invasion, and poor survival in OSCC patients (Tu et al., 2015; Troiano et al., 2018). Another report demonstrated upregulation of mesenchymal markers vimentin and N-cadherin by miR-373-3p, with downregulation of epithelial markers E-cadherin and CK18 and activation of the Wnt/ β-catenin pathway by directly targeting Dickkopf-1 (*DKK1*), suggesting the role of miR-373-3p in EMT phenotype (Weng et al., 2017). Additionally, miR-372 mediated chemoresistance in OSCC cells via the ZBTB7A-TRAIL-R2 axis (Yeh et al., 2020). Notably, miR-146 (miR-146a-3p, miR-146a-5p, miR-146b-3p and miR-146b-5p) has been identified predominantly as an oncomiR in context of OSCC which targets *IRAK1*, *TRAF6* and *NUMB* genes to aid in tumorigenesis and regulates the CD24/AKT/β-catenin axis to promote self-renewal capacity of oral cancer stem cells (Hung et al., 2013). While a few other contradicting reports in oral cancer have identified miR-146a (/b) as a tumour suppressor (Shi et al., 2015), its role in carcinogenesis is controversial, owing to its oncogenic or tumour suppressive properties in many other malignancies. Specifically in cancers of oral cavity, breast, colorectal, gastric, hepatocellular and lung, its role is inconclusive (Iacona et al., 2019).

1.13.10.2. Tumour suppressor miRNAs

Tumour suppressor miRNAs prevent cancer initiation through the modulation of oncoprotein levels. A prevalent mechanism of silencing/downregulating tumour suppressor miRNAs (e.g., miR-34b, miR-137, miR-193a and miR-203) is via DNA hypermethylation of the CpG sites in the CpG islands (Kozaki et al., 2008). This is exemplified via downregulation of tumour suppressors miR-137 and miR-193a, causing reduction in cell growth by regulating cyclin-dependent kinase 6 (*CDK6*) and E2F transcription factor 6 (*E2F6*), respectively (Kozaki et al., 2008). Further, miR-137 downregulation with promoter methylation was observed in patients with oral lichen planus (OLP), suggesting its role in malignant transformation (Dang et al., 2013; Ashbari et al., 2018a; Ashbari et al., 2018b). *MiR137* promoter methylation was also observed in tumour tissue and oral rinses and correlated with overall survival (Langevin et al., 2010; Langevin et al., 2011). Several miRNAs are downregulated in oral cancer and may act as tumour suppressors. The let-7 family members let-7a, let-7d, and let-7f are downregulated in 95%, 84% and 87% oral cancers with strong tendency for co-occurrence, respectively. Let-7f and let-7d levels can discriminate between G1 and G2 grades of OSCC, let-7d levels discriminate between males and females, and let-7a and let-7f levels discriminate

between tumours of the tongue and gingivo-buccal complex (Manikandan et al., 2016). The let-7a/STAT3 axis was found to be involved in niclosamide sensitivity in OSCC cells by promoting apoptosis and inhibiting cell-cycle related proteins, migration, and invasion (Li X et al., 2017). Additionally in retrospective studies, miR-99a-5p was found to be downregulated with significant up-regulation of genes regulating the PI3K-AKT signalling pathway as determined by the Gene Expression Profiling Interactive Analysis (GEPIA) (Lau et al., 2017; Chen et al., 2018).Tumour suppressor miR-139-5p has been identified as a potential salivary biomarker for tongue cancer with discriminatory potential between pre-operative and post-operative tongue squamous cell carcinoma (TSCC) patients (Duz et al., 2016; Chen et al., 2017; Yan et al., 2017). Decreased miR-139-5p was found to promote proliferation and invasion via WNT responsive elements MYC, CCND1 and BCL2, and target *CXCR4* in preclinical models (Jiang et al., 2020). It was also associated with poor survival in clinical specimens (Jiang et al., 2020). miR-143-3p was identified as a tumour suppressive microRNA in OSCC patients as well as OSCC cell lines, playing a crucial role in tumour cell invasion and migration (Sun et al., 2017; Irani et al., 2019; Mesgarzadeh et al., 2019; Duan et al., 2020). miR-184 has been found to be downregulated in OSCC tumour samples (Santhi et al., 2013). Additionally, lncRNA-*UCA1* was found to facilitate proliferation and cisplatin chemo-resistance via sponging miR-184 in OSCC cells (Fang et al., 2017). However, one contradictory report indicated the role of miR-184 in anti-apoptotic and pro-proliferative processes of tongue SCC (Wong et al., 2009). Literature suggests the downregulation of miR-375 in oral cancer and its utility as a biomarker in tongue cancer, malignant transformation of oral premalignant lesions, and poor prognosis of oral cancer patients (Shi et al., 2015; Zhang et al., 2017; Cao et al., 2017). Further, miR-375 has been found to mediate radio-sensitization of OSCC cells (Jia et al., 2017; Zhang et al., 2017).

Targeting several genes significant to oral malignancy is seen as an effective tool of therapeutic miRNA mimics. Therapeutic miRNA mimics form the basis of miRNA replacement therapy which entails the restoration of endogenously downregulated tumour suppressor miRNAs (Barger and Nana-Sinkam, 2015). miRNA restoration is best exemplified by let-7 miRNA, a developmental switch in *C. elegans*. The exogenous expression of let-7 obstructs the proliferation of malignant cells *in vitro* and reduces tumour growth *in vivo* (Lee et al., 2016). Another model example is miR-34a; wherein, a lipid-based formulation of synthetic miR-34a was systemically delivered to lung tumours in mice to downregulate its direct targets and retard tumour growth (Wiggins et al., 2010). Subsequently, this investigation recommended an

effective delivery mechanism for miR-34a and the specific anti-oncogenic action of miR-34a in tumour cells (Wiggins et al., 2010). While miRNA replacement therapy has been investigated in several preliminary preclinical studies with promising outcomes, the translation to the clinic has failed to advance (Hosseinahli et al., 2018).

1.13.11. Tumour suppressor miRNAs silenced by DNA hypermethylation in OSCC

Smoking and alcohol consumption have been reported to directly alter the DNA methylation status in OSCC tissues (Gasche and Goel, 2012). Gasche et al. (2011) have also reported the involvement of interleukin-6 in inducing chronic inflammation and promoting oral tumorigenesis by altering DNA methylation in cancer cells. Piyathilake et al. (2005) reported that DNA extracted from OSCC tissues and premalignant lesions exhibits more frequent and higher levels of DNA methylation compared to the DNA extracted from healthy or corresponding normal tissues adjacent to the tumour. Also, of the various mechanisms reported to be involved in miRNA deregulation such as loss or mutation of miRNA-encoding genes, defective biogenesis pathway, hypermethylation-mediated silencing of miRNA-encoding genes and/or histone modifications, epigenetic silencing through methylation of the promoter regions has emerged as the major mechanism of silencing/downregulation of tumour suppressor miRNAs (Kozaki et al., 2008; Kunej et al., 2011). An integrative study aimed at identifying epigenetically regulated miRNAs specific for cancer types undertaken by Kunej et al. (2011) revealed that compared to protein-coding genes, miRNA genes silenced in tumours showed an order of magnitude higher methylation frequency (11.6%; 122/1,048 known miRNAs) and that nearly half (45%; 55/122) of epigenetically regulated miRNAs are associated with different cancer types, but the rest 55% (67/122) miRNAs are present in only one cancer type, thereby representing cancer-specific biomarker potential. The data integration also revealed the presence of miRNA epigenomic hot spots on the chromosomes 1q, 7q, 11q, 14q, and 19q, and the CpG island analysis of corresponding miRNA precursors (pre-miRNAs) revealed that 20% (26/133) of epigenetically regulated miRNAs had a CpG island within the range of 5 kb upstream, among them, 14% (19/133) of miRNAs resided within the CpG island (Kunej et al., 2011). Kozaki et al. (2008) also reported that of the 148 miRNAs whose expression was tested by Taqman MicroRNA Assays Human Panel Early Access kit (Applied Biosystems, Massachusetts, USA), 54 (36.5%) miRNAs were frequently downregulated in 18 OSCC cell lines that were analysed compared to an immortalized oral keratinocyte cell line RT7. Also, in the same study, DNA methylation-mediated silencing was identified as the cause for the downregulation of four miRNAs, namely, miR-34b, miR-137, miR-193a, and miR-203

(Kozaki et al., 2008). In a case-control study by Langevin et al. (2010), hypermethylation of the *MIR137* promoter was relatively frequently detected in oral rinses of HNSCC patients and was shown to be associated with female gender and inversely associated with body mass index (BMI). *MIR137* promoter methylation was also found to be associated with poorer overall survival in patients with squamous cell carcinoma of the head and neck (Langevin et al., 2011).

The above observations underscore the importance of DNA methylation in the silencing of tumour suppressor miRNAs in OSCC. Thus, we set up the experimental design of the present study to identify, validate and investigate a novel putative tumour suppressor miRNA, silenced by DNA hypermethylation in OSCC pathogenesis.

Table 1: Major miRNA-based therapeutics in clinical trials*.

Therapeutic molecule	Disease	Target miRNA	Biotechnology or Biopharmaceutical Company	Stage of Development (Clinical trial/preclinical trial)	ClinicalTrials.gov Identifier
Miravirsen (SPC3649)	For the treatment of hepatitis C virus (HCV) infection	miR-122	SantarisPharma	Phase II clinical trials completed	NCT01200420, NCT01872936, NCT02031133,NCT02508090
MRX34	For the treatment of different types of cancers	miR-34a	miRNATherapeutics	Withdrawn during phase 1 clinical trial	NCT02862145
RG-101	For the treatment viral effect	miR-122	Regulus Therapeutics	Phase 1B clinical trial-terminated	-
RG-012	To prevent alport nephropathy	miRNA-21	Regulus therapeutics (with the strategic alliance with Genzyme)	Phase 1 completed	NCT03373786
RGLS4326	For the treatment of polycystic kidney disease (PKD)	miR-17	Regulus Therapeutics	Phase 1B completed	NCT04536688
MGN-1374	For the treatment of post-myocardial infarction	miRNA-15 and miR-195	miRagen therapeutics	Preclinical stage	-
MGN-2677	For the treatment of vascular disease	miR-143/145	miRagen therapeutics	Preclinical stage	-
MGN-4220	For the treatment of cardiac fibrosis	miR-29	miRagen therapeutics	Preclinical stage	-
MGN-4893	For the treatment of disorders like abnormal red blood cell production	miR-451	miRagen therapeutics.	Preclinical stage	-
MGN-5804	For the treatment of cardiometabolic disease	miR-378	miRagen therapeutics	Preclinical stage	-
MGN-6114	For the treatment of peripheral arterial disease	miR-92	miRagen therapeutics	Preclinical stage	-
MGN-9103	For the treatment of chronic heart failure	miR-208	miRagen therapeutics	Preclinical stage	-
Cobomarsen (MRG-106)	For the treatment of cutaneous T-cell lymphoma (CTCL)	miR-155	miRagen therapeutics	Phase-I clinical trial terminated	NCT02580552
MRG-107	For the treatment of amyotrophic lateral sclerosis (ALS)	miR-155	miRagen therapeutics	Completed preclinical trial and entering in clinical trial	-
MRG-110	To control ischemia and target blood vessel growth	miR-92a	miRagen therapeutics	Phase-I clinical trial completed	NCT03603431
Remlarsen (MRG-201)	For the treatment of different type of fibrosis such as cutaneous fibrosis, idiopathic pulmonary fibrosis etc.	miR-29	miRagen therapeutics	Phase II clinical trial completed	NCT03601052

*https://classic.clinicaltrials.gov Chakraborty et al., 2021.

RATIONALE AND OBJECTIVES OF THE STUDY

2. Rationale and Objectives of the Study

Recent investigations have emphasized and established the role of epigenetic modification and dysregulation in cancer development and progression. DNA methylation is one of the most studied epigenetic mechanisms in gene silencing and chromatin remodelling. Upon comparing OSCC patient samples with their matched normal oral tissue samples, distinct epigenetic signatures have been unearthed, which include genome-wide hypomethylation and promoter hypermethylation (Irimie et al., 2018). Promoter hypermethylation in OSCC involves methylated CpG sites in the promoter regions of tumour suppressor genes that impede access to transcription factors and implicitly silence/downregulate gene expression (Irimie et al., 2018). Concurrently, it has been shown that an astonishingly high proportion of miRNA genes are embedded in CpG islands susceptible to methylation (Morales et al., 2017). Consequently, human miRNA gene methylation frequency is nearly one order of magnitude higher than the protein-encoding genes (Morales et al., 2017). The first large-scale microRNA expression profiling revealed that 54/148 miRNAs were downregulated across 18 OSCC cell lines compared to an immortalized oral keratinocyte cell line R17 (Kozaki et al., 2008). DNA methylation-mediated silencing was identified as the cause for the downregulation of four miRNAs, namely, miR-34b, miR-137, miR-193a, and miR-203 (Kozaki et al., 2008).

The two prevalent methods employed in detecting the epigenetic status of miRNAs comprise strategies of pharmacologic and genetic unmasking. Most of the studies rely upon ways of pharmacologic unmasking for identifying epigenetically inactivated miRNAs, where they compare the miRNA expression profiles of the treated and untreated cells by pharmacologic drugs (Kunej et al., 2011). Chromatin-modifying agents or epigenetic drugs such as DNA hypomethylation agents (e.g., DNA methyltransferase inhibitor like 5-Azacytidine), histone deacetylase (HDAC) inhibitors [e.g., 4-phenyl butyric acid (PBA) and trichostatin A (TSA)] and in most cases a combination of both are used to treat cancer cell lines (Kunej et al., 2011). Following the treatment, a microarray-based approach is adopted to identify differentially expressed miRNAs between untreated and drug-treated cells. The miRNAs upregulated following the treatment are then validated using RT-qPCR (Kunej et al., 2011). Genetic unmasking strategies are less frequently used wherein double knockout (DKO) for DNA methyltransferases *DNMT1* and *DNMT3B* are generated and the miRNA expression profiles of the DKO and wild-type cells are compared thereafter (Kunej et al., 2011).

The pharmacologic drug 5-Azacytidine is a cytidine analogue, which incorporates into DNA and acts as a suicide substrate by covalent coupling with DNMT1 (DNA methyltransferase I). It causes unbiased global hypomethylation of the genome. It is widely used to reactivate tumour suppressor genes by following DNA hypermethylation. Therefore, by comparing the miRNA expression profiles between 5-Azacytidine and vehicle control (DMSO) treated OSCC cells by microRNA microarray, one should be able to identify miRNAs that are otherwise silenced by DNA hypermethylation but are reactivated upon 5-Azacytidine treatment. RT-qPCR can then validate the upregulated miRNAs, and their tumour suppressive properties, if any, can be explored by determining their role in regulating cell proliferation, apoptosis, anchorage-independent growth, tumour growth, and maintenance.

Thus, to identify epigenetically silenced/downregulated tumour suppressor microRNAs, cells from an OSCC cell line SCC131 were treated previously in our laboratory with 5-Azacytidine and vehicle control for five days (our unpublished laboratory data). Total RNA samples were then isolated using a mirVana™ miRNA isolation kit (cat#AM1561; Ambion, Austin, TX, USA), which enriches explicitly for small RNA (<200 nucleotides) to ensure enhanced sensitivity in microRNA microarray analysis. To validate the efficacy of 5-Azacytidine treatment of SCC131 cells, the expression of an epigenetically silenced tumour suppressor gene *MCPH1* reported earlier to show upregulation upon 5-Azacytidine treatment was assessed by RT-qPCR (Figure 1; Venkatesh et al., 2013). The results corroborated with the previous report (Venkatesh et al., 2013), thereby validating the efficacy of the 5-Azacytidine treatment. Following this, the total RNA samples underwent microRNA microarray analysis for investigating the expression of 2,549 mature miRNAs using SurePrint G3 8x60K Human miRNA Microarray platform (AMADID 70156; Agilent Technologies, Santa Clara, CA, USA). MicroRNA microarray data analysis subsequently showed that 78 miRNAs were differentially expressed in 5-Azacytidine-treated cells compared to those treated with the vehicle control; 50/78 miRNAs were found to be upregulated (cut-off: fold change ≥ 0.6 and mean-fold expression ≥ 0.8), and 28/78 miRNAs (cut-off: fold change ≤ -0.6 and mean fold expression ≤ -0.8) were found to be downregulated (Figure 2; Table 2; our unpublished laboratory data). MiR-885-5p was the most upregulated miRNA showing a mean fold expression of 6.21, while miR-5684 was the most downregulated miRNA with a mean fold expression of -5.57 following the 5-Azacytidine treatment of cells (Table 2). Since there are few reports exploring the functional aspects of miR-617 (Ge et al., 2020; Liu et al., 2021; Zhao and Liu, 2021), which is one of the 50 upregulated microRNAs (Table 2; a mean fold

expression of 3.5), it was chosen for further analysis during the present study. Therefore, the present study has focused on exploring, validating, and investigating the tumour suppressor properties of miR-617 in OSCC pathogenesis by identifying its downstream gene target and understanding the underlying mechanism for its upregulation following the 5-Azacytidine treatment. The specific objectives of the present study are as follows.

1. To validate the upregulation of miR-617 and elucidate its regulatory mechanism following 5-Azacytidine treatment of SCC131 cells.
2. To assess the role of miR-617 in cell proliferation of OSCC cells.
3. To identify and confirm a downstream gene target of miR-617 in OSCC pathogenesis.
4. To investigate the biological relevance of the interaction between miR-617 and its gene target in different human cell lines and OSCC patient samples.
5. To elucidate the effect of miR-617-mediated regulation of its gene target on the hallmarks of cancer.
6. To study the downstream effectors of miR-617 and its gene target.
7. To explore the therapeutic potential of miR-617 through OSCC xenograft studies in nude mice.

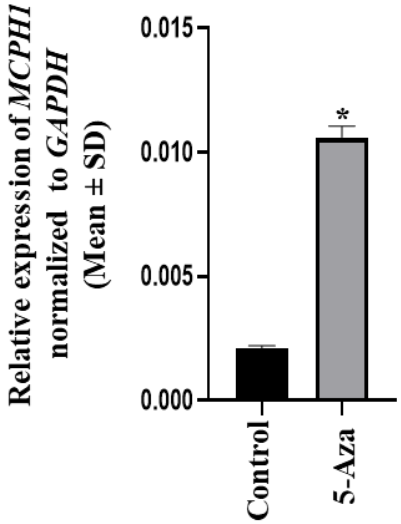

Figure 1: Validation of 5-Azacytidine treatment of SCC131 cells. The expression of the tumor suppressor gene *MCPH1* was found to be upregulated following 5-Azacytidine treatment of SCC131 cells by RT-qPCR. Each bar for RT-qPCR is an average of 2 technical replicates. *Abbreviation:* 5-Aza, 5-Azacytidine; and *, $p<0.05$.

A

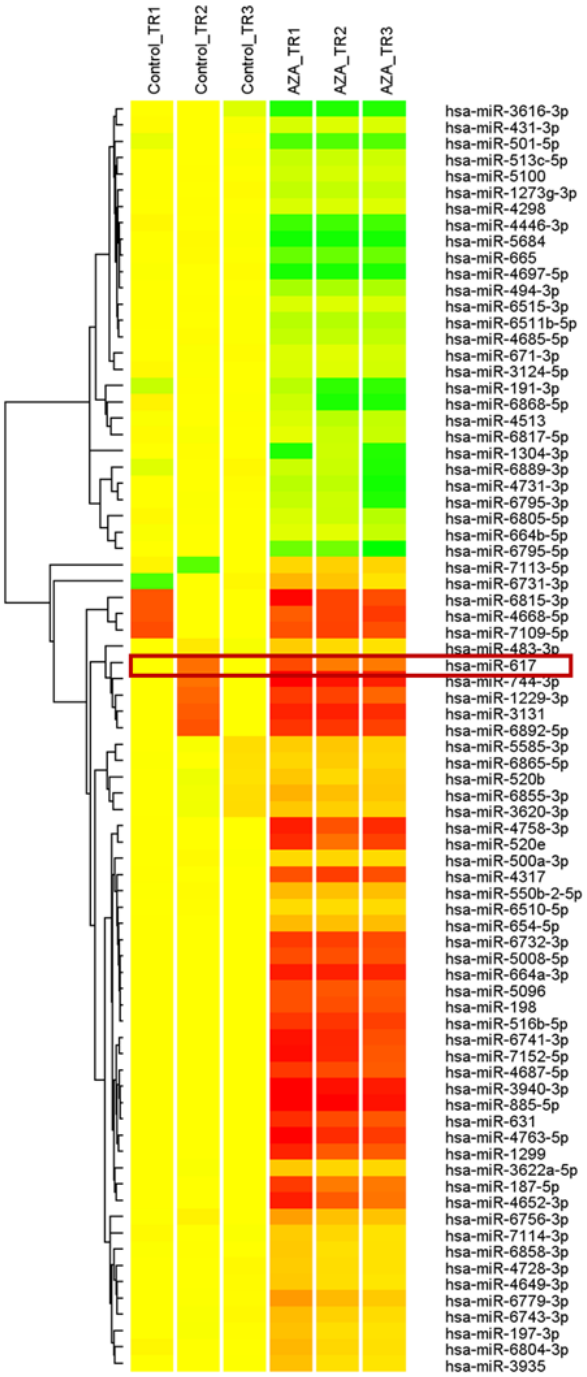

B

miRNA	Fold mean expression
miR-617	3.5

Figure 2. MicroRNA microarray analysis of 5-Azacytidine and control treated SCC131 cells. (A) A heatmap depicting the upregulation of 50 miRNAs and downregulation of 28 miRNAs expression following 5-Azacytidine treatment of SCC131 cells. Control_TR (1-3) represents technical replicates of RNA from cells treated with DMSO. AZA_TR (1-3) represents technical replicates of RNA from cells treated with 5-Azacytidine. The expression profile of miR-617 is also highlighted. **(B)** miR-617 showed fold mean expression change by the microRNA microarray analysis. *Abbreviation:* AZA, 5-Azacytidine.

Table 2: List of differentially regulated microRNAs identified by microRNA microarray analysis of 5-Azacytidine- and DMSO-treated SCC131 cells.

List of 50 upregulated microRNAs

Sl. No	Name of the microRNA	Mean fold expression	P-Value
1	miR-5008-5p	4.16	0.0000
2	miR-198	4.11	0.0000
3	miR-664a-3p	5.26	0.0000
4	miR-5096	4.00	0.0000
5	miR-516b-5p	4.67	0.0000
6	miR-654-5p	1.56	0.0000
7	miR-6510-5p	0.84	0.0000
8	miR-6732-3p	4.48	0.0000
9	miR-4317	4.27	0.0000
10	miR-550b-2-5p	1.52	0.0000
11	miR-4687-5p	4.28	0.0001
12	miR-3940-3p	5.82	0.0001
13	miR-885-5p	6.21	0.0001
14	miR-631	4.39	0.0001
15	miR-500a-3p	0.89	0.0001
16	miR-4758-3p	4.81	0.0002
17	miR-4763-5p	5.26	0.0003
18	miR-6741-3p	4.96	0.0003
19	miR-1299	4.31	0.0006
20	miR-7152-5p	4.93	0.0007
21	miR-3622a-5p	1.06	0.0007
22	miR-520e	4.27	0.0010
23	miR-187-5p	3.63	0.0019
24	miR-4652-3p	4.16	0.0024
25	miR-6756-3p	1.71	0.0054
26	miR-7114-3p	0.93	0.0058
27	miR-4728-3p	0.89	0.0063
28	miR-6779-3p	1.74	0.0066
29	miR-6743-3p	1.16	0.0070
28	miR-6779-3p	1.74	0.0066
29	miR-6743-3p	1.16	0.0070

Sl. No	Name of the miRNA	Mean fold expression	P-Value
30	miR-6858-3p	0.90	0.0098
31	miR-4649-3p	0.88	0.0129
32	miR-744-3p	5.59	0.0162
33	miR-197-3p	0.97	0.0165
34	miR-6855-3p	1.55	0.0181
35	miR-6804-3p	1.12	0.0230
36	miR-3935	0.94	0.0250
37	miR-5585-3p	1.20	0.0314
38	miR-520b	1.16	0.0347
39	miR-6865-5p	1.06	0.0355
40	miR-483-3p	0.90	0.0358
41	miR-3131	5.16	0.0395
42	miR-3620-3p	1.15	0.0488
43	miR-6815-3p	4.83	0.0716
44	miR-1229-3p	4.24	0.0722
45	miR-6892-5p	4.65	0.0735
46	miR-4668-5p	4.29	0.0940
47	miR-7109-5p	4.23	0.1159
48	miR-617	3.50	0.1182
49	miR-6731-3p	1.24	0.1499
50	miR-7113-5p	1.00	0.1733

List of 28 downregulated microRNAs

Sl. No	Name of the microRNA	Mean fold expression	P-Value
1	miR-4697-5p	-5.41	0.0000
2	miR-5684	-5.57	0.0000
3	miR-665	-3.55	0.0000
4	miR-494-3p	-2.01	0.0000
5	miR-4446-3p	-4.51	0.0000
6	miR-6511b-5p	-1.73	0.0000
7	miR-4685-5p	-1.43	0.0000
8	miR-1273g-3p	-1.40	0.0000
9	miR-4298	-0.85	0.0000
10	miR-6515-3p	-0.86	0.0000
11	miR-501-5p	-4.10	0.0000
12	miR-513c-5p	-1.26	0.0000
13	miR-3616-3p	-5.23	0.0000
14	miR-5100	-1.00	0.0001
15	miR-431-3p	-0.86	0.0003
16	miR-671-3p	-0.83	0.0007
17	miR-3124-5p	-0.90	0.0009
18	miR-4513	-1.31	0.0050
19	miR-6805-5p	-1.28	0.0059
20	miR-6817-5p	-1.05	0.0109
21	miR-664b-5p	-0.91	0.0201
22	miR-6795-5p	-4.70	0.0240
23	miR-6868-5p	-3.95	0.0443
24	miR-1304-3p	-3.90	0.0450
25	miR-191-3p	-3.79	0.0464
26	miR-4731-3p	-2.92	0.0939
27	miR-6795-3p	-2.62	0.1222
28	miR-6889-3p	-2.60	0.1578

MATERIALS AND METHODS

3. Methods and Materials

3.1. Bacterial cell culture

3.1.1. General procedures

The bacterial cell culture work was done under sterile conditions inside a laminar hood (Lab line Instruments, Mumbai, India). All the glass- and plastic-wares were autoclaved prior to their usage. The culture medium was sterilised by autoclaving, stored at 4°C and pre-warmed to room temperature (RT) before use. The hood was cleaned with 70% alcohol before and after every use.

3.1.2. Bacterial strains

The DH5α strain of *E.coli* (*Escherichia coli*) is genetically engineered to maximize transformation efficiency; therefore competent cells were prepared with it for subsequent use in cloning procedures. It harbours recA1$^-$ mutation which inhibits undesirable restriction of cloned DNA or its recombination with the host chromosomal DNA. Moreover, endA1$^-$ mutation leads to improved yield and quality of plasmid DNA isolated from this strain after transformation. It contains *lac*ZΔM15 mutation in the genomic copy of *lacZ* gene which permits α-complementation with the amino terminus of β-galactosidase encoded by appropriate vectors, thus providing the useful feature of blue-white colony selection for the screening of recombinants. The genotype of the strain is as follows.

DH5α strain- F$^-$φ80*lac*ZΔM15Δ (*lac*ZYA-*arg*F) U169 *rec*A1 *end*A1 *hsd*R17 (r_K^-, m_K^+) *pho*A *sup*E44 λ$^-$*thi*-1 *gyr*A96 *rel*A1.

3.1.3. Preparation of bacterial culture media

Unless commercially obtained in sterile condition, all media, solutions, and supplements used in bacterial culture work were sterilized by autoclaving. Lysogeny broth (LB) (2 g/100 mL) (HiMedia, Mumbai, India) was used for liquid bacterial culture. LB agar plates were prepared using LB and 1.5% (w/v) bacteriological agar (HiMedia, Mumbai, India). The molten LB agar was cooled to ~50°C before adding ampicillin (SRL, India) at a final concentration of 100 μg/mL. The LB agar was then poured in sterile 90 mm bacteriological plates in a laminar hood and allowed to solidify prior to use.

3.1.4. Preparation of glycerol stocks

Glycerol [50% (v/v) glycerol in Elix® water] was prepared and sterilized by autoclaving. Chilled 50% glycerol was used for preparing glycerol stocks from bacterial cultures grown for 16 hr at 37°C. A 500 µL aliquot of freshly grown culture (inoculated from a single isolated colony) was mixed with 200 µL of 50% glycerol. The glycerol stock was kept at RT for 30 min and then stored at -80°C for long term storage.

3.1.5. Preparation of competent cells by $CaCl_2$ method

To prepare competent cells, the DH5α strain of *E. coli* was streaked on a LB agar plate and incubated overnight at 37°C for the colonies to develop. A single bacterial colony was then inoculated in 5 mL of the sterile LB in a 50 mL sterile plastic tube. The tube was incubated overnight in an incubator-shaker (37°C and 180 rpm). In a 500 mL conical flask, 100 mL of the sterile LB in a 500 mL conical flask was inoculated with 1 mL inoculum of the overnight grown culture. The flask was incubated in an incubator-shaker for 2-3 hr till the OD_{600} of the culture reached 0.4-0.6. The culture was then incubated on ice for 30 min, divided in four 50 mL sterile plastic tubes and centrifuged at 4,000 rpm for 15 min at 4°C. The supernatant was discarded, and the cell pellet was resuspended in 12.5 mL of ice-cold sterile 100 mM $CaCl_2$ (Sigma-Aldrich, St. Louis, MO, USA) in a 50 mL tube and kept on ice for 30 min. The cells were centrifuged at 4,000 rpm for 15 min at 4°C, resuspended in 700 µL of ice-cold sterile 100 mM $CaCl_2$ and incubated at 4°C for 4 hr. The competent cells were supplemented with 300 µL of 50% ice-cold glycerol and after gently mixing the contents, 100 µL aliquots of the same were made in 1.5 mL microcentrifuge tubes and stored at -80°C until future use.

3.1.6. Restriction enzyme digestion of DNA

The restriction enzyme digestion of vectors or amplified PCR products was carried out in a 20 µL reaction volume containing 0.5-1 µg of the template DNA, 1X digestion buffer, 5-10 U of the specific restriction enzyme in a 1.5 mL tube which was then incubated at 37°C for 2 hr or overnight as per requirement. For the generation of different plasmid constructs used in the study, double digestion was performed with two compatible restriction enzymes to generate cohesive ends. The details of the plasmid vectors used in this study are mentioned in Appendix VI.

3.1.7. Ligation reaction

For setting up ligation, the double-digested and gel-eluted vector and insert DNAs were used at different molar ratios depending on the size of the insert with respect to the vector. The total volume of the ligation reaction was 10 µL with 5% PEG-4000, 1X ligation buffer and 1 U of the T4 DNA ligase (Thermo Fischer Scientific, Waltham, MA, USA). The ligation was carried out at 22°C for 18 hr.

3.1.8. Transformation of DH5α cells

For transformation, an aliquot of competent cells stored at -80°C in a 1.5 mL microcentrifuge tube was thawed on ice and gently tapped to get a uniform cell suspension. To the cell suspension, 5 µL of the ligation reaction or an appropriate amount of plasmid DNA (50 ng) was added. The tube was gently tapped and incubated on ice for 30 min. The cell suspension was then subjected to heat shock at 42°C in a water bath for 90 sec followed by snap chilling on ice for 2 min. Following this, 1 mL of LB was added to the cells in the tube, which was then incubated in an incubator-shaker (at 37°C and 180 rpm) for 45 min-1 hr. Cells were then pelleted by centrifugation at 12,000 rpm for 1 min, and the supernatant was discarded leaving behind ~100 uL of the supernatant. The cell pellet was resuspended in the residual supernatant and then plated onto sterile LB agar plates supplemented with 100 µg/mL of ampicillin. Plates were then incubated overnight at 37°C in an inverted position. For TA cloning in the pTZ57R vector, the transformants were selected by the blue-white colony screening method. It is known that the *lacZ* gene in the DH5α competent cells only codes for the ω-peptide while that in the pTZ57R vector codes for the α-peptide. Independently, these two peptides cannot form the functional β-galactosidase enzyme. However, the expression of both peptides in the same cell leads to the synthesis of a functional β-galactosidase enzyme by α-complementation. The multiple cloning site (MCS) of this vector is in the coding region of the lacZ gene expressing the α-peptide. Upon insertion of the fragment of interest at this MCS, the gene is disrupted to form a non-functional β-galactosidase due to the absence of α-complementation. It is established that β-galactosidase converts its colourless substrate X-Gal (an analogue of lactose) to form 5-bromo-4-chloro-indoxyl, which then spontaneously dimerizes and oxidizes to form a bright blue insoluble pigment 5,5'-dibromo-4,4'-dichloro-indigo. Thus, the non-recombinant colonies with the functional β-galactosidase enzyme turn blue in colour, whereas the recombinant colonies with the fragment of interest remain

colourless. For this, 100 μL of 100 mM IPTG (isopropyl-β-D-thio galactopyranoside; an artificial inducer of *lac* operon) and 20 μL of 20 mg/mL X-Gal (5-Bromo-4-chloro-3-indolyl-β-D-galactoside) were spread onto a 90 mm sterile LB agar plate supplemented with ampicillin in the dark. The plate was allowed to absorb X-Gal and IPTG for at least 30 min before plating the transformed cells. The plates were incubated overnight at 37°C for the colonies to develop. The recombinant colonies with the desired insert were white in colour, which were subsequently screened by plasmid isolation, restriction enzyme digestion and confirmed by Sanger sequencing using vector-specific M13 R primer.

3.1.9. Preparation of plasmid DNA by alkaline lysis method

The plasmid DNA from transformed DH5α cells was isolated by the alkaline lysis method, as described in Sambrook et al. (1995) with a few modifications. A single bacterial colony was inoculated in 5 mL of LB supplemented with ampicillin in a 50 mL tube, which was incubated overnight in an incubator-shaker. A glycerol stock was prepared from the overnight grown culture prior to the plasmid isolation. The remaining culture was then pelleted down at RT by centrifugation at 5,000 rpm for 10 min, and the supernatant was discarded. The cell pellet was resuspended in 150 μL of the ice-cold Solution I (50 mM glucose, 25 mM Tris-HCl pH 8.0 and 10 mM EDTA pH 8.0) by thorough vortexing and then the tube was incubated at RT for 5 min. For cell lysis, 200 μL of a freshly prepared Solution II (0.2 N NaOH and 1% SDS) was added to the tube. The contents were mixed by gentle inversion and incubated at RT for 3 min. A 200 μL aliquot of the Solution III (3 M sodium acetate pH 4.8) was then added to the tube for neutralization of the lysis solution. Contents of the tube were mixed by gentle inversion, followed by incubation on ice for about 5 min until a white cottony mass was seen. The tube was centrifuged at 12,000 rpm for 15 min at 4°C, and the supernatant was transferred to a fresh 1.5 mL tube. Ten μL of RNase A (10 mg/mL stock) was added to the supernatant, which was incubated for 1 hr at 37°C. Following incubation, the protein extraction was done by adding 500 μL of chloroform to the tube, and the contents were mixed by vortexing for 20 sec. After centrifugation at 12,000 rpm for 10 min at 4°C, the aqueous phase from the tube was transferred to a fresh 1.5 mL tube. This step was repeated once more, and the resultant aqueous phase was transferred to a fresh 1.5 mL tube. To the aqueous phase, 1 mL of isopropanol was added, followed by a gentle inversion of the contents and its centrifugation at 12,000 rpm for 10 min at 4°C to precipitate the plasmid DNA. The resulting DNA pellet was washed by adding 1 mL of ice-cold 70 % ethanol. The pellet was air dried to remove the

residual ethanol and dissolved in 20 µL of TE buffer (10 mM Tris-HCl, 1 mM EDTA, pH 8.0). The quality of the plasmid DNA was checked on a 1% agarose gel and quantified using a spectrophotometer.

3.1.10. Plasmid DNA preparation for sequencing and transfection

To obtain a highly pure form of plasmid DNA for sequencing and transient transfections in human cell lines, a single colony of the bacterial clone was inoculated in 5 mL of LB containing ampicillin in a 50 mL tube. The culture was grown overnight in a 37°C incubator-shaker at 180 rpm. The overnight grown culture was pelleted down, and the plasmid DNA was isolated using the GenElute™ plasmid mini prep kit (Sigma-Aldrich, St. Louis, MO, USA) as per the manufacturer's protocol. The quality of the plasmid DNA was checked on a 1% agarose gel and quantified using a spectrophotometer.

3.2. Plasmid constructs

To study the role of miR-617 and its gene target *DDX27* in OSCC cells, we generated 14 plasmid constructs (Tables 3-5) to perform transient transfections and the subsequent assays described in the forthcoming sections.

We generated pGL3-PrMIR617-F1 harbouring an 825 bp putative *MIR617* promoter fragment 1 (-365 bp to +460 bp relative to TSS) and pGL3-PrMIR617-F2 harbouring a 3,175 bp putative *MIR617* promoter fragment 2 (-2,925 bp to +250 bp relative to TSS) to determine their promoter activity. The fragments were bioinformatically chosen as described in section 3.5 and amplified from human genomic DNA using specific primers (Table 3) harbouring *Mlu*I and *Xho*I restriction enzyme sites for directional cloning. Then, the agarose gel-eluted PCR products and the cloning vector pGL3-Basic (Promega, Madison, WI, USA) were double-digested with *Mlu*I and *Xho*I at 37°C for 2 hr. The double-digested PCR products and the cloning vector were then ligated at a molar ratio of 1:4 (vector: insert) following a standard laboratory protocol described in section 3.1.7. The positive clones were screened by plasmid isolation, followed by restriction enzyme digestion and Sanger sequencing.

We generated pmiR-617 to study the effect of miR-617 in OSCC cells. To this end, we amplified a 206 bp fragment, bearing the pre-miR sequence of miR-617, using human genomic DNA as a template and specific primers (Table 3) harbouring *Hind*III and *Xho*I restriction enzyme sites. Then, the agarose gel-eluted PCR product and the cloning vector pcDNA3-EGFP were double-digested with *Hind*III and *Xho*I at 37°C for 2 hr. The double-digested PCR product

and the cloning vector were then ligated at a molar ratio of 1:6 (vector: insert). The positive clones were screened by plasmid isolation, followed by restriction enzyme digestion, and Sanger sequencing.

To delineate the specificity of mature miR-617 in regulating its gene target *DDX27*, the pmiR-617-M construct was generated by site-directed mutagenesis (SDM) according to Sambrook et al. (1995) using specific primers (Table 4) flanking the seed region (8 bp) of miR-617 in pmiR-617 such that the seed region is not included in the PCR product during amplification. Using pmiR-617 as the template, PCR product (nicked circular plasmids with deleted seed region) was visualized as a smear between the supercoiled and linear forms of the plasmid template (pmiR-617). The PCR product then underwent overnight digestion with *Dpn*I (digests methylated DNA) at 37°C to eliminate the methylated template plasmid DNA such that only the smear of nicked circular plasmids was visible on a 1% agarose gel. The digested product was then transformed in *E. coli* DH5α cells and a putative positive clone, pmiR-617-M, was isolated, and confirmed by Sanger sequencing.

We generated pGL3-PrDDX27 harbouring a 709 bp long putative *DDX27* promoter fragment (-642 bp to +67 bp relative to TSS) upstream to the *luc* gene in pGL3-Basic to determine its promoter activity. The fragment was bioinformatically chosen as described in section 3.5, and amplified from human genomic DNA using specific primers (Table 3) harbouring *Mlu*I and *Xho*I restriction enzyme sites. Then, the agarose gel-eluted PCR product and the cloning vector pGL3-Basic were double-digested with *Mlu*I and *Xho*I at 37°C for 2 hr. The double-digested PCR product and the cloning vector bearing cohesive ends were then ligated at a molar ratio of 1:4 (vector: insert). The positive clones were screened by plasmid isolation, followed by restriction enzyme digestion, and Sanger sequencing.

To validate the interaction between miR-617 and the 3'UTR of *DDX27*, the p3'UTR-S construct was generated as follows. A 186 bp long sequence of the 3'UTR of *DDX27* in a sense orientation was amplified from human genomic DNA using specific primers (Table 3) harbouring *Sac*I and *Mlu*I restriction enzyme sites. Then, the agarose gel-eluted PCR product and the cloning vector pMIR-REPORT™ vector (Thermo Fisher Scientific, Waltham, MA, USA) were double-digested overnight with *Sac*I and *Mlu*I at 37°C. The double-digested PCR product and the cloning vector bearing cohesive ends were then ligated at a molar ratio of 1:6 (vector: insert). The positive clones were screened by plasmid isolation, followed by restriction enzyme digestion and Sanger sequencing.

To validate the sequence specificity of the interaction between miR-617 and the *DDX27* promoter, the pGL3-PrDDX27-M construct harbouring the *DDX27* promoter with mutated target site upstream to the *luc* gene was generated by site-directed mutagenesis (SDM) according to Sambrook et al. (1995) using specific primers (Table 4) flanking the target site (19 bp) of miR-617 in pGL3-PrDDX27 such that the target site is not included in the PCR product during PCR amplification. Since it is easier to generate long stretch of deletions in smaller plasmids by PCR amplification, we first amplified the wild-type *DDX27* promoter with specific primers (Table 3; SL. No. 6) harbouring *Sac*I and *Eco*RV using pGL3-PrDDX27 as a template and then sub-cloned the agarose gel eluted *Sac*I and *Eco*RV double-digested PCR product in the pBluescript II KS (+) also double-digested with *Sac*I and *Eco*RV to generate pBSKS-PrDDX27. Then, nicked circular plasmids with the deleted target site were generated in PCR using pBSKS-PrDDX27 as a template and site-directed mutagenesis specific primers mentioned in Table 4; SL. No. 2. The resulting PCR product was digested overnight with *Dpn*I at 37°C, followed by its transformation in DH5α cells. A putative positive clone (pBSKS-PrDDX27-M) was isolated and confirmed by Sanger sequencing. The *DDX27* promoter fragment with the mutated target site in pBSKS-PrDDX27-M was released by double digestion with *Mlu*I and *Xho*I, followed by its agarose gel-elution. The double-digested and agarose gel-eluted fragment was then sub-cloned in pGL3-Basic (also double-digested with *Mlu*I and *Xho*I) to generate pGL3-PrDDX27-M.

The effect of *DDX27* overexpression was analysed using the pDDX27 overexpression construct. To generate pDDX27, a 2,413 bp long fragment harbouring the complete *DDX27* ORF and the consensus Kozak sequence [AXXATGc; obtained from ATGpr (https://atgpr.dbcls.jp/)] was amplified from human cDNA using specific primers harbouring *Kpn*I and *Eco*RV restriction enzyme sites (Table 3). Then, the agarose gel-eluted PCR product and the cloning vector pcDNA3.1 (+) were double-digested overnight with *Kpn*I and *Eco*RV at 37°C. The double-digested, gel-eluted PCR product and the cloning vector were then ligated at a molar ratio of 1:5 (vector: insert). The positive clones were screened by plasmid isolation followed by restriction enzyme digestion and confirmed by Sanger sequencing using vector specific primers (CMV-fwd and BGH-rev) and a *DDX27*-specific internal primer 1 (Table 3; SL. No. 2).

To study the effect of miR-617-mediated regulation of *DDX27* on various aspects of cancer, we generated a construct (pPr-DDX27) wherein *DDX27* ORF was transcribed by its own promoter. To accomplish this goal, we excised the *luc* ORF from the promoter-null pGL3-

Basic vector and cloned the *DDX27* ORF in its place to generate pPr-null-DDX27. This was achieved by amplifying the *DDX27* ORF using pDDX27 as a template with specific primers harbouring *Xho*I and *Xba*I restriction enzyme sites (Table 3; SL. No. 7). Then, the agarose gel-eluted PCR product and the cloning vector pGL3-Basic were double-digested overnight with *Xho*I and *Xba*I at 37°C. The double-digested, gel-eluted PCR product and the cloning vector were then ligated at a molar ratio of 1:5 (vector: insert). The positive clones (pPr-null-DDX27) were screened by plasmid isolation, followed by restriction enzyme digestion. Furthermore, we amplified the wild-type and target site mutated *DDX27* promoter fragments separately using pGL3-PrDDX27 and pGL3-PrDDX27-M as templates respectively and specific primers (Table 3, SL. No. 6) harbouring *Mlu*I and *Xho*I restriction enzyme sites. Following double-digestion of PCR products with *Mlu*I and *Xho*I, the agarose gel-eluted PCR products were then ligated to pPr-null-DDX27 (also double-digested with *Mlu*I and *Xho*I) at a molar ratio of 1:4 (vector: insert) to generate pPr-DDX27 (containing wild-type *DDX27* promoter+*DDX27* ORF) or pPr-M-DDX27 (containing *DDX27* promoter with mutated target site+*DDX27* ORF).

To further dissect the nature of interaction between miR-617 and *DDX27* 3'UTR, we amplified the 3'UTR of *DDX27* using p3'UTR-S as a template and specific primers (Table 3, SL. No. 10) harbouring *Eco*RV and *Not*I restriction enzyme sites. The PCR product was double-digested with *Eco*RV and *Not*I overnight at 37°C. The double-digested, gel-eluted PCR product was then ligated to pDDX27 (also double-digested by *Eco*RV and *Not*I) at a molar ratio of 1:6 (vector: insert) to generate pDDX27-3'UTR (containing *DDX27* ORF+ wild-type *DDX27* 3'UTR).

Table 5 summarizes the functional features of all the constructs generated during the present study.

3.3. Collection of patient samples

All the 36 matched normal oral tissue and OSCC patient samples used in the present study were ascertained at the Kidwai Memorial Institute of Oncology (KMIO), Bengaluru, Karnataka. The study was performed with informed consent from the patients and approval from the ethics committees of KMIO, Bengaluru, and IISc, Bengaluru. The samples were obtained as surgically resected tissues from oral cancerous lesions and adjacent normal tissues (taken from the farthest margin of surgical resection) in RNALater™ (Sigma-Aldrich, St Louis, MO, USA) and transferred to -80°C until further use. The tumours were staged according to the UICC's (union for international cancer control) TNM (tumour-node-metastasis)

classification (Sobin and Fleming, 1997). The details of the clinicopathological parameters obtained from the patients are summarised in Table 6 and Table 7.

3.4. Bioinformatics analysis to identify miR-617 gene target

MicroRNAs exert their effect through binding to one or more cognate target mRNAs to regulate their expression. To predict the mRNAs that may be regulated by miR-617 and avoid false prediction, we used a consensus approach by employing five different mRNA target prediction algorithms like TargetScanHuman 8.0 (https://www.targetscan.org/vert_80/), miRDB (https://mirdb.org/), MiRanda (https://cbio.mskcc.org/miRNA2003/miranda.html), microT-CDS (Diana Tools) [https://dianalab.e-ce.uth.gr/html/dianauniverse/index.php?r=microT_CDS], and PITA (https://genie.weizmann.ac.il/pubs/mir07/mir07_prediction.html). Thereafter, we chose one putative gene target of miR-617 that was predicted by all the target prediction tools and showed substantial role in carcinogenesis following a literature survey.

3.5. *In silico* identification of the *MIR617* and *DDX27* promoters

The putative promoter sequences of *MIR617* and *DDX27* were retrieved by an *in silico* search using different promoter prediction databases. For *MIR617*, the two putative promoter sequences were obtained based on analyses using three different databases: the DBTSS (http://dbtss.hgc.jp), Promoter 2.0 (https://services.healthtech.dtu.dk/services/Promoter-2.0/), and PROMO (http://alggen.lsi.upc.es). The putative promoter sequence of *DDX27* was retrieved from two different databases: DBTSS (https://dbtss.hgc.jp) and Promoter 2.0 (https://services.healthtech.dtu.dk/services/Promoter-2.0/).

3.6. Mammalian Cell Culture

3.6.1. General procedures

All cell culture work was performed under aseptic conditions in a bio-safety level II (BSL-II) vertical laminar flow hood using sterile disposable plastic-wares. The surface of the hood and all the plastic-wares introduced in the hood were sterilised with 70% ethanol before and after every use. To maintain sterile conditions in the tissue culture room (maintained at 25°C with an air-conditioner) and the bio-safety hood, they were exposed to UV light 30 min prior to every use.

3.6.2. Media and cell culture solutions

All media, solutions and supplements used in cell culture were prepared with autoclaved MilliQ water (Merck, Kenilworth, NJ, USA) and sterilised by a vacuum driven 0.22 µm membrane filtration system (Sartorius, Gottingen, Germany). The solutions, media and supplements stored at prescribed temperatures (4°C and –20°C) were pre-warmed in a 37°C incubator prior to use. The glass-wares used for storage of all media, solutions, and supplements were sterilized by autoclaving.

3.6.3. Cell lines and their maintenance

Cells were grown and maintained in T25 flasks, 6-well, 24-well plates or 35 mm dishes as required. Following cell lines were used in the study.

a. UPCI: SCC084 (Oral squamous cell carcinoma)

b. UPCI: SCC131 (Oral squamous cell carcinoma)

c. HeLa (Human papillomavirus-related endocervical adenocarcinoma)

d. HEK293T (Human embryonic kidney cells transformed with SV40 T-antigen)

e. Huh-7 (Adult hepatocellular carcinoma)

f. HepG2 (Hepatoblastoma)

g. MCF-7 (Invasive breast ductal carcinoma)

All the cell lines were maintained in Dulbecco's modified eagle medium (DMEM) supplemented with 10% (v/v) fetal bovine serum (FBS) and 1X antibiotic-antimycotic solution (henceforth called the complete DMEM) (all purchased from Sigma-Aldrich, St. Louis, MO).

Cell lines were cultured in polystyrene culture flasks provided with 0.2 µm hydrophobic vent caps and maintained in a humidified 5% CO_2 incubator set at 37°C. UPCI: SCC131 (SCC131) and UPCI: SCC084 (SCC084) cell lines were a kind gift from Dr. Susanne M. Gollin (University of Pittsburgh, Pittsburgh, PA, USA). These cell lines were generated following Institutional Review Board guidelines from consenting patients undergoing surgery for squamous cell carcinoma of the oral cavity at the University of Pittsburgh Medical Center (White et al., 2007). SCC131 cells were derived from a $T_2N_{2b}M_0$ lesion on the floor of the mouth of a 73-year-old Caucasian male, and SCC084 cells were derived from a $T_2N_2M_0$ lesion of the retromolar trigone of a 52-year-old Caucasian male (White et al., 2007). Both the cell lines have amplification of the 11q13 locus, possess wild-type *TP53* and are negative for HPV (White et al., 2007). HeLa and HEK293T cells were acquired from the National Centre for Cell Sciences, Pune, India. Huh-7 cell line was procured from Prof. Saumitra Das's laboratory in the Department of MCB, IISc, Bangalore, India. HepG2 cell line was procured from Prof. Deepak Saini's laboratory in the Department of DBG, IISc, Bangalore, India. MCF-7 cell line was obtained from Prof. P. Kondaiah's laboratory, Department of DBG, IISc, Bangalore, India.

3.6.4. Trypsinization of adherent cell monolayers

Cells from all the cell lines used were adherent in nature and grown as a monolayer. To subculture confluent monolayers, adherent cells were washed twice with 2 mL of DPBS (Dulbecco's phosphate buffered saline) (Sigma-Aldrich, St. Louis, MO) to remove residual medium. Then the monolayer of cells was dissociated using 1X Trypsin/EDTA solution (Sigma-Aldrich, St. Louis, MO) (500 µL per 25 cm^2 culture flask) for 1-2 min at RT, and thereafter trypsin was inactivated by adding 1 mL of complete DMEM. Then the content was pipette mixed into a homogenous cell suspension, centrifuged at 1,000 rpm for 30 sec, and the cell pellet was washed with 1 mL of complete DMEM. The cell pellet was resuspended in 1 mL complete DMEM and subcultured at 1:3 dilution in complete DMEM for growth and maintenance in fresh flasks.

3.6.5. Cell number determination

To determine cell density, cells were first trypsinized as described above, and a 1:10 dilution of the cell suspension was prepared with complete DMEM. A 10 µL aliquot of this diluted cell suspension was placed on a Neubauer haemocytometer (HyClone, Logan, UT), covered with a 22 x 22 mm^2 cover slip and number of cells in the four quadrants (WBC chambers of 0.1 mm^3 volume each) were counted under an Olympus CKX4 inverted

microscope (Olympus Optical Co., Japan). The total cell number was calculated by the following formula: number of cells per mL of original suspension = mean of the total number of cells counted in the four quadrants x dilution factor (10) x 10^4).

3.6.6. Cryopreservation and thawing of cells

Cells were cryopreserved by freezing them at a high cell density and at the least possible passage number for future use using DMSO as the cryoprotectant. Thus, cells were briefly cultured in T25 culture flasks till ~ 80% cell confluence and trypsinized as described before. To the cell pellet, 1 mL of cell freezing mixture [90% FBS and 10% DMSO (both from Sigma-Aldrich, St. Louis, MO)] was added. The cell suspension was kept on ice for 5 min, mixed intermittently and transferred in a pre-chilled 2 mL cryovial for overnight storage at -20°C, thereafter it was transferred to a -80°C freezer for overnight incubation and finally stored in liquid nitrogen until future use.

To revive cryopreserved cells, they were thawed rapidly at 37°C and transferred in a sterile 15 mL tube containing 1 mL of complete DMEM. Cells were washed twice with the complete DMEM by centrifuging it at 1,000 rpm for 15 sec to remove DMSO and transferred to a T25 culture flask containing pre-warmed complete DMEM to grow and attain morphology overnight in a 37°C incubator with 5% CO_2.

3.6.7. 5-Azacytidine treatment of SCC131 cells

SCC131 cells were seeded in T25 flasks at a density of 4×10^6 cells/flask and allowed to grow for 24 hr in complete DMEM. Post 24 hr of growth, cells were treated with 5-Azacytidine (Sigma-Aldrich, St. Louis, MO, USA), dissolved in DMSO (Sigma-Aldrich, St. Louis, MO, USA), at a final concentration of 5 μM and the vehicle-control DMSO for 5 days. Cells were treated daily with fresh media supplemented with 5-Azacytidine or DMSO separately and on day 5 of treatment, total RNA, protein, and genomic DNA were isolated from 5-Azacytidine- and DMSO-treated cells for further studies.

3.6.8. Sodium bisulphite treatment of SCC131 cells

To analyse the methylation status of the promoters of interest, the genomic DNA samples isolated from 5-Azacytidine- and DMSO-treated SCC131 cells were subjected to sodium bisulphite treatment according to the protocol described by Frommer et al. (1992) with some modifications. Briefly, 8 μg of genomic DNA was resuspended in a total volume of 70 μL and 10 μL of 3 M NaOH was added to it in a 0.6 mL PCR tube. Then the tube was kept at

37°C for 15 min, followed by incubation at 95°C for 3 min to denature the DNA and then snap chilling it on ice for 2 min. The bisulphite treatment of the denatured DNA was then carried out by the addition of 1 mL of the bisulphite reagent (3.25 M sodium bisulphite, 0.36 M NaOH, and 2.4 M hydroquinone) and incubation at 55°C for 17 hr in dark. Following the incubation, the treated DNA was purified and eluted in 100 µL of warm Elix® water by using the Wizard DNA clean-up columns (Promega, Madison, WI, USA) following the manufacturer's instructions. The desulphonation of the eluted DNA was done by addition of 10 µL of freshly prepared 3 M NaOH and incubation at 37°C for 15 min. The DNA was then precipitated by adding an equal volume of 6 M ammonium acetate and two volumes of ethanol and keeping it overnight at -20°C. Next day, the precipitated DNA was washed once with 70% ice-cold ethanol and then dissolved in an appropriate volume of TE buffer according to the DNA pellet size. The treated DNA was stored in dark at -20°C and used for setting up PCR using the primers designed for bisulphite-treated DNA (Table 8).

3.6.9. Analysis of *MIR617* and *DDX27* promoters by bisulphite sequencing PCR (BSP)

The bisulphite treated genomic DNA samples from 5-Azacytidine- and DMSO-treated cells were used as templates to amplify *MIR617* and *DDX27* promoters with the respective primers designed according to the MethPrimer database (http://www.urogene.org/methprimer; Table 8; Li and Dahiya, 2002). Following amplification, the PCR products were resolved on a 1% agarose gel, eluted, ligated to the pTZ57R TA cloning vector (Thermo Fisher Scientific, Waltham, MA, USA). Following transformation of DH5α competent cells with the ligated DNA, the clones were screened by blue-white screening and vector-specific restriction enzyme digestion as described above. Plasmid isolation was performed using the GenElute™ plasmid mini prepkit (Sigma-Aldrich, St. Louis, MO, USA). Ten clones from each experimental set were sequenced on an ABI PRISM A310-automated sequencer (Thermo Fisher Scientific, Waltham, MA, USA) to identify the methylation status of the CpG sites in *MIR617* and *DDX27* promoters in 5-Azacytidine- and DMSO-treated cells.

3.7. Genomic DNA isolation

3.7.1. DNA isolation from cell lines

The genomic DNA isolation from cell lines was performed using the Wizard® Genomic DNA Purification Kit (Promega, Madison, WI, USA) according to the manufacturer's guidelines. For cell lines, 1×10^6 trypsinized cells were lysed using 600 µL of the nuclei lysis solution in a 1.5 mL microcentrifuge tube. Then to denature protein, 18 µL of Proteinase K

solution was added, and the mixture was incubated at 65°C for 16 hr on a gently shaking platform in a hybridizer. The next day, RNA digestion was carried out by adding 15 µL of 10 mg/mL RNAse A (Bangalore Genei, Bangalore, India) to the lysed cells, and the tube was incubated at 37°C for 30 min. After the incubation, the tube was cooled to RT and 200 µL of the protein precipitation solution was added to it. The mixture was then vortexed vigorously for 20 sec and after incubating it on ice for 5 min, it was centrifuged at 12,000 rpm for 5 min at 4°C. The supernatant was then transferred to a fresh 1.5 mL microcentifuge tube, and the DNA was precipitated with 600 µL of isopropanol. The tube was gently swirled till the DNA strands were visible and centrifuged at 12,000 rpm for 10 min at 4°C. The DNA pellet thus obtained was washed with 600 µL of 70% ethanol at 12,000 rpm for 10 min at 4°C, air-dried and depending on the pellet size dissolved in 80-150 µL of the autoclaved TE buffer and incubated overnight at 4°C. The DNA was aliquoted and stored at -20°C till further use.

3.7.2. Quantitation of genomic DNA by spectrophotometric method

Quantification of genomic DNA was done using a NanoDrop™ 1000 spectrophotometer (Thermo Fisher Scientific, Waltham, MA, USA), which is based on the property of DNA to absorb radiation at a wavelength of 260 nm. The TE buffer was used to set a blank control. In the case of double-stranded DNA, an O.D. of 1 at 260 nm = 50 µg/mL. The concentration of double-stranded DNA in µg/mL was calculated using the following formula: O.D. at 260 nm x Dilution Factor (100) x 50/1000. The absorbance of the sample at 280 nm was also noted to estimate the protein or phenol content in the DNA sample. The ratio of absorbance at 260/280 for a pure DNA sample should be 1.8-2.0.

3.7.3. Agarose gel electrophoresis of DNA

The quality of the isolated genomic DNA was estimated by electrophoresing it in a 0.8% agarose gel containing 0.25 µg/mL ethidium bromide (Sigma-Aldrich, St. Louis, MO, USA). DNA gets intercalated with ethidium bromide and moves in the gel from the negative to positive direction under an electric current opposite to the direction of ethidium bromide. A 1 µL aliquot of DNA (50 ng/µL) was mixed with 2 µL of a gel loading dye (0.25% bromophenol blue prepared in 30% glycerol), electrophoresed in a 0.8% agarose gel, and visualized under UV light.

3.7.4. DNA Amplification by PCR

The polymerase chain reaction (PCR) is a method developed by Kary Mullis in the 1980s for a rapid *in vitro* amplification of specific DNA sequences using a thermostable DNA polymerase and commercially synthesized primers.

Primer designing

The primers for PCR were manually designed taking the following criteria under consideration.

1. The primer length was greater than 20 bases for higher specificity.
2. The GC content of the primer was >40%.
3. The 3' end of the primer did not end with a T residue and the last three bases included one T or A.
4. The annealing temperature was calculated as 2(A+T) + 4(G+C). The melting temperature (Tm) of the primers was between 65°C and 75°C and the difference in the Tm of the forward and reverse primers is not more than 2°C.
5. To ensure specific amplification, the BLAST (https://blast.ncbi.nlm.nih.gov/Blast.cgi) analysis was performed to exclude the homology of the primers to non-specific sequences using the DDBJ database (http://www.ddbj.nig.ac.jp/).

3.7.5. Thermal cycler parameters

The PCR was carried out in an automated thermal cycler that carries out temperature-controlled cycles of denaturation, annealing and extension. The specific conditions used for setting up the PCR reactions were as follows.

Initial denaturation	95°C, 5 min	
Denaturation	95°C, 30-60 sec	28-35 cycles
Annealing	54-72°C, 30-60 sec	
Extension	72°C, ~1 min/kb	
Final extension	72°C, 5-20 min	

The PCR was carried out in a total reaction volume of 25 µL which contains 50 ng of genomic DNA template or 50-100 ng of cDNA, 200 µmol of each dNTP, 50 ng each of forward and reverse primers, 1.5 mM of $MgCl_2$, and 1 U of *Taq* DNA Polymerase (Black Bio, India) or 1 U Phusion DNA Polymerase (Thermo Fisher Scientific, Waltham, MA, USA) in a

standard 1X PCR reaction buffer supplied by the manufacturer. The amplification was performed in an Eppendorf™ thermocycler (Eppendorf Corp., Hamburg, Germany). The total volume of PCR product was mixed with 4 µL of a gel loading dye (0.25% xylene cyanol prepared in 30% glycerol or 0.5% bromophenol blue in 30% glycerol) and depending on the product size, electrophoresed in a 0.8-2% agarose gel containing ethidium bromide and then visualized on a UV Transilluminator.

3.7.6. Recovery of DNA from agarose gels

The Genelute™ Gel Extraction Kit (Sigma-Aldrich, St. Louis, MO, USA) was used to recover DNA fragments of interest from ethidium bromide-stained agarose gels. The specific DNA band in an agarose gel was cut out using a sharp razor blade under UV light. The care was taken to prevent overexposure of DNA to UV light. The gel extraction kit combines the silica-binding ability of DNA with the convenience of a spin or vacuum column format to provide a typical recovery of DNA up to 80%. Briefly, the agarose gel piece containing the DNA was weighed (1 volume = weight in mg) and dissolved by incubating at 60ºC for 10-20 min in 3 volumes of the gel solubilization buffer. After ensuring the complete dissolution of the gel piece, DNA was precipitated from the homogenous mixture by adding one gel volume of isopropanol. The contents in the tube were invert mixed, and the mixture was then loaded onto a pre-treated DNA binding column, which was then centrifuged at 12,000 rpm for 1 min at RT. After discarding the flow-through, the column was washed with 700 µL of the wash buffer containing ethanol. The column was given an empty spin at 12,000 rpm for 2 min at RT to remove any residual ethanol. The column was then transferred to a fresh collection tube and the DNA was eluted from the column in 20 µL of the warm TE buffer by centrifugation at 12,000 rpm for 3 min at RT. The eluted DNA was quantitated spectrophotometrically and stored at -20ºC until further use.

3.8. Total RNA isolation

3.8.1. Isolation of total RNA from human cell lines and oral tissue samples

For RNA isolation from human cell lines and oral tissue samples, TRI Reagent™ (Sigma-Aldrich, St. Louis, MO, USA) was used as per the manufacturer's instructions with some modifications. For tissue samples, 50-100 mg of tissue was homogenized in 500 µL of TRI Reagent™. In case of cell lines, cells were allowed to grow till they were confluent and then scraped off the plate (35 mm) with a scraper in 1 mL of the TRI Reagent™ (Sigma-Aldrich, St. Louis, MO, USA). The cell or tissue lysate was pipette mixed to form a

homogenous lysate, transferred to a 1.5 mL microcentrifuge tube and kept at RT for 5 min to ensure complete dissociation of nucleoprotein complexes. For phase separation, 200 µL (one-fifth volume of TRI Reagent™ used) of chloroform was added to the tube, and the contents of the tube were mixed by vigorous shaking for 15-30 sec. The tube was kept at RT for 15 min followed by centrifugation at 12,000 rpm for 15 min at 4°C. The aqueous phase which contains the RNA was carefully transferred to a fresh 1.5 mL microcentrifuge tube, ensuring that the interphase is unperturbed. RNA in the tube was then precipitated by adding 500 µL (half the volume of TRI Reagent™ used) of isopropanol. The tube was kept at RT for 10 min, and then centrifuged at 12,000 rpm for 10 min at 4°C. The RNA pellet was washed with 1 mL of 75% ethanol made in DEPC-treated water by centrifugation at 12,000 rpm at 4°C for 5 min. The resultant RNA pellet was air-dried and dissolved in 20 µL of DEPC-treated water. It was subsequently stored at -80°C for future use.

3.8.2. Quantitation and visualization of total RNA

Total RNA quantitation was done spectrophotometrically by measuring its absorbance at 260 nm using the NanoDrop™ 1000 spectrophotometer (Thermo Fisher Scientific, Waltham, MA, USA). For RNA, an OD_{260} of 1.0 corresponds to 40 µg of RNA/mL, while OD_{280} determines the purity of the sample in terms of protein contamination. Protein and other impurities in the RNA preparation are quantitated by a ratio of OD_{260} to OD_{280}. An OD_{260}/OD_{280} ratio of < 1.8 indicates an impure RNA preparation. An aliquot of RNA (1 µg) was mixed with 5 µL of an RNA loading dye [95% (v/v) formamide, 10 mM EDTA pH 8.0, 1 mg/mL xylene cyanol and 1 mg/mL bromophenol blue] (all from Sigma-Aldrich, St. Louis, MO, USA). Upon heating the mixture at 70°C for 20 min, it was snap chilled on ice for 10 min. Following this, the mixture was loaded onto a 1.5% agarose gel with ethidium bromide (Sigma-Aldrich, St. Louis, MO, USA) and electrophoresed in 1X TAE buffer (40 mM Tris-HCl, 20 mM acetic acid, and 1 mM EDTA pH 8.0). The presence of intact 28S (5 kb) and 18S (1.9 kb) ribosomal RNA bands was used to ascertain good RNA preparation.

3.8.3. First-strand cDNA synthesis

The first-strand cDNA was synthesized using the Verso cDNA synthesis kit (Thermo Fischer Scientific, Waltham, MA, USA) using 1-2 µg of total RNA as per the manufacturer's protocol. Briefly, in a sterile 0.5 mL PCR tube, 400 ng of random hexamer primers and 1-2 µg of total RNA were added and the volume was made up to 12 µL using DEPC-treated water. Following incubation of the tube at 70°C for 5 min in an Eppendorf™

thermocycler (Eppendorf Corp., Hamburg, Germany), it was snap chilled on ice. A 7 µL cocktail containing 2 µL of 20 nM dNTPs mix, 1 µL of RT enhancer, and 4 µL of 5X cDNA synthesis buffer was added to the tube, which was then incubated at 25°C for 5 min. Finally, 1 µL of an enzyme mix, which contains Reverse Transcriptase and RNase inhibitor, was added in the tube, which was then incubated in a thermocycler at 25°C for 10 min, at 42°C for 1 hr and lastly at 70°C for 10 min. The newly synthesized first-strand cDNA was stored at -20°C until further use.

3.8.4. Quantitative reverse transcription PCR

For each RT-qPCR, cDNA synthesized from 100 ng of total RNA was used as a template. All RT-qPCR reactions were performed in a QuantStudio3 and StepOnePlus™ Real-Time PCR System (Thermo Fischer Scientific, Waltham, MA, USA) using the DyNAmo ColorFlash SYBR Green qPCR Kit (Thermo Fischer Scientific, Waltham, MA, USA). The fold change in expression was determined using the equation: $\Delta Ct_{(gene)} = Ct_{(gene)} - Ct_{(normalizing\ control)}$, where Ct is the cycle threshold value, and ΔCt represents the gene expression normalized to *GAPDH* or *5S rRNA*. The details of the primers used for RT-qPCR are listed in Table 9.

The miR-617-specific cDNA was synthesized using a miRNA-specific oligonucleotide primer (RT6-miR-617) having a 5' overhang and a 3' end of six bases complementary to the respective miRNAs (Table 9). Amplification of the resulting cDNA was performed using three different oligonucleotide primers (short-miR-617; MP-fw and MP-rev) within the same PCR reaction (Table 9). The detailed protocol for the miR-Q RT-PCR is discussed by Sharbati-Tehrani et al. (2008) and is depicted in Figure 3. The final detection and quantitation of miRNAs were performed by real-time acquisition of SYBR green fluorescence using *5S rRNA* as a normalizing control to equalize the amount of cDNA generated from each sample.

3.9. Isolation of total protein from cell lines and OSCC xenograft tissues

Protein lysates were prepared from cells grown in T25 flasks or 6-well plates depending on the experiment. After aspirating the culture media, cells (~$4x10^6$) were washed twice using 1 mL of DPBS. The adherent cells were then gently removed in DPBS solution using a cell scraper and transferred to a 1.5 mL tube, which was then centrifuged at 2,500 rpm for 5 min at RT. The cell pellet obtained was lysed by the addition of 150 µL of the CelLytic™ Cell Lysis Reagent (Sigma-Aldrich, St. Louis, MO, USA) and 1.5 µL of the 100X Protease Inhibitor Cocktail (Sigma-Aldrich, St. Louis, MO, USA). The pellet was gently resuspended

in the cell lysis buffer cocktail by pipette mixing, and the tube was then put on a rotator for 30 min at 4°C to ensure proper lysis, followed by centrifugation at 12,000 rpm for 30 min at 4°C to remove cell debris. The supernatant containing the protein lysate was aliquoted into small volumes in 0.5 mL microcentrifuge tubes, snap chilled in liquid nitrogen, and then stored at -80°C until further use. In the case of OSCC xenograft tissues, approximately 100-200 mg tissue sample was homogenized in 500 µL of the CelLytic™ MT Mammalian Tissue Lysis Reagent (Sigma-Aldrich, St. Louis, MO, USA) supplemented with 1X Protease Inhibitor Cocktail (Sigma-Aldrich, St. Louis, MO, USA) and further processed same as the protocol described above for protein isolation from cell lines.

3.9.1. Quantitation of total protein by Bradford assay

Total protein in the lysates was estimated using the Bradford assay (Bradford, 1976), which is based on the principle that the absorbance maximum for an acidic solution of the dye Coomassie Brilliant Blue G-250 (CBBG) shifts from 465 nm to 595 nm upon binding to proteins. There is a visible colour change when the dye is bound to proteins as both hydrophobic and ionic interactions with the proteins stabilize the anionic form of the dye. The amount of dye bound to the protein is therefore proportional to the amount of protein in the lysate and is measured at 595 nm using a spectrophotometer. For the assay, a stock solution of 5X Bradford reagent (100 mL) was prepared in an amber-coloured bottle by dissolving 50 mg of the CBBG dye (Sigma-Aldrich, St. Louis, MO, USA) in 25 mL of 95% ethanol at 4ºC, followed by the addition of 50 mL of concentrated ortho-phosphoric acid (Qualigens Fine Chemicals, Mumbai, India) and Elix® water to make up the volume to 100 mL. Bovine serum albumin (BSA) (SRL, India) was used as a standard sample. For the assay, dilutions of BSA (2 µg to 14 µg) and test sample (1 and 2 µL of the test sample in duplicate) were prepared in a total volume of 50 µL with Elix® water. The diluted test and standard protein samples were denatured using 50 µL of 1 N NaOH; 1 mL of 1X Bradford reagent was then added to each tube, which was kept for 3-5 min in dark for the colour to develop. The absorbance at 595 nm was read in an ELISA plate reader (Bio-Rad™, Hercules, CA, USA). The GraphPad Prism 8 software (http://www.graphpad.com) GraphPad Software Inc., San Diego, CA, USA) was used to generate the standard curve by plotting concentration vs. absorbance, and the amount of protein was then calculated from this graph.

3.9.2. SDS-polyacrylamide gel electrophoresis (SDS-PAGE)

All the reagents and buffers for SDS-PAGE were prepared in Elix® water. A low cross-linking 30% acrylamide-bisacrylamide was prepared by mixing 29% (w/v) of acrylamide and 1% (w/v) of N, N'-methylene bisacrylamide. Other reagents like 1.0 M Tris-HCl (pH 6.8), 1.5 M Tris-HCl (pH 8.8), 10% SDS, and 10% ammonium persulphate were all prepared in Elix® water.

Preparation of resolving gel (total volume 30 mL)

Elix® water	11.40 mL
30% Acrylamide mix	10.20 mL
1.5 M Tris-HCl (pH 8.8)	7.50 mL
10% SDS	0.30 mL
10% Ammonium persulphate	0.30 mL
TEMED	0.012 mL

Preparation of 5% stacking gel (total volume 10 mL)

Elix® water	6.84 mL
30% Acrylamide mix	1.70 mL
1.0 M Tris-HCl (pH 6.8)	1.25 mL
10% SDS	0.10 mL
10% Ammonium persulphate	0.10 mL
TEMED	0.01 mL

For casting the SDS-PAGE gel, the glass plates, spacers, and clamps were first cleaned and assembled. The bottom of the assembled plates was then sealed by using 1.5% (w/v) agarose (Sigma-Aldrich, St. Louis, MO, USA) prepared in Elix® water. After the agarose solidified, the required volume of freshly prepared resolving gel was poured between the plates, leaving space for the stacking gel. To prevent oxidation of the gel, Elix® water was then layered on top of the resolving gel which was then allowed to polymerize for ~45 min at RT or at 4°C overnight. Once the gel polymerized, the water on top was poured out completely for casting the stacking gel over the resolving gel. A clean Teflon comb was then inserted immediately between the plates to keep a distance of at least 1-1.5 cm between the wells and the resolving gel front. The stacking gel was allowed to polymerize for about 20 min at RT.

After polymerization, the comb was removed gently, the wells were cleaned with Elix® water, and the gel assembly was then placed on a vertical gel electrophoresis apparatus. The top and bottom reservoirs of the apparatus were filled with an adequate amount of 1X Tris-glycine buffer [25 mM Tris-HCl, 250 mM Glycine, and 0.1%(w/v) SDS]. A denaturing SDS-PAGE gel loading buffer was prepared by adding 10 µL each of β-mercaptoethanol and 10% SDS to 100 µL of 1X SDS-PAGE gel loading dye [50 mM Tris-HCl (pH 6.8), 2% (w/v) SDS, 0.1% (w/v) bromophenol blue and 10% (v/v) glycerol]. The required amount of the total protein lysate (5-40 µL containing 25-200 µg proteins) in a 1.5 mL tube was mixed with 10-15 µL of the denaturing SDS-PAGE gel loading buffer. The tube was then placed in a boiling water bath for 5 min, snap chilled on ice and then the lysate was loaded in a well of the gel. The initial voltage for the gel was set at 100 V until the dye front crossed the stacking front, after which the voltage was increased to and maintained at 150 V until the proteins resolved sufficiently.

3.9.3. Western blot analysis

For Western blot analysis, proteins resolved as described above by SDS-PAGE were transferred onto a PVDF membrane (Pall, USA), using a locally made conventional semi-dry transfer apparatus for blotting proteins up to 100 kDa or a wet transfer mini-Trans-Blot electrophoretic transfer cell (Bio-Rad™, Hercules, CA, USA) for proteins larger than 100 kDa. To this end, the PVDF membrane and the electrophoresed gel were sandwiched between Whatman filter paper no.1 soaked in either a semi-dry transfer buffer (Tris-1.74 gm, Glycine-0.87gm, 10% SDS-1.11 mL, Methanol-60 mL, and Elix® water-240 mL) or a wet transfer buffer (Tris-3 gm, Glycine-14.4 gm, Methanol- 200 mL, Elix® water-800 mL) based on the protein of interest. The semi-dry transfer was carried out at 150 mA for 1.5 hr at RT, while the wet transfer was set at 200 mA for 2 hr at 4°C. After the transfer, the membrane was stained with Ponceau S [0.1% Ponceau S (w/v) in 5% (v/v) acetic acid (Sigma-Aldrich, St. Louis, MO, USA)] to check the transfer efficiency. Next, the blotting membrane was washed with 1X PBST [1X phosphate-buffered saline (PBS-0.05 M Na_2HPO_4, 0.05 M NaH_2PO_4, and 0.15 M NaCl, pH 7.4) and 0.1% (v/v) Tween®20] to completely remove the Ponceau S stain, and then blocked using 5% (w/v) skimmed milk (Nandini, Bangalore, India) prepared in 1X PBST for 1 hr at RT or 4°C overnight with gentle rocking to prevent non-specific binding of the antibodies. Following the blocking step, an appropriate primary antibody was added to the membrane, which was incubated overnight on a slow rocker in the cold room (4°C). The next day, the membrane was washed three times for 10 min each with 1X PBST at RT on a fast rocker to remove excess of primary antibody, followed by incubation for 1 hr at RT on a slow rocker

with an appropriate HRP-conjugated goat anti-rabbit (1:2,500 dilution; Bangalore Genei, Bangalore, India) or goat anti-mouse secondary antibody (1:5,000 dilution; Bangalore Genei, Bangalore, India) prepared in the blocking solution. The excess unbound secondary antibody was removed from the membrane by washing with 1X PBST at RT for 10 min, three times each on the fast rocker. The immunoblot was developed by spreading an adequate amount of the Immobilon Western chemiluminescent HRP substrate (Merck, Darmstadt, Germany) evenly on the membrane, which was incubated in dark for around 1 min, and the signals were imaged by a ChemiDoc imaging system (ChemiDoc XRS+, Bio-Rad Laboratories, Inc, Hercules, CA, USA).

3.9.4. Antibodies for Western blot analysis

The following antibodies were used in this study: anti-DDX27 antibody (1:1,000 dilution; cat# ab177950; Abcam, Cambridge, MA, USA), anti-mouse β-actin antibody (1: 10,000 dilution; cat# A5441; Sigma-Aldrich, St. Louis, MO, USA), anti-phospho-p70 S6 Kinase (Thr421/Ser424) antibody (1: 1,000 dilution; cat# 9204; Cell Signaling Technology, Danvers, MA, USA) and anti-p70 S6 Kinase antibody (1: 1,000 dilution; cat# 9202; Cell Signaling Technology, Danvers, MA, USA). The primary and secondary antibodies were diluted in 5% BSA prepared in 1X PBST and 5% skimmed milk prepared in 1X PBST, respectively.

3.10. Transient transfection

Transient transfection/co-transfection of plasmid DNA in OSCC cells was done with Lipofectamine 2000 (Invitrogen, Carsland, CA, USA), according to the manufacturer's instructions. For each experiment, plasmid DNA quantity was kept constant in each well of the 6-wellplate. Briefly, 2×10^6 cells/well were seeded in a 6-well plate using complete DMEM. Cells were allowed to attach and grow for 18 hr prior to transfection. For transfection, the medium was removed, and the cells in a well were washed with 1 mL of 1X DPBS, following which 1.8 mL of Opti-MEM™ (Thermo Fisher Scientific, Waltham, MA, USA) was added to the cells and the plate was incubated at 37°C in a CO_2 incubator. Meanwhile, a DNA-Opti-MEM™ complex was made using an appropriate quantity of DNA in a total volume of 100 µL with Opti-MEM™. Lipofectamine-Opti-MEM™ complex was also prepared according to the manufacturer's instructions using an appropriate quantity of Lipofectamine reagent (2 µl of Lipofectamine/µg DNA) and Opti-MEM™ to a final volume of 100 µL. The DNA-Opti-

MEM™ complex (100 µL) and lipofectamine-Opti- MEM™ complex (100 µL) were incubated separately for 5 min at RT, followed by mixing the two complexes. This mixture was then incubated for 20 min at RT. Following incubation, it was added directly into a well of a 6-well plate, which was then gently rocked to ensure proper mixing. After 6 hr, the medium was removed, and cells were allowed to recover for 48 hr in 2 mL of the complete DMEM. After the recovery period, cells were trypsinized, and the total protein or RNA was extracted depending upon the requirement.

For transfection with TurboFect (Thermo Fisher Scientific, USA), a 24-well plate was seeded with 50,000 cells/ well and incubated at 37°C for 18 hr prior to transient transfection. Next day, the cells in each well were washed with 1X DPBS and supplemented with 400 µL of Opti-MEM™, 1 hr prior to transfection. Meanwhile, a single 100 µL cocktail of DNA, Opti-MEM™ and TurboFect (1 µL per 500 ng of DNA) was made, mixed well and incubated at room temperature for 20 min. Following incubation, it was added directly into each well of the 24-well plate and the plate was gently rocked to ensure proper mixing. For each experiment, plasmid DNA quantity was kept constant in each well of the 24-well plate. After 6 hr, the medium was removed, and cells were allowed to recover for 48 hr in 500 µL of the complete DMEM. After the recovery period, cells were lysed and the total protein was extracted at the end of the experiment.

3.11. Dual-luciferase reporter assay

The direct interaction between miR-617 and the promoter or 3'UTR of a target gene was determined using a dual-luciferase reporter assay kit (Promega, Madison, WI, USA), as suggested by the manufacture. Similarly, the promoter activity of the *MIR617* and *DDX27* putative promoter constructs was also tested using the dual-luciferase reporter assay. For both the assays, 50,000 SCC131 cells/well were seeded in triplicate for each experiment in a 24-well plate one day prior to transfection. Different combinations of the vector and constructs (total 500 ng or 800 ng) were then transiently co-transfected in SCC131 cells, using TurboFect as described above. The pRL-TK vector (20 ng) was also co-transfected to normalize for transfection efficiency by determining the renilla luciferase activity. Post 48 hr of transfection, cells in each well were washed with 1X DPBS and then lysed with 100 µL of the 1X Passive Lysis Buffer by gently rocking the plate for 30 min at RT. The cell lysate from each well was then transferred to a 1.5 mL microcentrifuge tube, centrifuged for 5 min at 12,000 rpm and the supernatant was used for dual-luciferase reporter assay. To quantify firefly luciferase activity,

10 µL of the cell lysate from each 1.5 mL tube was mixed with 10 µL of the Luciferase Assay Reagent-II (LAR-II) in a well of 96-well plate. Then the renilla luciferase activity was assayed by adding 10 µL of the Stop and Glow reagent to the same well. The VICTOR™ X Multilabel Plate Reader (PerkinElmer®, Waltham, MA, USA) or the Infinite 200 PRO Plate reader (Tecan Group Ltd, Mannedorf, Switzerland) was used for quantification of both the luciferase activities, and ratio of the two values (i.e., firefly and renilla luciferases) was used for analysis.

3.12. Cell proliferation assay by trypan blue dye exclusion assay

The rate of cell proliferation was assessed by employing trypan blue dye exclusion assay as described in Karimi et al. (2019). In brief, post 24 hr of transfection with Lipofectamine 2000 as described above, cells were trypsinized and re-seeded at a density of 30,000 cells/well in triplicates for each transfection experiment in 24-well plates. At the desired time point, cells from each well were washed with 500 uL of 1X DPBS and then treated with 200 uL of trypsin, followed by addition of 1 mL of complete DMEM to inactivate the trypsin. Cells were then pelleted by centrifugation at 2,500 rpm for 5 min at RT. The cell pellet was resuspended in 700 uL of complete DMEM and 50 uL of this cell suspension was mixed with 50uL of 0.4 % trypan blue dye (Sigma-Aldrich, USA) prepared in 1X PBS. For cell counting, 10 uL aliquot of the stained cells were added to a haemocytometer. The number of viable cells/mL was calculated using the following formula: Number of viable cells/ mL= mean of the total number of cells counted in the four quadrants (unstained cells) X dilution factor X 10^4. The number of live cells over a period of time or at a single timepoint was plotted using the GraphPad prism 8.0 software.

3.11.1. Coefficient of interaction (CI) to determine the synergistic effect of the interaction between miR-617 and *DDX27*

Synergism between two drugs is calculated by CDI; a CDI <1 indicates a synergistic relationship (Chen et al., 2014). In the present study, we employed the CDI formula to calculate the synergistic effect of the interaction between miR-617 and *DDX27* on cell proliferation by co-transfecting their overexpression constructs in SCC131 cells. Since we are calculating the interaction between miR-617 and *DDX27* promoter using the cell proliferation assay, we called it the coefficient of interaction (CI). The CI was calculated as follows.

CI = AB/ (A × B), where AB is the ratio of the viable cell count post 72 hr of cells co-transfected with the overexpression constructs of miR-617 (pmiR-617) and DDX27 (pPr-DDX27; *DDX27* ORF under its own promoter) to the viable cell count post 72 hr of cells co-transfected with

pPr-null-DDX27 (a promoter less construct with *DDX27* ORF) and pcDNA3-EGFP, and A or B is the ratio of the viable cell count post 72 hr of cells transfected with each overexpression construct (pmiR-617 or pPr-DDX27) to the viable cell count post 72 hr of cells co-transfected with the pPr-null-DDX27 and pcDNA3-EGFP.

3.12. Apoptosis assay

The CaspGLOW Fluorescein Active Caspase-3 Staining Kit (Biovision, Mountain View, CA) was used to quantify the apoptosis of cells co-transfected with the appropriate constructs. In brief, post 24 hr of transfection with Lipofectamine 2000 as described above, cells from a well representing one co-transfection experiment were trypsinized and counted to obtain a cell suspension of 1×10^6 cells/mL in a 1.5 mL tube. Two 300 µL aliquots of this cell suspension (0.3×10^6) was made in 1.5 mL tubes. Following addition of 1 uL of FITC-DEVD label to each tube and incubation for 1 hr at 37^0C, the cells were then washed twice at 3,000 rpm for 5 min with 500 µL of wash buffer at RT. The resultant cell pellet in each tube was resuspended in 100 µL of wash buffer, and transferred as 50 µL aliquots into 2 wells in a black 96-well microtiter plate. The fluorescence intensity was measured (excitation wavelength = 485 nm and emission wavelength = 535 nm) using the Infinite 200 PRO Plate reader (Tecan Group Ltd, Mannedorf, Switzerland). Similar procedure was followed for each co-transfection experiment.

3.13. Soft agar colony-formation assay

The soft agar colony-formation assay was used to measure a cell's ability to proliferate and form colonies in suspension within a semi-solid agarose gel (Horibata et al., 2015). In the absence of anchorage to the extracellular matrix (ECM), non-transformed cells fail to rapidly propagate and undergo apoptosis. This process is known as anoikis. In contrast, tumour cells lose their anchorage dependence due to activation of signalling pathways such as phosphatidylinositol 3-kinase (PI3K)/AKT and Rac/Cdc42/PAK and can therefore grow and form colonies within the semi-solid soft agar matrix (Horibata et al., 2015). The anchorage-independent growth of cells co-transfected with a combination of constructs was analysed by soft agar colony-forming assay in 35 mm tissue culture dishes as described below.

Briefly, 1% Difco Noble Agar (BD Biosciences, USA) prepared in MilliQ water was autoclaved and cooled to ~45°C in a water bath; 10 mL of this solution was diluted with an equal volume (10 mL) of pre-warmed (~45°C) complete DMEM and 1 mL of this mixture

was poured in each 35 mm dish as a base layer and allowed to solidify at RT for 20-30 min. Since three 35 mm dishes were used for each transfection experiment, 4 mL of 0.37% soft agar-complete DMEM mixture was prepared using 1.5 mL of 1% Difco Noble Agar prepared in MilliQ water and 2.5 mL pre-warmed complete DMEM. Cells transfected with appropriate constructs were trypsinized, harvested and 28,000 cells were then suspended in 4 mL of 0.37% of the soft agar-complete DMEM mixture, and 1 mL of this mixture was plated in each of three 35-mm dishes. A similar procedure was followed for other transfection experiments. The plates were allowed to solidify for 15-20 min at RT and then incubated at 37°C in a CO_2 incubator for two weeks till visible colonies developed. The colonies were stained by adding 1 mL of 0.01% crystal violet (Sigma-Aldrich, St. Louis, MO, USA) prepared in 10% ethanol to each dish at RT for 30 min. The extra dye was decanted, and each dish was washed for four times with 1 mL of Elix® water. Following removal of extra water, the colonies were imaged using Leica Inverted Microscope DMi1 (Leica Microsystems, Wetzlar, Germany) and counted by the OpenCFU software (https://opencfu.sourceforge.net/)

3.14. *In vivo* assay for tumour growth

The tumour suppressor property of miR-617 was investigated using an *in vivo* nude mice OSCC xenograft model. The effect of miR-617 overexpression on tumour growth was assessed in 6 weeks old female NU/J athymic nude mice, using a synthetic miR-617 mimic and a negative mimic control. The optimum dosage of miR-617 mimic was optimized by performing RT-qPCR, Western Blot analysis and cell proliferation assay. For the nude mice experiment, briefly, 2×10^6 SCC131 cells were seeded per well in two 6-well plates. Post 18 hr of cell seeding, cells in each well were transfected with 400 nM of mimic control or 400 nM of miR-617 mimic (6 wells each for mimic control and miR-617 mimic), using Lipofectamine 2000 as described before. Post 24 hr of transfection, cells transfected with mimic control, or miR-617 mimic were trypsinized and pooled separately. The pooled cells from each transfection group (mimic control or miR-617 mimic) were divided into six 1.5 mL tubes: each tube with $3x10^{\mathbf{6}}$ cells. Cells from a tube were suspended in 200 μL of 1:1 dilution of DPBS and Matrigel [Corning® Matrigel® Growth Factor Reduced (GFR) Basement Membrane Matrix, LDEV-free, cat # 354230, New York, USA]. Three female mice were assigned for each transfection group, and $3x10^{\mathbf{6}}$ cells were subcutaneously injected in each flank. Tumours were allowed to grow in nude mice and tumour volumes were measured using a Vernier's calliper every alternate day starting on day 13 till the termination of the experiment on day 27. Tumour volumes were calculated using the formula: $V= L\times W^2\times0.5$, where L and W represent

length and width of the tumour respectively. The nude mice were photographed, and the tumour xenografts were harvested at the end of the study. Harvested xenografts were also photographed and weighed. Thereafter, total RNA and protein were isolated from the xenograft tissues to perform RT-qPCR and Western blotting. The study was conducted following approval from the Institute Animals Ethics Committee. The miRNA mimic used in the study, miRIDIAN microRNA hsa-miR-617-Mimic (cat# C-300943-01-0020) and miRIDIAN microRNA Mimic Negative Control #1(cat # CN-001000-01-20) were purchased from Dharmacon, Inc (Lafayette, CO, USA).

3.15. Statistical Analysis

The comparison between any two experimental data sets was performed by calculating the statistical significance using the student's t test with Welch's correction in the GraphPad Prism 8 software. Differences in two data sets were considered significant when P-values were ≤0.05 (*), <0.01 (**), <0.001 (***), <0.0001 (****) or non-significant (ns) when the P-value was >0.05.

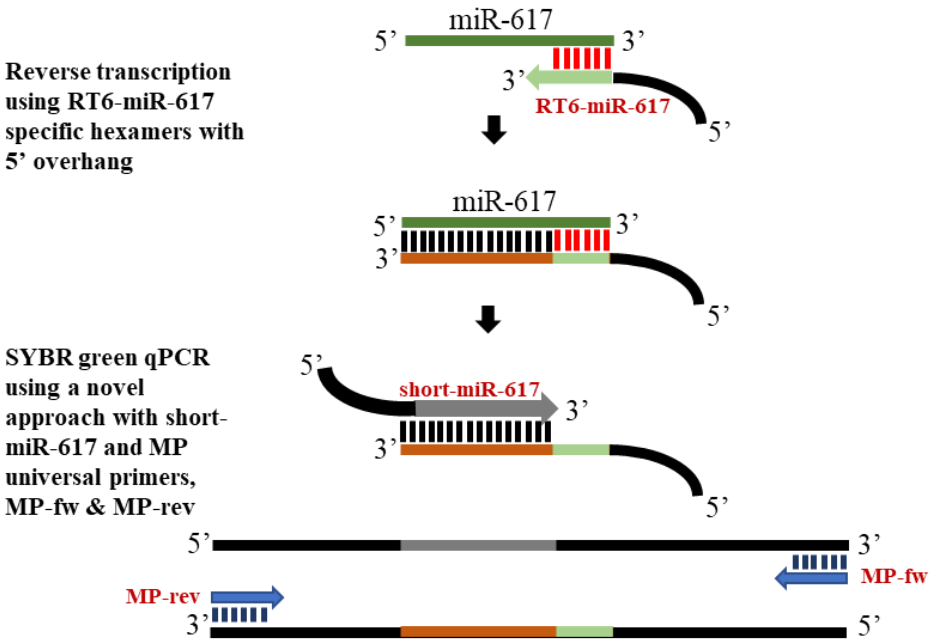

Figure 3: The miR-Q RT-PCR technique. miR-Q-RT-PCR assay for checking the expression of mature miR-617 (Adapted from Sharbati-Tehrani et al., 2008).

Table 3: Details of the plasmid constructs used in the study.

Sl. No.	Construct	Cloning vector	Primer sequence (5' to 3')	Amplicon size (bp)	Annealing temp. (°C)
1	pmiR-617	pcDNA3-*EGFP*	F: ATCGAAGCTTCCTGGAGCCATGTCACGGAAGCTA *Hind*III R: CTAGCTCGAGTGGGATCAACTCTGGTGCTCCTCC *Xho*I	206	56
2	p*DDX27*	pcDNA3.1(+)	F: GCTAGCGGCCGCGCTAGGTACCCGGAAGTGGCTTCTGCGACAAC *Kpn*I R:TAGCGATATCCTACTTCCTCCTCTTGTATCTGG *Eco*RV Internal primer 1: CTCCAGTCACCCGCGTGCTGGTG	2413	56
3	p3'UTR-S	pMIR-REPORT™	F: GCTAGAGCTCGTCGTGGCCTGAAGAAATTCATG *Sac*I R: TAGCACGCGTTCAGCAAGAAGGGAGATTGACAG *Mlu*I	186	56
4	pGL3-PrMIR617-F1	pGL3-Basic	F: TAGCACGCGTGGGATAATTCTTTCTGGGGGAG *Mlu*I R: GCTACTCGAGGGCAATTAGGAGTAGTGCATCC *Xho*I	825	62
5	pGL3-PrMIR617-F2	pGL3-Basic	F: GCTAACGCGTTAGAGTTAGACTCTCCGCCCAG *Mlu*I R: TAGCCTCGAGCCTGTAGAGACAGATTCAATACC *Xho*I	3175	60
6	pGL3-PrDDX27	pGL3-Basic	F: GCTAGAGCTCGCTAACGCGTGTGCCGTGACTAAAGGTGTGAACCAC *Sac*I *Mlu*I R: TAGCGATATCTAGCCTCGAGTACCATGCGTCACTTCCGTTCCAGAG *Eco*RV *Xho*I	709	56
7	pPr-null-DDX27	pGL3-Basic	F: GCTACTCGAGCGGAAGTGGCTTCTGCGACAAC *Xho*I R: TAGCTCTAGACTACTTCCTCCTCTTGTATCTGG *Xba*I	2413	56

Sl. No.	Plasmid constructs generated by sub-cloning				
8	pPr-DDX27	Template-pGL3-PrDDX27	Cloned upstream to *DDX27* ORF in pPr-null-DDX27	Cloning vector-pPr-null-DDX27	F:GCTAGAGCTCGCTAACGCGTGTGCCGTGACTAAAGGTGTGAACCAC *Sac*I *Mlu*I R: TAGCGATATCTAGCCTCGAGTACCATGCGTCACTTCCGTTCCAGAG *Eco*RV *Xho*I
9	pPr-M-DDX27	Template-pGL3-PrDDX27-M	Cloned upstream to *DDX27* ORF in pPr-null-DDX27		
10	pDDX27-3'UTR	Template-p3'UTR-S	Cloned downstream to *DDX27* ORF in pDDX27	Cloning vector-pDDX27	F: GCTAGATATCGTCGTGGCCTGAAGAAATTCATG *Eco*RV R: TAGCGCGGCCGCTCAGCAAGAAGGGAGATTGACAG *Not*I
11	pBSKS-PrDDX27	Template-pGL3-PrDDX27	Cloned at the MCS in pBSKS(+)	Cloning vector-pBSKS(+)	F: GCTAGAGCTCGCTAACGCGTGTGCCGTGACTAAAGGTGTGAACCAC *Sac*I *Mlu*I R: TAGCGATATCTAGCCTCGAGTACCATGCGTCACTTCCGTTCCAGAG *Eco*RV *Xho*I
12	pBSKS-PrDDX27-M	Template-pBSKS-PrDDX27	Cloned at the MCS in pBSKS(+)		F: CTGAGGCGGGAGGATGGGGTTGCAGTGATC R: GATCACTGCAACCCCATCCTCCCGCCTCAG

Abbreviations: F, forward primer; R, reverse primer; bp, base pair; and, temp, temperature.

Table 4: Details of constructs generated by site-directed mutagenesis in the study.

Construct	Template vector	Primer sequence (5' to 3')
pmiR-617-M	pmiR-617	F: CATCATAAGGAGCCTCATTTGAAGGTGGCC R: GGCCACCTTCAAATGAGGCTCCTTATGATG
pGL3-PrDDX27-M	pBSKS-PrDDX27 [*DDX27* promoter sub-cloned in pBSKS(+)]	F: CTGAGGCGGGAGGATGGGGTTGCAGTGATC R: GATCACTGCAACCCCATCCTCCCGCCTCAG

Table 5: Functional features of plasmid constructs generated during the present study.

SL. No.	Construct	Functional features
1	pGL3-PrMIR617-F1	F1 fragment of the *MIR617* promoter upstream to *luc* ORF at the MCS
2	pGL3-PrMIR617-F2	F2 fragment of the *MIR617* promoter upstream to *luc* ORF at the MCS
3	pmiR-617	Pre-miR-617 at the MCS
4	pmiR-617-M	Mutated seed region in pre-miR-617 at the MCS
5	pGL3-PrDDX27	*DDX27* promoter fragment upstream to *luc* ORF at the MCS
6	pGL3-PrDDX27-M	Target site mutated *DDX27* promoter fragment upstream to *luc* ORF at the MCS
7	pBSKS-PrDDX27	*DDX27* promoter fragment at the MCS
8	pBSKS-PrDDX27-M	Target site mutated *DDX27* promoter fragment at the MCS
9	p3'UTR-S	3'UTR of *DDX27* cloned downstream to *luc* ORF at the MCS
10	pDDX27	*DDX27* ORF at the MCS
11	pDDX27-3'UTR	*DDX27* ORF and its 3'UTR in a sense orientation at the MCS
12	pPr-null-DDX27	*DDX27* ORF in place of *luc* ORF without any promoter
13	pPr-DDX27	*DDX27* ORF in place of *luc* ORF with its own promoter at the MCS
14	pPr-M-DDX27	*DDX27* ORF in place of *luc* ORF with its own target-site mutated promoter at the MCS

Table 6: A summary of the clinicopathological features of patients included in the study.

Characteristics	No. of patients (36)
Mean Age/Range (yr)	56.1 (32-71)
50	15 (41.66%)
>51	21 (58.33%)
Gender	
Females	23 (63.88%)
Males	13 (36.11%)
Site of cancer	
BM	9 (25%)
Tongue	4 (11.11%)
GBS	7 (19.44%)
RMT	2 (5.55%)
Lip	1 (2.77%)
BM + RMT	1 (2.77%)
BM + GBS	9 (25%)
GBS + RMT	1 (2.77%)
BM + GBS + RMT	2 (5.55%)
Tumour classification	
T1	0 (0%)
T2	3 (8.33%)
T3	13 (36.11%)
T4	20 (55.55%)
Differentiation	
Well	16 (44.44%)
Moderate	13 (36.11%)
Poor	7 (19.44%)

Abbreviations: yr, years; BM, buccal mucosa; GBS, gingivo-buccal sulcus; RMT, retromolar trigone; and, T, tumour.

Table 7: Detailed clinicopathological parameters of the patients included in the study.

Sl. No.	Pt. No.	Age (yr)	Sex	Site of cancer	TNM	Differentiation	Habit
1	3	65	F	BM	T4aN2M0	Moderate	Nil
2	11	50	F	GBS+ BM	T2N0M0	Poor	Betel nut chewing
3	12	46	M	GBS+ BM	T3N2M1	Well	Tobacco chewing
4	25	52	M	GBS+ BM+ RMT	T3aN1M0	Well	Betel nut + Tobacco chewing
5	35	57	F	GBS+ BM+ RMT	T4aN1M1	Well	Betel nut chewing
6	36	65	F	GBS+BM	T4N1M0	Moderate	Betel nut chewing
7	37	32	F	Tongue	T3aN1M0	Poor	Areca nut chewing
8	38	47	M	GBS+ BM	T4aN1M0	Well	Paan + Tobacco chewing
9	39	45	M	BM+RMT	T4aN2M0	Well	Paan chewing
10	40	61	F	BM	T2aN2M0	Moderate	Tobacco chewing
11	41	58	F	Tongue	T4aN2M0	Well	Betel nut chewing
12	42	63	F	BM	T3aN1M0	Poor	Betel nut + Tobacco chewing
13	43	39	F	RMT	T4N1M0	Well	Betel nut + Tobacco chewing
14	47	54	M	GBS+ BM	T3aN1M0	Poor	Tobacco chewing
15	62	53	M	Tongue	T3aN1M0	Moderate	Nil
16	67	43	F	GBS + BM	T3aN2M0	Moderate	Tobacco chewing
17	71	56	F	GBS +BM	T4N2M0	Well	Areca Nut
18	72	44	M	GBS+ RMT	T4aN1M0	Well	Tobacco chewing
19	73	70	M	BM	T4aN1M0	Poor	Tobacco chewing
20	74	56	F	GBS + BM	T4aN1M0	Moderate	Betel nut + Tobacco chewing
21	75	42	M	GBS	T4aN1M0	Poor	Betel nut + Tobacco chewing
22	76	33	M	GBS	T3aN1M0	Moderate	Tobacco chewing
23	77	71	F	GBS	T2N1M0	Moderate	Tobacco chewing
24	78	65	F	GBS	T4aN1M0	Well	Betel nut + Tobacco chewing
25	79	56	M	BM	T4aN1M0	Well	Tobacco chewing
26	80	32	M	BM	T3aN1M0	Moderate	Tobacco chewing
27	81	52	F	BM	T4aN1M0	Well	Tobacco chewing
28	82	54	F	GBS	T4aN2M1	Poor	Tobacco chewing
29	83	71	F	Lower Lip	T4aN2bM0	Moderate	Betel nut chewing
30	84	55	F	RMT	T3aN2bM0	Well	Betel nut chewing
31	85	45	F	BM	T3N2bM0	Moderate	Betel nut chewing
32	86	68	F	BM+GBS	T4aN1M0	Well	Tobacco chewing
33	87	42	F	GBS	T4aN1M0	Well	Betel nut chewing
34	88	45	F	GBS	T3N2bM0	Moderate	Tobacco chewing
35	89	36	M	Tongue	T3N2bM0	Moderate	Gutkha
36	90	56	F	BM	T4aN1M0	Well	Nil

Abbreviations: Pt. No., patient number; yr, years; M, male; F, female; TNM, Tumour Node and Metastasis; BM, buccalmucosa; GBS, gingivo-buccal sulcus; and, RMT, retromolar trigone.

Table 8: Details of primers used in bisulphite sequencing PCR analysis.

Promoter	Sequence (5' to 3')	Amplicon size (bp)	Annealing temp. (°C)
miR-617 promoter F2-I	F:GAGGGAAAGATGGTAATTTAGAGG R:CCTCCATCAACCTATTCATTCTAAC	218	56
miR-617 promoter F2-II	F: TAGGGTTGAAGGGATGGGTTTGAG R: CACCTTACATATCCAATCAATCACC	344	63
DDX27 promoter	F: AAAGTTTCGGGGTTGTGCGTAG R: CGACCTCTTAAAAATACGCATACG	566	60

Table 9: Details of primers used in RT-qPCR.

Gene	Sequence (5' to 3')	Amplicon size (bp)	Annealing temp. (°C)	Reference
GAPDH	F: GAAGGGTGAAGGTCGGAGTC R: GAAGATGGTGATGGGATTTC	226	56	-
MIR617 (miR-617)	RT6-miR-617 TGTCAGGCAACCGTATTCACCGTGAGTGGTGCCACC Short-miR-617-rev CGTCAGATGTCCGAGTAGAGGGGGAACGGCGAGAC TTCCCATTTGAAGGT MP-fw: TGTCAGGCAACCGTATTCACC MP-rev: CGTCAGATGTCCGAGTAGAGG	83	63	Present study; Sharbati-Tehrani et al., 2008
5S rRNA	F: GCCCGATCTCGTCTGATCT R: AGCCTACAGCACCCGGTATT	93	60	-
MCPH1	F: TCACCACAGCGCAATGGAGAAGAGA R: ATCACGTGAAATGTTCAAAGGTGCTTC	109	60	Venkatesh et al., 2013
DDX27	F:TGCATTTGCCATTTCCTCAGC R: CCAGATCTTTCACCTCGTCTGT	159	60	-

RESULTS

4. Results

4.1. Validation of miR-617 upregulation following 5-Azacytidine treatment by RT-qPCR

The microRNA microarray data obtained from comparing the expression profiles of vehicle control (DMSO)- and 5-Azacytidine-treated SCC131 cells revealed that miR-617 was upregulated in 5-Azacytidine-treated cells in comparison to those treated with vehicle control (Table 2; Figure 2). Thus, miR-617 upregulation post 5-Azacytidine treatment was validated by RT-qPCR and semi-quantitative RT-PCR using RT6-miR-617 and short miR-617 primers specific to miR-617 (Table 9). Consequentially, statistically significant upregulation was observed in miR-617 expression in 5-Azacytidine-treated cells compared to those treated with the vehicle control (Figure 4), showing congruence with the microRNA microarray data.

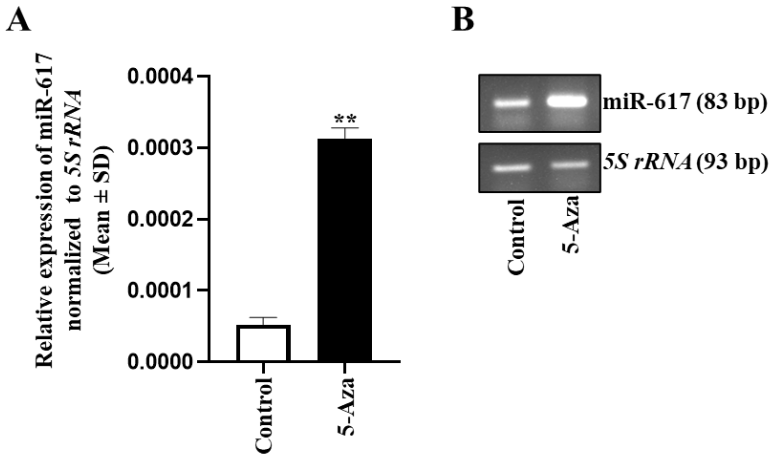

Figure 4: Validation of miR-617 upregulation following 5-Azacytidine treatment of SCC131 cells by RT-qPCR. (A) Upregulation of miR-617 in 5-Azacytidine-treated cells compared to vehicle control (DMSO)-treated cells. Each bar for RT-qPCR is an average of 2 technical replicates. (**B)** Representative agarose gel images to show the miR-617 upregulation in 5-Azacytidine-treated cells compared to DMSO-treated cells by semi-quantitative RT-PCR**.** *Abbreviation:* 5-Aza, 5-Azacytidine.

4.2. Characterization of the *MIR617* promoter

Since miR-617 showed upregulation in 5-Azacytidine treated cells compared to those treated with the vehicle control, we intended to elucidate the underlying mechanism of its upregulation after the 5-Azacytidine treatment. We hypothesized that the upregulation of miR-617 post 5-Azacytidine treatment was due to at least one of the following three mechanisms.

1. MiR-617 may be transcribed by its independent promoter that undergoes demethylation upon 5-Azacytidine treatment.
2. The host gene *LIN7A* and the intronic miR-617 have the same direction of transcription, indicating the possibility of *LIN7A* promoter-driven transcription of miR-617. Thus, the demethylation of *LIN7A* promoter may upregulate miR-617.
3. The promoter of transcription factors (activators) regulating miR-617 may be demethylated to cause miR-617 upregulation.

Thus, to explore the first possible mechanism, we decided to characterise the *MIR617* promoter as it was not previously reported in literature. The *MIR617* gene is located in the fourth intron (34 kb) of the host gene *LIN7A* (145.41 kb) (Figure 5). Therefore, we sought bioinformatics analysis to retrieve the putative *MIR617* promoter sequence (Fragment F1: 825 bp, from -365 bp to +460 bp relative to TSS) using the DBTSS database (Figure 6A). This fragment was then cloned in the promoter-null pGL3-Basic vector, and the resulting construct pGL3-PrMIR617-F1 was transfected in SCC131 cells along with the relevant negative (pGL3-Basic) and positive (pGL3-Control) controls to perform dual-luciferase reporter assay. The results showed that the fragment F1 did not have any promoter activity as compared to the pGL3-Basic vector (Figure 6B & C). Thus, we speculated the requirement of additional upstream sequences to show promoter activity and cloned a larger fragment (Fragment F2: 3175 bp, from -2925 bp to +250 bp relative to TSS), which was bioinformatically predicted by the Promoter 2.0 and PROMO databases (Figure 7A). Then the F2 fragment (construct pGL3-PrMIR617-F2) was transfected in SCC131 cells, and the results of dual-luciferase reporter assay demonstrated a significant increase in promoter activity compared to the pGL3-Basic vector (Figure 7B & C), suggesting that it represents the independent promoter of *MIR617.*

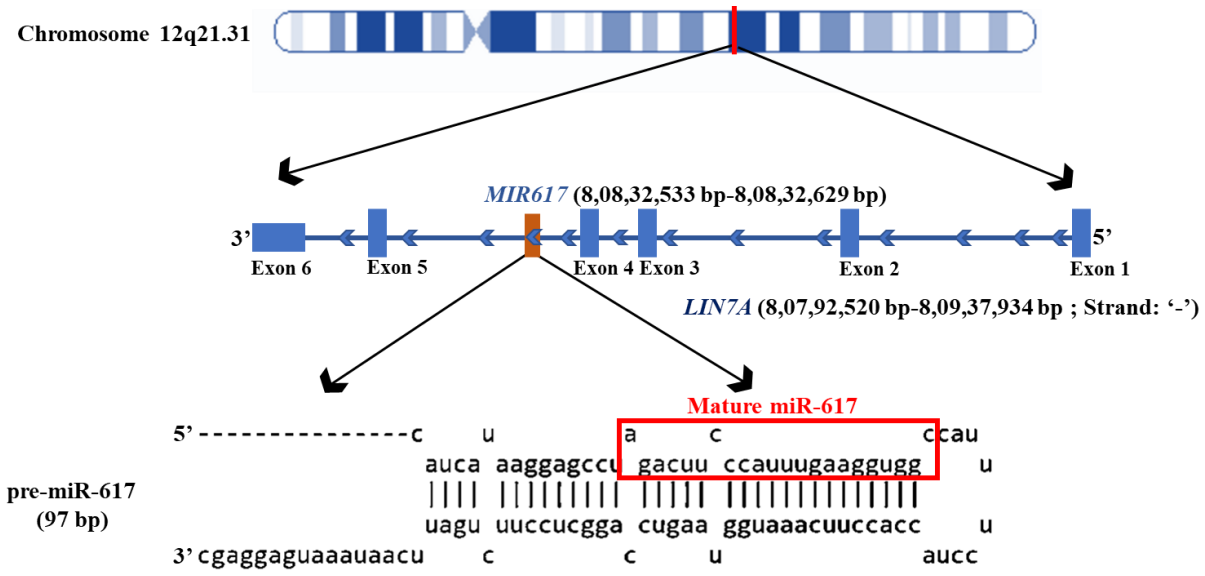

Figure 5: Schematic diagram to show the genomic location of intronic *MIR617* gene in its host gene *LIN7A* on chromosome 12q21.31. Note, *MIR617* is located between exons 4 and 5, and the direction of transcription of both *MIR617* and *LIN7A* is the same. In the pre-miR-617 stem-loop structure depicted above, the mature miR-617 is marked by a red rectangle.

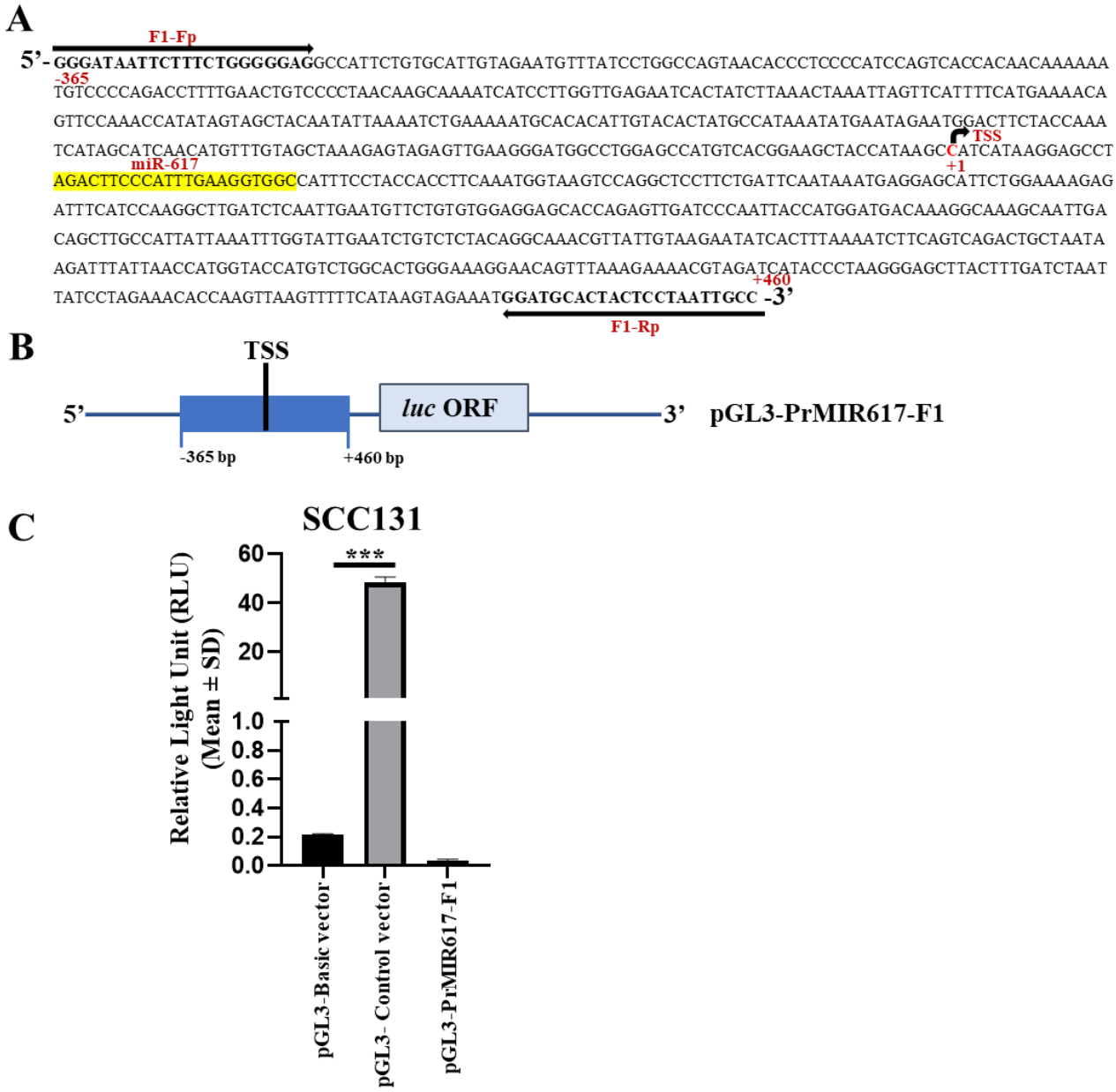

Figure 6: Characterization of the *MIR617* gene promoter. (A) The putative promoter sequence of *MIR617* retrieved from the DBTSS database. PCR primers for the putative promoter fragment F1 (F1-Fp and F1-Rp) are shown. The miR-617 is highlighted in yellow. **(B)** Schematic diagram of the putative promoter construct. **(C)** Dual-luciferase reporter assay to characterize the promoter of *MIR617* in SCC131 cells. Note, no significant promoter activity was observed for the pGL3-PrMIR617-F1 promoter construct. The pGL3-Control construct harbouring the SV40 promoter was used as a positive control. Each bar is an average of 3 biological replicates. *Abbreviation:* TSS, Transcription start site.

A

F2-Fp

5'-**TAGAGTTAGACTCTCCGCCCAG**TTTAAGTCATCTCCTCTGCTTTTTGTTTATCTTCAAGAGACAATAAAAGTCCCCCATTAAATACTCTAATTTCAG
-2925
AGGAAATTGGATCCTTGTCATTGGTGGGTTGATTATGGGCAAGTCATTGGAATTTTTGGTGTCTTTATATCTGCAGGACTGATGTAACAACACCTGT
CCTGTCTACCTTTCCTAATAGTAATTAGGATAAAAAAGAGAAATGATAAATACAGCATTAAAAGATAAGACTTATGCTTCCACAATTACACAGCAT
TGTTGCTGTATATTATTATTAAACAGCCTTTCACCAAACTTCCAGATGCATCTCTCCATGTTTCCTATTGCAACATTTTTCCTTAATTTACAAAAACA
GAATATGTAAACCAAGTAATGGTCCTTCTTCTGTTCTAGCTGAGAAATGTGTGGTTTATCTCAAATGAATAGAATATTTGTCTTGAAATCCTGTGCTG
GTCCAAAAAAGCATCATTTATATTTTGTGGAACTCACCAAGCCCAATTACCAGTGATTGCTTTAAACATTAGTGAAAAGCCAATGATTCGATTTAAT
CCTAACTTGGGAGGAACATTCTTCTAACTTATTTATGCTGGTCTACAGACTGTTGGCACTAGCCTAAAGCAAGGTTGGAATGTTAATATGCCACAGC
TACATGAGTATACCTAGTGAAATGCAAGCCAAGTGTAAGTCTAAGGGTTTATATAATTTTCCATAATGGATTTATATCTTGTTCTGTTTTTAATTATA
TTCTCAAAAACAGAAGACACTGATACATATGGCAATCAGATGACATGTCACAAGCCACATGTGATTGCTCACAGGTTCATGTGAGATAACCAAACT
TTAACTCAAATGTTGGTTGCTGAGTCTCAGATATGGGAAATGAGTATCAGCAATTGTGGTATTAGAACTACATCTTTCTAAGTTCAGCCAGGAGGTA
TGGGCTGTTTCAATAAATTTGCAAATGAATCACATTTGATCATAGGCCTTTCCTACTTGGGTTTCTTTCTCTTCTCTCATAGATACAAAATCATTAGT
TGCTAATTTTATCACAGCCAACCTTACTCTGAATTGTAAATTATTGACCTTGCCCTTCAGTGACACCAAATCACTTCTCAAGAGAAGTCATGTTTTCT
ATTTACAGAGGTGCCTATTATCACCAACTGTGTAAATATATAGCATATCTTAAGCTTTAAGAATATAAATTTGAATAAGAACCAAAGCATAAGACTT
TAGATCCTGAAGTCAAAATCTGTATATGTAGTATACAAGATTTGATCTAGCATCAGCCTGAACCTATCTTATCACCCAGCACTACCATTTCAACATA
GATTTTTCATTCTGAACTAATCACTATATATGTGGTAGTCCTTACATACTTAAAAATCGAGTAAAATGTGACATCAGAAGAGTTGAGGATTCTGGGC
AGTCTCTGAGCTTCTACCTCTGAAAGTCAAGGGAACATGACATTGTACTAGATTTGGTTTTGCAAAAGGCTATCCAGGAAGTAGGAGTGGTTAAATT
TGACTATTTTAGGGTCCAGAAGGAGATTAGATAAGTGAGCAGAGATAATCAAGAGGGAAAGATGGCAATCTAGAGGAGAAATGCCCTATTACAAT
TCTAGCCGGTTATTGCCATTTGGTACTGTGGACAGTGTAGCGAAAATTCAGAATTTAAAAACAAGCAAACAACACCTTCTGCCTTTGTAGAGGAAAT
GGTATATATAATAAGAAGCATTTTAAAGGATTAATAGTAGTTATCTATGGAATGTTAGAATGAATAGGTTGATGGAGGGCATTCTAGACAGAGGGA
CAACATCTACAGAAACATATAAGAAACAACATGTTTGTAGCTAAAGAGTAGGGTTGAAGGGATGGGCTTGAGCCACATCATGGAAGACACCATAA
GCCATCACAAGGAGCCCGGACTTAACATTTGAAAGTGGTAGGAAATTGCCAAAATGACATGAATTTTTATAGGTTATTCTGGCAATTGCCAACATG
TGGGCATAGGGTGTGTGAAGGCATGGAGGAAAAGCCGGAGGTGGAAGATCAACCAGGACACTCTTAGAAGTTCTGGAGGGACATGGTGGAGGTCT
TAACTGGAAGAGGGGCAATTTGGAGAGAAAGGAAAAGATTTGAAAATGACTTTGGATGTAACGGGACTATAAACAAGAACTGGTGATTGACTGGA
TATGCAAGGTGAAGAATAGGGAGTTACCAAGAACTCTTGGGTTTCTGACAAGGATCTTGCCTCTTGTTGACACAGCAGAAAAGATGGTTCAGGTGA
GAGTGAGCAGCTGAGTACTTGGAGGTTGTGTTGTCTATGGCTCAGCCATATGAACATAAACAAGGGCATAGGTTTTAATTTAGTTTTGCCTTTTCCA
AGATGTAAATTTAATTAACTGAGCTCTATCAAACTGACAGCATTTCGAAGTAGAACACTTAAAAATTATATTATGTAAACTTTTCACTCAATTACAT
TTGTCAACCAGGATTTCTCACCCTTGAAATTGCTGATATTTTGAATGGGATAATTCTTTCTGGGGGAGGCCATTCTGTGCATTGTAGAATGTTTATCC
TGGCCAGTAACACCCTCCCCATCCAGTCACCACAACAAAAAATGTCCCCAGACCTTTTGAACTGTCCCCTAACAAGCAAAATCATCCTTGGTTGAGA
ATCACTATCTTAAACTAAATTAGTTCATTTTCATGAAAACAGTTCCAAACCATATAGTAGCTACAATATTAAAATCTGAAAAATGCACACATTGTAC
ACTATGCCATAAATATGAATAGAATGGACTTCTACCAAATCATAGCATCAACATGTTTGTAGCTAAAGAGTAGAGTTGAAGGGATGGCCTGGAGCC
TSS miR-617
ATGTCACGGAAGCTACCATAAGCCATCATAAGGAGCCTAGACTTCCCATTTGAAGGTGGCCATTTCCTACCACCTTCAAATGGTAAGTCCAGGCTCC
+1
TTCTGATTCAATAAATGAGGAGCATTCTGGAAAAGAGATTTCATCCAAGGCTTGATCTCAATTGAATGTTCTGTGTGGAGGAGCACCAGAGTTGATC
+250
CCAATTACCATGGATGACAAAGGCAAAGCAATTGACAGCTTGCCATTATTAAATTT**GGTATTGAATCTGTCTCTACAGG** -3'
F2-Rp

B

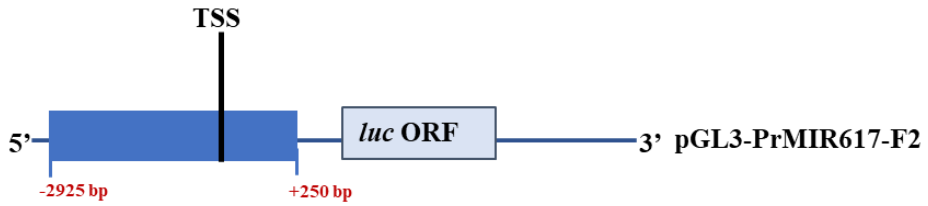

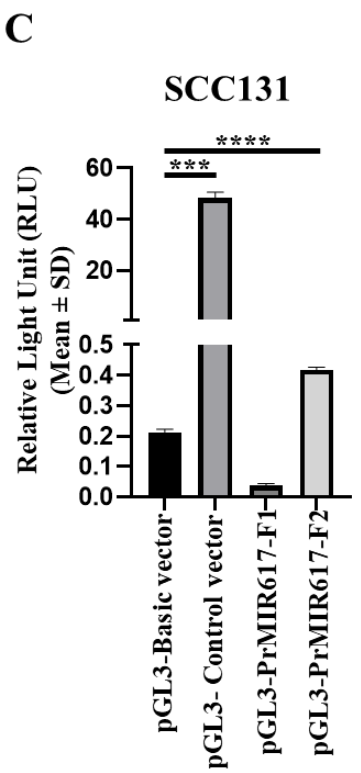

Figure 7: Characterization of the *MIR617* gene promoter. (A) The putative promoter sequence of *MIR617* retrieved from the promoter 2.0 and PROMO databases. PCR primers for the putative promoter fragment F2 (F2-Fp and F2-Rp) are shown. The miR-617 is highlighted in yellow. **(B)** Schematic diagram of the putative promoter construct. **(C)** Dual-luciferase reporter assay to characterize the promoter of *MIR617* in SCC131 cells. Note, a significant promoter activity was observed for the fragment F2 cloned in the pGL3-PrMIR617-F2 construct with respect to the pGL3-Basic vector. Each bar is an average of 3 biological replicates.

4.3. Analysis of the *MIR617* promoter by bisulphite sequencing PCR (BSP)

In order to decipher the mechanism of miR-617 upregulation post 5-Azacytidine treatment, we scanned the *MIR617* promoter for CpG sites to investigate their methylation status in SCC131 cells. The *MIR617* promoter has 10 CpG sites scattered across the 3,175 kb F2 fragment (Figure 8). Since it is difficult to amplify a large fragment using sodium bisulphite-treated DNA as a template, we first chose a 638 bp long CpG dense region comprising five CpG sites (Figure 8) and divided it into two subregions: F2-I (218 bp) and F2-II (344 bp) (Figure 9A). It is known that the treatment of genomic DNA with sodium bisulphite results in the deamination of unmethylated 'C' in CpG to 'U' and eventually to 'T' during PCR amplification, whereas methylated 'C' residue in CpG remains 'C'. Thus, genomic DNA isolated from DMSO- and 5-Azacytidine- treated SCC131 cells were treated separately with sodium bisulphite and F2-I and F2-II fragments were amplified with BSP-specific primers using sodium bisulphite-treated genomic DNA samples as templates. The PCR products were then cloned into a TA vector, and 10 random clones were sequenced for each experiment. The Sanger sequencing results showed that the methylation percentage of fragment F2-I decreased from 100% to 45% in 5-Azacytidine-treated cells as compared to DMSO-treated cells (Figure 9B). Similarly, the percentage of methylation in fragment F2-II decreased from 80% to 63.34% in 5-Azacytidine-treated cells as compared to DMSO-treated cells (Figure 9C). Overall, the

combined methylation percentage of fragments F2-I and F2-II significantly decreased from 88% to 56% in 5-Azacytidine-treated cells as compared to DMSO-treated cells (Figure 9D), suggesting that the demethylation of the *MIR617* promoter is one of the mechanisms for its upregulation following the 5-Azacytidine treatment of SCC131 cells.

```
                                CpG-1
5'-TAGAGTTAGACTCTCCGCCCAGTTTAAGTCATCTCCTCTGCTTTTTGTTTATCTTCAAGAGACAATAAAAGTCCCCCATTAAATACTCTAATTTCAGAGGAAATTGGAT
-2925
CCTTGTCATTGGTGGGTTGATTATGGGCAAGTCATTGGAATTTTTGGTGTCTTTATATCTGCAGGACTGATGTAACAACACCTGTCCTGTCTACCTTTCCTAATAGTAA
TTAGGATAAAAAAGAGAAATGATAAATACAGCATTAAAAGATAAGACTTATGCTTCCACAATTACACAGCATTGTTGCTGTATATTATTATTAAACAGCCTTTCACCA
AACTTCCAGATGCATCTCTCCATGTTTCCTATTGCAACATTTTTCCTTAATTTACAAAAACAGAATATGTAAACCAAGTAATGGTCCTTCTTCTGTTCTAGCTGAGAAA
TGTGTGGTTTATCTCAAATGAATAGAATATTTGTCTTGAAATCCTGTGCTGGTCCAAAAAAGCATCATTTATATTTTGTGGAACTCACCAAGCCCAATTACCAGTGATT
                                CpG-2
GCTTTAAACATTAGTGAAAAGCCAATGATTCGATTTAATCCTAACTTGGGAGGAACATTCTTCTAACTTATTTATGCTGGTCTACAGACTGTTGGCACTAGCCTAAAG
CAAGGTTGGAATGTTAATATGCCACAGCTACATGAGTATACCTAGTGAAATGCAAGCCAAGTGTAAGTCTAAGGGTTTATATAATTTTCCATAATGGATTTATATCTT
GTTCTGTTTTTAATTATATTCTCAAAAACAGAAGACACTGATACATATGGCAATCAGATGACATGTCACAAGCCACATGTGATTGCTCACAGGTTCATGTGAGATAAC
CAAACTTTAACTCAAATGTTGGTTGCTGAGTCTCAGATATGGGAAATGAGTATCAGCAATTGTGGTATTAGAACTACATCTTTCTAAGTTCAGCCAGGAGGTATGGGC
TGTTTCAATAAATTTGCAAATGAATCACATTTGATCATAGGCCTTTCCTACTTGGGTTTCTTTCTCTTCTCTCATAGATACAAAATCATTAGTTGCTAATTTTATCACAG
CCAACCTTACTCTGAATTGTAAATTATTGACCTTGCCCTTCAGTGACACCAAATCACTTCTCAAGAGAAGTCATGTTTTCTATTTACAGAGGTGCCTATTATCACCAAC
TGTGTAAATATATAGCATATCTTAAGCTTTAAGAATATAAATTTGAATAAGAACCAAAGCATAAGACTTTAGATCCTGAAGTCAAAATCTGTATATGTAGTATACAAG
ATTTGATCTAGCATCAGCCTGAACCTATCTTATCACCCAGCACTACCATTTCAACATAGATTTTTCATTCTGAACTAATCACTATATATGTGGTAGTCCTTACATACTT
      CpG-3
AAAAATCGAGTAAAATGTGACATCAGAAGAGTTGAGGATTCTGGGCAGTCTCTGAGCTTCTACCTCTGAAAGTCAAGGGAACATGACATTGTACTAGATTTGGTTTT
GCAAAAGGCTATCCAGGAAGTAGGAGTGGTTAAATTTGACTATTTTAGGGTCCAGAAGGAGATTAGATAAGTGAGCAGAGATAATCAAGAGGGAAAGATGGCAATC
                                CpG-4                   CpG-5
TAGAGGAGAAATGCCCTATTACAATTCTAGCCGGTTATTGCCATTTGGTACTGTGGACAGTGTAGCGAAAATTCAGAATTTAAAAACAAGCAAACAACACCTTCTGC
CTTTGTAGAGGAAATGGTATATATAATAAGAAGCATTTTAAAGGATTAATAGTAGTTATCTATGGAATGTTAGAATGAATAGGTTGATGGAGGGCATTCTAGACAGA
GGGACAACATCTACAGAAACATATAAGAAACAACATGTTTGTAGCTAAAGAGTAGGGTTGAAGGGATGGGCTTGAGCCACATCATGGAAGACACCATAAGCCATCA
          CpG-6
CAAGGAGCCCGGACTTAACATTTGAAAGTGGTAGGAAATTGCCAAAATGACATGAATTTTTATAGGTTATTCTGGCAATTGCCAACATGTGGGCATAGGGTGTGTGA
                CpG-7
AGGCATGGAGGAAAAGCCGGAGGTGGAAGATCAACCAGGACACTCTTAGAAGTTCTGGAGGGACATGGTGGAGGTCTTAACTGGAAGAGGGGCAATTTGGAGAGA
                                CpG-8
AAGGAAAAGATTTGAAAATGACTTTGGATGTAACGGGACTATAAACAAGAACTGGTGATTGACTGGATATGCAAGGTGAAGAATAGGGAGTTACCAAGAACTCTTG
GGTTTCTGACAAGGATCTTGCCTCTTGTTGACACAGCAGAAAAGATGGTTCAGGTGAGAGTGAGCAGCTGAGTACTTGGAGGTTGTGTTGTCTATGGCTCAGCCATAT
                                                                                CpG-9
GAACATAAACAAGGGCATAGGTTTTAATTTAGTTTTGCCTTTTCCAAGATGTAAATTTAATTAACTGAGCTCTATCAAACTGACAGCATTTCGAAGTAGAACACTTAA
AAATTATATTATGTAAACTTTTCACTCAATTACATTTGTCAACCAGGATTTCTCACCCTTGAAATTGCTGATATTTTGAATGGGATAATTCTTTCTGGGGGAGGCCATT
CTGTGCATTGTAGAATGTTTATCCTGGCCAGTAACACCCTCCCCATCCAGTCACCACAACAAAAAATGTCCCCAGACCTTTTGAACTGTCCCCTAACAAGCAAAATCA
TCCTTGGTTGAGAATCACTATCTTAAACTAAATTAGTTCATTTTCATGAAAACAGTTCCAAACCATATAGTAGCTACAATATTAAAATCTGAAAAATGCACACATTGT
                                                                                                CpG-10
ACACTATGCCATAAATATGAATAGAATGGACTTCTACCAAATCATAGCATCAACATGTTTGTAGCTAAAGAGTAGAGTTGAAGGGATGGCCTGGAGCCATGTCACGG
                TSS
AAGCTACCATAAGCCATCATAAGGAGCCTAGACTTCCCATTTGAAGGTGGCCATTTCCTACCACCTTCAAATGGTAAGTCCAGGCTCCTTCTGATTCAATAAATGAGG
                +1
AGCATTCTGGAAAAGAGATTTCATCCAAGGCTTGATCTCAATTGAATGTTCTGTGTGGAGGAGCACCAGAGTTGATCCCAATTACCATGGATGACAAAGGCAAAGCA
ATTGACAGCTTGCCATTATTAAATTTGGTATTGAATCTGTCTCTACAGG - 3'
                                                +250
```

Figure 8: Location of CpG sites in the *MIR617* promoter. Note, the CpG sites are marked in the *MIR617* promoter. The most CpG dense region containing five CpG sites (marked in red) chosen for bisulphite sequencing PCR (BSP) analysis is underlined.

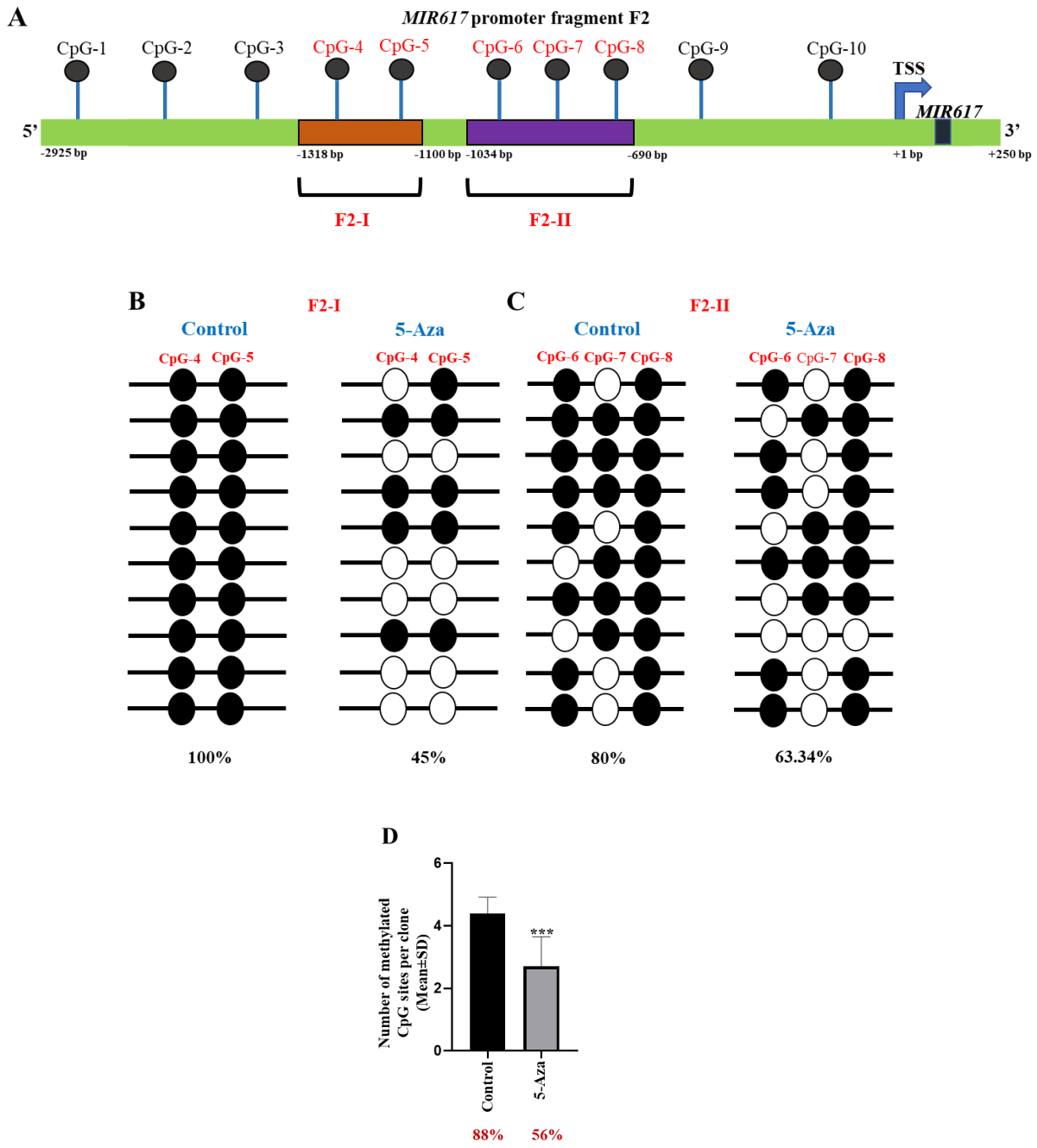

Figure 9: Analysis of the *MIR617* promoter by bisulphite sequencing PCR. (A) The schematic diagram of the two sub-regions F2-I and F2-II chosen for the BSP analysis. **(B)** The BSP analysis of F2-I fragment showed a drop in percentage methylation from 100% to 45% in 5-Azacytidine-treated cells. **(C)** The BSP analysis of F2-II fragment showed a drop in percentage methylation from 80% to 63.34% in 5-Azacytidine-treated cells. Note, each straight line with circles represents one TA clone. **(D)** Cumulative methylation percentage significantly reduces from 88% to 56% in 5-Azacytidine-treated cells compared to DMSO treated cells. Each bar is an average of 10 TA clones. The empty and filled circles represent unmethylated and methylated CpGs respectively.

4.4. miR-617 reduces the proliferation of SCC131 and SCC084 cells

Our next goal was to assess if miR-617 suppresses cell proliferation. To this end, we cloned the pre-miR-617 sequence downstream to the CMV promoter in the pcDNA3-EGFP vector. We then transiently transfected SCC131 and SCC084 cells with the pmiR-617 construct and the cloning vector pcDNA3-EGFP separately, and the cell proliferation was monitored at an interval of 24 hours for four days, using the trypan blue dye exclusion assay. The results showed that cells transfected with pmiR-617 have a significant reduction in cell proliferation as compared to those transfected with the pcDNA3-EGFP vector, thereby indicating its anti-proliferative role in OSCC cells (Figure 10).

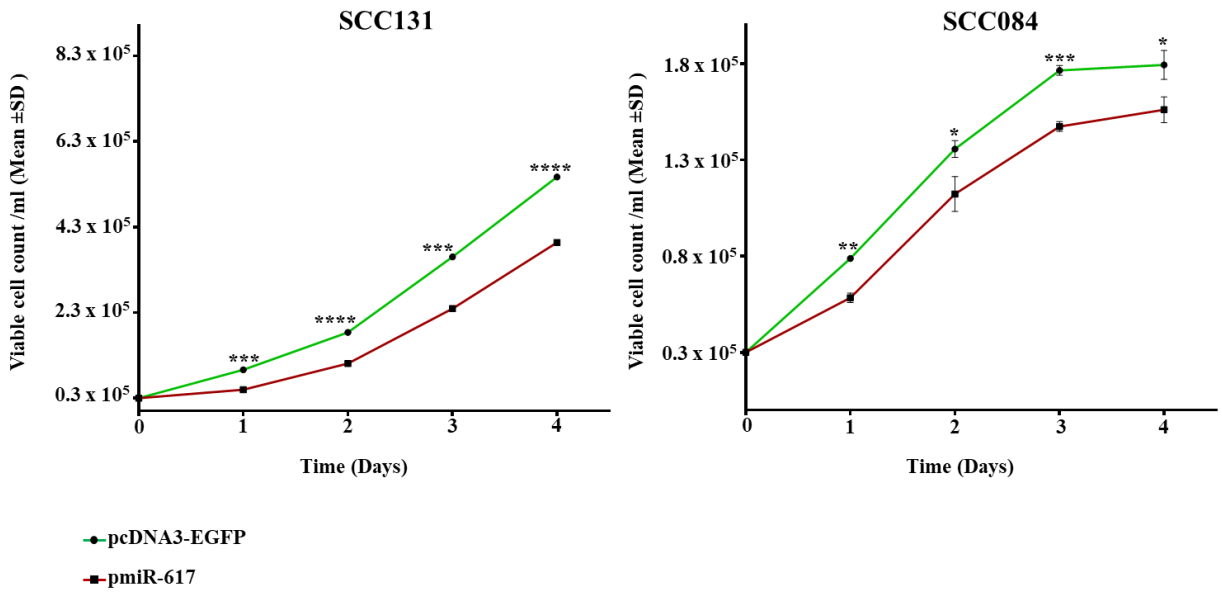

Figure 10: The transient overexpression of miR-617 reduces the proliferation of OSCC cells. Trypan blue dye exclusion assay revealed that the transient overexpression of miR-617 significantly decreases proliferation of both SCC131 and SCC084 cells compared to the vector control transfected cells. Each data point is an average of 3 technical replicates.

4.5. *In silico* identification of a potential gene target of miR-617

miRNAs exert their physiological functions by binding and regulating their cognate gene targets. The seed region of miRNAs usually binds to the target site in the 3'UTR of the gene targets to downregulate their expression. Since we have shown that miR-617 has an anti-proliferative role in OSCC cells, hence we expected its gene target to be an oncogene.

Emerging strategies for identifying miRNA targets include small-scale to large-scale genetic, molecular biology, and computational approaches. Thus, we chose to perform the

preliminary gene target screening for miR-617 by the computational method. To this end, we selected the target prediction tools according to the number of parameters considered by the algorithms for the target prediction of a particular miRNA (miR-617 in the present case), the frequency of each tool being used in miRNA-target prediction studies, the last time the software packages were updated, and their working status. Thus, we employed five target prediction tools [viz., TargetScanHuman 8.0, miRDB, MiRanda, microT-CDS (Diana Tools), and PITA] to look for miR-617 gene targets (Table 10). The following eight protein-coding genes were predicted by all the tools: *DDX27* (DEAD-Box Helicase 27), *ZFX* (Zinc finger X-chromosomal protein), *FAM179B* [(alias of TOGARAM1)-TOG array regulator of axonemal microtubules protein 1], *RFXAP* (Regulatory factor X-associated 41 protein), *MAP2K4* (Dual specificity mitogen-activated protein kinase 4), *SORBS1* (Sorbin and SH3 domain-containing protein 1), *MEX3C* (RNA-binding E3 ubiquitin protein ligase MEX3C), and *JPH1* (Junctophilin-1) (Table 10).Then we conducted a literature survey to select one of these eight genes with established oncogenic role and chose to work with *DDX27*, a known oncogene in breast, gastric, hepatocellular, and colorectal cancers. This gene codes for a protein that belongs to the family of DEAD-box proteins and is characterised by the conserved DEAD- (Asp-Glu-Ala-Asp) motif. The family of DEAD-box proteins are known to be putative RNA helicases, which are implicated in numerous cellular processes involving alteration of RNA secondary structure such as translation initiation, nuclear and mitochondrial splicing, and ribosome and spliceosome assembly (https://www.genecards.org). The structure and direct function of this protein have not been determined yet. Hence, the domain architecture of DDX27 was adapted from Uniprot, and its 3D predicted structure was obtained from the AlphaFold program for visual representation (Figure 11A & B). Moreover, this gene has not been validated as a gene target for any miRNA. Thus, we sought molecular biology approaches comprising RT-qPCR, Western blotting, and dual-luciferase reporter assay to confirm if miR-617 targets *DDX27*.

Table 10: *In silico* prediction of gene targets of miR-617 by microRNA target prediction tools. Gene targets highlighted in red were predicted by all the **five** target prediction programs**.**

Target prediction programs				
TargetScanHuman 8.0	**MiRDB**	**MiRanda**	**microT-CDS (Diana Tools)**	**PITA**
DDX27	*DDX27*	*DDX27*	*DDX27*	*DDX27*
ZFX	*ZFX*	*ZFX*	*ZFX*	*ZFX*
FAM179B	*FAM179B*	*FAM179B*	*FAM179B*	*FAM179B*
RFXAP	*RFXAP*	*RFXAP*	*RFXAP*	*RFXAP*
MAP2K4	*MAP2K4*	*MAP2K4*	*MAP2K4*	*MAP2K4*
-	*SOCS6*	*SOCS6*	*SOCS6*	*SOCS6*
SORBS1	*SORBS1*	*SORBS1*	*SORBS1*	*SORBS1*
-	*SCN9A*	*SCN9A*	*SCN9A*	*SCN9A*
HOXC4	-	*HOXC4*	*HOXC4*	*HOXC4*
-	*BTG1*	*BTG1*	*BTG1*	*BTG1*
MEX3C	*MEX3C*	*MEX3C*	*MEX3C*	*MEX3C*
JPH1	*JPH1*	*JPH1*	*JPH1*	*JPH1*
-	*WHSC1L1*	*WHSC1L1*	*WHSC1L1*	*WHSC1L1*

***Abbreviations**: DDX27*- DEAD-Box Helicase 27; *ZFX* - Zinc finger X-chromosomal protein; FAM179B (alias of TOGARAM1)-TOG array regulator of axonemal microtubules protein 1; *RFXAP*- Regulatory factor X-associated protein; *MAP2K4*- Dual specificity mitogen-activated protein kinase 4; *SOCS6*- Suppressor of cytokine signalling 6; *SORBS1*- Sorbin and SH3 domain-containing protein 1; *SCN9A*- Sodium channel protein type 9 subunit alpha; *HOXC4*- Homeobox protein Hox-C4; *BTG1*- B-cell translocation gene 1 protein; *MEX3C*- RNA-binding E3 ubiquitin-protein ligase MEX3C; *JPH1*- Junctophilin-1; and, *WHSC1L1*- Wolf-Hirschhorn syndrome candidate 1-like protein 1.

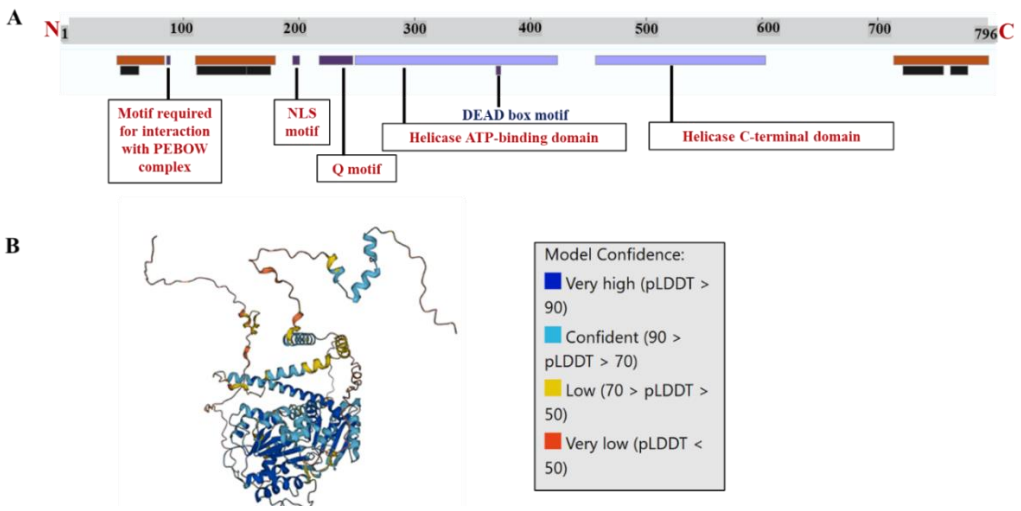

Figure 11: Domain architecture and 3D structure of DDX27. (A) Schematic diagram of the domain architecture of DDX27 protein, adapted from UniProt. **(B)** Predicted 3D structure of DDX27 from AlphaFold. *Abbreviation:* pLDDT, predicted local distance difference test.

4.6. Identification of *DDX27* as a gene target for miR-617

In order to determine if miR-617 targets *DDX27*, we transfected pmiR-617 in SCC131 cells and checked for the levels of miR-617 followed by transcript and protein levels of

DDX27. Contrary to our expectation, DDX27 was upregulated upon overexpression of miR-617 in SCC131 cells, both at the transcript and protein levels, instead of showing a presumed downregulation (Figure 12A). To further ascertain whether this was a dose-dependent regulation, SCC131 cells were transiently transfected with increasing quantities of pmiR-617. The results showed that DDX27 was upregulated by miR-617 at the transcript and protein levels in a dose-dependent manner (Figure 12B).

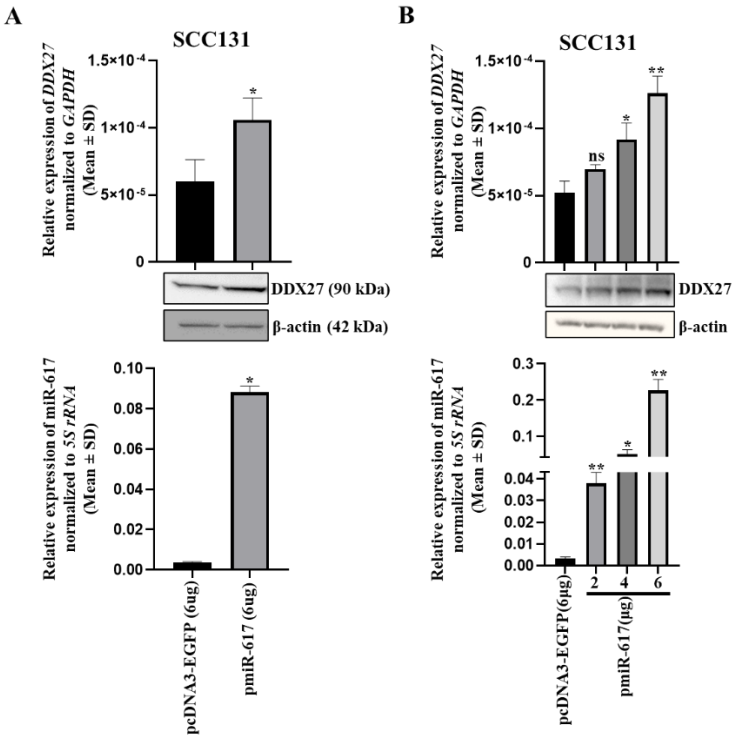

Figure 12: Identification of *DDX27* as a gene target for miR-617 in SCC131 cells. (A) Increased levels of DDX27 transcript and protein upon transient transfection of pmiR-617 in cells compared to those transfected with the vector control. **(B)** A dose-dependent regulation of DDX27 transcript and protein upon transient transfection of cells with increasing doses of pmiR-617 compared to those transfected with the vector control. For RT-qPCR data, each bar is an average of 3 technical replicates.

4.7. DDX27 upregulation is specific to the expression of miR-617

Next, we wanted to check if DDX27 upregulation was specific to the function of miR-617. To accomplish this, we deleted the seed region of miR-617 in pmiR-617 by site-directed mutagenesis to obstruct the formation of a functional miR-617. Deletion of the miR-617 seed region could either destabilize the pre-miRNA stem-loop to inhibit formation of miR-617 or re-optimise itself to generate a different small RNA entity. Therefore, the vector control, wild-type miR-617 construct (pmiR-617), and the miR-617 construct with the deleted seed region

(pmiR-617-M) were transiently transfected separately in SCC131 cells to check for the levels of miR-617 and DDX27 transcript and protein. We observed that the cells transfected with pmiR-617-M showed a comparable miR-617 level to those transfected with pcDNA3-EGFP indicating the lack of formation of a functional miR-617 from pmiR-617-M (Figure 13A). Further, the miR-617 levels were significantly increased in cells transfected with pmiR-617 in comparison to those transfected with pcDNA3-EGFP or pmiR-617-M, which was correlated with the concordant increase in DDX27 levels in pmiR-617 transfected cells compared to those transfected with pcDNA3-EGFP or pmiR-617-M. Thus, the upregulation of DDX27 is exclusively dependent on the functional miR-617 levels. To further ascertain the anti-proliferative role of miR-617, we checked for the differences in proliferation of SCC131 cells transfected separately with the vector control, pmiR-617 and pmiR-617-M constructs. As expected, cell proliferation was significantly reduced in cells transfected with pmiR-617 compared to those transfected with pcDNA3-EGFP or pmiR-617-M (Figure 13B). Therefore, the anti-proliferative function and upregulation of DDX27 were both specific to functional miR-617 formation.

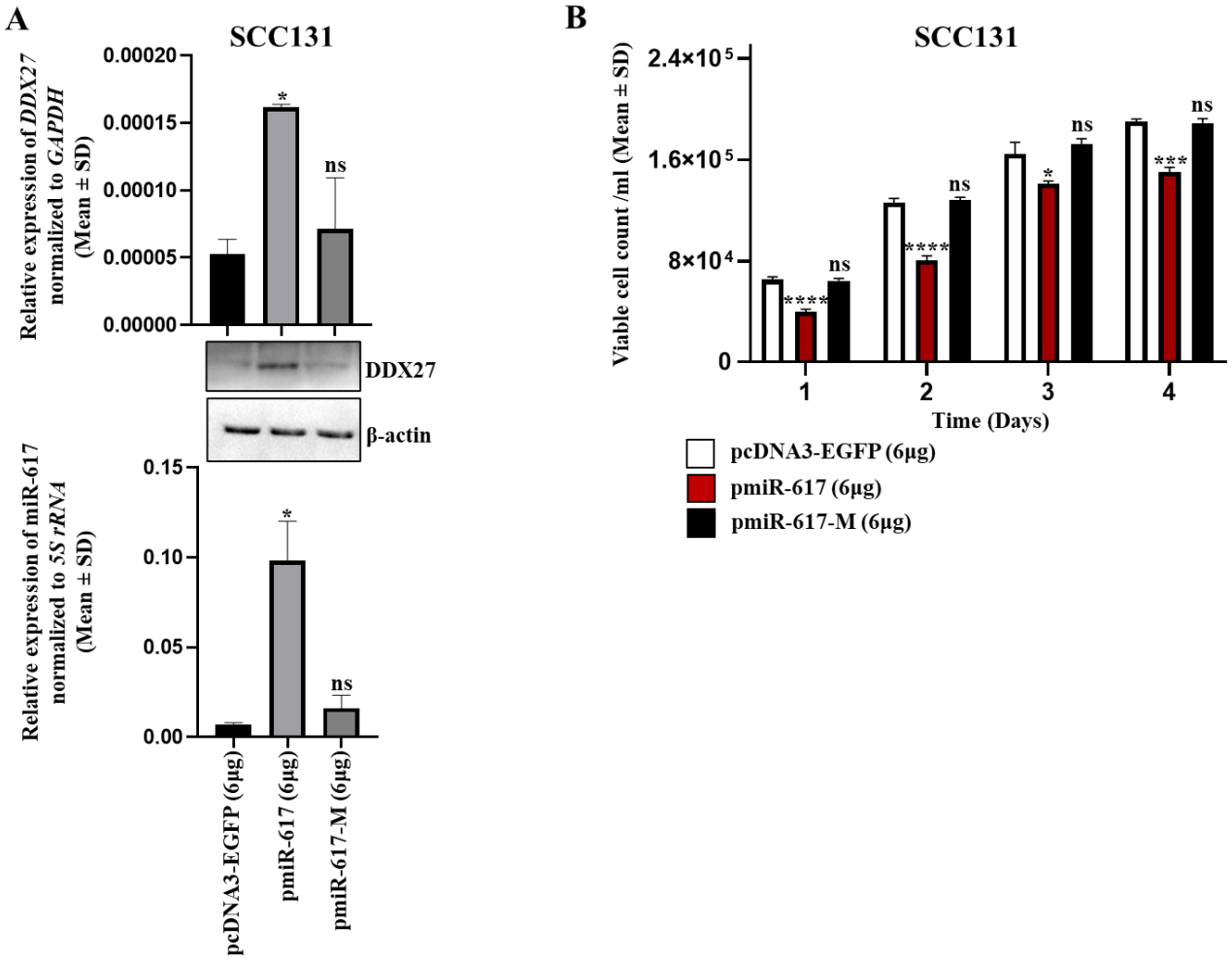

Figure 13: miR-617 upregulates DDX27 in SCC131 cells. (A) Transfection of the pmiR-617 construct in SCC131 cells increases the transcript and protein levels of DDX27 compared to those transfected with pmiR-617-M or the vector control. As expected, transfection of cells with pmiR-617-M, harbouring the deleted seed region of miR-617, does not increase the levels of DDX27 transcript and protein, due to the lack of a functional miR-617. **(B)** Reduced proliferation of cells transfected with pmiR-617 compared to those transfected with pmiR-617-M or the vector control. For RT-qPCR data, each bar is an average of 2 technical replicates.

4.8. DDX27 reduces cell proliferation of OSCC cells

Our data suggests that miR-617 has an anti-proliferative role in OSCC cells and positively regulates *DDX27* (Figures 10 and 12). Thus, we wanted to check if DDX27 has a role in cell proliferation of OSCC cells. To this end, we cloned the *DDX27* ORF sequence downstream to the CMV promoter in the pcDNA3.1(+) vector. Then, we transiently transfected SCC131 and SCC084 cells with pcDNA3.1(+) vector and pDDX27 construct separately, and cell proliferation was monitored at an interval of 24 hours for four days using the trypan blue

dye exclusion assay. OSCC cells transfected with pDDX27 showed a significant reduction in cell proliferation as compared to pcDNA3.1(+) transfected OSCC cells (Figure 14), suggesting that DDX27 has an anti-proliferative role in OSCC cells. This is contrary to the pro-proliferative role of DDX27, observed in other cancers.

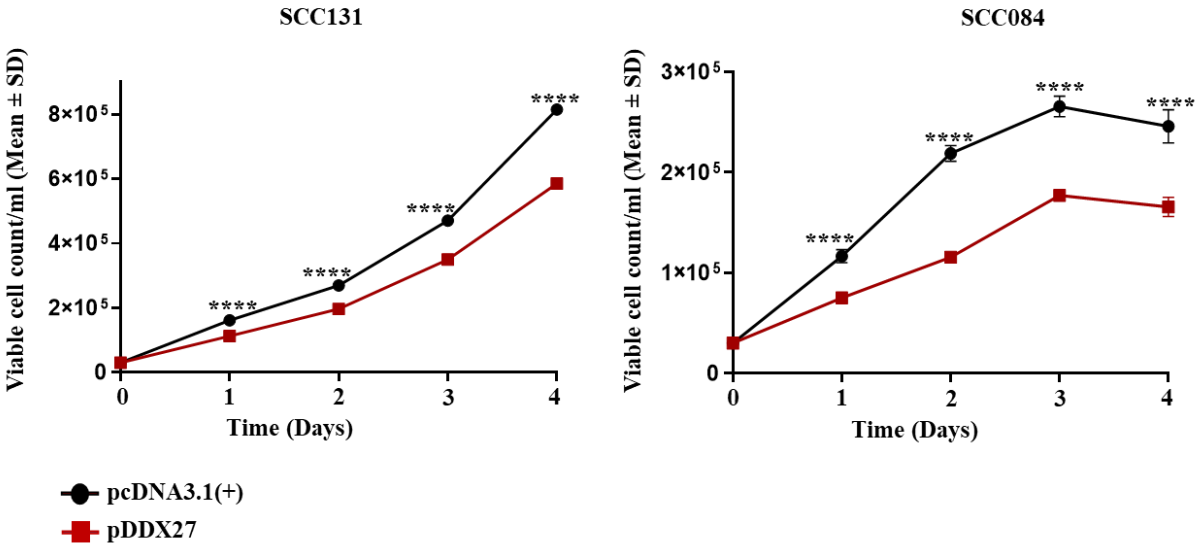

Figure 14: *DDX27* reduces proliferation of SCC131 and SCC084 cells. Transient overexpression of DDX27 decreases proliferation of both SCC131 and SCC084 cells compared to the vector control transfected cells. Each data point is an average of 3 technical replicates.

4.9. Characterization of the *DDX27* promoter

While canonically a miRNA binds to the 3'UTR of its cognate mRNA, our data on miR-617 clearly indicated the occurrence of a non-canonical mode of miRNA action. miRNAs are known to bind to the promoters of genes to cause their upregulation. Since the promoter of *DDX27* is not reported in literature, we first retrieved the putative promoter sequence of *DDX27* (-642 bp to +67 bp relative to TSS; 709 bp) using Promoter 2.0 and DBTSS databases (Figure 15A). Next, we cloned the putative promoter sequence of *DDX27* upstream to the *luc* ORF in pGL3-Basic (pGL3-PrDDX27), and transfected it along with relevant controls in SCC131 cells to perform dual-luciferase reporter assay (Figure 15B). The results showed a significant promoter activity for pGL3-PrDDX27 compared to pGL3-Basic (Figure 15B), suggesting that the bioinformatically predicted putative *DDX27* promoter sequence represents its promoter. Then, we looked for putative target sites complementary to the miR-617 seed region in the promoter of *DDX27*, using the multiple sequence alignment program. The results revealed the

presence of a putative miR-617 target binding site in the *DDX27* promoter (Figure 16). As already mentioned, a putative miR-617 target binding site was also observed in the 3'UTR of *DDX27* (Figure 16), using miRNA target prediction tools such as TargetScanHuman 8.0, miRDB, MiRanda, microT-CDS (Diana Tools), and PITA.

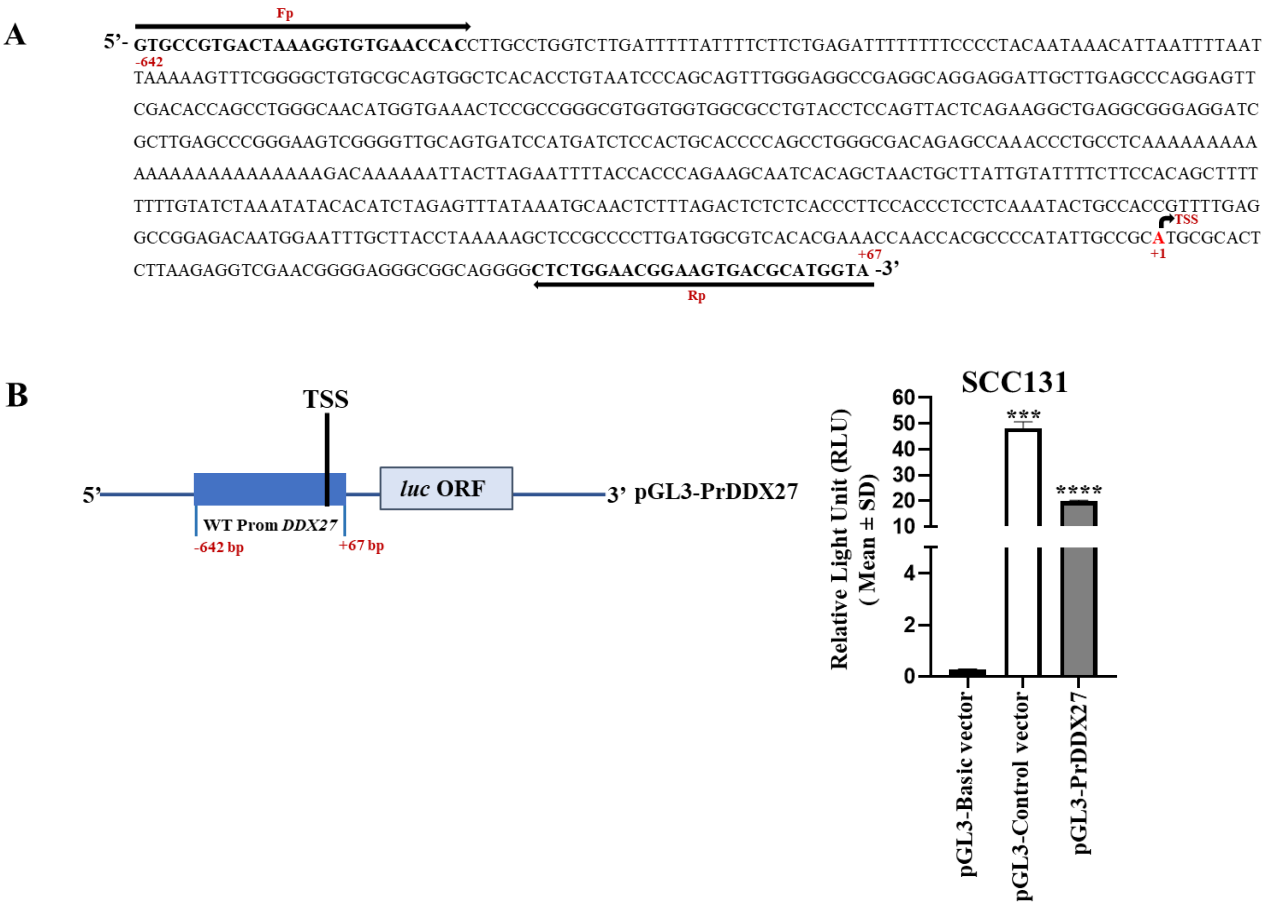

Figure 15: Identification of the *DDX27* promoter. (A) Putative promoter sequence of *DDX27*. PCR primers (Fp and Rp) used in cloning of the putative *DDX27* promoter are shown. **(B)** Schematic diagram of the putative *DDX27* promoter construct (left panel) and results of dual-luciferase reporter assay to characterize the *DDX27* promoter in SCC131 cells (right panel). Note, pPGL3-PrDDX27 showed a significant promoter activity compared to pGL3-Basic. Each bar is an average of 3 biological replicates.

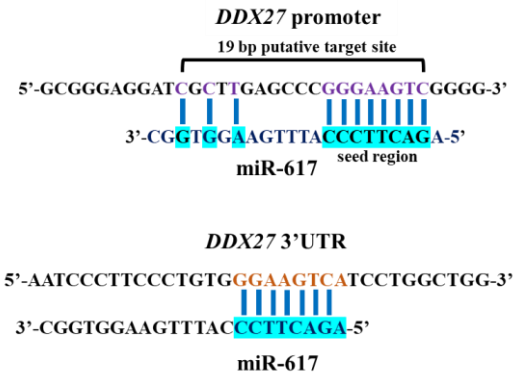

Figure 16: Putative miR-617 binding sites in the promoter and 3'UTR of *DDX27*. Note, the 11 bp complementarity in the 19 bp putative target site (TS) of miR-617 in the *DDX27* promoter.

4.10. miR-617 interacts with the promoter of *DDX27* instead of its 3'UTR

As stated above, the promoter and 3'UTR of *DDX27* harbour putative binding sites for miR-617 (Figure 16). Therefore, we wanted to determine if miR-617 had a binding preference for the *DDX27* promoter over its 3'UTR or vice versa. To this end, we generated following three constructs: p3'UTR-S, harbouring the 3'UTR of *DDX27* in a sense orientation downstream to the *luc* ORF in pMIR-REPORT, pGL3-PrDDX27, harbouring the wild-type *DDX27* promoter upstream to the *luc* ORF in pGL3-Basic and pGL3-PrDDX27-M, harbouring *DDX27* promoter with deleted 19 bp TS of miR-617 upstream to the *luc* ORF in pGL3-Basic (Figure 17, top panel). We then co-transfected different combinations of these constructs with pmiR-617 or the vector and estimated the interaction of miR-617 for the *DDX27* promoter or 3'UTR by dual-luciferase reporter assay. Remarkably, we observed a significant increase in luciferase activity in cells co-transfected with pGL3-PrDDX27 and pmiR-617 compared to those co-transfected with pGL3-PrDDX27 and the vector control (Figure 17, bottom panel), suggesting a direct interaction between miR-617 seed region and the target site in the *DDX27* promoter. Further, there was no significant change in luciferase activity in cells co-transfected with p3'UTR-S and pmiR-617 compared to those co-transfected with p3'UTR-S and the vector control, suggesting that miR-617 does not interact with the 3'UTR of *DDX27*. Next, we wanted to ascertain whether, in the cellular milieu, there was a competition between the 3'UTR and the promoter of *DDX27* to attract the binding of miR-617 or miR-617 showed a preferential binding towards either of them. Upon co-transfection of pGL3-PrDDX27, p3'UTR-S, and pmiR-617 in SCC131 cells there was a significant increase in luciferase activity compared to those co-transfected with pGL3-PrDDX27, p3'UTR-S, and the vector control (Figure 17, bottom panel). However, cells co-transfected with p3'UTR-S, pmiR-617, and pGL3-PrDDX27-M demonstrated comparable luciferase activity to those co-transfected with pGL3-PrDDX27, p3'UTR-S, and the vector control due to the lack of interaction of miR-617 with *DDX27* promoter in pGL3-PrDDX27-M. Therefore, even in the presence of miR-617 binding sites in both the promoter and 3'UTR of *DDX27*, miR-617 binds to the promoter of *DDX27* only (Figure 17).

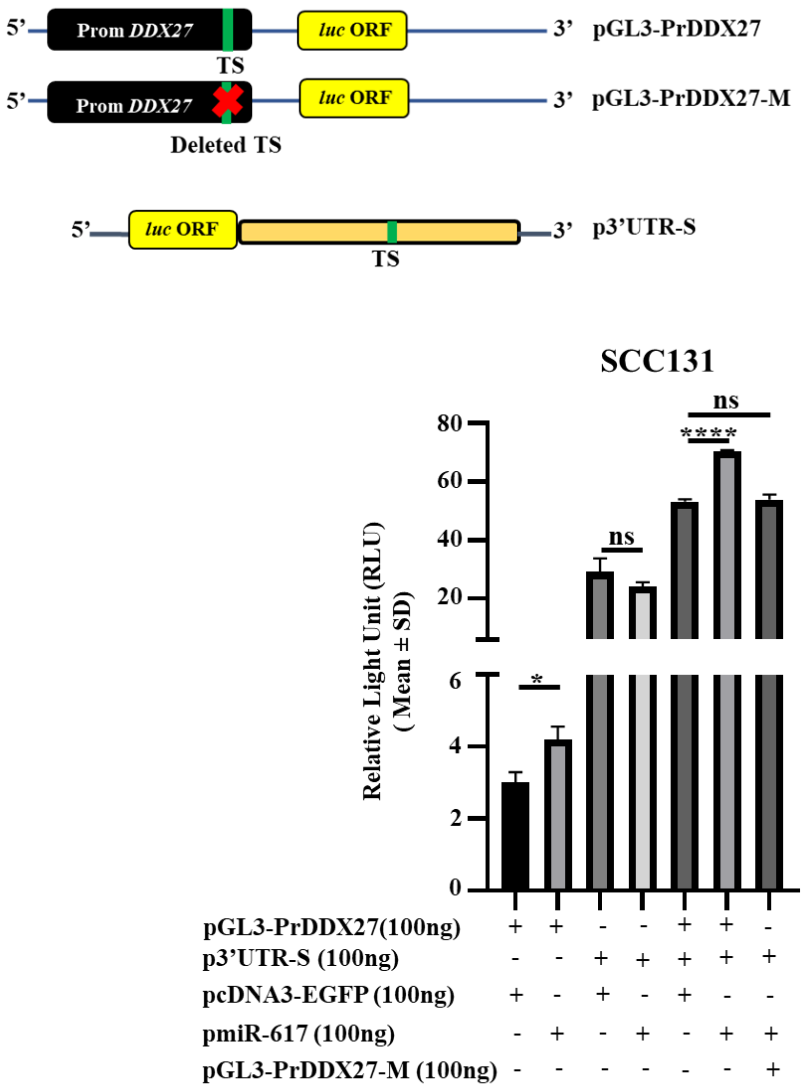

Figure 17: Dual-luciferase reporter assay to determine the interaction of miR-617 with 3'UTR and promoter of *DDX27* in SCC131 cells. Each bar is an average of 3 biological replicates. *Abbreviation:* TS, target-site.

4.11. miR-617 regulates the promoter activity of *DDX27* in a dose-dependent and sequence-specific manner

To further confirm the interaction of miR-617 with the promoter of *DDX27* by the dual-luciferase reporter assay, we co-transfected SCC131 cells with pGL3-PrDDX27 and an increasing dosage of pmiR-617 (Figure 18, left panel). The results showed that miR-617 regulates the *DDX27* promoter activity in a dose-dependent manner (Figure 18, left panel). Moreover, the cells co-transfected with pGL3-PrDDX27 and pmiR-617-M (miR-617 construct with deleted seed region) showed no significant change in luciferase activity compared to those co-transfected with pGL3-PrDDX27 and the vector control due to the lack of formation of a

functional miR-617 from pmiR-617-M (Figure 18, right panel). Similarly, cells co-transfected with pmiR-617 and pGL3-PrDDX27-M (*DDX27* promoter construct with deleted target site) showed no significant change in luciferase activity compared to those co-transfected with pGL3-PrDDX27 (the wild-type *DDX27* promoter construct) and the vector control (pcDNA3-EGFP) (Figure 18, right panel) as the target site for miR-617 was abrogated in pGL3-PrDDX27-M (Figure 17, top panel). The above observations thus suggested that miR-617 interacts with the promoter of *DDX27* and positively regulates its activity in a dose-dependent and sequence-specific manner.

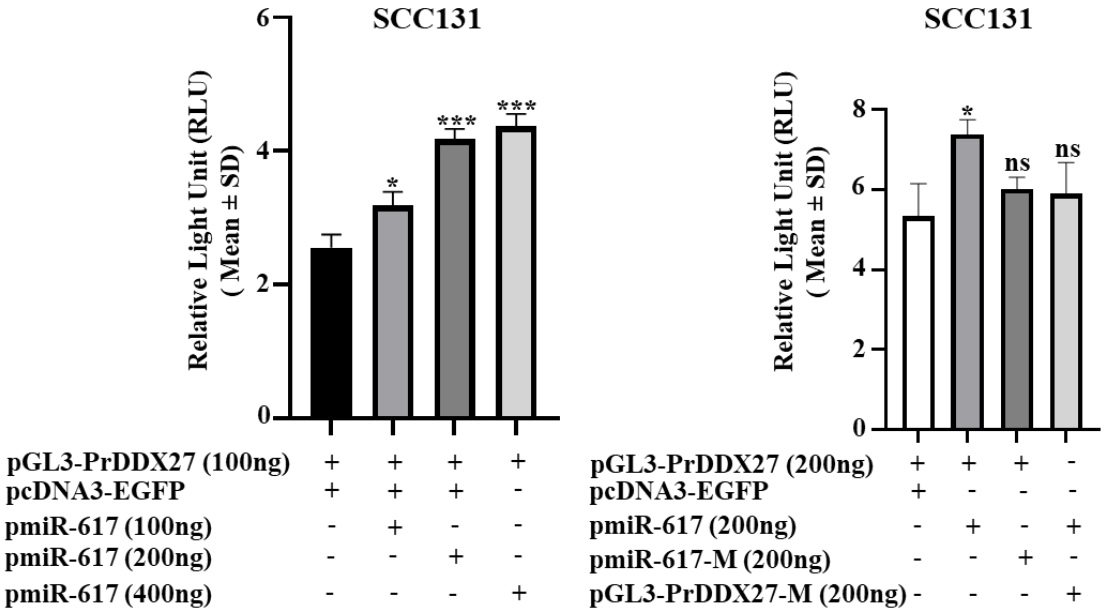

Figure 18: miR-617 regulates the promoter activity of *DDX27* in a dose-dependent and sequence-specific manner in SCC131 cells. The promoter activity of *DDX27* increases in a dose-dependent manner upon overexpression of miR-617 in increasing quantities in cells (left panel). No change in promoter activity was observed in cells co-transfected with pGL3-PrDDX27 and pmiR-617-M or pGL3-PrDDX27-M and pmiR-617 compared to those co-transfected with pGL3-PrDDX27 and the vector control (right panel). Each bar is an average of 3 biological replicates.

4.12. 5-Azacytidine treatment of SCC131 cells upregulates DDX27

We have shown that miR-617 was significantly upregulated in 5-Azacytidine-treated SCC131 cells compared to the DMSO-treated cells. Since *DDX27* was identified as the gene target of miR-617, we next checked the levels of DDX27 transcript and protein in DMSO- and 5-Azacytidine-treated SCC131 cells. As expected, DDX27 was upregulated at both the

transcript and protein levels following 5-Azacytidine treatment of SCC131 cells, suggesting that 5-Azacytidine treatment of SCC131 cells also upregulates DDX27 (Figure 19).

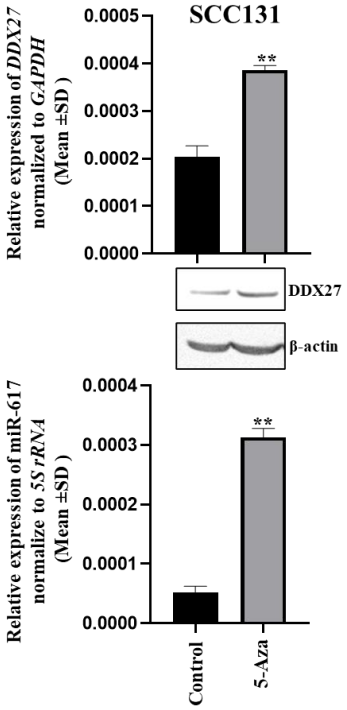

Figure 19: 5-Azacytidine treatment of SCC131 cells upregulates DDX27 at both transcript and protein levels. For RT-qPCR data, each bar is an average of 2 technical replicates.

4.13. Upregulation of DDX27 levels post 5-Azacytidine treatment of SCC131 cells is not due to demethylation of its promoter

We have shown that DDX27 was upregulated at the transcript and protein levels post 5-Azacytidine treatment of SCC131 cells (Figure 19). Thus, the next question was to address whether the upregulation of DDX27 post 5-Azacytidine treatment resulted from the upregulation of miR-617 or if it was a combination of demethylation of the *DDX27* promoter and miR-617 upregulation. To this end, we scanned the *DDX27* promoter for CpG sites and chose a CpG dense (566 bp, from -545 bp to +21 bp relative to the TSS) sequence harbouring 22 CpG sites to check for their methylation status in DMSO- and 5-Azacytidine-treated gDNA samples (Figure 20A). Thus, to distinguish between methylated and unmethylated CpGs in the selected region, the DMSO- and 5-Azacytidine-treated gDNA samples were treated with sodium bisulphite. Then, using BSP-specific primers (Table 8) the region of interest was PCR amplified, cloned into a TA vector, and 10 random clones were sequenced for each experiment.

The Sanger sequencing results showed no significant change in the methylation percentage of the *DDX27* promoter in 5-Azacytidine-treated cells (64.5%) as compared to DMSO-treated cells (67.2%) (Figure 20B and C), suggesting that the *DDX27* promoter is not demethylated post 5-Azacytidine treatment. This indicates that the upregulation of DDX27 levels is caused by an upregulation of miR-617 post 5-Azacytidine treatment.

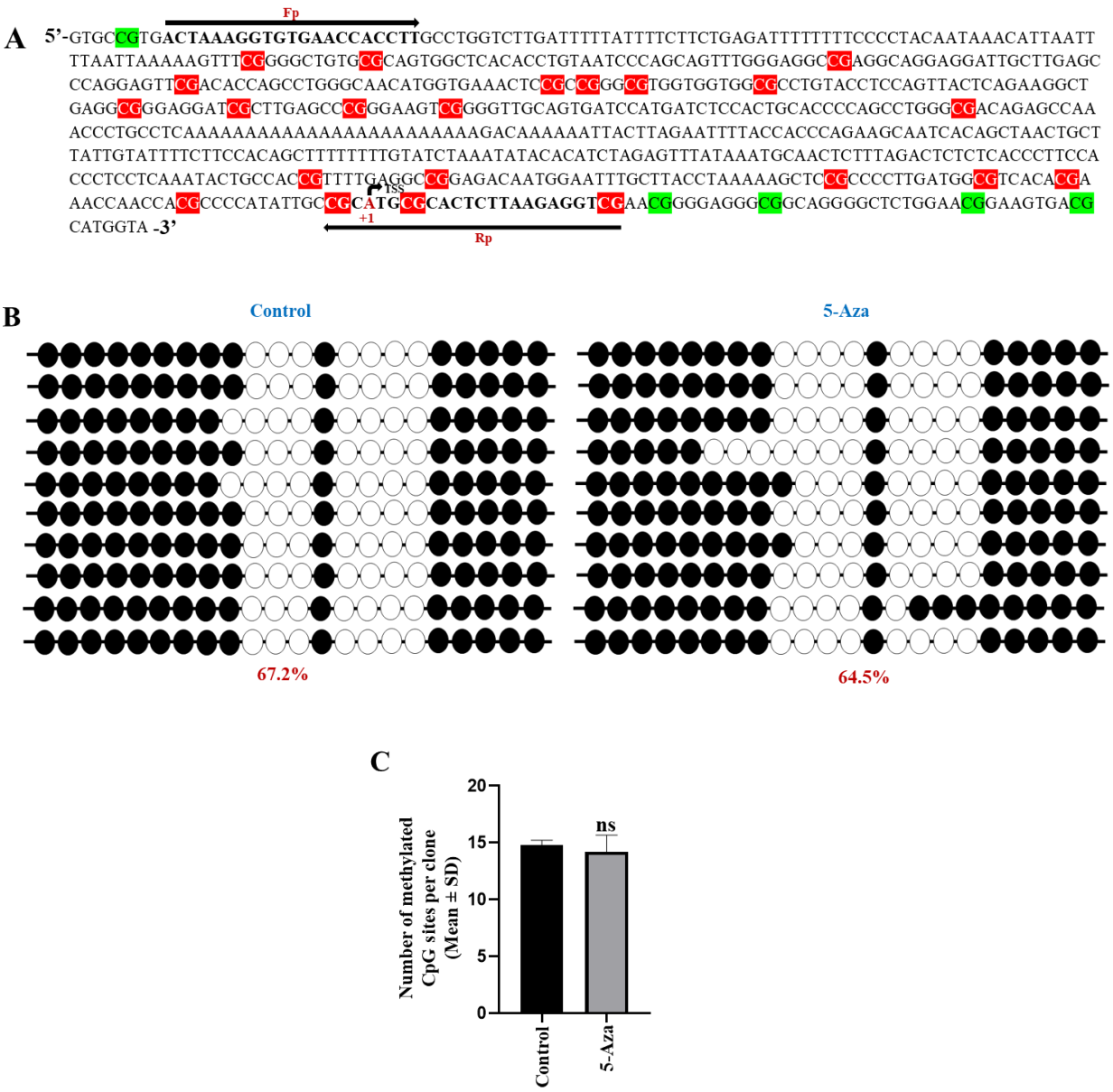

Figure 20: Analysis of the *DDX27* promoter by bisulphite sequencing PCR (BSP). (A) *DDX27* promoter sequence. Fp and Rp primers for BSP analysis of CpG sites are shown. **(B)** BSP analysis of the *DDX27* promoter showed a drop in percentage methylation from 67.2% in control treated cells to 64.5% in 5-Azacytidine-treated cells. Note, each straight line with circles represents a single TA clone. The empty and filled circles represent unmethylated and methylated CpGs respectively. **(C)** There is no significant change in percentage methylation of CpGs in the *DDX27* promoter post 5-Azacytidine treatment. Each bar is an average of 10 biological replicates.

4.14. Biological relevance of the interaction between miR-617 and *DDX27* in human cell lines

We have shown that miR-617 positively regulates DDX27 at the transcript and protein levels. Thus, to assess the biological relevance of their interaction, we checked for the levels of miR-617 and *DDX27* transcripts across seven different cell lines, namely HeLa, HEK293T, Huh-7, HepG2, MCF-7, SCC131, and SCC084 by RT-qPCR. In general, a positive correlation was observed between miR-617 and *DDX27* transcript levels across the seven cell lines, indicating the biological relevance of their interaction. For example, miR-617 and *DDX27* transcripts showed concomitantly high and low levels in HepG2 and SCC084 cells respectively, further exemplifying a positive correlation between the levels of miR-617 and DDX27 (Figure 21).

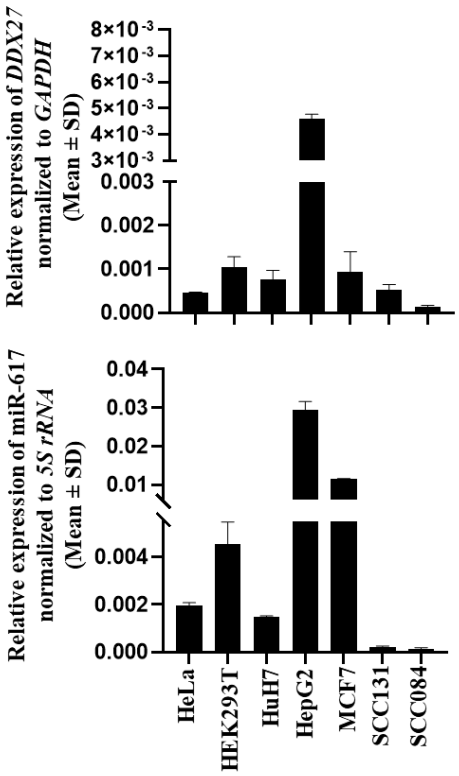

Figure 21: Biological relevance of the interaction between miR-617 and *DDX27* in human cell lines. In general, a positive correlation is observed between the expression of miR-617 and *DDX27* across these seven cell lines, indicating the biological relevance of their interaction. Each bar is an average of 2 technical replicates.

4.15. Biological relevance of the interaction between miR-617 and *DDX27* in OSCC patient samples

Next, we aimed to assess the biological relevance of the interaction between miR-617 and *DDX27* in 36 matched normal oral tissue and OSCC patient samples (Tables 6 and 7) by RT-qPCR (Figure 22). The results showed that miR-617 was significantly downregulated in 11/36 (viz., patient no. 3,11,36,39,62,71,73,75,81,86, and 40) OSCC patient samples in comparison to their matched normal oral tissue samples (Figure 22, top panel). Alongside, *DDX27* was significantly downregulated in 19/36 (viz., patient no. 3,11,36,39,62,71,73,75,81,86,35,74,76,80,82,83,87,47, and 67) OSCC patient samples when compared to their matched normal oral tissue samples (Figure 22, bottom panel). Moreover, there was a significant upregulation in the levels of miR-617 in 18/36 (viz., patient no. 12,25,41,43,72,77,35,74,76,80,82,83,87,38,42,78,88, and 89) and of *DDX27* in 8/36 (viz., patient no. 12,25,41,43,72,77,79, and 85) OSCC patient samples compared to their matched normal oral tissue samples (Figure 22). The levels of miR-617 and *DDX27* did not show any change in 7/36 (viz., patient no. 37,47,67,79,84,85, and 90) and 9/36 (viz., patient no. 37,38,40,42,78,84,88,89, and 90) OSCC patient samples, respectively, when compared to their matched normal oral tissue samples (Figure 22). It is noteworthy that miR-617 and *DDX27* were concomitantly downregulated in 10/36 (viz., patient no. 3,11,36,39,62,71,73,75,81, and 86) and upregulated in 6/36 (viz., patient no. 12,25,41,43,72, and 77) OSCC samples compared to their matched normal oral tissue samples (Figure 22). Taken together, a positive correlation in the levels of miR-617 and *DDX27* was observed in 16/36 (viz., patient no. 3,11,36,39,62,71,73,75,81,86,12,25,41,43,72, and 77) OSCC samples compared to their matched normal tissues, exemplifying the biological relevance of their interaction.

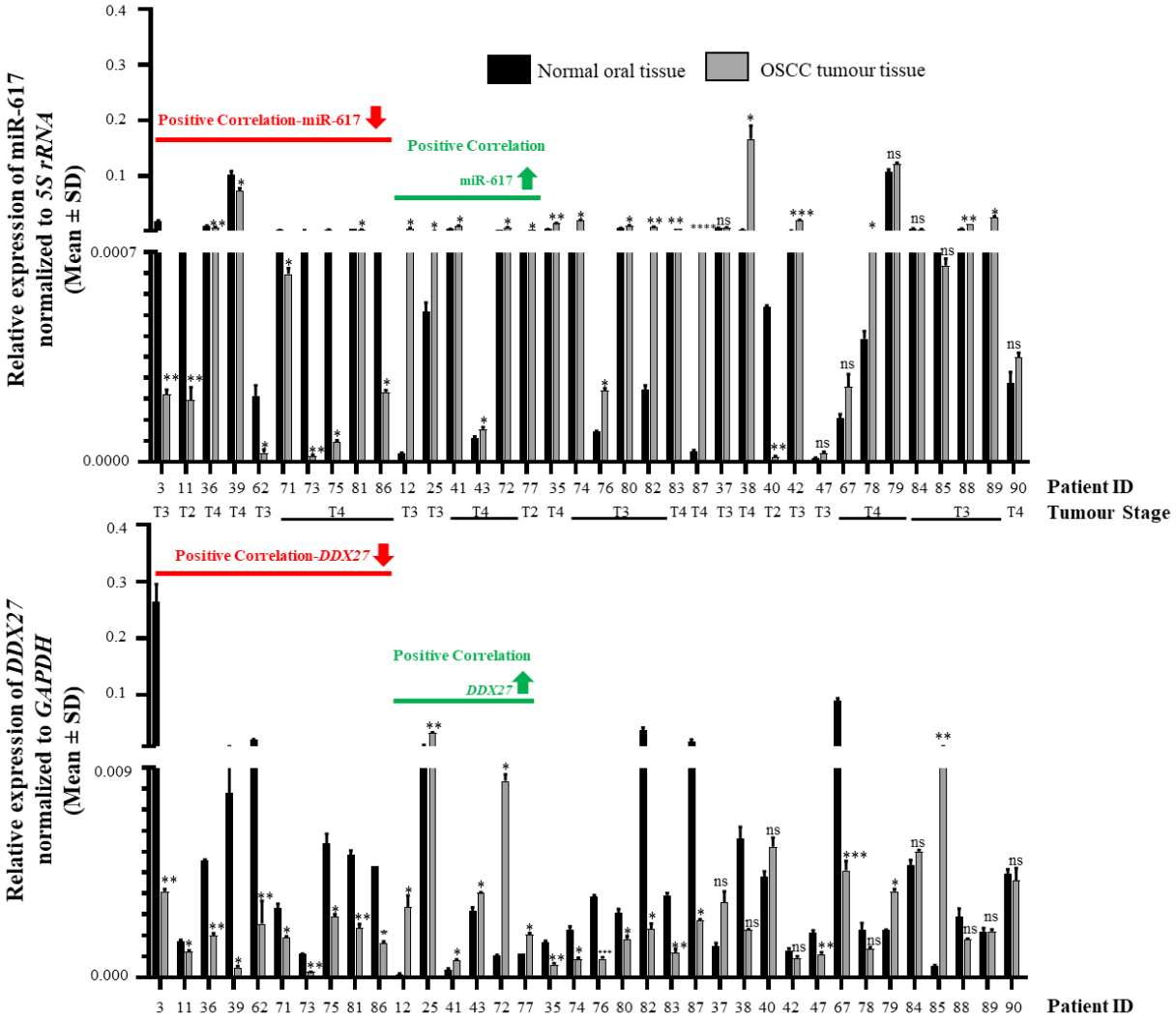

Figure 22: Biological relevance of the interaction between miR-617 and *DDX27* in OSCC patient samples. miR617 levels were downregulated in 11/36 OSCC samples (top panel) and *DDX27* levels were downregulated in 19/36 OSCC samples (bottom panel) compared to their matched normal oral tissue samples. miR-617 levels were upregulated in 18/36 OSCC samples (top panel) and *DDX27* levels were upregulated in 8/36 OSCC samples (bottom panel) compared to their matched normal oral tissue samples. Overall, 16/36 OSCC samples showed a positive correlation in the levels of miR-617 and *DDX27*. Each bar is an average of 2 technical replicates.

4.16. *In vitro* construct system recapitulates the DDX27 upregulation upon miR-617 overexpression

We have shown that miR-617 interacts with the promoter of *DDX27* to upregulate its promoter activity by dual-luciferase reporter assay (Figure 17, bottom panel). Thus, it was imperative to show that miR-617 directly interacts with the *DDX27* promoter to upregulate its expression with an *in vitro* construct system to validate our proposition further. To accomplish

this goal, we excised the *luc* ORF from the promoter-null pGL3-Basic vector and cloned the *DDX27* ORF in its place to generate the pPr-null-DDX27 construct (Figure 23A). Furthermore, we cloned the *DDX27* promoter upstream to the *DDX27* ORF in the pPr-null-DDX27 construct to generate pPr-DDX27 (Figure 23A; Table 3). Thus, we generated a construct (pPr-DDX27) wherein *DDX27* ORF was transcribed by its own promoter, mimicking the endogenous transcriptional unit (Figure 23A).

Then, to show that miR-617 interacts with the *DDX27* promoter to upregulate its expression, we co-transfected pPr-DDX27 with pmiR-617 in equal dosage (2 µg of plasmid DNA each) in SCC131 cells and observed that DDX27 was upregulated at the transcript and protein levels in comparison to cells co-transfected with pPr-DDX27 and pcDNA3-EGFP, thereby validating our proposition (Figure 23B). To dismiss the possibility of an interaction between miR-617 and the 3'UTR of *DDX27* to regulate DDX27 levels, we inserted the 3'UTR of *DDX27* downstream to the *DDX27* ORF in the pDDX27 construct to generate pDDX27-3'UTR (Figure 23A) and co-transfected it with the pmiR-617 construct in equal dosage (2 µg of plasmid DNA each) in SCC131 cells (Figure 23B). As expected, there was no change in DDX27 transcript and protein levels in these cells compared to those co-transfected with pDDX27-3'UTR and pcDNA3-EGFP, thereby validating the absence of a functional interaction between miR-617 and the 3'UTR of *DDX27* as observed by dual-luciferase reporter assay in Figure 17. Therefore, the *in vitro* construct system recapitulates the DDX27 upregulation observed upon miR-617 overexpression (Figure 23B).

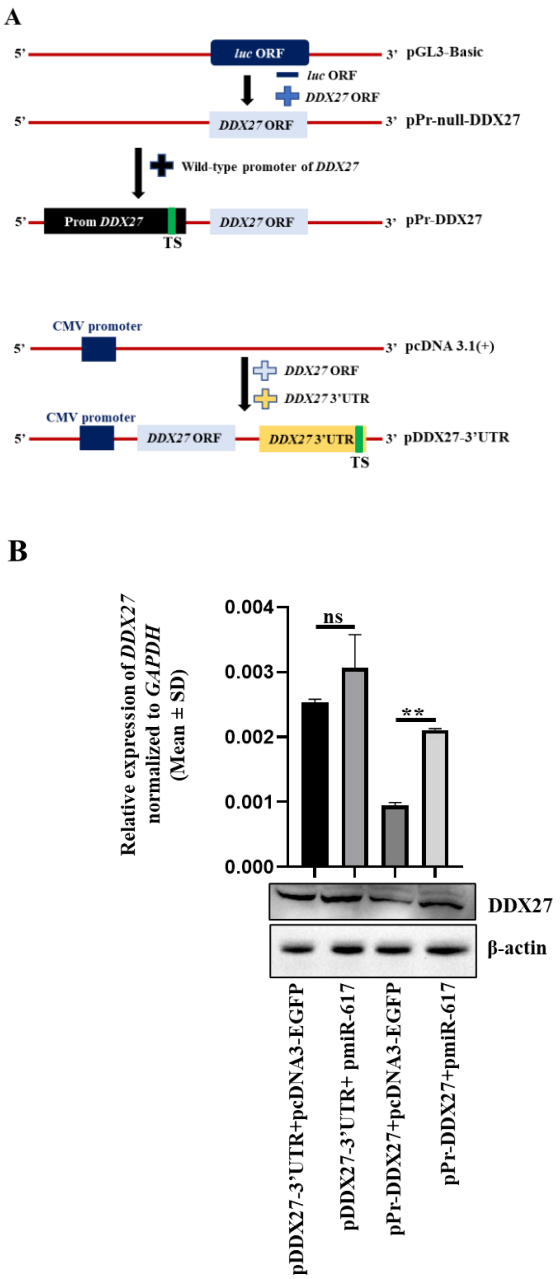

Figure 23: *In vitro* construct system recapitulates the endogenous DDX27 upregulation by miR-617 in SCC131 cells. (A) Schematic diagram to show generation of a *DDX27* ORF construct driven by its own promoter and another *DDX27* ORF construct with its 3'UTR in a sense orientation. **(B)** Cells co-transfected with pPr-DDX27 and miR-617 show a significant induction in the level of DDX27 compared to those co-transfected with pPr-DDX27 and the vector control. For RT-qPCR data, each bar is an average of 2 technical replicates.

4.17. DDX27 upregulation is specific to the interaction of miR-617 with the *DDX27* promoter

We showed that the *in vitro* construct system recapitulates the DDX27 upregulation observed upon miR-617 overexpression (Figure 23B). Thus, we wanted to explore if the upregulation of DDX27 is specific to the interaction of miR-617 to the *DDX27* promoter. We therefore co-transfected SCC131 and SCC084 cells separately with the following five combinations of overexpression constructs of miR-617 and *DDX27* in equal dosage (4 μg of plasmid DNA each), and performed Western blot analysis.

1. The promoter-null *DDX27* ORF construct, pPr-null-DDX27, was co-transfected with pcDNA3-EGFP to show the endogenous DDX27 level in OSCC cells, serving as the negative control.
2. The promoter-null *DDX27* ORF construct, pPr-null-DDX27, was co-transfected with pmiR-617 to show the change in endogenous DDX27 level in OSCC cells upon miR-617 overexpression.
3. The promoter-driven *DDX27* ORF construct, pPr-DDX27, was co-transfected with pcDNA3-EGFP to show the exogenous as well as endogenous DDX27 levels in OSCC cells upon DDX27 overexpression.
4. The promoter-driven *DDX27* ORF construct, pPr-DDX27, was co-transfected with pmiR-617 to show the change in exogenous as well as endogenous DDX27 levels in OSCC cells upon the interaction of miR-617 with the *DDX27* promoter in pPr-DDX27 and the endogenous promoter of *DDX27*.
5. The promoter-driven *DDX27* ORF construct, pPr-DDX27, was co-transfected with pmiR-617-M to show the extent of change in exogenous as well as endogenous levels of DDX27 in OSCC cells. Since pmiR-617-M will not generate a functional miR-617, thus it will not interact with exogenous and endogenous promoters of *DDX27*.

The Western blot analysis showed that the endogenous DDX27 was upregulated in OSCC cells co-transfected with pPr-null-DDX27 and pmiR-617 in comparison to those co-transfected with pPr-null-DDX27 and pcDNA3-EGFP as a result of the interaction of miR-617 with the endogenous promoter of *DDX27*. Next, co-transfection of OSCC cells with pPr-DDX27 and pcDNA3-EGFP showed the exogenous overexpression of DDX27 compared to those co-transfected with pPr-null-DDX27 and pcDNA3-EGFP. Then, following co-transfection of OSCC cells with pPr-DDX27 and pmiR-617, there was an increase in the level of DDX27 in

comparison to those co-transfected with pPr-DDX27 and pcDNA3-EGFP as a result of the interaction between miR-617 and endogenous and exogenous promoters of *DDX27*. Moreover, when cells were co-transfected with pPr-DDX27 and pmiR-617-M, the level of DDX27 was comparable to those co-transfected with pPr-DDX27 and pcDNA3-EGFP due to the absence of formation of functional miR-617 from pmiR-617-M (Figure 24). Thus, in the absence of exogenously expressed miR-617, neither the endogenous *DDX27* promoter in the genome nor the exogenously introduced *DDX27* promoter in pPr-DDX27 was targeted by miR-617 to cause DDX27 upregulation. Therefore, DDX27 upregulation is specific to the interaction of miR-617 with the *DDX27* promoter in SCC131 (Figure 24, left panel) and SCC084 (Figure 24, right panel) cells.

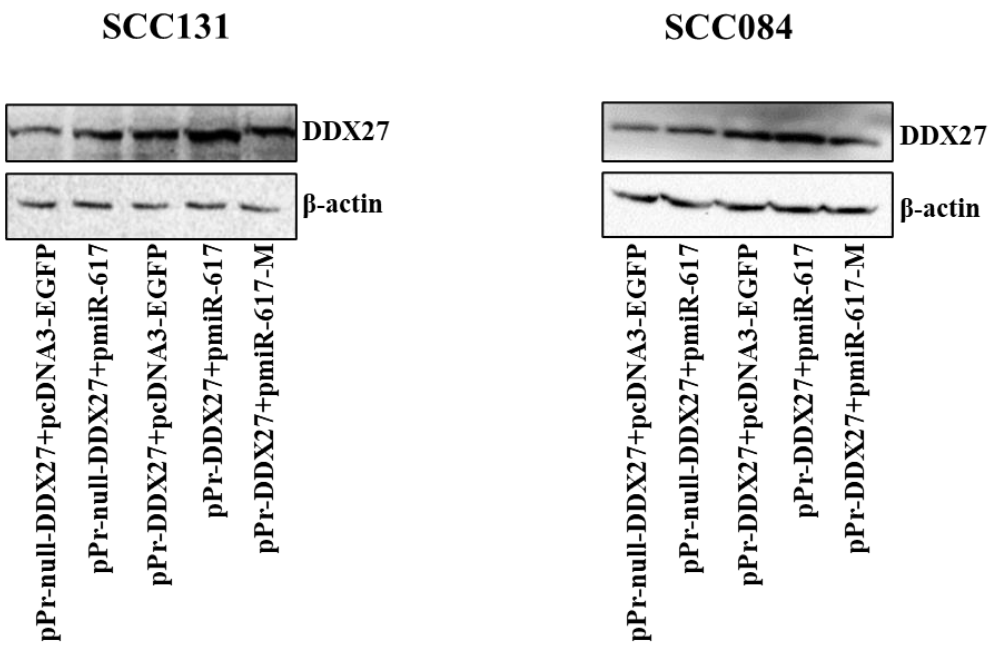

Figure 24: DDX27 upregulation occurs as a result of interaction between miR-617 and the promoter of *DDX27*. DDX27 levels are upregulated in cells co-transfected with pPr-DDX27 and pmiR-617 in comparison to those transfected with pPr-DDX27 and pcDNA3-EGFP or pmiR-617-M.

4.18. miR-617 negatively regulates cell proliferation, in part, by interacting with the *DDX27* promoter

Next, we decided to check for the effect of miR-617-mediated upregulation of DDX27 on some of the cancer hallmarks like cell proliferation, apoptosis, and anchorage-independent

growth. Incidentally, our data suggested that miR-617 and DDX27 have an anti-proliferative role in OSCC cells (Figures 10 and 14). Thus, to check for the effect of miR-617-mediated upregulation of DDX27 on cell proliferation, OSCC cells were co-transfected with the same set of constructs (Figure 24) and the cell proliferation was assessed by the trypan blue dye exclusion assay, 72 hours post transfection. The results demonstrated that the cell proliferation was significantly reduced in cells co-transfected with pPr-null-DDX27 and pmiR-617 in comparison to those co-transfected with pPr-null-DDX27 and pcDNA3-EGFP as a result of upregulation of endogenous DDX27 level by miR-617. Similarly, cell proliferation was significantly reduced in cells co-transfected with pPr-DDX27 and pcDNA3-EGFP compared to those co-transfected with pPr-null-DDX27 and pcDNA3-EGFP due to the exogenous expression of DDX27 from pPr-DDX27. Furthermore, there was a significant decrease in the proliferation of cells co-transfected with pPr-DDX27 and pmiR-617 in comparison to those co-transfected with pPr-DDX27 and pcDNA3-EGFP. This is due to the cumulative effect of pmiR-617 and pPr-DDX27 in increasing DDX27 levels in cells co-transfected with pPr-DDX27 and pmiR-617. As expected, no difference in cell proliferation was observed between cells co-transfected with pPr-DDX27 and pcDNA3-EGFP as compared to those co-transfected with pPr-DDX27 and pmiR-617-M (Figure 25). Thus, in the absence of exogenously expressed miR-617, neither the endogenous *DDX27* promoter in the genome nor the exogenously introduced *DDX27* promoter in pPr-DDX27 was induced to cause DDX27 upregulation and subsequently reduce cell proliferation. These observations indicated that miR-617 regulates cell proliferation, in part, by targeting the promoter of *DDX27*.

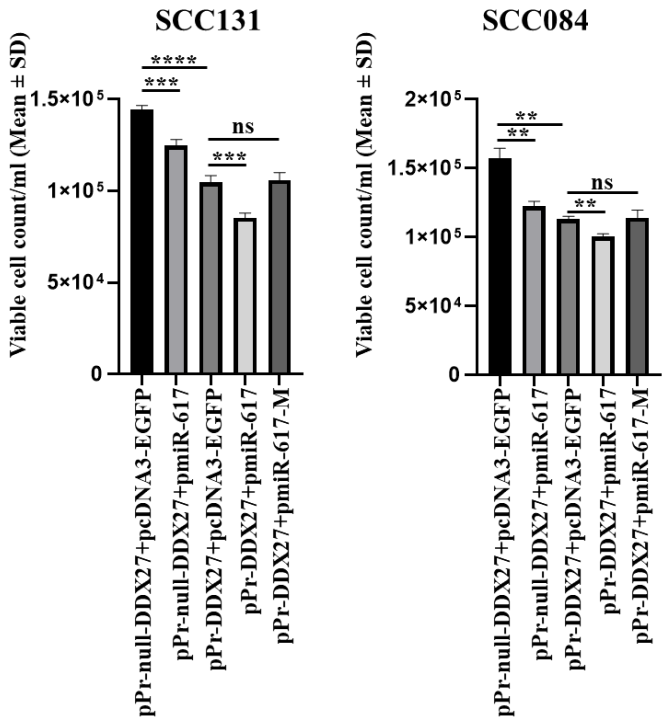

Figure 25: miR-617 negatively regulates cell proliferation, in part, by targeting the promoter of *DDX27*. The analysis of cell proliferation by trypan blue dye exclusion assay in SCC131 and SCC084 cells co-transfected with miR-617 and different DDX27 overexpression constructs. Note, cell proliferation is significantly reduced in cells co-transfected with pPr-DDX27 and pmiR-617 in comparison to those co-transfected with pPr-DDX27 and pcDNA3-EGFP or pPr-DDX27 and pmiR-617-M. Each bar is an average of 3 technical replicates.

4.19. Functional synergism between miR-617 and *DDX27*

We showed that miR-617 regulates cell proliferation, in part, by interacting with the promoter of *DDX27* and upregulating its expression. To further ascertain the functional synergy between miR-617 and DDX27, we generated pPr-M-DDX27 harbouring the promoter of *DDX27* with the deleted target site for miR-617 (Figure 26). Then, we decided to check for a quantifiable parameter like cell proliferation to detect functional synergy between miR-617 and *DDX27* by the trypan blue dye exclusion assay and calculated the same using the coefficient of interaction (CI) formula in SCC131 cells. To this end, we co-transfected SCC131 cells with different combinations of overexpression constructs of *DDX27* (viz., pPr-null-DDX27, pPr-DDX27 and pPr-M-DDX27) with pcDNA3-EGFP or pmiR-617 or pmiR-617-M in equal dosage and checked for cell proliferation, 72 hours post transfection. The results showed a significant reduction of 10.4% (100%-89.6%) in proliferation of cells co-transfected with pmiR-617, pPr-null-DDX27 and pcDNA3-EGFP in comparison to those co-transfected with

pPr-null-DDX27 and pcDNA3-EGFP (Figure 26). Similarly, a significant reduction of 13.9 % (100%-86.1%) in cell proliferation was observed in cells co-transfected with pPr-DDX27, pPr-null-DDX27 and pcDNA3-EGFP in comparison to those co-transfected with pPr-null-DDX27 and pcDNA3-EGFP (Figure 26). Furthermore, there was a significant decrease of 35.8% (100%-64.2%) in proliferation of cells co-transfected with pPr-DDX27 and pmiR-617 in comparison to those co-transfected with pPr-null-DDX27 and pcDNA3-EGFP. As mentioned before, this is due to cumulative effect of pPr-DDX27 and pmiR-617 in increasing DDX27 levels in cells co-transfected with pPr-DDX27 and pmiR-617. Also, cells co-transfected with an equal dosage of pPr-M-DDX27 and pmiR-617 showed a significant reduction in cell proliferation of 24.3% compared to those co-transfected with pPr-null-DDX27 and pcDNA3-EGFP due to increase in DDX27 levels as a result of DDX27 expression from pPr-M-DDX27 and the interaction of exogenous miR-617 with the endogenous *DDX27* promoter (Figure 26). It is noteworthy that the exogenous miR-617 did not interact with the *DDX27* promoter in pPr-M-DDX27 as the target site for miR-617 was deleted. As expected, a significant reduction of 13.3% (100%-86.7%) was observed in proliferation of cells co-transfected with pPr-DDX27 and pmiR-617-M in comparison to those co-transfected with pPr-null-DDX27 and pcDNA3-EGFP (Figure 26). Thus, in the absence of exogenously expressed miR-617, neither the endogenous *DDX27* promoter nor the exogenously introduced *DDX27* promoter was targeted by miR-617 to upregulate DDX27 and reduce cell proliferation.

Next, we calculated the CI in cells co-transfected with pPr-DDX27 and pmiR-617 or pPr-M-DDX27 (DDX27 overexpression construct with the deleted miR-617 target site) and pmiR-617 to ascertain the functional synergy between miR-617 and DDX27 as a result of the interaction between miR-617 and the *DDX27* promoter. It is established that CI<1 indicates a synergistic relationship. We observed that the CI in cells co-transfected with pPr-DDX27 and pmiR-617 was 0.83, indicating functional synergism. As expected, CI was 1 (actual value 0.99) in cells co-transfected with pPr-M-DDX27 and pmiR-617. These observations suggested that there is a functional synergism between miR-617 and DDX27 due to the interaction of miR-617 with the *DDX27* promoter (Figure 26).

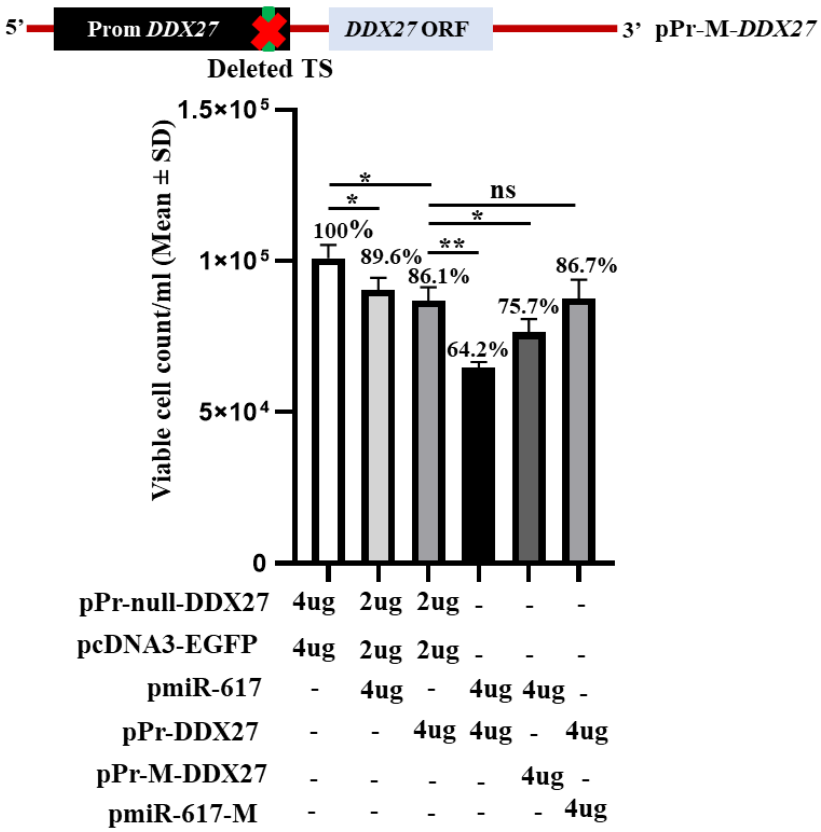

Figure 26: Functional synergism between miR-617 and *DDX27*. miR-617 and *DDX27* synergistically regulate cell proliferation in SCC131 cells. Note, there is a significant decrease in proliferation of cells co-transfected with pPr-DDX27 and pmiR-617 compared to those co-transfected with pPr-null-DDX27, pPr-DDX27 and pcDNA3-EGFP. Each bar is an average of 3 technical replicates.

4.20. miR-617 positively regulates apoptosis, in part, by targeting the *DDX27* promoter

Resisting apoptosis is one of the key tenets of cancer hallmarks. Based on our data of decreased cell proliferation by miR-617 and DDX27, we hypothesized that the reduced cell number could be caused by apoptotic induction. Thus, to check for the effect of miR-617-mediated regulation of DDX27 on cellular apoptosis, OSCC cells were co-transfected with the same set of constructs (Figure 24) to determine caspase-3 activity after 24 hours of transfection using the caspase-3 activity assay. The results showed that the caspase-3 activity was significantly increased in cells co-transfected with pPr-null-DDX27 and pmiR-617 or pPr-DDX27 and pcDNA3-EGFP in comparison to those co-transfected with pPr-null-DDX27 and pcDNA3-EGFP, suggesting that miR617 positively regulates apoptosis via upregulating DDX27 level. Furthermore, there was a significant increase in caspase-3 activity in cells co-

transfected with pPr-DDX27 and pmiR-617 in comparison to those co-transfected with pPr-DDX27 and pcDNA3-EGFP in OSCC cells as a result of the cumulative increase in endogenous and exogenous DDX27 levels by miR-617. As expected, no difference in the caspase-3 activity was observed between cells co-transfected with pPr-DDX27 and pcDNA3-EGFP and those co-transfected with pPr-DDX27 and pmiR-617-M (Figure 27). These observations suggested that miR-617 positively regulates apoptosis, in part, by targeting the promoter of *DDX27*.

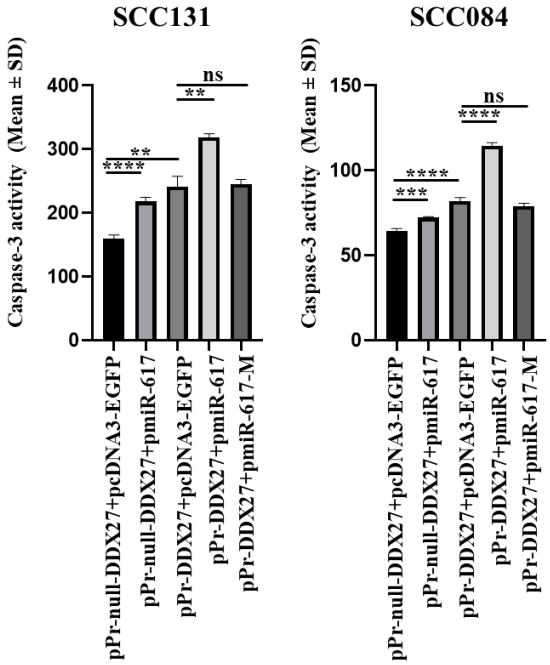

Figure 27: miR-617 positively regulates apoptosis, in part, by targeting the promoter of *DDX27*. The quantitative analysis of caspase-3 activity in SCC131 and SCC084 cells transfected with miR-617 and different DDX27 overexpression constructs. Caspase-3 activity is significantly increased in cells co-transfected with pPr-DDX27 and pmiR-617 in comparison to those transfected with pPr-DDX27 and pcDNA3-EGFP or pPr-DDX27 and pmiR-617-M. Each bar is an average of 4 technical replicates.

4.21. miR-617 negatively regulates anchorage-independent growth, in part, by targeting the *DDX27* promoter

Anchorage-independent growth is the ability of cancer cells to grow without a solid substratum and is a hallmark of carcinogenesis. Thus, we wanted to explore the impact of miR-617-mediated upregulation of DDX27 on the colony forming ability of OSCC cells by soft agar colony formation assay upon transfecting them with the same set of constructs (Figure 24). We used microscopic examination to score for visible colonies at the end of the experiment by the

OpenCFU software. The results showed that the number of colonies significantly reduced in cells co-transfected with pPr-null-DDX27 and pmiR-617 or pPr-DDX27 and pcDNA3-EGFP in comparison to those co-transfected with pPr-null-DDX27 and pcDNA3-EGFP, suggesting that miR617 negatively regulates anchorage-independent growth by upregulating DDX27 levels. Furthermore, there was a significant decrease in the number of colonies in cells co-transfected with pPr-DDX27 and pmiR-617 in comparison to those co-transfected with pPr-DDX27 and pcDNA3-EGFP as a result of the cumulative increase in endogenous and exogenous DDX27 levels by miR-617. As expected, no significant difference in the number of colonies was observed between cells co-transfected with pPr-DDX27 and pcDNA3-EGFP and those co-transfected with pPr-DDX27 and pmiR-617-M. (Figure 28). These observations suggested that miR-617 negatively regulates anchorage-independent growth, in part, by targeting the *DDX27* promoter.

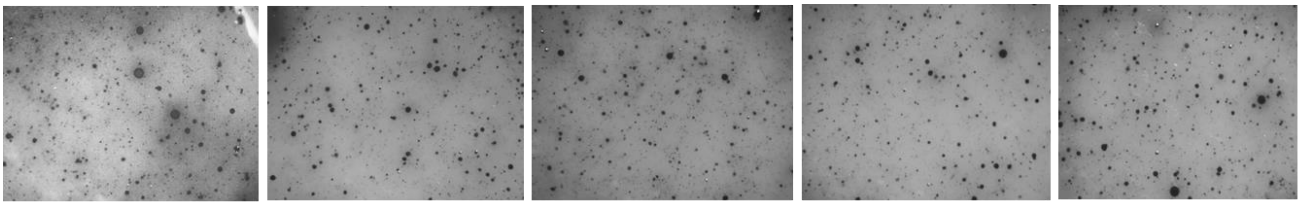

pPr-null-DDX27+ pcDNA3-EGFP | pPr-null-DDX27+pmiR-617 | pPr-DDX27+ pcDNA3-EGFP | pPr-DDX27+ pmiR-617 | pPr-DDX27+ pmiR-617-M

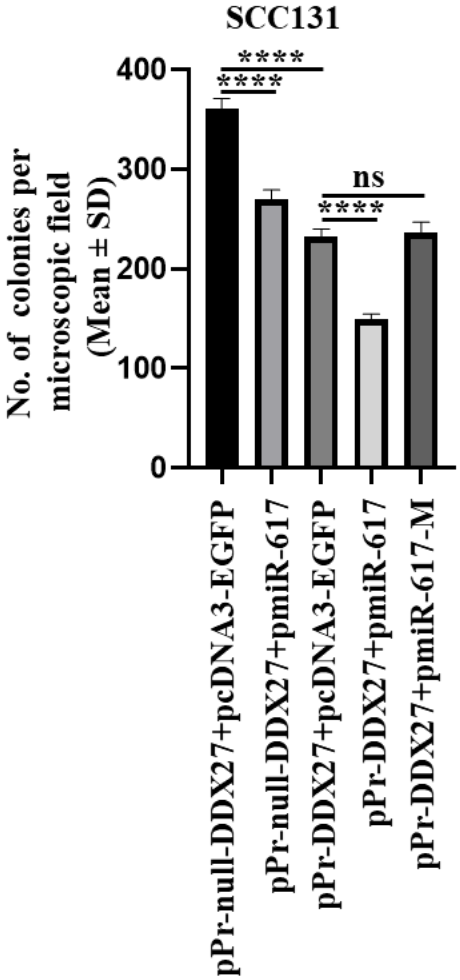

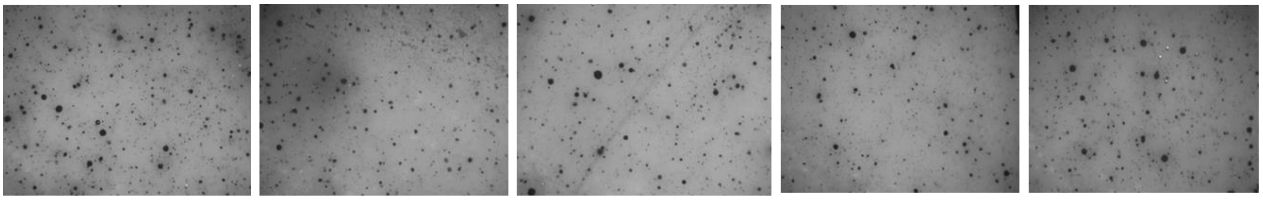

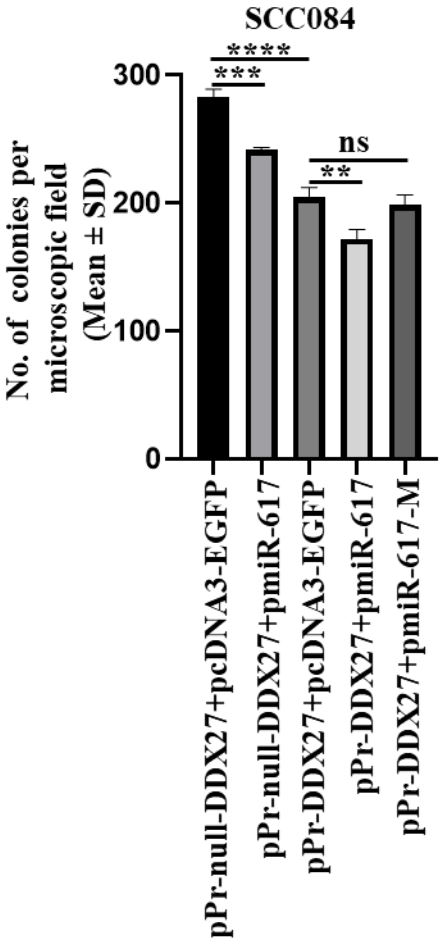

Figure 28: miR-617 negatively regulates anchorage-independent growth, in part, by targeting the promoter of *DDX27* in OSCC cells. Quantitative assessment of anchorage-independent growth in OSCC cells transfected with miR-617 and different DDX27 overexpression constructs accompanied by the representative microphotographs (magnification: 25X). Note, the number of colonies significantly reduced in cells co-transfected with pPr-DDX27 and pmiR-617 in comparison to those co-transfected with pPr-DDX27 and pcDNA3-EGFP or pPr-DDX27 and pmiR-617-M. Each bar is an average of 4 technical replicates.

4.22. Indication of a positive feedback loop between miR-617 and DDX27

While it is evident that miR-617 upregulates DDX27 and catalyses some of the tumour-protective functions in OSCC cells, it is imperative to explore whether they regulate each other to form a feedback loop. DDX27 is a putative RNA helicase and is implicated in RNA metabolism. Therefore, we wanted to explore if DDX27 affects the transcription and /or biogenesis of mature miR-617. Thus, we overexpressed pDDX27 in increasing quantities in SCC131 cells and checked for the level of miR-617 by RT-qPCR. Interestingly, endogenous miR-617 was significantly upregulated upon overexpressing pDDX27 at 4ug and 6ug, whereas no change in miR-617 level was observed in cells transfected with 2ug of pDDX27 in SCC131 cells (Figure 29). Thus, the above data suggested that DDX27, in turn, regulates miR-617 at the transcriptional level and/or in its biogenesis.

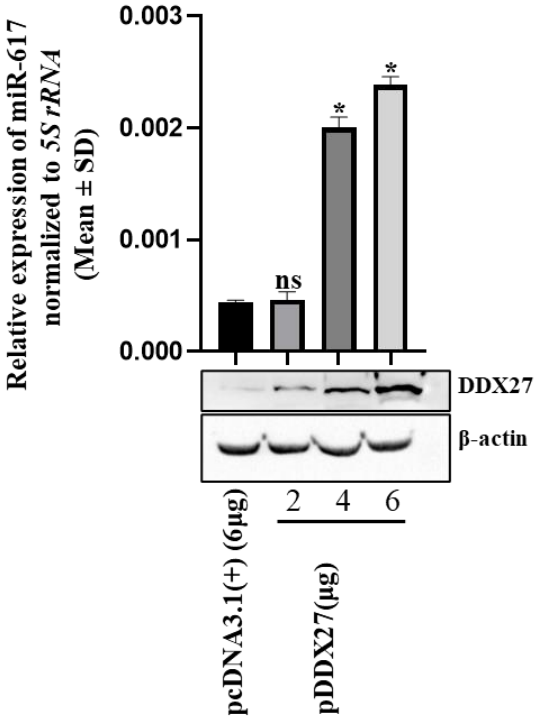

Figure 29: DDX27, in turn, regulates miR-617. Transient overexpression of DDX27 in SCC131 cells increases miR-617 levels. Note, DDX27 positively regulates miR-617 at the level of transcription or biogenesis of miR-617. For RT-qPCR data, each bar is an average of 2 technical replicates.

4.23. Reduced activation of the PI3K/AKT/MTOR pathway by miR-617 and DDX27

MiR-617 and DDX27 demonstrated tumour suppressive functions in OSCC cells, as shown by the cancer hallmarks experiments (Figures 25-28). However, there is no report about

the downstream signalling pathways that they affect in facilitating these functions. In this regard, we decided to check the PI3K/AKT/MTOR pathway, the master regulator of cell proliferation and growth, as it is the most frequently activated pathway in OSCC and other cancers. Therefore, we decided to detect the activation of this critical pathway upon overexpression of pmiR-617 or pDDX27 using the Western blot analysis. As read-outs for the activated PI3K-AKT-MTOR pathway, we decided to check the levels of phospho- and total S6K1. The results showed decreased phospho-S6K1 (p-S6K1) levels in SCC131 and SCC084 cells following overexpression of miR-617, along with that there was a reduction in total S6K1 levels only in SCC084 cells (Figure 30). As expected, overexpression of miR-617 led to an increased level of DDX27 in both SCC131 and SCC084 cells (Figure 30). Overexpression of DDX27 also showed decreased levels of p-S6K1 but there was no change in the levels of total S6K1 in both SCC131 and SCC084 cells (Figure 30). The above observations showed that miR-617 suppresses the activation of the PI3K/AKT/MTOR pathway, in part, by regulating DDX27, thereby indicating the existence of a functional miR-617-DDX27-S6K1 axis to regulate OSCC cell proliferation.

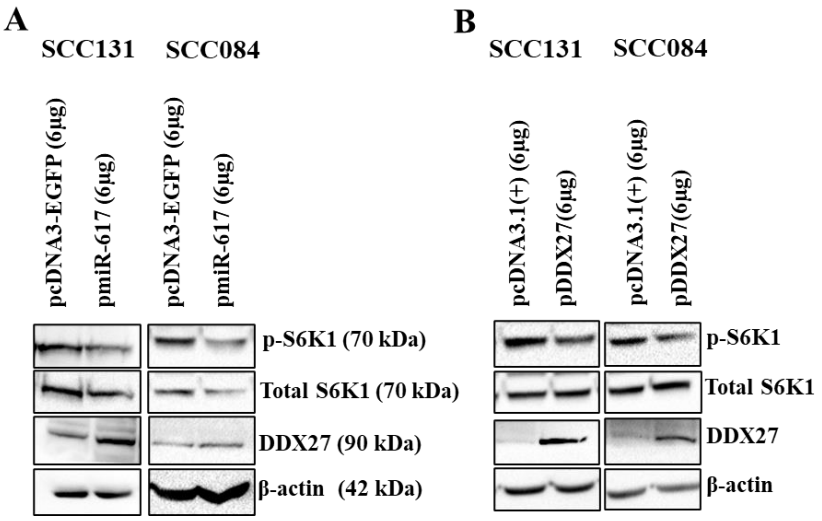

Figure 30: miR-617 downregulates the PI3K/AKT/MTOR pathway, in part, by regulating DDX27 in OSCC cells. (A) Overexpression of miR-617 reduces phospho-S6K1 levels in OSCC cells. **(B)** DDX27 downregulates p-S6K1 levels in OSCC cells.

4.24. Optimization of dosage for miR-617 mimic in SCC131 cells

Our final goal was to assess the therapeutic potential of miR-617-mediated regulation of DDX27 on tumour growth by OSCC xenograft studies in nude mice. We therefore wanted to explore the potential of a synthetic miR-617 mimic on regulating the levels of DDX27. Thus, we transfected SCC131 cells with different quantities of a synthetic miR-617 mimic and a

relevant mimic control separately to optimize the dosage. The results showed that both 200 nM and 400 nM dosages of miR-617 mimic effectively increased the levels of DDX27 in SCC131 cells in a dose-dependent manner (Figure 31A). As expected, the RT-qPCR analysis showed a significantly robust expression of miR-617 in mimic-transfected cells compared to those transfected with the mimic control, confirming its specificity (Figure 31A). To further ascertain the exact dosage to perform OSCC xenograft studies, we checked for the effect of miR-617 mimic on proliferation of SCC131 cells. We observed that the cell proliferation is significantly reduced in cells transfected with 200 nM and 400 nM of miR-617 mimic in comparison to those transfected with the mimic control (Figure 31B). However, a maximum reduction in cell proliferation was observed in cells transfected with 400 nM of miR-617 mimic, suggesting that 400 nM of miR-617 mimic is optimum to perform OSCC xenograft study in nude mice.

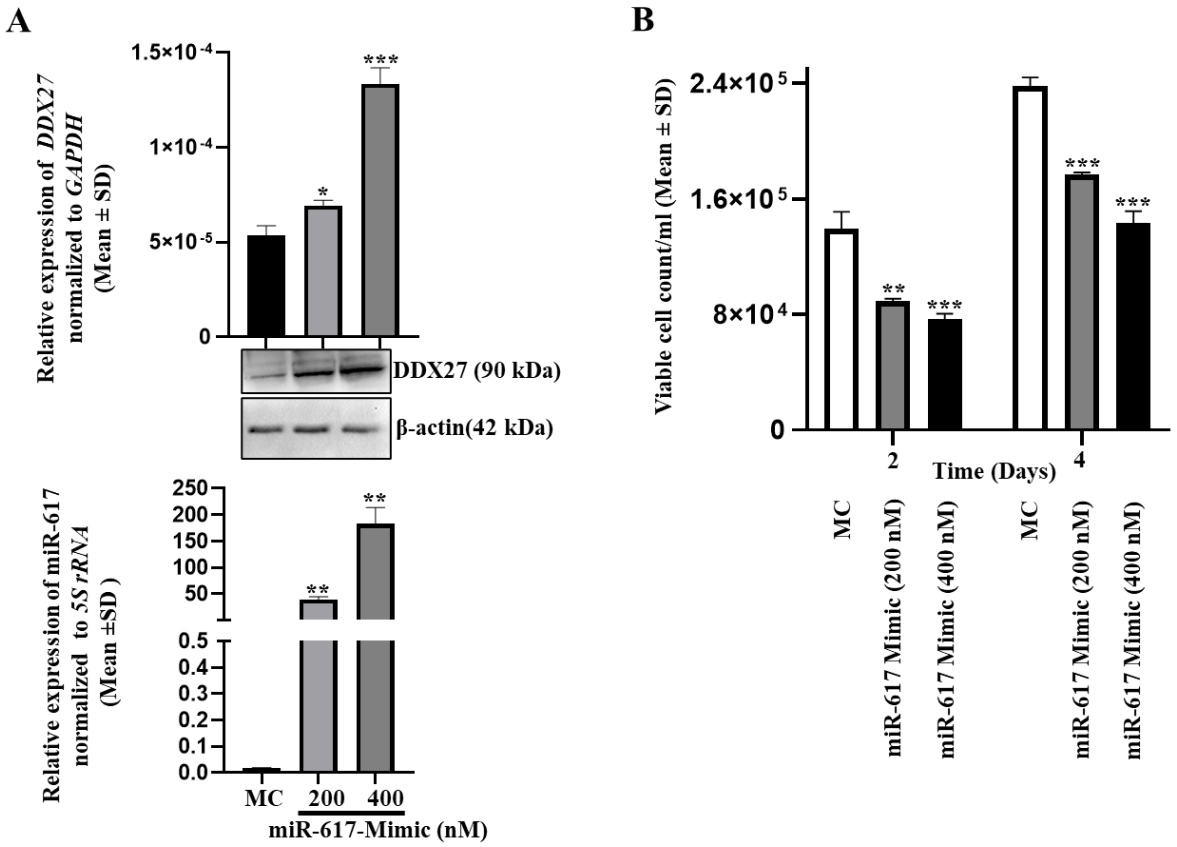

Figure 31: Optimization of dosage for miR-617 mimic in SCC131 cells. (A) miR-617 mimic upregulates DDX27. Note, DDX27 is upregulated at both the transcript and protein levels upon transient transfection of 200 and 400 nM of a synthetic miR-617 mimic. **(B)** miR-617 mimic reduces cell proliferation of SCC131 cells. For RT-qPCR data, each bar is an average of 3 technical replicates. For cell proliferation assay, each data point is an average of 3 technical replicates. *Abbreviation*: MC, mimic control #1 (400 nM).

4.25. Restoration of miR-617 by a mimic suppresses *in vivo* tumour growth in nude mice

Our *in vitro* studies have established the tumour suppressive functions of miR-617 via targeting *DDX27*. Based on these observations, we have hypothesized that restoring the miR-617 level by a synthetic miR-617 mimic and in turn increasing the level of DDX27 in OSCC cells may have an anti-tumorigenic effect *in vivo*. Thus, we decided to test this hypothesis using an *in vivo* OSCC tumour xenograft nude mouse model. To this end, we injected three female nude mice with SCC131 cells pre-transfected with 400 nM of a miR-617 mimic or 400 nM of a mimic control into their left and right flanks. The OSCC tumour xenografts were monitored for 27 days post injection (Figure 32A). As expected, there was a significant reduction in tumour volume and weight of nude mice xenografts with miR-617 mimic compared to those with the mimic control (Figure 32B and C). As expected, the RT-qPCR analysis showed a significant upregulation of miR-617 in nude mice xenografts derived from SCC131 cells transfected with the miR-617 mimic compared to those derived from SCC131 cells transfected with the mimic control. Moreover, we observed a concordant increase in DDX27 at the RNA and protein levels in nude mice xenografts derived from SCC131 cells transfected with the miR-617 mimic compared to those derived from SCC131 cells transfected with the mimic control (Figure 32D). These observations suggested that miR-617 acts as a tumour suppressor and inhibits tumour growth *in vivo*, in part, by interacting with the promoter of *DDX27* to upregulate DDX27 expression.

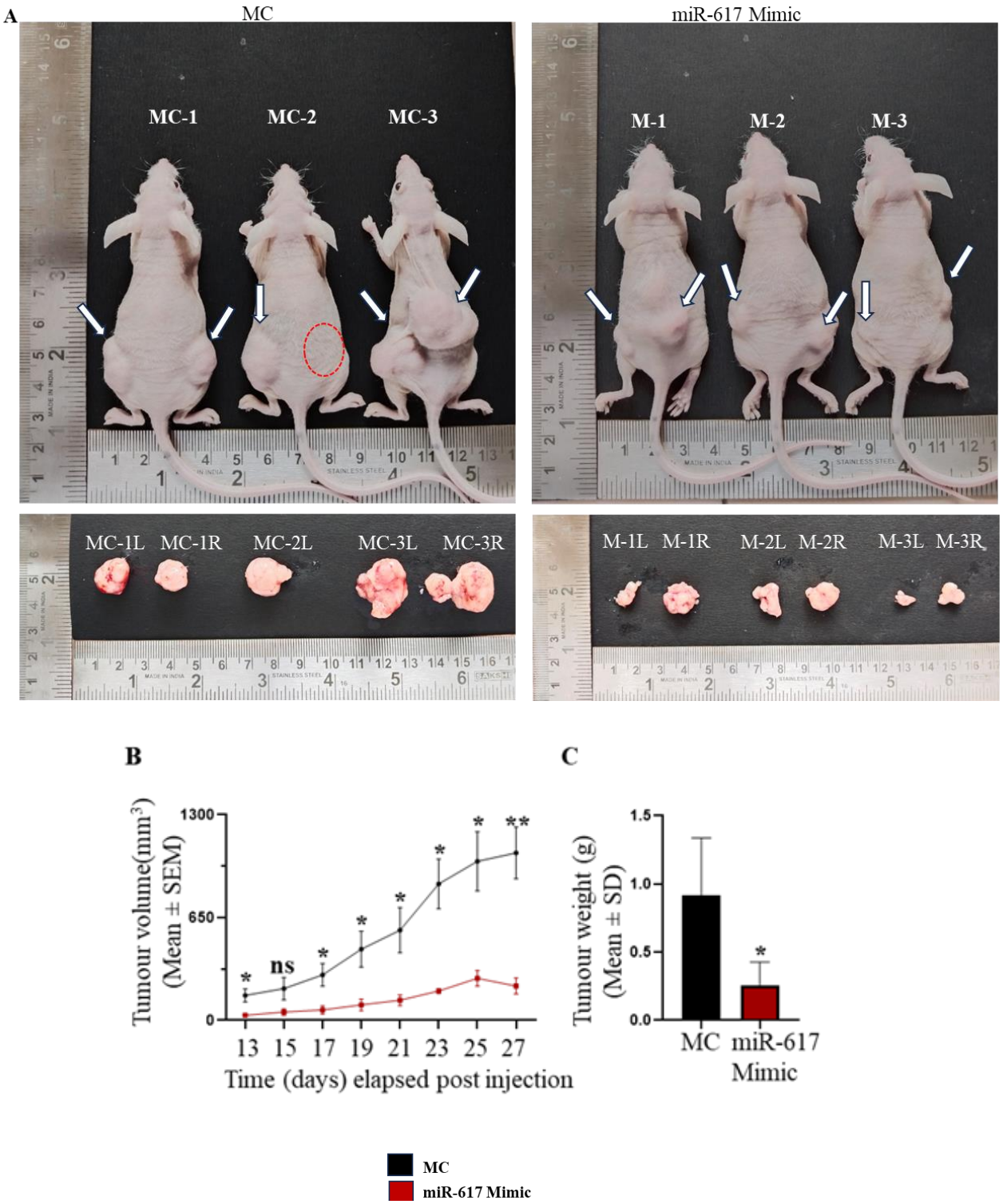
A
MC
miR-617 Mimic
MC-1
MC-2
MC-3
M-1
M-2
M-3
MC-1L
MC-1R
MC-2L
MC-3L
MC-3R
M-1L
M-1R
M-2L
M-2R
M-3L
M-3R
B
Tumour volume(mm³)
(Mean ± SEM)
1300
650
0
ns
*
**
13 15 17 19 21 23 25 27
Time (days) elapsed post injection
C
Tumour weight (g)
(Mean ± SD)
1.5
1.0
0.5
0.0
MC
miR-617
Mimic
MC
miR-617 Mimic

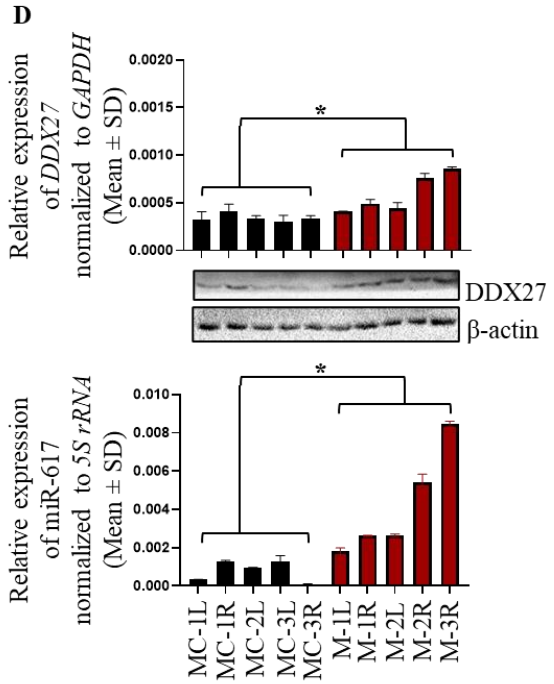

Figure 32. The effect of synthetic miR-617 mimic on SCC131 cells-derived xenografts derived from SCC131 cells in nude mice. (A) Top panel: photographs of nude mice showing tumour growth on Day 27 post injection of cells pre-transfected with miR-617 mimic and mimic control. Bottom panel: Excised xenografts from cells pre-transfected with miR-617 mimic and mimic control on Day 27. **(B)** Effect of miR-617 mimic on the volume of xenografts during a time course of 13-27 days. For mimic control group: n=5, Day 13-27 and, for miR-617 mimic group: n=4, Day 13; n=3, Day 15-21; n=4, Day 23; n=6, Day 25-27 (n=number of tumours measured). **(C)** Effect of miR-617 mimic on the weight of xenografts on Day 27. For miR-617 mimic and the mimic control groups, 3 animals were injected per group. **(D)** The levels of miR-617 and DDX27 in OSCC xenografts. Note, the M-3L xenograft was not considered for this analysis due to the inadequacy of tissue sample for both RNA and protein isolation. *Abbreviations:* L, left posterior flank; R, right posterior flank; MC, mimic control; and, M, mimic-617. The dotted red circle denotes the absence of tumour development.

DISCUSSION

5. Discussion

The present study focuses on characterising the role of a putative epigenetically inactivated tumour suppressor microRNA (miRNA), miR-617, for the first time in OSCC pathogenesis. As stated before, it is one of the 50 upregulated miRNAs, which were identified by microRNA microarray analysis upon treating cells from an OSCC cell line, SCC131 with 5-Azacytidine. Therefore, we first validated the microRNA microarray data by RT-qPCR, which showed a significant upregulation of miR-617 following the 5-Azacytidine treatment of SCC131 cells (Figure 4). *MIR617* is a primate-specific microRNA gene located in the 12th chromosome (cytogenetic band 12q21.31) of humans. miR-617 was discovered by Cummins et al. (2006) in human colorectal cells. In a previous study by Venturelli et al. (2014), microRNA expression chip analysis showed that miR-617 levels were significantly upregulated in metastatic melanoma cells treated with 8 mM pharmacological dosage of ascorbate, which inhibited DNMT (DNA methyltransferase) activity. This is in congruence with our finding wherein miR-617 is transcriptionally reactivated following 5-Azacytidine (an inhibitor of DNA methyltransferase) treatment of SCC131 cells. In a rectal cancer study aiming to explore the association between cigarette smoking and differential miRNA expression by microRNA microarray analysis, miR-617 was one of the 99 miRNAs, which were positively associated with cigarette smoking (Mullany et al., 2016). It was also shown as one of the significantly upregulated miRNAs in oesophageal cancer cells following treatment with the chemotherapeutic drug 5-fluorouracil (Hummel et al., 2011). In this study, the analysis of the predicted gene targets of the differentially regulated miRNAs including miR-617 suggested that these miRNAs could regulate functions in response to a cytotoxic stimulus (Hummel et al., 2011). In a subsequent study, chromatin immunoprecipitation sequencing (ChIP-Seq) was performed on lymphoid cells treated with the NRF2 activator, sulforaphane, to identify NRF2 target transcripts, and miR-617 was one of the upregulated miRNAs upon NRF2 activation (Chorley et al., 2012). Since NRF2 is upregulated following 5-fluorouracil treatment as well (Shibata et al., 2011), there is a speculation that it upregulates miR-617 to resist cellular damage upon cytotoxic stimuli (Shah et al., 2013). Another microRNA microarray study showed a significant downregulation of miR-617 in oesophageal adenocarcinoma samples compared to their paired normal tissues (Yang et al., 2009). Further, microRNA microarray analysis revealed a significant downregulation of >8 fold in miR-617 levels in OSCC samples compared to normal gingival tissue samples (Lajer et al., 2011). In a study of tongue squamous cell carcinoma with 21 formalin fixed paraffin embedded tissue samples and 8 control samples,

microRNA microarray analysis revealed that miR-617 was one of the significantly downregulated miRNAs (Rentoft et al., 2012). A recent study showed that miR-617 expression was reduced in OSCC tissues compared to their matched normal tissues, and it displayed a negative association with the clinical TNM stages of OSCC patients (Zhao and Liu, 2021).

MicroRNA microarray analysis by Mao et al. (2010) showed that miR-617 was significantly downregulated in GH-secreting pituitary adenomas compared to normal pituitaries. LncRNAs act as miRNA sponges to regulate miRNA functions through competing endogenous RNA (ceRNA) networks (Karreth et al., 2015). In this regard, high-throughput sequencing of multiple myeloma samples suggested that novel aberrantly expressed lncRNAs, MSTRG.255209, MSTRG.42167, and MSTRG.42200 harboured microRNA recognition elements (MREs) for miR-617 to act as ceRNAs in regulating its functions. Similarly, microarray analysis of the same samples indicated that BMS1P5 could act as a ceRNA for miR-617 (Lu et al., 2023). Vecchione et al. (2013) analysed miRNA signatures associated with chemoresistance in 198 serous ovarian cancer samples along with clinical data and concluded that the presence of miR-617 along with miR-217 and miR-484 was able to predict the chemoresistance of these tumours. In lung cancer, miR-617 was one of the downregulated miRNAs in lung adenocarcinoma samples compared to squamous cell carcinoma samples in microRNA microarray analysis (Kim HK et al., 2014). MiR-617 was also downregulated in recurrence vs no-recurrence case groups of stage I non-small-cell lung carcinoma (NSCLC) (Leidinger et al., 2012).

MIR617 is transcribed to generate an intronic miRNA from the fourth intron (34 kb) of its host gene *LIN7A* (145.41 kb) (Figure 5). Thus, we hypothesized that the upregulation of miR-617 post 5-Azacytidine treatment is due to at least one of the following three mechanisms: *MIR617* may be transcribed by its independent promoter, thus the demethylation of the *MIR617* promoter can cause upregulation of miR-617; in a host gene *LIN7A* dependent transcription of *MIR617*, demethylation of *LIN7A* promoter can cause miR-617 upregulation; and, promoters of transcription activators of *MIR617* may be demethylated to cause miR-617 upregulation. Steiman-Shimony et al. (2018) showed that 866 pre-miRNAs are encoded within introns of 786 protein-coding genes, and 158 pre-miRNAs among these are clustered in 67 introns. Among the intronic miRNAs, those encoded in clusters are more conserved than those that are not (Steiman-Shimony et al., 2018). *MIR617* is not a part of any microRNA gene cluster, and the mature miR-617 shows a 100% sequence conservation in chimpanzee and bonobo (Ensembl; https://www.ensembl.org), whereas in other primates the sequence conservation is

maintained with a few base mismatches in the seed region (https://blast.ncbi.nlm.nih.gov/Blast.cgi). There are conflicting evidences correlating the expression patterns of host genes and the corresponding intronic miRNAs. While some studies, using small data sets, found correlation between the expression patterns of the intronic miRNAs and their host genes (Baskerville and Bartel, 2005; Hinske et al., 2010; França et al., 2016), other studies using more extensive data have demonstrated a low correlation between the two (Monteys et al., 2010; Marsico et al., 2013; Budach et al., 2016). Steiman-Shimony et al. (2018) showed that intronic miRNAs are transcribed independently of their host genes in most of the cases, especially if they are situated in a large intron (Li et al., 2007). Most of the introns are much longer than the full-length transcriptional units of known intergenic miRNAs, implying that some introns indeed are long enough to carry the entire transcription units of pre-miRNA genes (Li et al., 2007). In humans, most of the intragenic miRNAs are located within introns (Hinske et al., 2010), and these intronic miRNAs constitute more than 85% of all intragenic miRNAs (Hinske et al., 2014). Intronic miRNAs that are present in introns longer than 5,000 bp are likely to have their independent transcription units regulated by RNA Pol II or III (Li et al., 2007). MiR-617 is present in the 34,045 bp long 4th intron of host gene *LIN7A,* and thus we speculated its transcription to be driven by an independent promoter. Since the promoter of *MIR617* is not reported in literature, we retrieved two putative promoter regions: a short fragment (-365 bp to +460 bp relative to TSS; 825 bp) and a long fragment (-2925 bp to +250 bp relative to TSS; 3175 bp) with additional proximal regulatory elements by employing bioinformatic promoter prediction databases such as DBTSS, Promoter 2.0 and PROMO (Figures 6A and 7A). These fragments were then cloned in the promoter-null pGL3-Basic vector, and the resulting constructs pGL3-PrMIR617-F1 with a short fragment and pGL3-PrMIR617-F2 with a long fragment were transfected in SCC131 cells along with the relevant negative (pGL3-Basic) and positive (pGL3-Control) controls to perform dual-luciferase reporter assay. The results showed that the pGL3-PrMIR617-F2 construct was able to significantly enhance the luciferase activity by >2 fold compared to pGL3-Basic. Thus, we have shown for the first time that *MIR617* is transcribed by its independent promoter.

Epigenetic silencing of tumour suppressor genes (TSGs) is a common and crucial event in cancer development and progression. Similarly, epigenetic silencing through methylation of the promoter regions has emerged as the major mechanism of silencing/downregulating tumour suppressor miRNAs (Kozaki et al., 2008; Kunej et al., 2011). We therefore wanted to explore if upregulation of miR-617 following 5-Azacytidine treatment of OSCC cells is due to

demethylation of its promoter. We chose to assess the methylation status of five CpG sites adjoining the TSS in the *MIR617* promoter by using bisulphite sequencing PCR analysis. We observed that there was a reduction in methylation percentage of the *MIR617* promoter from 88% to 56% in 5-Azacytidine treated cells compared to DMSO treated cells, thereby suggesting *MIR617* promoter demethylation to be one of the mechanisms of miR-617 upregulation post 5-Azacytidine treatment of OSCC cells. There is no report on the transcriptional regulation of miR-617 till date, thus our finding is the first report on the epigenetic reactivation of miR-617 transcription by altering the promoter DNA methylation status in OSCC cells, indicating DNA hypermethylation of the *MIR617* promoter to be one of its silencing/downregulating mechanisms in OSCC pathogenesis.

DNA methylation-mediated silencing/downregulating mechanism was identified earlier as the cause for downregulation of four miRNAs namely, miR-34b, miR-137, miR-193a, and miR-203 in OSCC cell lines (Kozaki et al., 2008). DNA methylation is also recognized as a silencing/downregulating mechanism for the deregulation of miR-127, miR-375, miR-205, and miR-137 in OSCC samples (Wiklund et al., 2011). Therefore, transcriptional reactivation of miR-617 post 5-Azacytidine treatment of OSCC cells prompted us to investigate the role of this miRNA in the proliferation of OSCC cells. Like the classical tumour suppressor genes, one of the defining characteristics of a tumour suppressor miRNA is its ability to suppress the proliferation of cancer cells. In our study, the ectopic expression of miR-617 in SCC131 and SCC084 cells reduced their proliferation compared to the vector control transfected cells, indicating its anti-proliferative role in OSCC cells (Figure 10). In a recent study, ectopic expression of miR-617 mimic in OSCC cells (SCC-090-HPV positive and PE/CA-PJ41-HPV negative) led to a significant reduction in cell proliferation, which corroborates our finding in OSCC cells from HPV negative cell lines SCC131 and SCC084 in the present study (Zhao and Liu, 2021). Apart from our study, Zhao and Liu (2021) have also explored the cancer-associated roles of miR-617 and taken together, these two studies indicate the tumour suppressive nature of miR-617 in OSCC cells, independent of its HPV infection status. Further, studies have also explored the tumour suppressive nature of other miRNAs in OSCC pathogenesis. For instance, miRNAs having tumour suppressive potential like let-7a, let-7b, let-7c, let-7d, let-7e, let-7f, let-7g, let-7i, miR-26a, miR-99a-5p, miR-137, miR-139-5p, miR-143-3p, miR-184 and miR-375 are shown to be downregulated in oral cancer through *in vitro* and *in vivo* studies (D'Souza and Kumar, 2021).

MicroRNAs exert their downstream function by regulating their cognate gene targets, primarily by binding to their 3'UTRs. Till date, only 3 gene targets of miR-617 are reported (Ge et al., 2020; Liu et al., 2021; Zhao and Liu, 2021). MiR-617 directly targets *SMAD3* in dental pulp stem cells and the circular RNA SIPA1L1 sponges miR-617 to promote osteogenesis by regulating the miR-617/*SMAD3* axis in dental pulp stem cells (Ge et al., 2020). miR-617 increases the growth of IL-22-stimulated keratinocytes through targeting *FOXO4*, which provides a new therapeutic target for psoriasis (Liu et al., 2021). *In vitro* experiments suggest that miR-617 could function as a tumour suppressor in OSCC cells by negatively regulating SERPINE1 levels (Zhao and Liu, 2021). A miRNA may target 100s of genes and the scarcity of studies pertaining to the biological role of miR-617 necessitated a comprehensive study to explore its downstream gene targets to understand its complex regulatory network in the cell. Thus, after establishing miR-617 as an epigenetically regulated miRNA with anti-proliferative functions, we aimed to identify its novel downstream gene target. MiRNAs with tumour suppressive functions repress their cognate oncogenic gene targets to keep tumorigenesis under check (Otmani and Lewalle, 2021). Thus, we employed five target prediction tools [viz., TargetScanHuman 8.0, miRDB, MiRanda, microT-CDS (Diana Tools), and PITA] to look for miR-617 gene targets (Table 10). Eight protein-coding genes were predicted by all the tools (Table 10). Then, we conducted a literature survey to select one of these eight genes with established oncogenic role in cancers and chose to work with *DDX27*. It is a known oncogene in breast, gastric, hepatocellular, and colorectal cancers (Tsukamoto et al., 2015; Tang et al., 2018; Xiaoqian et al., 2021; Li et al., 2021). This gene codes for a protein that belongs to the family of DEAD-box proteins and is characterised by the conserved DEAD- (Asp-Glu-Ala-Asp) motif. DDX27 modulates skeletal muscle growth and regeneration through translational processes (Bennett et al., 2018). It is also involved in the 3' end generation of ribosomal 47S rRNA and is established as a constituent of the PeBoW complex by mass spectrometric analysis (Kellner et al., 2015). It is discovered as a characteristic RNA binding protein showing potential to be a diagnostic biomarker for IgA nephropathy patients (Zhang et al., 2021). The structure and direct function of this protein have not been determined yet. Moreover, this gene has not been experimentally validated to be targeted by any miRNA.

Contrary to our expectation, DDX27 was upregulated upon overexpression of miR-617 in SCC131 cells, both at the transcript and protein levels, instead of showing a presumed downregulation (Figure 12A). To further ascertain whether this was a dose-dependent

regulation, SCC131 cells were transiently transfected with increasing quantities of pmiR-617. The results showed that DDX27 was upregulated by miR-617 at the transcript and protein levels in a dose-dependent manner (Figure 12B). Moreover, the levels of DDX27 in cells transfected with seed-region deleted pmiR-617-M construct were comparable to those transfected with the vector control (pcDNA3-EGFP), indicating that pmiR-617-M does not generate a functional miR-617 (Figure 13A).

Previous evidence has demonstrated the oncogenic role of DDX27 in tumorigenesis of hepatocellular carcinoma *via* activating ERK signalling (Xiaoqian et al., 2021). DDX27 enhances the stem cell-like features with undesirable survival outcome of breast (Li et al., 2021) and colorectal cancers (Yang et al., 2018). Moreover, DDX27 contributes to colony formation by gastric cancer cells through cell cycle control and may be a potential therapeutic target for gastric cancer patients with chromosome gain at 20q13. (Tsukamoto et al., 2015). It strengthens colorectal cancer growth and metastasis (Tang et al., 2018). Converse to our expectation, miR-617 upregulated DDX27 in SCC131 cells (Figure 12). Therefore, we wanted to decipher the role of DDX27 in OSCC pathogenesis. Contrary to its oncogenic role in other cancers, cell proliferation assay in OSCC cells showed a reduction in cell proliferation upon DDX27 overexpression, thereby suggesting an anti-proliferative role of DDX27 for the first time in OSCC (Figure 14). Interestingly, DEAD-box proteins have dual roles in cancer progression. The precise role of DEAD-box proteins depends on their interacting partners, the expression and/or function of which may also be independently altered during cancer development (Fuller-Pace, 2013). In this respect, changes in post-translational modification of DEAD-box proteins will also influence their interactions with partners and their impact on different cellular processes, adding further complexity (Fuller-Pace, 2013). Thus, a given DEAD-box protein could have a growth promoting or pro-proliferative role in some contexts and a growth- or tumour suppressive role in others (Fuller-Pace, 2013). This context dependence would clearly have profound implications for the consideration of DEAD-box proteins as possible biomarkers or therapeutic targets in cancer. For example, *DDX3*, *DDX5*, and *DDX17* act as oncogenes or tumour suppressors in a context-dependent manner (Fuller-Pace, 2013). Therefore, both our assumptions of *DDX27* being an oncogene and miR-617 inhibiting its expression in OSCC cells were refuted. These data served as an impetus to explore alternative ways of miRNA-mediated regulation of gene targets.

Canonically, a miRNA binds to the 3'UTR of its cognate mRNA to inhibit its expression, but our data on miR-617 clearly indicated some non-canonical mode of miRNA

action at play. MiRNAs are known to interact with the 5'UTRs, AU-rich elements (AREs) in the 3'UTRs of their cognate mRNAs and promoters of genes to cause their upregulation (Vasudevan et al., 2007; Ørom et al., 2008; Place et al., 2008). We therefore characterized the promoter of *DDX27* for the first time and observed that miR-617 has a putative binding site in it (Figure 16). Since, *DDX27* was primarily predicted to be a gene target of miR-617 based on its putative binding site in 3'UTR of *DDX27* (Figure 16), we thus decided to check if miR-617 interacts with the *DDX27* promoter or its 3'UTR. By dual-luciferase reporter assay, we demonstrated that miR-617 interacts with the *DDX27* promoter only (Figure 17). Moreover, miR-617 regulates the promoter activity of *DDX27* in a dose-dependent and sequence-specific manner (Figure 18). This is a novel finding wherein despite the presence of a putative binding site in the 3'UTR of *DDX27*, miR-617 interacts with the *DDX27* promoter to upregulate its expression. This phenomenon can be attributed to a biologically irrelevant interaction between miR-617 and the *DDX27* 3'UTR or a biased localization of miR-617 to the cell nucleus, thereby limiting cytoplasmic functions. Moreover, according to the miRNALoc server (http://cabgrid.res.in:8080/mirnaloc/) prediction, miR-617 has a greater propensity to localize to the nucleus over the cell cytoplasm, further implying its nuclear function. Interestingly, Miao et al. (2016) have shown that miR-552 inhibits the expression of human cytochrome P450 2E1 (*CYP2E1*) in two independent manners. First, the 3′ UTR of the *CYP2E1* mRNA contains an imperfect miR-552 binding site with one mismatch in the miR-552 seed region, which leads to its translational repression in the cytoplasm (Miao et al., 2016). Second, the *CYP2E1* promoter folds in a DNA cruciform structure, and its loop contains the miR-552 binding site (Miao et al., 2016). The *CYP2E1* promoter and miR-552 form a DNA:RNA hybrid to downregulate *CYP2E1* expression (Miao et al., 2016). An increase in miR-552 expression causes a decrease in RNA polymerase II and transcription factor binding at the *CYP2E1* promoter, thereby silencing *CYP2E1* transcription (Miao et al., 2016). However, it needs further investigation whether additional recruitment of downstream proteins is required or simply the occupation of RISC on the promoter region is sufficient to bring about this silencing action.

Generally, instances of transcriptional gene activation (TGA) by miRNAs have been associated with an increase in target gene expression by interacting with their promoter regions (Table 11). The first ever study of TGA by miRNAs dates to 2007, when the authors showed that ectopic expression of miR-373 in prostate cancer cells induced the levels of E-cadherin (*CDH1*) and cold shock domain containing C2 (*CSCD2*) by interacting with the reverse complementary sequences in their promoters (Place et al., 2008). In 2010, another report from

the same group demonstrated that, in prostate cancer cells, ectopic expression of miR-205 increased the expression of *IL35* and *IL24* by binding to complementary sequences in their promoters, accompanied by enrichment of RNA polymerase II and histone marks associated with active transcription (Majid et al., 2010). A subsequent study in mice showed that *Ccnb1* (cyclin B1) expression is enhanced by two miRNAs (744-5p and miR-466d-3p) that are complementary to a sequence motif in its promoter (Huang et al., 2012). This induction in *Ccnb1* expression was associated with miRNA biogenesis factors such as Drosha, Dicer, Ago1, and Ago2 (Huang et al., 2012). Furthermore, the transcriptional upregulation was accompanied by the enrichment of Ago1, RNA polymerase II and an increase in histone H3 Lysine 4 trimethylation (H3K4me3) near the transcriptional start site of *Ccnb1* (Huang et al., 2012). Another study showed that, in PC12 cells, miR-324-3p induced endogenous *RelA* mRNA and protein expression by binding to its promoter and the induction was dependent on the presence of Ago2 protein (Dharap et al., 2013).

Moreover, miR-877-3p acts as a tumour suppressor miRNA in bladder cancer cells by activating the expression of *CDKN2A* gene, which is achieved through its binding to the promoter of *CDKN2A* gene (Li et al., 2016). Interestingly, oncomiR miR551b-3p binds to a complementary sequence on the *STAT3* promoter, thereby recruiting RNA Polymerase II and the *TWIST1* transcription factor to activate *STAT3* transcription and thus directly upregulates *STAT3* expression in ovarian cancer cells leading to carcinogenesis (Chaluvally-Raghavan et al., 2016). MiR-4281, a miRNA specifically expressed in hominids, potently and specifically upregulated *FOXP3* expression by directly interacting with the TATA-box motif in the human *FOXP3* promoter. As a result, miR-4281 significantly accelerated the differentiation of human naive cells to induced Tregs (iTregs) that possess immune suppressor functions and weaken the development of graft-versus-host disease in a humanized mouse model (Zhang Y et al., 2018). Studies on miRNA-mediated TGA indicate that this is cell type-specific. For example, miR-1236-3p, miR-370-5p, and miR-3619-5p, all binding to matching sites in the *CDKN1A* promoter, acted as tumour suppressor microRNAs by inducing *CDKN1A* expression in human endometrial cancer, pancreatic cancer, and lung carcinoma cell lines, but not in liver cancer cells (Li C et al., 2017; Li S et al., 2017).

Next, we aimed to assess the biological relevance of the interaction between miR-617 and *DDX27* in human cell lines and 36 matched normal oral tissue and OSCC patient samples by RT-qPCR (Figures 21 and 22). In general, a positive correlation was observed between miR-617 and *DDX27* transcript levels across different human cell lines, indicating the biological

relevance of their interaction. Moreover, a positive correlation in the levels of miR-617 and *DDX27* was observed in 16/36 (44.44%) OSCC samples compared to their matched normal tissues, exemplifying the biological relevance of their interaction. Up until now, the biological relevance of this miRNA-target gene pair was unexplored in cancer, thus we are the first to report a positive correlation between miR-617 and *DDX27* levels in OSCC. As mentioned above, a study by Zhao and Liu (2021) also explored the tumour suppressive property of miR-617 wherein it displayed a negative association with the clinical TNM stages of OSCC patients. They also showed that miR-617 levels were reduced in OSCC tissues compared to their matched normal tissues. Similarly, miR-617 levels were significantly reduced in 11/36 samples in our OSCC patient cohort in comparison to the matched normal tissue samples. Till date, increased DDX27 levels have been correlated with poor prognosis and outcome in gastric, breast, colorectal, and hepatocellular cancer patients, indicating a positive association with carcinogenesis (Tsukamoto et al., 2015; Tang et al., 2018; Xiaoqian et al., 2021; Li et al., 2021). However, we found that 19/36 (52.77%) OSCC samples showed significant reduction in *DDX27* levels compared to their matched normal sample. This is the first time that *DDX27* gene has been associated with reduced cell proliferation in OSCC cell lines and decreased levels in OSCC patients in comparison to the matched normal tissues. However, we did not observe a positive correlation between miR-617 and *DDX27* levels in 20/36 (55.56%) OSCC samples, indicating the involvement of additional molecular players such as tumour heterogeneity, variable etiopathogenesis, and heterogenous genetic composition of each patient (Michor and Polyak, 2010; Ghosh et al., 2020). Taken together, our study is the first of its kind to explore the biological relevance of a miRNA-target gene pair in context to transcriptional gene activation by miRNAs. Remarkably, a pan-cancer analysis of 8,375 patient samples across 31 major human cancers from the TCGA (The Cancer Genome Atlas) database showed that the positive miRNA-gene correlations are surprisingly prevalent and consistent across cancer types and show distinct patterns than negative correlations. The top-ranked positive correlations are significantly involved in the immune cell differentiation and cell membrane signalling related processes and display strong power in stratifying patients in terms of survival rate (Tan et al., 2019). Therefore, this analysis further corroborates our finding in the present study, which has determined the biological relevance of the positive correlation between miR-617 and *DDX27* levels.

After establishing the interaction between miR-617 and the *DDX27* promoter, using the dual-luciferase reporter assay, we generated a construct (pPr-DDX27) wherein *DDX27* ORF

was transcribed by its own promoter, mimicking the endogenous transcriptional unit (Figure 23A). Then, to show that miR-617 interacts with the *DDX27* promoter to upregulate its expression, we co-transfected pPr-DDX27 with pmiR-617 in SCC131 cells in equal dosage and observed that DDX27 was upregulated at the transcript and protein levels in comparison to those co-transfected with pPr-DDX27 and pcDNA3-EGFP, thereby validating our proposition (Figure 23B). Moreover, co-transfection of pDDX27-3'UTR with pmiR-617 in SCC131 cells showed no significant change in *DDX27* transcript and an unaltered protein level compared to those co-transfected with pDDX27-3'UTR and pcDNA3-EGFP, thereby validating the absence of an interaction between miR-617 and the 3'UTR of *DDX27* (Figures 16 and 23B). Thus, the *in vitro* construct system recapitulated the endogenous DDX27 upregulation observed upon miR-617 overexpression (Figure 23B). Western blot analysis with the different combination of constructs (as described in Results section 4.17) also showed that DDX27 upregulation is specific to the interaction of miR-617 to the *DDX27* promoter in SCC131 (Figure 24, left panel) and SCC084 (Figure 24, right panel) cells.

Next, we decided to check for the effect of miR-617-mediated upregulation of DDX27 on some of the cancer hallmarks like cell proliferation, apoptosis, and anchorage-independent growth. Incidentally, our data suggested that miR-617 and DDX27 have an anti-proliferative role as they reduce cell proliferation of OSCC cells (Figures 10 and 14). Thus, to check for the effect of miR-617-mediated upregulation of DDX27 on cell proliferation, OSCC cells were co-transfected with the same set of constructs (Figure 24), and cell proliferation was assessed by the trypan blue dye exclusion assay, 72 hours post transfection (Karimi et al., 2019). Notably, in the absence of exogenously expressed miR-617, neither the endogenous *DDX27* promoter in the genome nor the exogenously introduced *DDX27* promoter in pPr-DDX27 was induced to cause DDX27 upregulation and subsequently reduce cell proliferation. This indicated that miR-617 regulates cell proliferation, in part, by targeting the promoter of *DDX27* and regulating it. We also deduced the functional synergy between miR-617 and DDX27 as a result of the interaction between miR-617 and the *DDX27* promoter by calculating the CI (coefficient of interaction) in cells co-transfected with pPr-DDX27 and pmiR-617 or pPr-M-DDX27 (DDX27 overexpression construct with the deleted miR-617 target site) and pmiR-617. It is established that CI<1 indicates a synergistic relationship (Chen et al., 2014). We observed that the CI in cells co-transfected with pPr-DDX27 and pmiR-617 was 0.83, indicating marked functional synergism. As expected, CI was 1 (actual value 0.99) in cells co-transfected with pPr-M-DDX27 and pmiR-617. These observations suggested that there is a functional

synergism between miR-617 and DDX27 due to the interaction of miR-617 with the *DDX27* promoter (Figure 26). Similarly, miR-617 acts as a positive regulator of apoptosis and negative regulator of anchorage-independent growth, in part, by regulating DDX27 levels as per our finding (Figures 27 and 28). This is in line with a recent study wherein Zhao and Liu (2021) demonstrated miR-617 as a negative regulator of cell proliferation and has a positive impact on apoptotic induction in OSCC cells. We have demonstrated that DDX27 also acts as a negative regulator of cell proliferation and anchorage-independent growth and a positive regulator of apoptotic induction, which is the first report of tumour suppressive functions of DDX27. However, up until now, increased DDX27 levels have been positively associated with acquiring stem cell-like features with undesirable survival outcome of breast (Li et al., 2021) and colorectal cancers (Yang et al., 2018). Increased levels of *DDX27* are also correlated with enhanced colony-forming ability of gastric cancer cells (Tsukamoto et al., 2015). Moreover, it also enhances colorectal cancer growth and metastasis (Tang et al., 2018). Therefore, our report has explored and established the tumour suppressive effects of DDX27 in OSCC for the first time.

The functional synergism between miR-617 and DDX27 provided us with an impetus to explore any possible feedback mechanism between them to regulate each other. There is an instance of miR-200 family demonstrating a negative feedback loop with its gene targets (e.g., *ZEB1* and *ZEB2*). MiR-200 family can effectively upregulate cellular E-cadherin level to maintain a cell in a more epithelial-like state by downregulating ZEB1 and ZEB2 expression. However, ZEB1 and ZEB2 can also bind to the E-box sites close to the transcription start site of each of the miR-200 clusters inhibiting their transcription, resulting in a negative feedback loop (Bracken et al., 2008; Burk et al., 2008). In our case, DDX27 belongs to a family of putative RNA helicases implicated in a number of cellular processes involving alteration of RNA secondary structure such as translation initiation, nuclear and mitochondrial splicing, ribosome and spliceosome assembly (https://www.genecards.org). In a recent study, the plant DEAD-box RNA helicase 27 (RH27) was associated with the biogenesis of miRNAs (Hou et al., 2021). Thus, we wanted to explore if DDX27 regulates miR-617 expression. Interestingly, endogenous miR-617 was significantly upregulated upon overexpression of pDDX27 at 4ug and 6ug in SCC131 cells, whereas no significant change in the miR-617 level was observed in those transfected with 2ug of pDDX27 (Figure 29). We have already established that miR-617 upregulates DDX27, and our preliminary data suggests that, in turn, DDX27 can also

upregulate miR-617 either by modulating the transcription machinery and/or in its biogenesis, thereby indicating a positive feedback loop.

Till date, there is no report on the downstream signalling pathways that are affected by miR-617 and DDX27 to bring about their tumour suppressive functions. However, DDX27 has been shown to bring about oncogenic functions via activating ERK signalling in hepatocellular cancer (Xiaoqian et al., 2021). Thus, we resorted to assess the phospho-S6K1 (p-S6K1) levels, a molecular read-out for the PI3K/AKT/MTOR pathway, which is one of the most aberrantly regulated signalling pathways in cancers including OSCC (Bernardes et al., 2010). We found a discernible reduction in p-S6K1 levels in both miR-617 and DDX27 overexpressed SCC131 and SCC084 cells, thereby connecting the link between the observed reduction in cell proliferation and reduced activation of the pro-survival pathway PI3K/AKT/MTOR (Figure 30).

Furthermore, our *in vitro* studies have established the anti-tumorigenic activity of miR-617 via targeting *DDX27*. As expected, there was a significant reduction in tumour weight and volume of nude mice xenografts with miR-617 mimic compared to those with the mimic control (Figure 32B and C). These observations suggested that miR-617 inhibits tumour growth *in vivo*, in part, by targeting the promoter of *DDX27*. Till date, this is the first study which explores the anti-tumorigenic potential of miR-617 *in vivo*.

To conclude, our study clearly demonstrated that miR-617 is a tumour suppressor miRNA transcribed by its independent promoter and is silenced/downregulated by DNA hypermethylation of its promoter in OSCC. MiR-617 positively regulates DDX27 levels by interacting with its promoter in a dose-dependent and sequence-specific manner, and this interaction is biologically relevant. Moreover, there is a functional synergism between miR-617 and *DDX27* with the speculation of a positive feedback loop between them to regulate each other. We substantiate these conclusions with a combination of *in silico*, *in vitro,* and *in vivo* assays. Further, we suggest that the restoration of miR-617 levels by using DNA demethylating drugs (e.g., 5-Azacytidine, and Decitabine) or synthetic miR-617 mimics can be a potent strategy to treat OSCC and perhaps other cancers.

Table 11: List of microRNAs that upregulate gene expression by binding to their cognate sites in the target gene promoters.

Sl. No.	miRNA	Target gene	Reference
1	miR-551	*STAT3*	Chaluvally-Raghavan et al., 2016
2	miR-4281	*FOXP3*	Zhang et al., 2018
3	miR-877-3p	*CDKN2A*	Li et al., 2016
4	miR-370	*CDKN1A*	Li C et al., 2017
5	miR- 1180	*CDKN1A*	Wang et al., 2014
6	miR-1236	*CDKN1A*	Li C et al., 2017
7	miR-6734	*CDKN1A*	Kang et al., 2016
8	miR-744	*CCNB1*	Huang et al., 2012
9	miR-1186	*CCNB1*	Huang et al., 2012
10	miR-3619-5p	*CDKN1A*	Li S et al., 2017
11	miR-324-3p	*RELA*	Dharap et al., 2013
12	miR-205	*IL24* and *IL32*	Majid et al., 2010
13	miR-373	*CSDC2*	Place et al., 2008

CONCLUSIONS

6. Conclusions

The main conclusions from the present study are as follows.

1. To validate the miR-617 upregulation post 5-Azacytidine treatment of SCC131 cells, we compared the miR-617 levels between 5-Azacytidine-treated and vehicle control (DMSO) treated cells by RT-qPCR. As expected, miR-617 was significantly upregulated in 5-Azacytidine-treated cells compared to DMSO-treated cells. Next, we hypothesized that the upregulation of miR-617 in 5-Azacytidine-treated cells could be due to the demethylation of its independent *MIR617* promoter or its host gene *LIN7A* promoter owing to their same direction of transcription, or the promoters of transcription activators involved in *MIR617* transcription. To explore the first possible mechanism, we characterized the *MIR617* promoter, which was not previously reported in the literature, by the dual-luciferase reporter assay in SCC131 cells. We retrieved two putative *MIR617* promoter fragments from bioinformatic promoter prediction databases such as DBTSS, Promoter 2.0 and PROMO: a short 825 bp fragment F1 (-365 bp to +460 bp relative to TSS) and a long 3,175 bp fragment F2 (-2925 bp to +250 bp relative to TSS). Only the long fragment F2 showed a significant increase in promoter activity compared to pGL3-Basic in SCC131 cells. Upon scanning the *MIR617* promoter for CpG sites, we chose a CpG rich region and divided it into two fragments (218 bp long F2-I and 344 bp long F2-II) to check for the methylation status of the promoter post 5-Azacytidine treatment by bisulphite sequencing PCR. The Sanger sequencing results showed a significant decrease in cumulative methylation percentage of fragments F2-I and F2-II from 88% to 56% in 5-Azacytidine-treated cells compared to DMSO-treated cells, indicating demethylation of the *MIR617* promoter as one of the mechanisms responsible for miR-617 upregulation post 5-Azacytidine treatment. In other words, methylation of the *MIR617* promoter is responsible for its downregulation in OSCC cells.

2. To assess if miR-617 has an anti-proliferative potential, miR-617 was ectopically expressed in cells from OSCC cell lines SCC131 and SCC084, and the cell proliferation assay was determined using the trypan blue dye exclusion assay. The results showed that it reduces proliferation of SCC084 and SCC131 cells, indicating its anti-proliferative function.

3. MiRNAs usually bring about their physiological functions in cells by downregulating its cognate gene targets. Thus, we expected the gene targets of miR-617 to have pro-proliferative functions. We employed five miRNA target prediction tools [viz., TargetScanHuman 8.0, miRDB, MiRanda, microT-CDS (Diana Tools), and PITA] to look for miR-617 gene targets.

As a result, we obtained the following eight protein-coding putative target genes predicted by all the tools*: DDX27, ZFX, FAM179B, RFXAP, MAP2K4, SORBS1, MEX3C,* and *JPH1*. We chose to further investigate *DDX27* as a putative gene target for miR-617 because it is known to be overexpressed in cancers and function as a proto-oncogene. To determine if miR-617 regulates *DDX27*, we transfected pmiR-617 and the cloning vector pcDNA3-EGFP separately in SCC131 cells and assessed the levels of DDX27 transcript and protein. Contrary to our expectation, we observed that miR-617 upregulated DDX27 at both transcript and protein levels, instead of downregulating it. The DDX27 upregulation was also observed to be dose-dependent, as demonstrated by a transient overexpression of miR-617 in increasing quantities in SCC131 cells. Following transfection of SCC131 cells with pmiR-617-M, harbouring the pre-miR-617 sequence with deleted seed region, we demonstrated that miR-617 and DDX27 levels were comparable to those transfected with pcDNA3-EGFP due to the lack of formation of a functional miR-617 from pmiR-617-M. As expected, the wild-type pmiR-617 transfected cells showed upregulation of miR-617 levels and a corresponding upregulation of DDX27 levels in comparison to pcDNA3-EGFP or pmiR-617-M transfected cells. Further, to check the role of DDX27 in cell proliferation, we generated the pDDX27 construct with a complete *DDX27* ORF and transfected it and the vector control, pcDNA3.1(+), separately in OSCC cells. The results showed a significant reduction in proliferation of cells transfected with pDDX27 compared to those transfected with the vector control. This suggests that DDX27 has an anti-proliferative role in OSCC cells, contrary to its oncogenic role in other cancers.

4. To determine the mechanism of miR-617-mediated upregulation of DDX27, we did a literature survey to speculate on the possible mechanism of action, and this suggested that there could be a non-canonical interaction of miR-617 with the promoter of *DDX27* to upregulate it. Since the *DDX27* promoter was previously unknown in the literature, we characterised its promoter using the dual-luciferase reporter assay in SCC131 cells. Thereafter, we observed putative miR-617 binding sites in the promoter and 3’UTR of *DDX27*. Then, we aimed to determine if miR-617 interacts with the *DDX27* promoter over its 3'UTR or vice versa by the dual-luciferase reporter assay in SCC131 cells. To this end, we generated following constructs: p3’UTR-S, harbouring the 3’UTR of *DDX27* in pMIR-REPORT downstream to *luc* ORF; pGL3-PrDDX27, harbouring the *DDX27* promoter upstream to the *luc* ORF in pGL3-Basic; and pGL3-PrDDX27-M, harbouring the *DDX27* promoter with deleted target site for miR-617 upstream to the *luc* ORF in pGL3-Basic. These constructs were transfected separately or in combination with pmiR-617 in SCC131 cells to assess of miR-617 interacts with the promoter

or 3'UTR of *DDX27*. The results showed that miR-617 interacts with the *DDX27* promoter only. Next, we co-transfected SCC131 cells with pGL3-PrDDX27 with an increasing dosage of pmiR-617 and showed that miR-617 positively regulates *DDX27* promoter activity in a dose-dependent manner. We also showed that miR-617 regulates the *DDX27* promoter activity in a sequence-specific manner by co-transfecting SCC131 cells with pmiR-617 and pGL3-PrDDX27-M or pmiR-617-M and pGL3-PrDDX27.

5. To check if miR-617 upregulation coincides with DDX27 upregulation in 5-Azacytidine-treated cells compared to DMSO-treated SCC131 cells, we assessed the DDX27 levels by RT-qPCR and Western blotting. We have already established that miR-617 was significantly upregulated in 5-Azacytidine-treated SCC131 cells compared to those treated with DMSO, and it upregulates its gene target *DDX27*. As expected, DDX27 was also upregulated at both transcript and protein levels in 5-Azacytidine-treated SCC131 cells compared to those treated with DMSO as a result of an increased level of miR-617 and not due to the demethylation of *DDX27* promoter post 5-Azacytidine treatment as demonstrated by a non-significant change in methylation status of *DDX27* promoter post 5-Azacytidine treatment.

6. To determine the biological relevance of the interaction between miR-617 and *DDX27*, we assessed their levels in seven human cell lines and 36 matched normal oral tissues and OSCC patient samples by RT-qPCR. The RT-qPCR analysis showed a positive correlation between miR-617 and *DDX27* transcript levels across seven cell lines, indicating the biological relevance of the interaction between miR-617 and *DDX27* promoter. For example, miR-617 and *DDX27* levels were concomitantly high and low in HepG2 and SCC084 cells respectively, highlighting the biological relevance of their interaction. Overall, miR-617 and *DDX27* levels concomitantly increased or decreased in 16/36 (44.44%) OSCC samples compared to their matched normal tissues, highlighting the biological relevance of their interaction.

7. To further investigate the interaction of miR-617 with the *DDX27* promoter, a *DDX27* overexpression construct driven by its own promoter, pPr-DDX27 was generated in pGL3-Basic to mimic the endogenous transcriptional unit. When pPr-DDX27 was co-transfected with pmiR-617 in SCC131 cells, DDX27 was upregulated at transcript and protein levels compared to those transfected with pPr-DDX27 and the vector control. Thus, the *in vitro* construct system recapitulated the DDX27 upregulation observed upon miR-617 overexpression. As expected, no change was observed in the levels of DDX27 transcript and protein in SCC131 cells co-transfected with pDDX27-3'UTR harbouring the complete *DDX27* ORF and 3'UTR with

pmiR-617 compared to those co-transfected with pDDX27-3'UTR and the vector control, thereby validating the absence of functional interaction between miR-617 and the 3'UTR of *DDX27*. Next, we co-transfected SCC131 and SCC084 cells with different combinations of pmiR-617, pmiR-617-M and *DDX27* constructs (viz., pPr-null-DDX27, harbouring the *DDX27* ORF without any promoter in pGL3-Basic, and pPr-DDX27), and performed Western blot analysis using an anti-DDX27 antibody. The results showed that the upregulation of DDX27 was specific to the interaction of miR-617 with the *DDX27* promoter. As expected, the endogenous DDX27 level was upregulated in OSCC cells co-transfected with pPr-null-DDX27 and pmiR-617 compared to those co-transfected with pPr-null-DDX27 and the vector control (pcDNA3-EGFP), while its level was upregulated in OSCC cells co-transfected with pPr-DDX27 and pcDNA3-EGFP compared to those co-transfected with pPr-null-DDX27 and pcDNA3-EGFP. Moreover, there was a further increase in DDX27 levels in cells co-transfected with pPr-DDX27 and pmiR-617 in comparison to those co-transfected with pPr-DDX27 and pcDNA3-EGFP by virtue of the interaction between miR-617 and the endogenous and exogenous *DDX27* promoters. We have already shown that cells transfected with only pmiR-617-M demonstrated comparable miR-617 levels to those transfected with pcDNA3-EGFP due to the lack of formation of a mature miR-617 from pmiR-617-M. Therefore, in OSCC cells co-transfected with pPr-DDX27 and pmiR-617-M, neither the endogenous *DDX27* promoter nor the *DDX27* promoter in pPr-DDX27 was targeted by miR-617 to cause DDX27 upregulation in comparison to those co-transfected with pPr-DDX27 and pcDNA3-EGFP. This data further underscores the exclusivity of DDX27 upregulation by miR-617.

8. To investigate the effect of miR-617-mediated upregulation of DDX27 on cancer hallmarks like cell proliferation, apoptosis, and anchorage-independent growth, we co-transfected different combinations of pmiR-617, pmiR-617-M and *DDX27* constructs in OSCC cells. We have already demonstrated the anti-proliferative role of miR-617 and DDX27 in OSCC cells. As expected, cell proliferation was significantly reduced in cells co-transfected with pPr-null-DDX27 and pmiR-617 or pPr-DDX27 and pcDNA3-EGFP compared to those co-transfected with pPr-null-DDX27 and pcDNA3-EGFP. Moreover, the interaction of miR-617 with the exogenous and endogenous *DDX27* promoters reduced cell proliferation in cells co-transfected with pPr-DDX27 and pmiR-617 compared to those co-transfected with pPr-DDX27 and pcDNA3-EGFP, and this interaction was abolished in those co-transfected with pPr-DDX27 and pmiR-617-M, indicating that miR-617 regulates cell proliferation, in part, by targeting the *DDX27* promoter. We also showed that there is a functional synergism between miR-617 and

DDX27 by calculating the CI (co-efficient of interaction). The CI was calculated as follows: CI = AB/ (A × B), where AB is the ratio of the viable cell count post 72 hr of cells co-transfected with the overexpression constructs of miR-617 (pmiR-617) and DDX27 (pPr-DDX27) to the viable cell count post 72 hr of cells co-transfected with pPr-null-DDX27 (a promoter less construct with *DDX27* ORF) and pcDNA3-EGFP, and A or B is the ratio of the viable cell count post 72 hr of cells transfected with each overexpression construct (pmiR-617 or pPr-DDX27) to the viable cell count post 72 hr of cells co-transfected with the pPr-null-DDX27 and pcDNA3-EGFP. It is established that CI<1 indicates a synergistic relationship. We observed that the CI in cells co-transfected with pPr-DDX27 and pmiR-617 was 0.83, indicating marked functional synergism. As expected, CI was 1 (actual value 0.99) in cells co-transfected with pPr-M-DDX27 and pmiR-617. These observations suggested that there is a functional synergism between miR-617 and *DDX27* due to the interaction of miR-617 with the *DDX27* promoter. Similarly, we also showed that miR-617 positively regulates apoptotic induction and negatively regulates anchorage-independent growth of SCC131 and SCC084 cells, in part, via targeting the promoter of *DDX27*.

9. To check if there is a positive feedback loop between miR-617 and *DDX27*, prompted by their functional synergism, we overexpressed DDX27 in SCC131 cells. We observed that DDX27 overexpression in SCC131 cells showed a significant upregulation of endogenous miR-617, suggesting that, in turn, it can also upregulate miR-617 at the transcriptional level and/or in its biogenesis.

10. To determine the downstream molecular effectors of the miR-617 and DDX27 axis, we chose to examine the PI3K/AKT/MTOR pathway, which is one of the most frequently activated pathways in cancers, including OSCC. We transfected cells from both cell lines with pmiR-617 or pDDX27 constructs separately and assessed the levels of phospho-S6K1 (p-S6K1), the terminal molecular readout of this pathway. The results showed that miR-617 and DDX27 suppress the PI3K/AKT/MTOR pathway activation by reducing p-S6K1 levels, indicating that miR-617 modulates this pathway, in part, via targeting DDX27. This indicates the existence of a functional miR-617-DDX27-S6K1 axis, correlating the reduced cell proliferation to the decreased activation of the pro-survival PI3K/AKT/MTOR pathway.

11. To explore the therapeutic potential of miR-617-mediated upregulation of DDX27 on OSCC xenografts in nude mice, we hypothesized that increasing the level of miR-617 by a synthetic miR-617 mimic would induce the level of the anti-proliferative DDX27 in OSCC

cells, thereby reducing tumour size *in vivo* in nude mice. Indeed, we observed that nude mice OSCC xenografts derived from SCC131 cells pre-transfected with 400 nM of the miR-617 mimic showed significant reduction in tumour weight and volume compared to those derived from SCC131 cells pre-transfected with 400 nM of the miR-617 mimic control. As expected, RT-qPCR of the OSCC xenografts revealed that the miR-617 levels were significantly high in OSCC xenografts obtained from SCC131 cells transfected with 400 nM of the miR-617 mimic in comparison to the xenografts obtained from cells transfected with 400 nM of the mimic control. Subsequent RT-qPCR and Western blot analysis showed that DDX27 was also upregulated in OSCC xenografts obtained from SCC131 cells transfected with the miR-617 mimic in comparison to the xenografts obtained from cells transfected with the mimic control. Therefore, these results indicated that miR-617 acts as a tumour suppressor in OSCC, in part, by activating DDX27 levels.

REFERENCES

7. References

Abdelfattah A, Park C, & Choi M. (2014). Update on non-canonical microRNAs. *Biomolecular Concepts*, 5:275. https://doi.org/10.1515/bmc-2014-0012.

Aghbari SMH, Abushouk AI, Shakir OG, Zayed SO, & Attia A. (2018a). Correlation between tissue expression of microRNA-137 and CD8 in oral lichen planus. *Clinical Oral Investigations*, 22:1463. https://doi.org/10.1007/s00784-017-2252-6.

Aghbari SMH, Gaafar SM, Shaker OG, Ashiry SE, & Zayed SO. (2018b). Evaluating the accuracy of microRNA27b and microRNA137 as biomarkers of activity and potential malignant transformation in oral lichen planus patients. *Archives of Dermatological Research*, 310:209. https://doi.org/10.1007/s00403-018-1805-0.

Ajay P, Ashwinirani SR, Nayak A, Suragimath G, Kamala KA, Sande A, & Naik R. (2018). Oral cancer prevalence in western population of Maharashtra, India, for a period of 5 years. *Journal of Oral Research and Review*, 10:11. https://doi.org/10.4103/jorr.jorr_23_17.

Al-Hashimi I, Schifter M, Lockhart PB, Wray D, Brennan M, Migliorati CA, Axéll T, Bruce AJ, Carpenter W, Eisenberg E, Epstein JB, Holmstrup P, Jontell M, Lozada-Nur F, Nair R, Silverman B, Thongprasom K, Thornhill M, Warnakulasuriya S, & van der Waal I. (2007). Oral lichen planus and oral lichenoid lesions: diagnostic and therapeutic considerations. *Oral Surgery, Oral Medicine, Oral Pathology, Oral Radiology, and Endodontics*, 103:e1. https://doi.org/10.1016/j.tripleo.2006.11.001.

Ali K. (2022). Oral cancer - the fight must go on against all odds... *Evidence-Based Dentistry*, 23:4. https://doi.org/10.1038/s41432-022-0243-1.

Alrashdan MS, Cirillo N, & McCullough M. (2016). Oral lichen planus: a literature review and update. *Archives of Dermatological Research*, 308:539. https://doi.org/10.1007/s00403-016-1667-2.

Al-Rawi NH, & Talabani NG. (2008). Squamous cell carcinoma of the oral cavity: a case series analysis of clinical presentation and histological grading of 1,425 cases from Iraq. *Clinical Oral Investigations*, 12:15. https://doi.org/10.1007/s00784-007-0141-0.

Aminuddin A, & Ng PY. (2016). Promising druggable target in head and neck squamous cell carcinoma: Wnt Signaling. *Frontiers in Pharmacology*, 7:244. https://doi.org/10.3389/fphar.2016.00244.

Amit M, Yen TC, Liao CT, Chaturvedi P, Agarwal JP, Kowalski LP, Ebrahimi A, Clark JR, Kreppel M, Zöller J, Fridman E, Bolzoni VA, Shah JP, Binenbaum Y, Patel SG, Gil Z, & International Consortium for Outcome Research (ICOR) in Head and Neck Cancer. (2013). Improvement in survival of patients with oral cavity squamous cell carcinoma: an international collaborative study. *Cancer*, 119:4242. https://doi.org/10.1002/cncr.28357.

Ang KK, Berkey BA, Tu X, Zhang HZ, Katz R, Hammond EH, Fu KK, & Milas L. (2002). Impact of epidermal growth factor receptor expression on survival and pattern of relapse in patients with advanced head and neck carcinoma. *Cancer Research*, 62:7350. PMID: 12499279.

Ankathil, R, Bhattathiri NV, Francis JV, Ratheesan K, Jyothish B, Chandini R, Roy DD, Elizabeth AK, & Nair MK. (1996). Mutagen sensitivity as a predisposing factor in familial oral cancer. *International Journal of Cancer*, 69:265. https://doi.org/10.1002/(SICI)1097-0215(19960822)69:4<265::AID-IJC4>3.0.CO;2-V.

Arakeri G, & Brennan PA. (2013). Oral submucous fibrosis: an overview of the aetiology, pathogenesis, classification, and principles of management. *The British Journal of Oral & Maxillofacial Surgery*, 51:587. https://doi.org/10.1016/j.bjoms.2012.08.014.

Arellano-Garcia ME, Hu S, Wang J, Henson B, Zhou H, Chia D, & Wong DT. (2008). Multiplexed immunobead-based assay for detection of oral cancer protein biomarkers in saliva. *Oral Diseases*, 14:705. https://doi.org/10.1111/j.1601-0825.2008.01488.x.

Awasthi N. (2017). Role of salivary biomarkers in early detection of oral squamous cell carcinoma. *Indian Journal of Pathology & Microbiology*, 60:464. https://doi.org/10.4103/IJPM.IJPM_140_16.

Baba O, Hasegawa S, Nagai H, Uchida F, Yamatoji M, Kanno NI, Yamagata K, Sakai S, Yanagawa T, & Bukawa H. (2016). MicroRNA-155-5p is associated with oral squamous cell carcinoma metastasis and poor prognosis. *Journal of Oral Pathology & Medicine: Official Publication of the International Association of Oral Pathologists and the American Academy of Oral Pathology*, 45:248. https://doi.org/10.1111/jop.12351.

Babiarz JE, Ruby JG, Wang Y, Bartel DP, & Blelloch R. (2008). Mouse ES cells express endogenous shRNAs, siRNAs, and other microprocessor-independent, Dicer-dependent small RNAs. *Genes & Development*, 22:2773. https://doi.org/10.1101/gad.1705308.

Bader AG, Brown D, Stoudemire J, & Lammers P. (2011). Developing therapeutic microRNAs for cancer. *Gene Therapy*, 18:1121. https://doi.org/10.1038/gt.2011.79.

Bagnardi V, Blangiardo M, La Vecchia C, & Corrao G. (2001). A meta-analysis of alcohol drinking and cancer risk. *British Journal of Cancer*, 85:1700. https://doi.org/10.1054/bjoc.2001.2140.

Bakhshandeh B, Soleimani M, Hafizi M, & Ghaemi N. (2012). A comparative study on nonviral genetic modifications in cord blood and bone marrow mesenchymal stem cells. *Cytotechnology*, 64:523. https://doi.org/10.1007/s10616-012-9430-9.

Balaram P, Sridhar H, Rajkumar T, Vaccarella S, Herrero R, Nandakumar A, Ravichandran K, Ramdas K, Sankaranarayanan R, Gajalakshmi V, Muñoz N, & Franceschi S. (2002). Oral cancer in southern India: the influence of smoking, drinking, paan-chewing and oral hygiene. *International Journal of Cancer*, 98:440. https://doi.org/10.1002/ijc.10200.

Balzeau J, Menezes MR, Cao S, & Hagan JP. (2017). The LIN28/let-7 Pathway in Cancer. *Frontiers in Genetics*, 8:31. https://doi.org/10.3389/fgene.2017.00031.

Barger JF, & Nana-Sinkam SP. (2015). MicroRNA as tools and therapeutics in lung cancer. *Respiratory Medicine*, 109:803. https://doi.org/10.1016/j.rmed.2015.02.006.

Barnes L, Everson JW, Reichart P, Sidransky D, editors. (2005). Pathology and genetics of head and neck tumours. Lyon, France: IARC Press (Paperback, ISBN:9283224175).

Bartel DP. (2018). Metazoan microRNAs. *Cell*, 173:20. https://doi.org/10.1016/j.cell.2018.03.006.

Baskerville S, & Bartel DP. (2005). Microarray profiling of microRNAs reveals frequent coexpression with neighboring miRNAs and host genes. *RNA*, 11:241. https://doi.org/10.1261/rna.7240905.

Bast RC, Jr Hennessy B, & Mills GB. (2009). The biology of ovarian cancer: new opportunities for translation. *Nature Reviews Cancer*, 9:415. https://doi.org/10.1038/nrc2644.

Bau DT, Chang CH, Tsai MH, Chiu CF, Tsou YA, Wang RF, Tsai CW, & Tsai RY. (2010). Association between DNA repair gene ATM polymorphisms and oral cancer susceptibility. *The Laryngoscope*, 120:2417. https://doi.org/10.1002/lary.21009.

Beg MS, Brenner AJ, Sachdev J, Borad M, Kang YK, Stoudemire J, Smith S, Bader AG, Kim S, & Hong DS. (2017). Phase I study of MRX34, a liposomal miR-34a mimic, administered twice weekly in patients with advanced solid tumors. *Investigational New Drugs*, 35:180. https://doi.org/10.1007/s10637-016-0407-y.

Bennett AH, O'Donohue MF, Gundry SR, Chan AT, Widrick J, Draper I, Chakraborty A, Zhou Y, Zon LI, Gleizes PE, Beggs AH, & Gupta VA. (2018). RNA helicase, DDX27 regulates skeletal muscle growth and regeneration by modulation of translational processes. *PLoS Genetics*, 14:e1007226. https://doi.org/10.1371/journal.pgen.1007226.

Berindan-Neagoe I, Monroig PdelC, Pasculli B, & Calin GA. (2014). MicroRNAome genome: a treasure for cancer diagnosis and therapy. *CA: A Cancer Journal for Clinicians*, 64:311. https://doi.org/10.3322/caac.21244.

Bernardes VF, Gleber-Netto FO, Sousa SF, Silva TA, & Aguiar MC. (2010). Clinical significance of EGFR, Her-2 and EGF in oral squamous cell carcinoma: a case control study. *Journal of Experimental & Clinical Cancer Research,* 29:40. https://doi.org/10.1186/1756-9966-29-40.

Bernardo BC, Gregorevic P, Ritchie RH, & McMullen JR. (2018). Generation of microRNA-34 sponges and tough decoys for the heart: developments and challenges. *Frontiers in Pharmacology*, 9:1090. https://doi.org/10.3389/fphar.2018.01090.

Bersani C, Mints M, Tertipis N, Haeggblom L, Näsman A, Romanitan M, Dalianis T, & Ramqvist T. (2018). MicroRNA-155, -185 and-193b as biomarkers in human papillomavirus positive and negative tonsillar and base of tongue squamous cell carcinoma. *Oral Oncology*, 82:8. https://doi.org/10.1016/j.oraloncology.2018.04.021.

Bhatt P, Manjunath M, Khakhla D, Gubrellay P, Bhargava R, & Guruprasad L. (2019). Assessment and correlation between functional and histological staging of oral submucous fibrosis: a clinicohistopathologic study. *National Journal of Maxillofacial Surgery*, 10:27. https://doi.org/10.4103/njms.NJMS_15_18.

Bhide SA, & Nutting CM. (2010). Advances in radiotherapy for head and neck cancer. *Oral Oncology*, 46:439. https://doi.org/10.1016/j.oraloncology.2010.03.005.

Bonner JA, Harari PM, Giralt J, Azarnia N, Shin DM, Cohen RB, Jones CU, Sur R, Raben D, Jassem J, Ove R, Kies MS, Baselga J, Youssoufian H, Amellal N, Rowinsky EK, & Ang KK.

(2006). Radiotherapy plus cetuximab for squamous-cell carcinoma of the head and neck. *The New England Journal of Medicine*, 354:567. https://doi.org/10.1056/NEJMoa053422.

Bonner JA, Harari PM, Giralt J, Cohen RB, Jones CU, Sur RK, Raben D, Baselga J, Spencer SA, Zhu J, Youssoufian H, Rowinsky EK, Ang KK. (2010). Radiotherapy plus cetuximab for locoregionally advanced head and neck cancer: 5-year survival data from a phase 3 randomised trial, and relation between cetuximab-induced rash and survival. *The Lancet-Oncol*ogy,11:21. https://doi.org/10.1016/S1470-2045(09)70311-0.

Borchert GM, Lanier W, & Davidson BL. (2006). RNA polymerase III transcribes human microRNAs. *Nature Structural & Molecular Biology*, 13:1097. https://doi.org/10.1038/nsmb1167.

Boroumand F, Saadat I. & Saadat M. (2019). Non-randomness distribution of micro-RNAs on human chromosomes. *Egyptian Journal of Medical Human Genetics*, 20:33. https://doi.org/10.1186/s43042-019-0041-2.

Bracken CP, Gregory PA, Kolesnikoff N, Bert AG, Wang J, Shannon MF, & Goodall GJ. (2008). A double-negative feedback loop between ZEB1-SIP1 and the microRNA-200 family regulates epithelial-mesenchymal transition. *Cancer Research*, 68:7846. https://doi.org/10.1158/0008-5472.CAN-08-1942.

Bråte J, Neumann RS, Fromm B, Haraldsen AAB, Tarver JE, Suga H, Donoghue PCJ, Peterson KJ, Ruiz-Trillo I, Grini PE, & Shalchian-Tabrizi K. (2018). Unicellular origin of the animal microRNA machinery. *Current Biology: CB*, 28:3288. https://doi.org/10.1016/j.cub.2018.08.018.

Bray F, Ferlay J, Soerjomataram I, Siegel RL, Torre LA, & Jemal A. (2018). Global cancer statistics 2018: GLOBOCAN estimates of incidence and mortality worldwide for 36 cancers in 185 countries. *CA: A Cancer Journal for Clinicians*, 68:394. https://doi.org/10.3322/caac.21492.

Bruni L, Diaz M, Barrionuevo-Rosas L, Herrero R, Bray F, Bosch FX, de Sanjosé S, & Castellsagué X. (2016). Global estimates of human papillomavirus vaccination coverage by region and income level: a pooled analysis. *The Lancet-Global Health*, 4:e453. https://doi.org/10.1016/S2214-109X(16)30099-7.

Budach S, Heinig M, & Marsico A. (2016). Principles of microRNA regulation revealed through modeling microRNA expression quantitative trait loci. *Genetics*, 203:1629. https://doi.org/10.1534/genetics.116.187153.

Burk U, Schubert J, Wellner U, Schmalhofer O, Vincan E, Spaderna S, & Brabletz T. (2008). A reciprocal repression between ZEB1 and members of the miR-200 family promotes EMT and invasion in cancer cells. *EMBO Reports*, 9:582. https://doi.org/10.1038/embor.2008.74.

Byatnal AA, Byatnal A, Sen S, Guddattu V, & Solomon MC. (2015). Cyclooxygenase-2-an imperative prognostic biomarker in oral squamous cell carcinoma-an immunohistochemical study. *Pathology Oncology Research: POR*, 21:1123. https://doi.org/10.1007/s12253-015-9940-9.

Calin GA, Dumitru CD, Shimizu M, Bichi R, Zupo S, Noch E, Aldler H, Rattan S, Keating M, Rai K, Rassenti L, Kipps T, Negrini M, Bullrich F, & Croce CM. (2002). Frequent deletions and down-regulation of micro-RNA genes miR15 and miR16 at 13q14 in chronic lymphocytic leukemia. *Proceedings of the National Academy of Sciences of the United States of America*, 99:15524. https://doi.org/10.1073/pnas.242606799.

Calin GA, Ferracin M, Cimmino A, Di Leva G, Shimizu M, Wojcik S E, Iorio MV, Visone R, Sever NI, Fabbri M, Iuliano R, Palumbo T, Pichiorri F, Roldo C, Garzon R, Sevignani C, Rassenti L, Alder H, Volinia S, Liu CG, Kipps TJ, Negrini M, & Croce CM. (2005). A microRNA signature associated with prognosis and progression in chronic lymphocytic leukemia. *The New England Journal of Medicine*, 353:1793. https://doi.org/10.1056/NEJMoa050995.

Calin GA, Sevignani C, Dumitru CD, Hyslop T, Noch E, Yendamuri S, Shimizu M, Rattan S, Bullrich F, Negrini M, & Croce CM. (2004). Human microRNA genes are frequently located at fragile sites and genomic regions involved in cancers. *Proceedings of the National Academy of Sciences of the United States of America* ,101:2999. https://doi.org/10.1073/pnas.242606799.

Campisi G, Panzarella V, Giuliani M, Lajolo C, Di Fede O, Falaschini S, Di Liberto C, Scully C, & Lo Muzio L. (2007). Human papillomavirus: its identity and controversial role in oral oncogenesis, premalignant and malignant lesions (review). *International Journal of Oncology*, 30:813. PMID: 177332919.

Cao ZH, Cheng JL, Zhang Y, Bo CX, & Li YL. (2017). MicroRNA-375 inhibits oral squamous cell carcinoma cell migration and invasion by targeting platelet-derived growth factor-A. *Molecular Medicine Reports*, 15:922. https://doi.org/10.3892/mmr.2016.6057.

Capella DL, Gonçalves JM, Abrantes AAA, Grando LJ, & Daniel FI. (2017). Proliferative verrucous leukoplakia: diagnosis, management and current advances. *Brazilian Journal of Otorhinolaryngology*, 83:585. https://doi.org/10.1016/j.bjorl.2016.12.005.

Carreras-Torras C, & Gay-Escoda C. (2015). Techniques for early diagnosis of oral squamous cell carcinoma: systematic review. *Medicina Oral, Patologia Oral y Cirugia Bucal*, 20:e305. https://doi.org/10.4317/medoral.20347.

Cervigne NK, Reis PP, Machado J, Sadikovic B, Bradley G, Galloni NN, Pintilie M, Jurisica I, Perez-Ordonez B, Gilbert R, Gullane P, Irish J, & Kamel-Reid S. (2009). Identification of a microRNA signature associated with progression of leukoplakia to oral carcinoma. *Human Molecular Genetics*, 18:4818. https://doi.org/10.1093/hmg/ddp446.

Cesana M, Cacchiarelli D, Legnini I, Santini T, Sthandier O, Chinappi M, Tramontano A, & Bozzoni I. (2011). A long noncoding RNA controls muscle differentiation by functioning as a competing endogenous RNA. *Cell*, 147:358. https://doi.org/10.1016/j.cell.2011.09.028.

Chakraborty C, Sharma AR, Sharma G, & Lee SS. (2021). Therapeutic advances of miRNAs: a preclinical and clinical update. *Journal of Advanced Research*, 28:127, https://doi.org/10.1016/j.jare.2020.08.012.

Chaluvally-Raghavan P, Jeong KJ, Pradeep S, Silva AM, Yu S, Liu W, Moss T, Rodriguez-Aguayo C, Zhang D, Ram P, Liu J, Lu Y, Lopez-Berestein G, Calin GA, Sood AK, & Mills GB. (2016). Direct upregulation of STAT3 by microRNA-551b-3p deregulates growth and metastasis of ovarian cancer. *Cell Reports*, 15:1493. https://doi.org/10.1016/j.celrep.2016.04.034.

Chamoli A, Gosavi AS, Shirwadkar UP, Wangdale KV, Behera SK, Kurrey NK, Kalia K, & Mandoli A. (2021). Overview of oral cavity squamous cell carcinoma: risk factors, mechanisms, and diagnostics. *Oral Oncology*, 121:105451. https://doi.org/10.1016/j.oraloncology.2021.105451.

Chan G, Boyle JO, Yang EK, Zhang F, Sacks PG, Shah JP, Edelstein D, Soslow RA, Koki AT, Woerner BM, Masferrer JL, & Dannenberg AJ (1999). Cyclooxygenase-2 expression is up-

regulated in squamous cell carcinoma of the head and neck. *Cancer Research*, 59:991. PMID: 10070952.

Chang HH, Chiang CP, Hung HC, Lin CY, Deng YT, & Kuo MY. (2009). Histone deacetylase 2 expression predicts poorer prognosis in oral cancer patients. *Oral Oncology*, 45:610. https://doi.org/10.1016/j.oraloncology.2008.08.011.

Chang S. (2018). Construction of multi-Potent microRNA sponge and its functional evaluation. *Methods in Molecular Biology,* 1699:201. https://doi.org/10.1007/978-1-4939-7435-1_15.

Chatterjee SJ, George B, Goebell PJ, Alavi-Tafreshi M, Shi SR, Fung YK, Jones PA, Cordon-Cardo C, Datar RH, & Cote RJ. (2004). Hyperphosphorylation of pRb: a mechanism for RB tumour suppressor pathway inactivation in bladder cancer. *The Journal of Pathology*, 203:762. https://doi.org/10.1002/path.1567.

Cheloufi S, Dos Santos CO, Chong MM, & Hannon GJ. (2010). A dicer-independent miRNA biogenesis pathway that requires Ago catalysis. *Nature*, 465:584. https://doi.org/10.1038/nature09092.

Chen C, Zhang Y, Loomis MM, Upton MP, Lohavanichbutr P, Houck JR, Doody DR, Mendez E, Futran N, Schwartz SM, & Wang P. (2015). Genome-wide loss of heterozygosity and DNA copy number aberration in HPV-negative oral squamous cell carcinoma and their associations with disease-specific survival. *PloS One*, 10:e0135074. https://doi.org/10.1371/journal.pone.0135074.

Chen L, Ye HL, Zhang G, Yao WM, Chen XZ, Zhang FC, & Liang G. (2014). Autophagy inhibition contributes to the synergistic interaction between EGCG and doxorubicin to kill the hepatoma Hep3B cells. *PloS One*, 9:e85771. https://doi.org/10.1371/journal.pone.0085771.

Chen LL, & Yang L. (2015). Regulation of circRNA biogenesis. *RNA Biology*, 12:381. https://doi.org/10.1080/15476286.2015.1020271.

Chen SW, Zhang Q, Guo ZM, Chen WK, Liu WW, Chen YF, Li QL, Liu XK, Li H, Ou-Yang D, Chen WC, Fu XY, Wang XD, Yang AK, Bei JX, & Song M. (2018). Trends in clinical features and survival of oral cavity cancer: fifty years of experience with 3,362 consecutive cases from a single institution. *Cancer Management and Research*, 10:4523. https://doi.org/10.2147/CMAR.S171251.

Chen Z, Yu T, Cabay RJ, Jin Y, Mahjabeen I, Luan X, Huang L, Dai Y, & Zhou X. (2017). miR-486-3p, miR-139-5p, and miR-21 as biomarkers for the detection of oral tongue squamous cell carcinoma. *Biomarkers in Cancer*, 9:1. https://doi.org/10.4137/BIC.S40981.

Chiang YT, Chien YC, Lin YH, Wu HH, Lee DF, & Yu YL. (2021). The Function of the Mutant p53-R175H in Cancer. *Cancers*, 13:4088. https://doi.org/10.3390/cancers13164088.

Chinn SB, & Myers JN. (2015). Oral cavity carcinoma: current management, controversies, and future directions. *Journal of Clinical Oncology*, 33:3269. https://doi.org/10.1200/JCO.2015.61.2929.

Chorley BN, Campbell MR, Wang X, Karaca M, Sambandan D, Bangura F, Xue P, Pi J, Kleeberger SR, & Bell DA. (2012). Identification of novel NRF2-regulated genes by ChIP-Seq: influence on retinoid X receptor alpha. *Nucleic Acids Research*, 40:7416. https://doi.org/10.1093/nar/gks409.

Chu TH, Yang CC, Liu CJ, Lui MT, Lin SC, & Chang KW. (2013). miR-211 promotes the progression of head and neck carcinomas by targeting TGFβRII. *Cancer Letters*, 337:115. https://doi.org/10.1016/j.canlet.2013.05.032.

Coleman N, Marcelo KL, Hopkins JF, Khan NI, Du R, Hong L, Park E, Balsara B, Leoni M, Pickering C, Myers J, Heymach J, Albacker LA, Hong D, Gillison M, & Le X. (2023). *HRAS* mutations define a distinct subgroup in head and neck squamous cell carcinoma. *JCO Precision Oncology*, 7:e2200211. https://doi.org/10.1200/PO.22.00211.

Conde J, Oliva N, Atilano M, Song HS, & Artzi N. (2016). Self-assembled RNA-triple-helix hydrogel scaffold for microRNA modulation in the tumour microenvironment. *Nature Materials*, 15:353. https://doi.org/10.1038/nmat4497.

Corney DC, Flesken-Nikitin A, Godwin AK, Wang W, & Nikitin AY. (2007). MicroRNA-34b and microRNA-34c are targets of p53 and cooperate in control of cell proliferation and adhesion-independent growth. *Cancer Research*, 67:8433. https://doi.org/10.1158/0008-5472.CAN-07-1585.

Cristaldi M, Mauceri R, Di Fede O, Giuliana G, Campisi G, & Panzarella V. (2019). Salivary biomarkers for oral squamous cell carcinoma diagnosis and follow-up: current status and perspectives. *Frontiers in Physiology*, 10:1476. https://doi.org/10.3389/fphys.2019.01476.

Cuffari L, Tesseroli de Siqueira JT, Nemr K, & Rapaport A. (2006). Pain complaint as the first symptom of oral cancer: a descriptive study. *Oral Surgery, Oral Medicine, Oral Pathology, Oral Radiology, and Endodontics*, 102:56. https://doi.org/10.1016/j.tripleo.2005.10.041.

Cummins JM, He Y, Leary RJ, Pagliarini R, Diaz LA, Jr Sjoblom T, Barad O, Bentwich Z, Szafranska AE, Labourier E, Raymond CK, Roberts BS, Juhl H, Kinzler KW, Vogelstein B, & Velculescu VE. (2006). The colorectal microRNAome. *Proceedings of the National Academy of Sciences of the United States of America*, 103:3687. https://doi.org/10.1073/pnas.0511155103.

Dai Q, Li J, Zhou K, & Liang T. (2015). Competing endogenous RNA: a novel posttranscriptional regulatory dimension associated with the progression of cancer. *Oncology Letters*, 10:2683. https://doi.org/10.3892/ol.2015.3698.

Dang J, Bian YQ, Sun JY, Chen F, Dong GY, Liu Q, Wang XW, Kjems J, Gao S, & Wang QT. (2013). MicroRNA-137 promoter methylation in oral lichen planus and oral squamous cell carcinoma. *Journal of Oral Pathology & Medicine: Official Publication of the International Association of Oral Pathologists and the American Academy of Oral Pathology*, 42:315. https://doi.org/10.1111/jop.12012.

Das BR, & Nagpal JK. (2002). Understanding the biology of oral cancer. *Medical Science Monitor: International Medical Journal of Experimental and Clinical Research*, 8:RA258. PMID: 12444391.

Das S, Kohr M, Dunkerly-Eyring B, Lee DI, Bedja D, Kent OA, Leung AK, Henao-Mejia J, Flavell RA, & Steenbergen C. (2017). Divergent effects of miR-181 family members on myocardial function through protective cytosolic and detrimental mitochondrial microRNA Targets. *Journal of the American Heart Association*, 6:e004694. https://doi.org/10.1161/JAHA.116.004694.

Davis-Dusenbery BN, & Hata A. (2010). Mechanisms of control of microRNA biogenesis. *Journal of Biochemistry*, 148:381. https://doi.org/10.1093/jb/mvq096.

D'Cruz AK, Vaish R, & Dhar H. (2018). Oral cancers: current status. *Oral Oncology*, 87:64. https://doi.org/10.1016/j.oraloncology.2018.10.013.

de la Cour CD, Sperling CD, Belmonte F, Syrjänen S, & Kjaer SK. (2021). Human papillomavirus prevalence in oral potentially malignant disorders: systematic review and meta-analysis. *Oral Diseases*, 27:431. https://doi.org/10.1111/odi.13322.

de Rie D, Abugessaisa I, Alam T, Arner E, Arner P, Ashoor H, Åström G, Babina M, Bertin N, Burroughs AM, Carlisle AJ, Daub CO, Detmar M, Deviatiiarov R, Fort A, Gebhard C, Goldowitz D, Guhl S, Ha TJ, Harshbarger J, … & de Hoon MJL. (2017). An integrated expression atlas of miRNAs and their promoters in human and mouse. *Nature Biotechnology*, 35:872. https://doi.org/10.1038/nbt.3947.

Denli AM, Tops BB, Plasterk RH, Ketting RF, & Hannon GJ. (2004). Processing of primary microRNAs by the microprocessor complex. *Nature*, 432:231. https://doi.org/10.1038/nature03049.

DeVeale B, Swindlehurst-Chan J, & Blelloch R. (2021). The roles of microRNAs in mouse development. *Nature Reviews Genetics*, 22:307. https://doi.org/10.1038/s41576-020-00309-5.

Dharap A, Pokrzywa C, Murali S, Pandi G, & Vemuganti R. (2013). MicroRNA miR-324-3p induces promoter-mediated expression of RelA gene. *PloS One*, 8:e79467. https://doi.org/10.1371/journal.pone.0079467.

Dhull AK, Atri R, Dhankhar R, Chauhan AK, & Kaushal V. (2018). Major risk factors in head and neck cancer: a retrospective analysis of 12-year experiences. *World Journal of Oncology*, 9:80. https://doi.org/10.14740/wjon1104w.

Di Leva G, Garofalo M, & Croce CM. (2014). MicroRNAs in cancer. *Annual Review of Pathology*, 9:287. https://doi.org/10.1146/annurev-pathol-012513-104715.

Dioguardi M, Spirito F, Sovereto D, Alovisi M, Aiuto R, Garcovich D, Crincoli V, Laino L, Cazzolla AP, Caloro GA, Di Cosola M, Ballini A, Lo Muzio L, & Troiano G. (2022). The prognostic role of miR-31 in head and neck squamous cell carcinoma: systematic review and meta-analysis with trial sequential analysis. *International Journal of Environmental Research and Public Health*, 19:5334. https://doi.org/10.3390/ijerph19095334.

Dodson TB. (2010). The frequency of human papilloma virus (HPV) is higher in premalignant and malignant oral mucosal lesions than normal mucosa. *The Journal of Evidence-Based Dental Practice*, 10:174. https://doi.org/10.1016/j.jebdp.2010.05.012.

Dragomir MP, Knutsen E, & Calin GA. (2018). SnapShot: unconventional miRNA functions. *Cell*, 174:1038. https://doi.org/10.1016/j.cell.2018.07.040.

D'Souza G, Kreimer AR, Viscidi R, Pawlita M, Fakhry C, Koch WM, Westra WH, & Gillison ML. (2007). Case-control study of human papillomavirus and oropharyngeal cancer. *The New England Journal of Medicine*, 356:1944. https://doi.org/10.1056/NEJMoa065497.

D'Souza W, & Kumar A. (2020). microRNAs in oral cancer: moving from bench to bed as next generation medicine. *Oral Oncology*, 111:104916. https://doi.org/10.1016/j.oraloncology.2020.104916.

Duan Q, Xu M, Wu M, Zhang X, Gan M, & Jiang H. (2020). Long noncoding RNA UCA1 promotes cell growth, migration, and invasion by targeting miR-143-3p in oral squamous cell carcinoma. *Cancer Medicine*, 9:3115. https://doi.org/10.1002/cam4.2808.

Duz MB, Karatas OF, Guzel E, Turgut NF, Yilmaz M, Creighton CJ, & Ozen M. (2016). Identification of miR-139-5p as a saliva biomarker for tongue squamous cell carcinoma: a pilot study. *Cellular Oncology*, 39:187. https://doi.org/10.1007/s13402-015-0259-z.

Ebert MS, & Sharp PA. (2010). MicroRNA sponges: progress and possibilities. *RNA*, 16:2043. https://doi.org/10.1261/rna.2414110.

Elango KJ, Anandkrishnan N, Suresh A, Iyer SK, Ramaiyer SK, & Kuriakose MA. (2011). Mouth self-examination to improve oral cancer awareness and early detection in a high-risk population. *Oral Oncology*, 47:620. https://doi.org/10.1016/j.oraloncology.2011.05.001.

Elashoff D, Zhou H, Reiss J, Wang J, Xiao H, Henson B, Hu S, Arellano M, Sinha U, Le A, Messadi D, Wang M, Nabili V, Lingen M, Morris D, Randolph T, Feng Z, Akin D, Kastratovic D. A, Chia D, … & Wong DT. (2012). Prevalidation of salivary biomarkers for oral cancer detection. *Cancer Epidemiology, Biomarkers & Prevention: A Publication of the American Association for Cancer Research, cosponsored by the American Society of Preventive Oncology*, 21:664. https://doi.org/10.1158/1055-9965.EPI-11-1093.

Eling TE, Thompson DC, Foureman GL, Curtis JF, & Hughes MF. (1990). Prostaglandin H synthase and xenobiotic oxidation. *Annual Review of Pharmacology and Toxicology*, 30:1. https://doi.org/10.1146/annurev.pa.30.040190.000245.

Ellis MA, Graboyes EM, Wahlquist AE, Neskey DM, Kaczmar JM, Schopper HK, Sharma AK, Morgan PF, Nguyen SA, & Day TA. (2018). Primary surgery vs radiotherapy for early stage

oral cavity cancer. *Otolaryngology-Head and Neck Surgery: Official Journal of American Academy of Otolaryngology-Head and Neck Surgery*, 158:649. https://doi.org/10.1177/0194599817746909.

Endo-Takahashi Y, Negishi Y, Nakamura A, Ukai S, Ooaku K, Oda Y, Sugimoto K, Moriyasu F, Takagi N, Suzuki R, Maruyama K, & Aramaki Y. (2014). Systemic delivery of miR-126 by miRNA-loaded bubble liposomes for the treatment of hindlimb ischemia. *Scientific Reports,* 4:3883.https://doi.org/10.1038/srep03883.

Esteller M. (2008). Epigenetics in cancer. *The New England Journal of Medicine*, 358:1148. https://doi.org/10.1056/NEJMra072067.

Fabbri M, Calore F, Paone A, Galli R, & Calin GA. (2013). Epigenetic regulation of miRNAs in cancer. *Advances in Experimental Medicine and Biology*, 754:137. https://doi.org/10.1007/978-1-4419-9967-2_6.

Fabbri M, Garzon R, Cimmino A, Liu Z, Zanesi N, Callegari E, Liu S, Alder H, Costinean S, Fernandez-Cymering C, Volinia S, Guler G, Morrison CD, Chan KK, Marcucci G, Calin GA, Huebner K, & Croce CM. (2007). MicroRNA-29 family reverts aberrant methylation in lung cancer by targeting DNA methyltransferases 3A and 3B. *Proceedings of the National Academy of Sciences of the United States of America*, 104:15805. https://doi.org/10.1073/pnas.0707628104.

Fabian M, & Sonenberg N. (2012) The mechanics of miRNA-mediated gene silencing: a look under the hood of miRISC. *Nature Structural and Molecular Biology,* 19:586. https://doi.org/10.1038/nsmb.2296.

Fang Z, Zhao J, Xie W, Sun Q, Wang H, & Qiao B. (2017). LncRNA UCA1 promotes proliferation and cisplatin resistance of oral squamous cell carcinoma by suppressing miR-184 expression. *Cancer Medicine*, 6:2897. https://doi.org/10.1002/cam4.1253.

Farah CS, Woo SB, Zain RB, Sklavounou A, McCullough MJ, & Lingen M. (2014). Oral cancer and oral potentially malignant disorders. *International Journal of Dentistry*, 2014:853479. https://doi.org/10.1155/2014/853479.

Farsi NJ, El-Zein M, Gaied H, Lee YC, Hashibe M, Nicolau B, & Rousseau MC. (2015). Sexual behaviours and head and neck cancer: a systematic review and meta-analysis. *Cancer Epidemiology*, 39:1036. https://doi.org/10.1016/j.canep.2015.08.010.

Feller L, Altini M, & Lemmer J. (2013). Inflammation in the context of oral cancer. *Oral Oncology*, 49:887. https://doi.org/10.1016/j.oraloncology.2013.07.003.

Felli N, Fontana L, Pelosi E, Botta R, Bonci D, Facchiano F, Liuzzi F, Lulli V, Morsilli O, Santoro S, Valtieri M, Calin GA, Liu CG, Sorrentino A, Croce CM, & Peschle C. (2005). MicroRNAs 221 and 222 inhibit normal erythropoiesis and erythroleukemic cell growth via kit receptor down-modulation. *Proceedings of the National Academy of Sciences of the United States of America*, 102:18081. https://doi.org/10.1073/pnas.0506216102.

Ferris RL, Blumenschein G Jr, Fayette J, Guigay J, Colevas AD, Licitra L, Harrington K, Kasper S,Vokes EE, Even C, Worden F, Saba NF, Iglesias Docampo LC, Haddad R, Rordorf T, Kiyota N, Tahara M, Monga M, Lynch M, Geese WJ, Kopit J, Shaw JW, & Gillison ML. (2016). Nivolumab for recurrent squamous-cell carcinoma of the head and neck. *The New England Journal of Medicine*, 375:1856. https://doi.org/10.1056/NEJMoa1602252.

Ferris RL, Blumenschein G Jr, Fayette J, Guigay J, Colevas AD, Licitra L, Harrington KJ, Kasper S, Vokes EE, Even C, Worden F, Saba NF, Docampo LCI, Haddad R, Rordorf T, Kiyota N, TaharaM, Lynch M, Jayaprakash V, Li L, & Gillison ML. (2018). Nivolumab vs investigator's choice in recurrent or metastatic squamous cell carcinoma of the head and neck: 2-year long-term survival update of CheckMate 141 with analyses by tumor PD-L1 expression. *Oral Oncology*, 81:45. https://doi.org/10.1016/j.oraloncology.2018.04.008.

Flausino CS, Daniel FI, & Modolo F. (2021). DNA methylation in oral squamous cell carcinoma: from its role in carcinogenesis to potential inhibitor drugs. *Critical Reviews in Oncology/Hematology*, 164:103399. https://doi.org/10.1016/j.critrevonc.2021.103399.

França GS, Vibranovski MD, & Galante PA. (2016). Host gene constraints and genomic context impact the expression and evolution of human microRNAs. *Nature Communications*, 7:11438. https://doi.org/10.1038/ncomms11438.

Franceschi S, Talamini R, Barra S, Barón AE, Negri E, Bidoli E, Serraino D, & La Vecchia C. (1990). Smoking and drinking in relation to cancers of the oral cavity, pharynx, larynx, and esophagus in northern Italy. *Cancer Research*, 50:6502. PMID: 2208109.

Franzmann EJ, Reategui EP, Carraway KL, Hamilton KL, Weed DT, & Goodwin WJ. (2005). Salivary soluble CD44: a potential molecular marker for head and neck cancer. *Cancer Epidemiology, Biomarkers & Prevention: A Publication of the American Association for*

Cancer Research, Cosponsored by the American Society of Preventive Oncology, 14:735. https://doi.org/10.1158/1055-9965.EPI-04-0546.

Fridman E, Na'ara S, Agarwal J, Amit M, Bachar G, Villaret AB, Brandao J, Cernea CR, Chaturvedi P, Clark J, Ebrahimi A, Fliss DM, Jonnalagadda S, Kohler HF, Kowalski LP, Kreppel M, Liao CT, Patel SG, Patel RS, Robbins KT, Shah JP, Shpitzer T, Yen TC, Zöller JE, Gil Z & International Consortium for Outcome Research in Head and Neck Cancer. (2018). The role of adjuvant treatment in early-stage oral cavity squamous cell carcinoma: an international collaborative study. *Cancer*, 124:2948. https://doi.org/10.1002/cncr.31531.

Friedländer MR, Lizano E, Houben AJ, Bezdan D, Báñez-Coronel M, Kudla G, Mateu-Huertas E, Kagerbauer B, González J, Chen KC, LeProust EM, Martí E, & Estivill X. (2014). Evidence for the biogenesis of more than 1,000 novel human microRNAs. *Genome Biology*, 15:R57. https://doi.org/10.1186/gb-2014-15-4-r57.

Friedman RC, Farh KK, Burge CB, & Bartel DP. (2009). Most mammalian mRNAs are conserved targets of microRNAs. *Genome Research*, 19:92. https://doi.org/10.1101/gr.082701.108.

Frommer M, McDonald LE, Millar DS, Collis CM, Watt F, Grigg GW, Molloy PL, & Paul CL. (1992). A genomic sequencing protocol that yields a positive display of 5-methylcytosine residues in individual DNA strands. *Proceedings of the National Academy of Sciences of the United States of America*, 89:1827. https://doi.org/10.1073/pnas.89.5.1827.

Fu S, Chen HH, Cheng P, Zhang CB, & Wu Y. (2017). MiR-155 regulates oral squamous cell carcinoma Tca8113 cell proliferation, cycle, and apoptosis via regulating p27Kip1. *European Review for Medical and Pharmacological Sciences*, 21:937. PMID: 28338203.

Fuller-Pace FV. (2013). The DEAD box proteins DDX5 (p68) and DDX17 (p72): multi-tasking transcriptional regulators. *Biochimica et Biophysica Acta*, 1829:756. https://doi.org/10.1016/j.bbagrm.2013.03.004.

García-Pola MJ, González-Álvarez L, & Garcia-Martin JM. (2017). Treatment of oral lichen planus. Systematic review and therapeutic guide. *Medicina Clinica*, 149:351. https://doi.org/10.1016/j.medcli.2017.06.024.

Garibaldi F, Falcone E, Trisciuoglio D, Colombo T, Lisek K, Walerych D, Del Sal G, Paci P, Bossi G, Piaggio G, & Gurtner A. (2016). Mutant p53 inhibits miRNA biogenesis by interfering with the microprocessor complex. *Oncogene*, 35:3760. https://doi.org/10.1038/onc.2016.51.

Garofalo M, Quintavalle C, Romano G, Croce CM, & Condorelli G. (2012). miR221/222 in cancer: their role in tumor progression and response to therapy. *Current Molecular Medicine*, 12:27. https://doi.org/10.2174/156652412798376170.

Garzon R, Liu S, Fabbri M, Liu Z, Heaphy CE, Callegari E, Schwind S, Pang J, Yu J, Muthusamy N, Havelange V, Volinia S, Blum W, Rush LJ, Perrotti D, Andreeff M, Bloomfield CD, Byrd JC, Chan K, Wu LC, … & Marcucci G. (2009). MicroRNA-29b induces global DNA hypomethylation and tumor suppressor gene reexpression in acute myeloid leukemia by targeting directly DNMT3A and 3B and indirectly DNMT1. *Blood*, 113:6411. https://doi.org/10.1182/blood-2008-07-170589.

Gasche JA, & Goel A. (2012). Epigenetic mechanisms in oral carcinogenesis. *Future Oncology*, 8:1407. https://doi.org/10.2217/fon.12.138.

Gasche JA, Hoffmann J, Boland CR, & Goel A. (2011). Interleukin-6 promotes tumorigenesis by altering DNA methylation in oral cancer cells. *International Journal of Cancer*, 129:1053. https://doi.org/10.1002/ijc.25764.

Ge X, Li Z, Zhou Z, Xia Y, Bian M, & Yu J. (2020). Circular RNA SIPA1L1 promotes osteogenesis via regulating the miR-617/Smad3 axis in dental pulp stem cells. *Stem Cell Research & Therapy*, 11:364. https://doi.org/10.1186/s13287-020-01877-3.

Gebert LF, Rebhan MA, Crivelli SE, Denzler R, Stoffel M, & Hall J. (2014). Miravirsen (SPC3649) can inhibit the biogenesis of miR-122. *Nucleic Acids Research*, 42:609. https://doi.org/10.1093/nar/gkt852.

Georgaki M, Theofilou VI, Pettas E, Stoufi E, Younis RH, Kolokotronis A, Sauk JJ, & Nikitakis NG. (2021). Understanding the complex pathogenesis of oral cancer: a comprehensive review. *Oral Surgery, Oral Medicine, Oral Pathology and Oral Radiology*, 132:566. https://doi.org/https://doi.org/10.1016/j.oooo.2021.04.004.

Ghafouri-Fard S, Dashti S, Farsi M, & Taheri M. (2021). HOX transcript antisense RNA: an oncogenic lncRNA in diverse malignancies. *Experimental and Molecular Pathology*, 118:104578. https://doi.org/10.1016/j.yexmp.2020.104578.

Ghanghoria S, Ghanghoria A, & Shukla A. (2015). P53 Expression in oral cancer: a study of 50 cases. *Journal of Pathology of Nepal*, 5:747. https://doi.org/10.3126/jpn.v5i9.13785.

Ghosh R, Singh LC, Shohet JM, & Gunaratne PH. (2013). A gold nanoparticle platform for the delivery of functional microRNAs into cancer cells. *Biomaterials*, 34:807. https://doi.org/10.1016/j.biomaterials.2012.10.023.

Ghosh RD, Pattatheyil A, & Roychoudhury S. (2020). Functional landscape of dysregulated microRNAs in oral squamous cell carcinoma: clinical implications. *Frontiers in Oncology,* 10:619. https://doi.org/10.3389/fonc.2020.00619.

Gilardi M, Wang Z, Proietto M, Chillà A, Calleja-Valera JL, Goto Y, Vanoni M, Janes MR, Mikulski Z, Gualberto A, Molinolo AA, Ferrara N, Gutkind JS, & Burrows F. (2020). Tipifarnib as a precision therapy for *HRAS*-mutant head and neck squamous cell carcinomas. *Molecular Cancer Therapeutics*, 19:1784. https://doi.org/10.1158/1535-7163.MCT-19-0958.

Gillison ML, Broutian T, Pickard RK, Tong ZY, Xiao W, Kahle L, Graubard BI, & Chaturvedi AK. (2012). Prevalence of oral HPV infection in the United States, 2009-2010. *Journal of the American Medical Association*, 307:69. https://doi.org/10.1001/jama.2012.101.

Gilot D, Migault M, Bachelot L, Journé F, Rogiers A, Donnou-Fournet E, Mogha A, Mouchet N, Pinel-Marie ML, Mari B, Montier T, Corre S, Gautron A, Rambow F, El Hajj P, Ben Jouira R, Tartare-Deckert S, Marine JC, Felden B, Ghanem G, … & Galibert MD. (2017). A non-coding function of TYRP1 mRNA promotes melanoma growth. *Nature Cell Biology*, 19:1348. https://doi.org/10.1038/ncb3623.

Gkouveris I, & Nikitakis NG. (2017). Role of JNK signaling in oral cancer: a mini review. *Tumour Biology: The Journal of the International Society for Oncodevelopmental Biology and Medicine*, 39. https://doi.org/10.1177/1010428317711659.

Gleber-Netto FO, Yakob M, Li F, Feng Z, Dai J, Kao HK, Chang YL, Chang KP, & Wong DT. (2016). Salivary biomarkers for detection of oral squamous cell carcinoma in a Taiwanese population. *Clinical Cancer Research: An Official Journal of the American Association for Cancer Research*, 22:3340. https://doi.org/10.1158/1078-0432.CCR-15-1761.

Goertzen C, Mahdi H, Laliberte C, Meirson T, Eymael D, Gil-Henn H, & Magalhaes M. (2018). Oral inflammation promotes oral squamous cell carcinoma invasion. *Oncotarget*, 9:29047. https://doi.org/10.18632/oncotarget.25540.

Goldenberg D, Begum S, Westra WH, Khan Z, Sciubba J, Pai SI, Califano JA, Tufano RP, & Koch WM. (2008). Cystic lymph node metastasis in patients with head and neck cancer: an HPV-associated phenomenon. *Head & Neck*, 30:898. https://doi.org/10.1002/hed.20796.

Gomes RS, das Neves RP, Cochlin L, Lima A, Carvalho R, Korpisalo P, Dragneva G, Turunen M, Liimatainen T, Clarke K, Ylä-Herttuala S, Carr C, & Ferreira L. (2013). Efficient pro-survival/angiogenic miRNA delivery by an MRI-detectable nanomaterial. *ACS nano*, 7:3362. https://doi.org/10.1021/nn400171w.

González-Losa MdelR, Manzano-Cabrera L, Rueda-Gordillo F, Hernández-Solís SE, & Puerto-Solís L. (2008). Low prevalence of high risk human papillomavirus in normal oral mucosa by hybrid capture 2. *Brazilian Journal of Microbiology: Publication of the Brazilian Society for Microbiology*, 39:32. https://doi.org/10.1590/S1517-83822008000100008.

Gonzalez-Zulueta M, Bender CM, Yang AS, Nguyen T, Beart RW, Van Tornout JM, & Jones PA. (1995). Methylation of the 5' CpG island of the p16/CDKN2 tumor suppressor gene in normal and transformed human tissues correlates with gene silencing. *Cancer Research*, 55: 4531. PMID: 7553622.

Gopinath D, Menon RK, Wie CC, Banerjee M, Panda S, Mandal D, Behera PK, Roychoudhury S, Kheur S, Botelho MG, & Johnson NW. (2021). Differences in the bacteriome of swab, saliva, and tissue biopsies in oral cancer. *Scientific Reports*, 11:1181. https://doi.org/10.1038/s41598-020-80859-0.

Gorsky M, & Epstein JB. (2002). The effect of retinoids on premalignant oral lesions: focus on topical therapy. *Cancer*, 95:1258. https://doi.org/10.1002/cncr.10874.

Gorsky M, Epstein JB, Oakley C, Le ND, Hay J, & Stevenson-Moore P. (2004). Carcinoma of the tongue: a case series analysis of clinical presentation, risk factors, staging, and outcome. *Oral Surgery, Oral Medicine, Oral Pathology, Oral Radiology, and Endodontics*, 98:546. https://doi.org/10.1016/j.tripleo.2003.12.041.

Gorsky M, Littner MM, Sukman Y, & Begleiter A. (1994). The prevalence of oral cancer in relation to the ethnic origin of Israeli Jews. *Oral surgery, Oral Medicine, and Oral Pathology*, 78:408. https://doi.org/10.1016/0030-4220(94)90077-9.

Grandis JR, Drenning SD, Zeng Q, Watkins SC, Melhem MF, Endo S, Johnson DE, Huang L, He Y, & Kim JD. (2000). Constitutive activation of Stat3 signaling abrogates apoptosis in

squamous cell carcinogenesis *in vivo*. *Proceedings of the National Academy of Sciences of the United States of America*, 97:4227. https://doi.org/10.1073/pnas.97.8.4227.

Greither T, Vorwerk F, Kappler M, Bache M, Taubert H, Kuhnt T, Hey J, & Eckert AW. (2017). Salivary miR-93 and miR-200a as post-radiotherapy biomarkers in head and neck squamous cell carcinoma. *Oncology Reports*, 38:1268. https://doi.org/10.3892/or.2017.5764.

Guerrero-Preston R, Godoy-Vitorino F, Jedlicka A, Rodríguez-Hilario A, González H, Bondy J, Lawson F, Folawiyo O, Michailidi C, Dziedzic A, Thangavel R, Hadar T, Noordhuis MG, Westra W, Koch W, & Sidransky D. (2016). 16S rRNA amplicon sequencing identifies microbiota associated with oral cancer, human papilloma virus infection and surgical treatment. *Oncotarget*, 7:51320. https://doi.org/10.18632/oncotarget.9710.

Gupta AA, Kheur S, Varadarajan S, Parveen S, Dewan H, Alhazmi YA, Raj TA, Testarelli L, & Patil S. (2021). Chronic mechanical irritation and oral squamous cell carcinoma: a systematic review and meta-analysis. *Bosnian Journal of Basic Medical Sciences*, 21:647. https://doi.org/10.17305/bjbms.2021.5577.

Gupta B. (2013). Burden of smoked and smokeless tobacco consumption in India - results from the Global adult Tobacco Survey India (GATS-India)- 2009-2010. *Asian Pacific Journal of Cancer Prevention*, 14:3323. https://doi.org/10.7314/apjcp.2013.14.5.3323.

Gupta PC, & Ray CS. (2003). Smokeless tobacco and health in India and South Asia. *Respirology*, 8:419. https://doi.org/10.1046/j.1440-1843.2003.00507.x.

Gupta PC, & Warnakulasuriya S. (2002). Global epidemiology of areca nut usage. *Addiction Biology*, 7:77. https://doi.org/10.1080/13556210020091437.

Gupta PC, Bhonsle RB, Murti PR, Daftary DK, Mehta FS, & Pindborg JJ. (1989). An epidemiologic assessment of cancer risk in oral precancerous lesions in India with special reference to nodular leukoplakia. *Cancer*, 63:2247. https://doi.org/10.1002/1097-0142(19890601)63:11%3C2247::AID-CNCR2820631132%3E3.0.CO;2-D.

Gupta S, & Gupta S. (2015). Role of human papillomavirus in oral squamous cell carcinoma and oral potentially malignant disorders: A review of the literature. *Indian Journal of Dentistry*, 6:91. https://doi.org/10.4103/0975-962X.155877.

Gupta S, Gupta R, Sinha DN, & Mehrotra R. (2018). Relationship between type of smokeless tobacco & risk of cancer: a systematic review. *Indian Journal of Medical Research*, 148:56.

https://doi.org/10.1046/j.1440-1843.2003.00507.x.

Gupta S, Jawanda MK, & Madhushankari GS. (2020). Current challenges and the diagnostic pitfalls in the grading of epithelial dysplasia in oral potentially malignant disorders: a review. *Journal of Oral Biology and Craniofacial Research*, 10:788. https://doi.org/10.1016/j.jobcr.2020.09.005.

Gurtner A, Falcone E, Garibaldi F, & Piaggio G. (2016). Dysregulation of microRNA biogenesis in cancer: the impact of mutant p53 on Drosha complex activity. *Journal of Experimental & Clinical Cancer Research*, 35:45. https://doi.org/10.1186/s13046-016-0319-x.

Ha M, & Kim VN. (2014). Regulation of microRNA biogenesis. *Nature Reviews Molecular Cell Biology*, 15:509. https://doi.org/10.1038/nrm3838.

Han J, Lee Y, Yeom KH, Kim YK, Jin H, & Kim VN. (2004). The Drosha-DGCR8 complex in primary microRNA processing. *Genes & Development*, 18:3016. https://doi.org/10.1101/gad.1262504.

Hanahan D, & Weinberg A. (2000). The hallmarks of cancer. *Cell*, 100:57. https://doi.org/10.1016/s0092-8674(00)81683-9.

Hao L, Patel PC, Alhasan AH, Giljohann DA, & Mirkin CA. (2011). Nucleic acid-gold nanoparticle conjugates as mimics of microRNA. *Small (Weinheim an der Bergstrasse, Germany)*, 7:3158. https://doi.org/10.1002/smll.201101018.

Haya-Fernández MC, Bagán JV, Murillo-Cortés J, Poveda-Roda R, & Calabuig C. (2004). The prevalence of oral leukoplakia in 138 patients with oral squamous cell carcinoma. *Oral Diseases*, 10:346. https://doi.org/10.1111/j.1601-0825.2004.01031.x.

He L, He X, Lim LP, de Stanchina E, Xuan Z, Liang Y, Xue W, Zender L, Magnus J, Ridzon D, Jackson AL, Linsley PS, Chen C, Lowe SW, Cleary MA, & Hannon GJ. (2007). A microRNA component of the p53 tumour suppressor network. *Nature*, 447:1130. https://doi.org/10.1038/nature05939.

He T, Li X, Xie D, & Tian L. (2019). Overexpressed circPVT1 in oral squamous cell carcinoma promotes proliferation by serving as a miRNA sponge. *Molecular Medicine Reports*, 20:3509. https://doi.org/10.3892/mmr.2019.10615.

Hendawi N, Niklander S, Allsobrook O, Khurram SA, Bolt R, Doorbar J, Speight PM, & Hunter KD. (2020). Human papillomavirus (HPV) can establish productive infection in

dysplastic oral mucosa, but HPV status is poorly predicted by histological features and p16 expression. *Histopathology*, 76:592. https://doi.org/10.1111/his.14019.

Heo I, Joo C, Cho J, Ha M, Han J, & Kim VN. (2008). Lin28 mediates the terminal uridylation of let-7 precursor MicroRNA. *Molecular Cell*, 32:276. https://doi.org/10.1016/j.molcel.2008.09.014.

Heravi-Moussavi A, Anglesio MS, Cheng SW, Senz J, Yang W, Prentice L, Fejes AP, Chow C, Tone A, Kalloger SE, Hamel N, Roth A, Ha G, Wan AN, Maines-Bandiera S, Salamanca C, Pasini B, Clarke BA, Lee AF, Lee CH, … & Huntsman DG. (2012). Recurrent somatic DICER1 mutations in nonepithelial ovarian cancers. *The New England Journal of Medicine*, 366:234. https://doi.org/10.1056/NEJMoa1102903.

Hientz K, Mohr A, Bhakta-Guha D, & Efferth T. (2017). The role of p53 in cancer drug resistance and targeted chemotherapy. *Oncotarget*, 8:8921. https://doi.org/10.18632/oncotarget.13475.

Hinske LC, França GS, Torres HA, Ohara DT, Lopes-Ramos CM, Heyn J, Reis LF, Ohno-Machado L, Kreth S, & Galante PA. (2014). miRIAD-integrating microRNA inter- and intragenic data. *Database: The Journal of Biological Databases and Curation*, 2014:bau099. https://doi.org/10.1093/database/bau099.

Hinske LC, Galante PA, Kuo WP, & Ohno-Machado L. (2010). A potential role for intragenic miRNAs on their hosts' interactome. *BMC Genomics*, 11:533. https://doi.org/10.1186/1471-2164-11-533.

Ho AS, Kraus DH, Ganly I, Lee NY, Shah JP, & Morris LG. (2014) Decision making in the management of recurrent head and neck cancer. *Head & Neck*, 36:144. https://doi.org/10.1002/hed.23227.

Hoffmann TK, Sonkoly E, Homey B, Scheckenbach K, Gwosdz C, Bas M, Chaker A, Schirlau K, & Whiteside TL. (2007). Aberrant cytokine expression in serum of patients with adenoid cystic carcinoma and squamous cell carcinoma of the head and neck. *Head & Neck*, 29:472. https://doi.org/10.1002/hed.20533.

Hong DS, Kang YK, Borad M, Sachdev J, Ejadi S, Lim HY, Brenner AJ, Park K, Lee JL, Kim TY, Shin S, Becerra CR, Falchook G, Stoudemire J, Martin D, Kelnar K, Peltier H, Bonato V, Bader AG, Smith S, … & Beg MS. (2020). Phase 1 study of MRX34, a liposomal miR-34a

mimic, in patients with advanced solid tumours. *British Journal of Cancer*, 122:1630. https://doi.org/10.1038/s41416-020-0802-1.

Horibata S, Vo TV, Subramanian V, Thompson PR, & Coonrod SA. (2015). Utilization of the soft agar colony formation assay to identify inhibitors of tumorigenicity in breast cancer cells. *Journal of Visualized Experiments-JoVE*, 99:e52727. https://doi.org/10.3791/52727.

Hosseinahli N, Aghapour M, Duijf PHG, & Baradaran B. (2018). Treating cancer with microRNA replacement therapy: a literature review. *Journal of Cellular Physiology*, 233:5574. https://doi.org/10.1002/jcp.26514.

Hou HA, Chou WC, Kuo YY, Liu CY, Lin LI, Tseng MH, Chiang YC, Liu MC, Liu CW, Tang JL, Yao M, Li CC, Huang SY, Ko BS, Hsu SC, Chen CY, Lin CT, Wu SJ, Tsay W, Chen YC, … & Tien HF. (2015). TP53 mutations in de novo acute myeloid leukemia patients: longitudinal follow-ups show the mutation is stable during disease evolution. *Blood Cancer Journal*, 5:e331. https://doi.org/10.1038/bcj.2015.59.

Hou XL, Chen WQ, Hou Y, Gong HQ, Sun J, Wang Z, Zhao H, Cao X, Song XF, & Liu CM. (2021). DEAD-BOX RNA HELICASE 27 regulates microRNA biogenesis, zygote division, and stem cell homeostasis. *The Plant Cell*, 33:66. https://doi.org/10.1093/plcell/koaa001.

Hu J, Ge W, & Xu J. (2016). HPV 16 E7 inhibits OSCC cell proliferation, invasion, and metastasis by upregulating the expression of miR-20a. *Tumour Biology: The Journal of the International Society for Oncodevelopmental Biology and Medicine*, 37:9433. https://doi.org/10.1007/s13277-016-4817-4.

Hu QL, Jiang QY, Jin X, Shen J, Wang K, Li YB, Xu FJ, Tang GP, & Li ZH. (2013). Cationic microRNA-delivering nanovectors with bifunctional peptides for efficient treatment of PANC-1 xenograft model. *Biomaterials*, 34:2265. https://doi.org/10.1016/j.biomaterials.2012.12.016.

Huang R, Guo G, Lu L, Fu R, Luo J, Liu Z, Gu Y, Yang W, Zheng Q, Chao T, He L, Wang Y, Niu Z, Wang H, Lawrence T, Malissen M, Malissen B, Liang Y, & Zhang L. (2019). The three members of the Vav family proteins form complexes that concur to foam cell formation and atherosclerosis. *Journal of Lipid Research*, 60:2006. https://doi.org/10.1194/jlr.M094771.

Huang V, Place RF, Portnoy V, Wang J, Qi Z, Jia Z, Yu A, Shuman M, Yu J, & Li LC. (2012). Upregulation of Cyclin B1 by miRNA and its implications in cancer. *Nucleic Acids Research*, 40:1695. https://doi.org/10.1093/nar/gkr934.

Hummel R, Wang T, Watson DI, Michael MZ, Van der Hoek M, Haier J, & Hussey DJ. (2011). Chemotherapy-induced modification of microRNA expression in esophageal cancer. *Oncology Reports*, 26:1011. https://doi.org/10.3892/or.2011.1381.

Hung PS, Liu CJ, Chou CS, Kao SY, Yang CC, Chang KW, Chiu TH, & Lin SC. (2013). miR-146a enhances the oncogenicity of oral carcinoma by concomitant targeting of the IRAK1, TRAF6 and NUMB genes. *PloS One*, 8:e79926. https://doi.org/10.1371/journal.pone.0079926.

Hung PS, Tu HF, Kao SY, Yang CC, Liu CJ, Huang TY, Chang KW, & Lin SC. (2014). miR-31 is upregulated in oral premalignant epithelium and contributes to the immortalization of normal oral keratinocytes. *Carcinogenesis*, 35:1162. https://doi.org/10.1093/carcin/bgu024.

Hurst DR, Edmonds MD, & Welch DR. (2009). Metastamir: the field of metastasis-regulatory microRNA is spreading. *Cancer Research*, 69:7495. https://doi.org/10.1158/0008-5472.CAN-09-2111.

Hwang HW, Wentzel EA, & Mendell JT. (2007). A hexanucleotide element directs microRNA nuclear import. *Science,* 315:97. https://doi.org/10.1126/science.1136235.

Iacona JR, & Lutz CS. (2019). miR-146a-5p: Expression, regulation, and functions in cancer. *Wiley Interdisciplinary Reviews- RNA*, 10:e1533. https://doi.org/10.1002/wrna.1533.

Ibáñez-Ventoso C, Vora M, & Driscoll M. (2008). Sequence relationships among C. elegans, D. melanogaster and human microRNAs highlight the extensive conservation of microRNAs in biology. *PloS One*, 3:e2818. https://doi.org/10.1371/journal.pone.0002818.

Iliopoulos D, Lindahl-Allen M, Polytarchou C, Hirsch HA, Tsichlis PN, & Struhl K. (2010). Loss of miR-200 inhibition of Suz12 leads to polycomb-mediated repression required for the formation and maintenance of cancer stem cells. *Molecular Cell*, 39:761. https://doi.org/10.1016/j.molcel.2010.08.013.

Iocca O, Sollecito TP, Alawi F, Weinstein GS, Newman JG, De Virgilio A, Di Maio P, Spriano G, Pardiñas López S, & Shanti RM. (2020). Potentially malignant disorders of the oral cavity and oral dysplasia: a systematic review and meta-analysis of malignant transformation rate by subtype. *Head & Neck*, 42:539. https://doi.org/10.1002/hed.26006.

Irani S, & Shokri G. (2019). The role of miR-143, miR-145, and miR-590 in expression levels of CD44 and vascular endothelial cadherin in oral squamous cell carcinoma. *Middle East Journal of Cancer*, 10*:*194. https://doi.org/10.1016/j.vph.2018.11.006.

Irimie AI, Ciocan C, Gulei D, Mehterov N, Atanasov AG, Dudea D, & Berindan-Neagoe I. (2018). Current Insights into Oral Cancer Epigenetics. *International Journal of Molecular Sciences*, 19:670. https://doi.org/10.3390/ijms19030670.

Jacobson AS, Alpert E, Persky M, Okay D, Buchbinder D, & Lazarus C. (2015). Transoral mandibulectomy and double barrel fibular flap reconstruction. *The Laryngoscope*, 125:2119. https://doi.org/10.1002/lary.25051.

Jainkittivong A, Swasdison S, Thangpisityotin M, & Langlais RP. (2009). Oral squamous cell carcinoma: a clinicopathological study of 342 Thai cases. *The Journal of Contemporary Dental Practice*, *10*:E033. PMID: 19838608.

Jang JH, & Lee TJ. (2021). The role of microRNAs in cell death pathways. *Yeungnam University Journal of Medicine*, 38:107. https://doi.org/10.12701/yujm.2020.00836.

Javed Z, Muhammad Farooq H, Ullah M, Zaheer Iqbal M, Raza Q, Sadia H, Pezzani R, Salehi B, Sharifi-Rad J, & Cho WC. (2019). Wnt signaling: a potential therapeutic target in head and neck squamous cell carcinoma. *Asian Pacific Journal of Cancer Prevention: APJCP*, 20:995. https://doi.org/10.31557/APJCP.2019.20.4.995.

Jefferies S, Eeles R, Goldgar D, A'Hern R, Henk JM, & Gore M. (1999). The role of genetic factors in predisposition to squamous cell cancer of the head and neck. *British Journal of Cancer*, 79:865. https://doi.org/10.1038/sj.bjc.6690138.

Jeffries CD, Fried HM, & Perkins DO. (2011). Nuclear and cytoplasmic localization of neural stem cell microRNAs. *RNA,*17:675. https://doi.org/10.1261/rna.2006511.

Jehn P, Dittmann J, Zimmerer R, Stier R, Jehn M, Gellrich NC, Tavassol F, & Spalthoff S. (2019). Survival rates according to tumour location in patients with surgically treated oral and oropharyngeal squamous cell carcinoma. *Anticancer Research*, 39:2527. https://doi.org/10.21873/anticanres.13374.

Jia L, Zhang S, Huang Y, Zheng Y, & Gan Y. (2017). Trichostatin A increases radiosensitization of tongue squamous cell carcinoma via miR-375. *Oncology Reports*, 37:305. https://doi.org/10.3892/or.2016.5261.

Jiang F, Zhao W, Zhou L, Liu Z, Li W, & Yu D. (2014). MiR-222 targeted PUMA to improve sensitization of UM1 cells to cisplatin. *International Journal of Molecular Sciences*, 15:22128. https://doi.org/10.3390/ijms151222128.

Jiang FZ, He YY, Wang HH, Zhang HL, Zhang J, Yan XF, Wang XJ, Che Q, Ke JQ, Chen Z, Tong H, Zhang YL, Wang FY, Li YR, & Wan XP. (2015). Mutant p53 induces EZH2 expression and promotes epithelial-mesenchymal transition by disrupting p68-Drosha complex assembly and attenuating miR-26a processing. *Oncotarget*, 6:44660. https://doi.org/10.18632/oncotarget.6350.

Jiang Q, Cao Y, Qiu Y, Li C, Liu L, & Xu G. (2020). Progression of squamous cell carcinoma is regulated by miR-139-5p/CXCR4. *Frontiers in Bioscience (Landmark edition)*, 25:1732. https://doi.org/10.2741/4875.

Jiang X, Wu J, Wang J, & Huang R. (2019). Tobacco and oral squamous cell carcinoma: A review of carcinogenic pathways. *Tobacco Induced Diseases,* 17:29. https://doi.org/10.18332/tid/105844.

Jie M, Feng T, Huang W, Zhang M, Feng Y, Jiang H, & Wen Z. (2021). Subcellular localization of miRNAs and implications in cellular homeostasis. *Genes*, 12:856. https://doi.org/10.3390/genes12060856.

Jordan RC, Bradley G, & Slingerland J. (1998). Reduced levels of the cell-cycle inhibitor p27Kip1 in epithelial dysplasia and carcinoma of the oral cavity. *The American Journal of Pathology,* 152:585. PMID: 9466585.

Jung J, Yeom C, Choi YS, Kim S, Lee E, Park MJ, Kang SW, Kim SB, & Chang S. (2015). Simultaneous inhibition of multiple oncogenic miRNAs by a multi-potent microRNA sponge. *Oncotarget*, 6:20370. https://doi.org/10.18632/oncotarget.4827.

Jung YS, & Park JI. (2020). Wnt signaling in cancer: therapeutic targeting of Wnt signaling beyond β-catenin and the destruction complex. *Experimental & Molecular Medicine,* 52:183. https://doi.org/10.1038/s12276-020-0380-6.

Jurel SK, Gupta DS, Singh RD, Singh M, & Srivastava S. (2014). Genes and oral cancer. *Indian Journal of Human Genetics*, 20:4. https://doi.org/10.4103/0971-6866.132745.

Kaminagakura E, Villa LL, Andreoli MA, Sobrinho JS, Vartanian JG, Soares FA, Nishimoto IN, Rocha R, & Kowalski LP. (2012). High-risk human papillomavirus in oral squamous cell

carcinoma of young patients. *International Journal of Cancer*, 130:1726. https://doi.org/10.1002/ijc.26185.

Kang MR, Park KH, Yang JO, Lee CW, Oh SJ, Yun J, Lee MY, Han SB, & Kang JS. (2016). miR-6734 up-regulates p21 gene expression and induces cell cycle arrest and apoptosis in colon cancer cells. *PloS One*, 11:e0160961. https://doi.org/10.1371/journal.pone.0160961.

Kao SY, Tsai MM, Wu CH, Chen JJ, Tseng SH, Lin SC, & Chang KW. (2016). Co-targeting of multiple microRNAs on factor-inhibiting hypoxia-inducible factor gene for the pathogenesis of head and neck carcinomas. *Head & Neck*, 38:522. https://doi.org/10.1002/hed.23912.

Kao YY, Chou CH, Yeh LY, Chen YF, Chang KW, Liu CJ, Fan Chiang CY, & Lin SC. (2019). MicroRNA miR-31 targets SIRT3 to disrupt mitochondrial activity and increase oxidative stress in oral carcinoma. *Cancer Letters*, 456:40. https://doi.org/10.1016/j.canlet.2019.04.028.

Karimi L, Zeinali T, Hosseinahli N, Mansoori B, Mohammadi A, Yousefi M, Asadi M, Sadreddini S, Baradaran B, & Shanehbandi D. (2019). miRNA-143 replacement therapy harnesses the proliferation and migration of colorectal cancer cells in vitro. *Journal of Cellular Physiology,* 234:21359. https://doi.org/10.1002/jcp.28745.

Karlsen TA, & Brinchmann JE. (2013). Liposome delivery of microRNA-145 to mesenchymal stem cells leads to immunological off-target effects mediated by RIG-I. *Molecular Therapy: The Journal of the American Society of Gene Therapy*, 21:1169. https://doi.org/10.1038/mt.2013.55.

Karreth FA, Reschke M, Ruocco A, Ng C, Chapuy B, Léopold V, Sjoberg M, Keane TM, Verma A, Ala U, Tay Y, Wu D, Seitzer N, Velasco-Herrera MdelC, Bothmer A, Fung J, Langellotto F, Rodig SJ, Elemento O, Shipp MA, … & Pandolfi PP. (2015). The BRAF pseudogene functions as a competitive endogenous RNA and induces lymphoma *in vivo*. *Cell*, 161:319. https://doi.org/10.1016/j.cell.2015.02.043.

Karreth FA, Tay Y, Perna D, Ala U, Tan SM, Rust AG, DeNicola G, Webster KA, Weiss D, Perez-Mancera PA, Krauthammer M, Halaban R, Provero P, Adams DJ, Tuveson DA, & Pandolfi PP. (2011). *In vivo* identification of tumor- suppressive PTEN ceRNAs in an oncogenic BRAF-induced mouse model of melanoma. *Cell*, 147:382. https://doi.org/10.1016/j.cell.2011.09.032.

Kawakita A, Yanamoto S, Yamada S, Naruse T, Takahashi H, Kawasaki G, & Umeda M. (2014). MicroRNA-21 promotes oral cancer invasion via the Wnt/β-catenin pathway by targeting DKK2. *Pathology Oncology Research: POR*, 20:253. https://doi.org/10.1007/s12253-013-9689-y.

Kawamata T, & Tomari Y. (2010). Making RISC. *Trends in Biochemical Sciences*, 35:368. https://doi.org/10.1016/j.tibs.2010.03.009.

Kellner M, Rohrmoser M, Forné I, Voss K, Burger K, Mühl B, Gruber-Eber A, Kremmer E, Imhof A, & Eick D. (2015). DEAD-box helicase DDX27 regulates 3' end formation of ribosomal 47S RNA and stably associates with the PeBoW-complex. *Experimental Cell Research*, 334:146. https://doi.org/10.1016/j.yexcr.2015.03.017.

Khan A, Huque R, Shah SK, Kaur J, Baral S, Gupta PC, Cherukupalli R, Sheikh A, Selvaraj S, Nargis N, Cameron I, & Siddiqi K. (2014). Smokeless tobacco control policies in South Asia: a gap analysis and recommendations. *Nicotine & Tobacco Research: Official Journal of the Society for Research on Nicotine and Tobacco*, 16:890. https://doi.org/10.1093/ntr/ntu020.

Khanal S, Trainor PJ, Zahin M, Ghim SJ, Joh J, Rai SN, Jenson AB, & Shumway BS. (2017). Histologic variation in high grade oral epithelial dysplasia when associated with high-risk human papillomavirus. *Oral Surgery, Oral Medicine, Oral Pathology and Oral Radiology*, 123:566. https://doi.org/10.1016/j.oooo.2017.01.008.

Khvorova A, Reynolds A, & Jayasena SD. (2003). Functional siRNAs and miRNAs exhibit strand bias. *Cell*, 115:209. https://doi.org/10.1016/s0092-8674(03)00801-8.

Kim HK, Lim NJ, Jang SG, & Lee GK. (2014). miR-592 and miR-552 can distinguish between primary lung adenocarcinoma and colorectal cancer metastases in the lung. *Anticancer Research*, 34:2297. PMID: 24778034.

Kim KS, Park SA, Ko KN, Yi S, & Cho YJ. (2014). Current status of human papillomavirus vaccines. *Clinical and Experimental Vaccine Research*, 3:168. https://doi.org/10.7774/cevr.2014.3.2.168.

Kirave P, Gondaliya P, Kulkarni B, Rawal R, Garg R, Jain A, & Kalia K. (2020). Exosome mediated miR-155 delivery confers cisplatin chemoresistance in oral cancer cells via epithelial-mesenchymal transition. *Oncotarget*, 11:1157. https://doi.org/10.18632/oncotarget.27531.

Kluiver J, Slezak-Prochazka I, Smigielska-Czepiel K, Halsema N, Kroesen BJ, & van den Berg A. (2012). Generation of miRNA sponge constructs. *Methods,* 58:113. https://doi.org/10.1016/j.ymeth.2012.07.019.

Kowal J, Tkach M, & Théry C. (2014). Biogenesis and secretion of exosomes. *Current Opinion in Cell Biology*, 29:116. https://doi.org/10.1016/j.ceb.2014.05.004.

Kozaki K, Imoto I, Mogi S, Omura K, & Inazawa J. (2008). Exploration of tumor-suppressive microRNAs silenced by DNA hypermethylation in oral cancer. *Cancer Res*earch, 68:2094. https://doi.org/10.1186/1743-422X-10-175.

Kramer IR, Lucas RB, Pindborg JJ, & Sobin LH. (1978). Definition of leukoplakia and related lesions: an aid to studies on oral precancer. *Oral Surgery, Oral Medicine, and Oral Pathology*, 46:518. PMID: 280847.

Kreth S, Hübner M, & Hinske LC. (2018). MicroRNAs as clinical biomarkers and therapeutic tools in perioperative medicine. *Anesthesia and Analgesia*, 126:670. https://doi.org/10.1213/ANE.0000000000002444.

Krishna A, Singh S, Singh V, Kumar V, Singh US, & Sankhwar SN. (2018). Does Harvey-Ras gene expression lead to oral squamous cell carcinoma? a clinicopathological aspect. *Journal of Oral and Maxillofacial Pathology: JOMFP*, 22:65. https://doi.org/10.4103/jomfp.JOMFP_246_17.

Krishnan P, & Damaraju S. (2018). The challenges and opportunities in the clinical application of noncoding RNAs: the road map for miRNAs and piRNAs in cancer diagnostics and prognostics. *International Journal of Genomics*, 2018:5848046. https://doi.org/10.1155/2018/5848046.

Kristoffersen AK, Enersen M, Kverndokk E, Sunde PT, Landin M, Solheim T, Olsen I, & Grinde B. (2012). Human papillomavirus subtypes in oral lesions compared to healthy oral mucosa. *Journal of Clinical Virology: The Official Publication of the Pan American Society for Clinical Virology*, 53:364. https://doi.org/10.1016/j.jcv.2011.12.023.

Krützfeldt J, Rajewsky N, Braich R, Rajeev KG, Tuschl T, Manoharan M, & Stoffel M. (2005). Silencing of microRNAs *in vivo* with 'antagomirs'. *Nature*, 438:685. https://doi.org/10.1038/nature04303.

Kulkarni SS, Kulkarni SS, Vastrad PP, Kulkarni BB, Markande AR, Kadakol GS, Hiremath SV, Kaliwal S, Patil BR, & Gai PB. (2011). Prevalence and distribution of high risk human papillomavirus (HPV) types 16 and 18 in carcinoma of cervix, saliva of patients with oral squamous cell carcinoma and in the general population in Karnataka, India. *Asian Pacific Journal of Cancer Prevention: APJCP*, 12:645. PMID: 21627358.

Kumar MS, Pester RE, Chen CY, Lane K, Chin C, Lu J, Kirsch DG, Golub TR, & Jacks T. (2009). Dicer1 functions as a haploinsufficient tumor suppressor. *Genes & Development*, 23:2700. https://doi.org/10.1101/gad.1848209.

Kunej T, Godnic I, Ferdin J, Horvat S, Dovc P, & Calin GA. (2011). Epigenetic regulation of microRNAs in cancer: An integrated review of literature. *Mutation Research*, 717:77. https://doi.org/10.1016/j.mrfmmm.2011.03.008.

Kurago ZB. (2016). Etiology and pathogenesis of oral lichen planus: an overview. *Oral Surgery, Oral Medicine, Oral Pathology and Oral Radiology*, 122:72. https://doi.org/10.1016/j.oooo.2016.03.011.

Lai YH, Liu H, Chiang WF, Chen TW, Chu LJ, Yu JS, Chen SJ, Chen HC, & Tan BC. (2018). MiR-31-5p-ACOX1 axis enhances tumorigenic fitness in oral squamous cell carcinoma via the promigratory prostaglandin E2. *Theranostics*, 8:486. https://doi.org/10.7150/thno.22059.

Laimer K, Spizzo G, Gastl G, Obrist P, Brunhuber T, Fong D, Barbieri V, Jank S, Doppler W, Rasse M, & Norer B. (2007). High EGFR expression predicts poor prognosis in patients with squamous cell carcinoma of the oral cavity and oropharynx: a TMA-based immunohistochemical analysis. *Oral Oncology*, 43:193. https://doi.org/10.1016/j.oraloncology.2006.02.009.

Lajer CB, Nielsen FC, Friis-Hansen L, Norrild B, Borup R, Garnæs E, Rossing M, Specht L, Therkildsen MH, Nauntofte B, Dabelsteen S, & von Buchwald C. (2011). Different miRNA signatures of oral and pharyngeal squamous cell carcinomas: a prospective translational study. *British Journal of Cancer*, 104:830. https://doi.org/10.1038/bjc.2011.29.

Lakshminarayana S, Augustine D, Rao RS, Patil S, Awan KH, Venkatesiah SS, Haragannavar VC, Nambiar S, & Prasad K. (2018). Molecular pathways of oral cancer that predict prognosis and survival: a systematic review. *Journal of Carcinogenesis*, 17:7. https://doi.org/10.4103/jcar.JCar_17_18.

Lambertz I, Nittner D, Mestdagh P, Denecker G, Vandesompele J, Dyer MA, & Marine JC. (2010). Monoallelic but not biallelic loss of Dicer1 promotes tumorigenesis *in vivo*. *Cell Death and Differentiation*, 17:633. https://doi.org/10.1038/cdd.2009.202.

Langevin SM, Stone RA, Bunker CH, Grandis JR, Sobol RW, & Taioli E. (2010). MicroRNA-137 promoter methylation in oral rinses from patients with squamous cell carcinoma of the head and neck is associated with gender and body mass index. *Carcinogenesis,* 31:864. https://doi.org/10.1093/carcin/bgq051.

Langevin SM, Stone RA, Bunker CH, Lyons-Weiler MA, LaFramboise WA, Kelly L, Seethala RR,Grandis JR, Sobol RW, & Taioli E. (2011). MicroRNA-137 promoter methylation is associated with poorer overall survival in patients with squamous cell carcinoma of the head and neck. *Cancer*,117:1454. https://doi.org/10.1002/cncr.25689.

Lau HK, Wu ER, Chen MK, Hsieh MJ, Yang SF, Wang LY, & Chou YE. (2017). Effect of genetic variation in microRNA binding site in WNT1-inducible signaling pathway protein 1 gene on oral squamous cell carcinoma susceptibility. *PloS One*, 12:e0176246. https://doi.org/10.1371/journal.pone.0176246.

Lee CH, Ko YC, Huang HL, Chao YY, Tsai CC, Shieh TY, & Lin LM. (2003). The precancer risk of betel quid chewing, tobacco use and alcohol consumption in oral leukoplakia and oral submucous fibrosis in southern Taiwan. *British Journal of Cancer*, 88:366. https://doi.org/10.1038/sj.bjc.6600727.

Lee H, Han S, Kwon CS, & Lee D. (2016). Biogenesis and regulation of the let-7 miRNAs and their functional implications. *Protein & Cell*, 7:100. https://doi.org/10.1007/s13238-015-0212-y.

Lee RC, Feinbaum RL, & Ambros V. (1993). The C. elegans heterochronic gene lin-4 encodes small RNAs with antisense complementarity to lin-14. *Cell*, 75:843. https://doi.org/10.1016/0092-8674(93)90529-y.

Lee Y, Kim M, Han J, Yeom KH, Lee S, Baek SH, & Kim VN. (2004). MicroRNA genes are transcribed by RNA polymerase II. *The EMBO Journal*, 23:4051. https://doi.org/10.1038/sj.emboj.7600385.

Leemans CR, Braakhuis BJ, & Brakenhoff RH. (2011). The molecular biology of head and neck cancer. *Nature Reviews Cancer*, 11:9. https://doi.org/10.1038/nrc2982.

Leidinger P, Keller A, Backes C, Huwer H, & Meese E. (2012). MicroRNA expression changes after lung cancer resection: a follow-up study. *RNA Biology*, 9:900. https://doi.org/10.4161/rna.20107.

Lerman MA, Almazrooa S, Lindeman N, Hall D, Villa A, & Woo SB. (2017). HPV-16 in a distinct subset of oral epithelial dysplasia. *Modern Pathology: An Official Journal of the United States and Canadian Academy of Pathology, Inc*, 30:1646. https://doi.org/10.1038/modpathol.2017.71.

Li C, Ge Q, Liu J, Zhang Q, Wang C, Cui K, & Chen Z. (2017). Effects of miR-1236-3p and miR-370-5p on activation of p21 in various tumors and its inhibition on the growth of lung cancer cells. *Tumour Biology: The Journal of the International Society for Oncodevelopmental Biology and Medicine*, 39:1010428317710824. https://doi.org/10.1177/1010428317710824.

Li G, Ren S, Su Z, Liu C, Deng T, Huang D, Tian Y, Qiu Y, & Liu Y. (2015). Increased expression of miR-93 is associated with poor prognosis in head and neck squamous cell carcinoma. *Tumour Biology: The Journal of the International Society for Oncodevelopmental Biology and Medicine*, 36:3949. https://doi.org/10.1007/s13277-015-3038-6.

Li J, Huang H, Sun L, Yang M, Pan C, Chen W, Wu D, Lin Z, Zeng C, Yao Y, Zhang P, & Song E. (2009). MiR-21 indicates poor prognosis in tongue squamous cell carcinomas as an apoptosis inhibitor. *Clinical Cancer Research: An Official Journal of the American Association for Cancer Research*, 15:3998. https://doi.org/10.1158/1078-0432.CCR-08-3053.

Li L, Lu S, Liang X, Cao B, Wang S, Jiang J, Luo H, He S, Lang J, & Zhu G. (2019). γδTDEs: an efficient delivery system for miR-138 with anti-tumoral and immunostimulatory roles on oral squamous cell carcinoma. *Molecular Therapy-Nucleic Acids*, 14:101. https://doi.org/10.1016/j.omtn.2018.11.009.

Li L, Xu J, Yang D, Tan X, & Wang H. (2010). Computational approaches for microRNA studies: a review. *Mammalian Genome: Official Journal of the International Mammalian Genome Society*, 21:1. https://doi.org/10.1007/s00335-009-9241-2.

Li LC, & Dahiya R. (2002). MethPrimer: designing primers for methylation PCRs. Bioinformatics,18:1427. https://doi.org/10.1093/bioinformatics/18.11.1427.

Li S, Jiang M, Wang L, & Yu S. (2020). Combined chemotherapy with cyclooxygenase-2 (COX-2) inhibitors in treating human cancers: Recent advancement. *Biomedicine &*

Pharmacotherapy = Biomedecine & Pharmacotherapie, 12:110389. https://doi.org/10.1016/j.biopha.2020.110389.

Li S, Ma J, Zheng A, Song X, Chen S, & Jin F. (2021). DEAD-box helicase 27 enhances stem cell-like properties with poor prognosis in breast cancer. *Journal of Translational Medicine*, 19:334. https://doi.org/10.1186/s12967-021-03011-0.

Li S, Wang C, Yu X, Wu H, Hu J, Wang S, & Ye Z. (2017). miR-3619-5p inhibits prostate cancer cell growth by activating CDKN1A expression. *Oncology Reports*, 37:241. https://doi.org/10.3892/or.2016.5250.

Li S, Zhu Y, Liang Z, Wang X, Meng S, Xu X, Xu X, Wu J, Ji A, Hu Z, Lin Y, Chen H, Mao Y, Wang W, Zheng X, Liu B, & Xie L. (2016). Up-regulation of p16 by miR-877-3p inhibits proliferation of bladder cancer. *Oncotarget*, 7:51773. https://doi.org/10.18632/oncotarget.10575.

Li SC, Tang P, & Lin WC. (2007). Intronic microRNA: discovery and biological implications. *DNA and Cell Biology*, 26:195. https://doi.org/10.1089/dna.2006.0558.

Li X, Ding R, Han Z, Ma Z, & Wang Y. (2017). Targeting of cell cycle and let-7a/STAT3 pathway by niclosamide inhibits proliferation, migration and invasion in oral squamous cell carcinoma cells. *Biomedicine & Pharmacotherapy = Biomedecine & Pharmacotherapie*, 96:434. https://doi.org/10.1016/j.biopha.2017.09.149.

Li X, Xu M, Ding L, & Tang J. (2019). MiR-27a: a novel biomarker and potential therapeutic target in tumors. *Journal of Cancer*, 10:2836. https://doi.org/10.7150/jca.31361.

Li Y, Shen Z, & Yu XY. (2015). Transport of microRNAs via exosomes. *Nature Reviews Cardiology*, 12:198. https://doi.org/10.1038/nrcardio.2014.207-c1.

Li YC, Cheng AJ, Lee LY, Huang YC, & Chang JT. (2019). Multifaceted mechanisms of areca nuts in oral carcinogenesis: the molecular pathology from precancerous condition to malignant transformation. *Journal of Cancer*, 10:4054. https://doi.org/10.7150/jca.29765.

Lin DT, Yarlagadda BB, Sethi RK, Feng AL, Shnayder Y, Ledgerwood LG, Diaz JA, Sinha P, Hanasono MM, Yu P, Skoracki RJ, Lian TS, Patel UA, Leibowitz J, Purdy N, Starmer H, & Richmon JD. (2015). Long-term functional outcomes of total glossectomy with or without total laryngectomy. *JAMA Otolaryngology- Head & Neck Surgery*, 141:797. https://doi.org/10.1001/jamaoto.2015.1463.

Liu B, Shen M, Xiong J, Yuan Y, Wu X, Gao X, Xu J, Guo F, & Jian X. (2015). Synergistic effects of betel quid chewing, tobacco use (in the form of cigarette smoking), and alcohol consumption on the risk of malignant transformation of oral submucous fibrosis (OSF): a case-control study in Hunan Province, China. *Oral Surgery, Oral Medicine, Oral Pathology and Oral Radiology*, 120:337. https://doi.org/10.1016/j.oooo.2015.04.013.

Liu CJ, Kao SY, Tu HF, Tsai MM, Chang KW, & Lin SC. (2010). Increase of microRNA miR-31 level in plasma could be a potential marker of oral cancer. *Oral Diseases*, 16:360. https://doi.org/10.1111/j.1601-0825.2009.01646.x.

Liu CJ, Lin SC, Yang CC, Cheng HW, & Chang KW. (2012). Exploiting salivary miR-31 as a clinical biomarker of oral squamous cell carcinoma. *Head & Neck*, 34:219. https://doi.org/10.1002/hed.21713.

Liu CJ, Shen WG, Peng SY, Cheng HW, Kao SY, Lin SC, & Chang KW. (2014). miR-134 induces oncogenicity and metastasis in head and neck carcinoma through targeting WWOX gene. *International Journal of Cancer*, 134:811. https://doi.org/10.1002/ijc.28358.

Liu J, Wang X, Ren Y, Li X, Zhang X, & Zhou B. (2014). Effect of single nucleotide polymorphism Rs189037 in ATM gene on risk of lung cancer in Chinese: a case-control study. *PloS One,* 9:e115845. https://doi.org/10.1371/journal.pone.0115845.

Liu T, Chen G, Sun D, Lei M, Li Y, Zhou C, Li X, Xue W, Wang H, Liu C, & Xu J. (2017). Exosomes containing miR-21 transfer the characteristic of cisplatin resistance by targeting PTEN and PDCD4 in oral squamous cell carcinoma. *Acta Biochimica et Biophysica Sinica*, 49:808. https://doi.org/10.1093/abbs/gmx078.

Liu T, Feng X, & Liao Y. (2021). miR-617 promotes the growth of IL-22-stimulated keratinocytes through regulating FOXO4 expression. *Biochemical Genetics, 59*:547. https://doi.org/10.1007/s10528-020-09997-4.

Liu X, Sempere LF, Ouyang H, Memoli VA, Andrew AS, Luo Y, Demidenko E, Korc M, Shi W, Preis M, Dragnev KH, Li H, Direnzo J, Bak M, Freemantle SJ, Kauppinen S, & Dmitrovsky E. (2010). MicroRNA-31 functions as an oncogenic microRNA in mouse and human lung cancer cells by repressing specific tumor suppressors. *The Journal of Clinical Investigation*, 120:1298. https://doi.org/10.1172/JCI39566.

Loayza-Puch F, Yoshida Y, Matsuzaki T, Takahashi C, Kitayama H, & Noda M. (2010). Hypoxia and RAS-signaling pathways converge on, and cooperatively downregulate, the RECK tumor-suppressor protein through microRNAs. *Oncogene*, 29:2638. https://doi.org/10.1038/onc.2010.23.

Londin E, Loher P, Telonis AG, Quann K, Clark P, Jing Y, Hatzimichael E, Kirino Y, Honda S, Lally M, Ramratnam B, Comstock CE, Knudsen KE, Gomella L, Spaeth GL, Hark L, Katz LJ, Witkiewicz A, Rostami A, Jimenez SA, … & Rigoutsos I. (2015). Analysis of 13 cell types reveals evidence for the expression of numerous novel primate- and tissue-specific microRNAs. *Proceedings of the National Academy of Sciences of the United States of America*, 112:E1106. https://doi.org/10.1073/pnas.1420955112.

Lopez Guerr JL, Song YP, Nguyen QN, Gomez DR, Liao Z, & Xu T. (2018). Functional promoter rs189037 variant of *ATM* is associated with decrease in lung diffusing capacity after irradiation for non-small-cell lung cancer. *Chronic Diseases and Translational Medicine*, 4:59. https://doi.org/10.1016/j.cdtm.2018.02.006.

Lopez-Serra P, & Esteller M. (2012). DNA methylation-associated silencing of tumor-suppressor microRNAs in cancer. *Oncogene*, 31:1609. https://doi.org/10.1038/onc.2011.354.

Lu J, Getz G, Miska EA, Alvarez-Saavedra E, Lamb J, Peck D, Sweet-Cordero A, Ebert BL, Mak RH, Ferrando AA, Downing JR, Jacks T, Horvitz HR, & Golub TR. (2005). MicroRNA expression profiles classify human cancers. *Nature*, 435:834. https://doi.org/10.1038/nature03702.

Lu MQ, He YQ, Wu Y, Zhou HX, Jian Y, Gao W, Bao L, & Chen WM. (2023). Identification of aberrantly expressed lncRNAs and ceRNA networks in multiple myeloma: a combined high-throughput sequencing and microarray analysis. *Frontiers in Oncology*, 13:1160342. https://doi.org/10.3389/fonc.2023.1160342.

Lu YC, Chang JT, Huang YC, Huang CC, Chen WH, Lee LY, Huang BS, Chen YJ, Li HF, & Cheng AJ. (2015). Combined determination of circulating miR-196a and miR-196b levels produces high sensitivity and specificity for early detection of oral cancer. *Clinical Biochemistry*, 48:115. https://doi.org/10.1016/j.clinbiochem.2014.11.020.

Lujambio A, Ropero S, Ballesta E, Fraga MF, Cerrato C, Setién F, Casado S, Suarez-Gauthier A, Sanchez-Cespedes M, Git A, Spiteri I, Das PP, Caldas C, Miska E, & Esteller M. (2007).

Genetic unmasking of an epigenetically silenced microRNA in human cancer cells. *Cancer Research*, 67:1424. https://doi.org/10.1158/0008-5472.CAN-06-4218.

Majid S, Dar AA, Saini S, Yamamura S, Hirata H, Tanaka Y, Deng G, & Dahiya R. (2010). MicroRNA-205-directed transcriptional activation of tumor suppressor genes in prostate cancer. *Cancer*, 116:5637. https://doi.org/10.1002/cncr.25488.

Majumder S, Crabtree JS, Golde TE, Minter LM, Osborne BA, & Miele L. (2021). Targeting Notch in oncology: the path forward. *Nature Reviews Drug Discovery*, 20:125. https://doi.org/10.1038/s41573-020-00091-3.

Mallela K, Shivananda S, Gopinath KS, & Kumar A. (2021). Oncogenic role of MiR-130a in oral squamous cell carcinoma. *Scientific Reports*, 11:7787. https://doi.org/10.1038/s41598-021-87388-4.

Manikandan M, Deva Magendhra Rao AK, Arunkumar G, Manickavasagam M, Rajkumar KS, Rajaraman R, & Munirajan AK. (2016). Oral squamous cell carcinoma: microRNA expression profiling and integrative analyses for elucidation of tumourigenesis mechanism. *Molecular Cancer*, 15:28. https://doi.org/10.1186/s12943-016-0512-8.

Mao ZG, He DS, Zhou J, Yao B, Xiao WW, Chen CH, Zhu YH, & Wang HJ. (2010). Differential expression of microRNAs in GH-secreting pituitary adenomas. *Diagnostic Pathology*, 5:79. https://doi.org/10.1186/1746-1596-5-79.

Marsico A, Huska MR, Lasserre J, Hu H, Vucicevic D, Musahl A, Orom U, & Vingron M. (2013). PROmiRNA: a new miRNA promoter recognition method uncovers the complex regulation of intronic miRNAs. *Genome Biology*, 14:R84. https://doi.org/10.1186/gb-2013-14-8-r84.

Marur S, D'Souza G, Westra WH, & Forastiere AA. (2010). HPV-associated head and neck cancer: a virus-related cancer epidemic. *The Lancet-Oncology*, 11:781. https://doi.org/10.1016/S1470-2045(10)70017-6.

Marziliano A, Teckie, S, & Diefenbach MA. (2020). Alcohol-related head and neck cancer: summary of the literature. *Head & Neck*, 42:732. https://doi.org/10.1002/hed.26023.

Mascolo M, Siano M, Ilardi G, Russo D, Merolla F, De Rosa G, & Staibano S. (2012). Epigenetic disregulation in oral cancer. *International Journal of Molecular Sciences*, 13:2331. https://doi.org/10.3390/ijms13022331.

Matta A, & Ralhan R. (2009). Overview of current and future biologically based targeted therapies in head and neck squamous cell carcinoma. *Head & Neck Onco*logy, 1:6. https://doi.org/10.1186/1758-3284-1-6.

Mayr C, & Bartel DP. (2009). Widespread shortening of 3'UTRs by alternative cleavage and polyadenylation activates oncogenes in cancer cells. *Cell*, 138:673. https://doi.org/10.1016/j.cell.2009.06.016.

McCord C, Xu J, Xu W, Qiu X, McComb RJ, Perez-Ordonez B, & Bradley G. (2013). Association of high-risk human papillomavirus infection with oral epithelial dysplasia. *Oral Surgery, Oral Medicine, Oral Pathology and Oral Radiology*, 115:541. https://doi.org/10.1016/j.oooo.2013.01.020.

Mehdipour M, Shahidi M, Manifar S, Jafari S, Mashhadi Abbas F, Barati M, Mortazavi H, Shirkhoda M, Farzanegan A, & Elmi Rankohi Z. (2018). Diagnostic and prognostic relevance of salivary microRNA-21, -125a, -31 and -200a levels in patients with oral lichen planus - a short report. *Cellular Oncology (Dordrecht)*, 41:329. https://doi.org/10.1007/s13402-018-0372-x.

Meijer HA, Smith EM, & Bushell M. (2014). Regulation of miRNA strand selection: follow the leader?. *Biochemical Society Transactions*, 42:1135. https://doi.org/10.1042/BST20140142.

Melo SA, Moutinho C, Ropero S, Calin GA, Rossi S, Spizzo R, Fernandez AF, Davalos V, Villanueva A, Montoya G, Yamamoto H, Schwartz S Jr, & Esteller, M. (2010). A genetic defect in exportin-5 traps precursor microRNAs in the nucleus of cancer cells. *Cancer Cell*, 18:303. https://doi.org/10.1016/j.ccr.2010.09.007.

Mendell JT, Hwang HW, & Wentzel EA. (2007). (Patent)

Merritt WM, Lin YG, Han LY, Kamat AA, Spannuth WA, Schmandt R, Urbauer D, Pennacchio LA, Cheng JF, Nick AM, Deavers MT, Mourad-Zeidan A, Wang H, Mueller P, Lenburg ME, Gray JW, Mok S, Birrer MJ, Lopez-Berestein G, Coleman RL, … & Sood AK. (2008). Dicer, Drosha, and outcomes in patients with ovarian cancer. *The New England Journal of Medicine*, 359:2641. https://doi.org/10.1056/NEJMoa0803785.

Mesgarzadeh AH, Aali M, Farhadi F, Noorolyai S, Baghbani E, Mohammadnejad F, & Baradaran B. (2019). Transfection of microRNA-143 mimic could inhibit migration of HN-5

cells through down-regulating of metastatic genes. *Gene*, 716:144033. https://doi.org/10.1016/j.gene.2019.144033.

Miao L, Yao H, Li C, Pu M, Yao X, Yang H, Qi X, Ren J, & Wang Y. (2016). A dual inhibition: microRNA-552 suppresses both transcription and translation of cytochrome P450 2E1. *Biochimica et Biophysica Acta*, 1859:650. https://doi.org/10.1016/j.bbagrm.2016.02.016.

Michor F, & Polyak K. (2010). The origins and implications of intratumor heterogeneity. *Cancer Prevention Research,* 3:1361. https://doi.org/10.1158/1940-6207.CAPR-10-0234.

Migaldi M, Pecorari M, Forbicini G, Nanni N, Grottola A, Grandi T, Delle Donne G, Leocata P, Trovato D, & Sgambato A. (2012). Low prevalence of human papillomavirus infection in the healthy oral mucosa of a Northern Italian population. *Journal of Oral Pathology & Medicine: Official Publication of the International Association of Oral Pathologists and the American Academy of Oral Pathology*, 41:16. https://doi.org/10.1111/j.1600-0714.2011.01062.x.

Milian A, Bagan JV, & Vera F. (1993). Squamous cell carcinoma of the oral cavity: a follow up study of 85 cases and analysis of prognostic variables. *Bulletin du Groupement International Pour la Recherche Scientifique en Stomatologie & Odontologie*, 36:29. PMID: 8318820.

Miller CS, & Johnstone BM. (2001). Human papillomavirus as a risk factor for oral squamous cell carcinoma: a meta-analysis, 1982-1997. *Oral surgery, Oral Medicine, Oral Pathology, Oral Radiology, and Endodontics*, 91:622. https://doi.org/10.1067/moe.2001.115392.

Minor J, Wang X, Zhang F, Song J, Jimeno A, Wang XJ, Lu X, Gross N, Kulesz-Martin M, Wang D, & Lu SL (2012). Methylation of microRNA-9 is a specific and sensitive biomarker for oral and oropharyngeal squamous cell carcinomas. *Oral Oncology*, 48:73. https://doi.org/10.1016/j.oraloncology.2011.11.006.

Minter HA, Eveson JW, Huntley S, Elder DJ, & Hague A. (2003). The cyclooxygenase 2-selective inhibitor NS398 inhibits proliferation of oral carcinoma cell lines by mechanisms dependent and independent of reduced prostaglandin E2 synthesis. *Clinical Cancer Research: An Official Journal of the American Association for Cancer Research,* 9:1885. PMID: 12738747.

Misra S, Chaturvedi A, & Misra NC. (2008). Management of gingivobuccal complex cancer. *Annals of the Royal College of Surgeons of England*, 90:546. https://doi.org/10.1308/003588408X301136.

Miyahara LAN, Pontes FSC, Burbano RMR, Conte Neto N, Guimarães DM, Fonseca FP, & Pontes HAR. (2018). PTEN allelic loss is an important mechanism in the late stage of development of oral leucoplakia into oral squamous cell carcinoma. *Histopathology*, 72:330. https://doi.org/10.1111/his.13381.

Mogedas-Vegara A, Hueto-Madrid JA, Chimenos-Küstner E, & Bescós-Atín C. (2015). The treatment of oral leukoplakia with the CO2 laser: A retrospective study of 65 patients. *Journal of Cranio-Maxillo-Facial Surgery: Official Publication of the European Association for Cranio-Maxillo-Facial Surgery*, 43:677. https://doi.org/10.1016/j.jcms.2015.03.011.

Mogedas-Vegara A, Hueto-Madrid JA, Chimenos-Küstner E, & Bescós-Atín C. (2016). Oral leukoplakia treatment with the carbon dioxide laser: a systematic review of the literature. *Journal of Cranio-maxillo-facial Surgery: Official Publication of the European Association for Cranio-Maxillo-Facial Surgery*, 44:331. https://doi.org/10.1016/j.jcms.2016.01.026.

Mohan M, & Jagannathan N. (2014). Oral field cancerization: an update on current concepts. *Oncology Reviews*, 8:244. https://doi.org/10.4081/oncol.2014.244.

Monteys AM, Spengler RM, Wan J, Tecedor L, Lennox KA, Xing Y, & Davidson BL. (2010). Structure and activity of putative intronic miRNA promoters. *RNA*, 16:495. https://doi.org/10.1261/rna.1731910.

Moraes RC, Dias FL, Figueredo CM, & Fischer RG. (2016). Association between chronic periodontitis and oral/oropharyngeal cancer. *Brazilian Dental Journal*, 27:261. https://doi.org/10.1590/0103-6440201600754.

Morales S, Monzo M, & Navarro A. (2017). Epigenetic regulation mechanisms of microRNA expression. *Biomolecular Concepts*, 8:203. https://doi.org/10.1515/bmc-2017-0024.

More Y, & D'Cruz AK. (2013). Oral cancer: Review of current management strategies. *The National Medical Journal of India*. 26:152. PMID: 24476162.

Mullany LE, Herrick JS, Wolff RK, Stevens JR, & Slattery ML. (2016). Association of cigarette smoking and microRNA expression in rectal cancer: Insight into tumor phenotype. *Cancer Epidemiology*, 45:98. https://doi.org/10.1016/j.canep.2016.10.011.

Müller S. (2018). Oral epithelial dysplasia, atypical verrucous lesions and oral potentially malignant disorders: focus on histopathology. *Oral Surgery, Oral Medicine, Oral Pathology and Oral Radiology*, 125:591. https://doi.org/10.1016/j.oooo.2018.02.012.

Murakami K, & Miyagishi M. (2014). Tiny masking locked nucleic acids effectively bind to mRNA and inhibit binding of microRNAs in relation to thermodynamic stability. *Biomedical Reports*, 2:509. https://doi.org/10.3892/br.2014.260.

Murphy J, Isaiah A, Wolf JS, & Lubek JE. (2016). The influence of intraoperative frozen section analysis in patients with total or extended maxillectomy. *Oral Surgery, Oral Medicine, Oral Pathology and Oral Radiology*, 121:17. https://doi.org/10.1016/j.oooo.2015.07.014.

Murugan AK, Munirajan AK, & Tsuchida N. (2012). Ras oncogenes in oral cancer: the past 20 years. *Oral Oncology*, 48:383. https://doi.org/10.1016/j.oraloncology.2011.12.006.

Nagler R, Bahar G, Shpitzer T, & Feinmesser R. (2006). Concomitant analysis of salivary tumor markers--a new diagnostic tool for oral cancer. *Clinical Cancer Research: An Official Journal of the American Association for Cancer Research*, 12:3979. https://doi.org/10.1158/1078-0432.CCR-05-2412.

Nagpal JK, & Das BR. (2003). Oral cancer: reviewing the present understanding of its molecular mechanism and exploring the future directions for its effective management. *Oral Oncology*, 39:213. https://doi.org/10.1016/s1368-8375(02)00162-8.

Nagpal JK, Mishra R, & Das BR. (2002). Activation of Stat-3 as one of the early events in tobacco chewing- mediated oral carcinogenesis. *Cancer*, 94:2393. https://doi.org/10.1002/cncr.10499.

Nakagaki T, Tamura M, Kobashi K, Koyama R, Fukushima H, Ohashi T, Idogawa M, Ogi K, Hiratsuka H, Tokino T, & Sasaki Y. (2017). Profiling cancer-related gene mutations in oral squamous cell carcinoma from Japanese patients by targeted amplicon sequencing. *Oncotarget*, 8:59113. https://doi.org/10.18632/oncotarget.19262.

Niaz K, Maqbool F, Khan F, Bahadar H, Ismail Hassan F, & Abdollahi M. (2017). Smokeless tobacco (paan and gutkha) consumption, prevalence, and contribution to oral cancer. *Epidemiology and Health*, 39:e2017009. https://doi.org/10.4178/epih.e2017009.

Nishimura G, Yanoma S, Mizuno H, Kawakami K, & Tsukuda M. (1999). A selective cyclooxygenase-2 inhibitor suppresses tumor growth in nude mouse xenografted with human head and neck squamous carcinoma cells. *Japanese Journal of Cancer Research: Gann*, 90:1152. https://doi.org/10.1111/j.1349-7006.1999.tb00690.x.

Nishiyama A, & Nakanishi M. (2021). Navigating the DNA methylation landscape of cancer. *Trends in Genetics: TIG*, 37:1012. https://doi.org/10.1016/j.tig.2021.05.002.

O'Brien J, Hayder H, Zayed Y, & Peng C. (2018). Overview of microRNA biogenesis, mechanisms of actions, and circulation. *Frontiers in Endocrinology*, 9:402. https://doi.org/10.3389/fendo.2018.00402.

Odell E, Gale N, Thavaraj S, Nadal A, Zidar N, & Gnepp DR. (2021). 1 - Precursor Lesions for Squamous Carcinoma in the Upper Aerodigestive Tract. In D. R. Gnepp & J. A. Bishop (Eds.), *Gnepp's Diagnostic Surgical Pathology of the Head and Neck (Third Edition)* (pp. 1–62). Elsevier. https://doi.org/https://doi.org/10.1016/B978-0-323-53114-6.00001-8.

O'Donnell KA, Wentzel EA, Zeller KI, Dang CV, & Mendell JT. (2005). c-Myc-regulated microRNAs modulate E2F1 expression. *Nature*, 435:839. https://doi.org/10.1038/nature03677.

Ogawa H, Nakashiro K I, Tokuzen N, Kuribayashi N, Goda H, & Uchida D. (2020). MicroRNA-361-3p is a potent therapeutic target for oral squamous cell carcinoma. *Cancer Science*, 111:1645. https://doi.org/10.1111/cas.14359.

Okada C, Yamashita E, Lee SJ, Shibata S, Katahira J, Nakagawa A, Yoneda Y, & Tsukihara T. (2009). A high-resolution structure of the pre-microRNA nuclear export machinery. *Science* 326:1275. https://doi.org/10.1126/science.1178705.

Olena AF, & Patton JG. (2010). Genomic organization of microRNAs. *Journal of Cellular Physiology*, 222:540. https://doi.org/10.1002/jcp.21993.

Omar E. (2015). Current concepts and future of noninvasive procedures for diagnosing oral squamous cell carcinoma-a systematic review. *Head & Face Medicine*, 11:6. https://doi.org/10.1186/s13005-015-0063-z.

Ørom UA, Nielsen FC, & Lund AH. (2008). MicroRNA-10a binds the 5'UTR of ribosomal protein mRNAs and enhances their translation. *Molecular Cell*, 30:460. https://doi.org/10.1016/j.molcel.2008.05.001.

Otmani K, & Lewalle P. (2021). Tumor suppressor miRNA in cancer cells and the tumor microenvironment: mechanism of deregulation and clinical implications. *Frontiers in Oncology*, 11:708765. https://doi.org/10.3389/fonc.2021.708765.

Ozaki H, Ishikawa S, Kitabatake K, Yusa K, Sakurai H, & Iino M. (2016). Functional and aesthetic rehabilitation with maxillary prosthesis supported by two zygomatic implants for maxillary defect resulting from cancer ablative surgery: a case report/technique article. *Odontology*, 104:233. https://doi.org/10.1007/s10266-015-0222-5.

Pan L, Chen H, Bai Y, Wang Q, & Chen L. (2019). Long non-coding RNA CASC2 serves as a ceRNA of microRNA-21 to promote PDCD4 expression in oral squamous cell carcinoma. *OncoTargets and Therapy*, 12:3377. https://doi.org/10.2147/OTT.S198970.

Pasquinelli AE, Reinhart BJ, Slack F, Martindale MQ, Kuroda MI, Maller B, Hayward DC, Ball EE, Degnan B, Müller P, Spring J, Srinivasan A, Fishman M, Finnerty J, Corbo J, Levine M, Leahy P, Davidson E, & Ruvkun G. (2000). Conservation of the sequence and temporal expression of let-7 heterochronic regulatory RNA. *Nature*, 408:86. https://doi.org/10.1038/35040556.

Patel VD, & Capra JA. (2017). Ancient human miRNAs are more likely to have broad functions and disease associations than young miRNAs. *BMC Genomics* 18:672. https://doi.org/10.1186/s12864-017-4073-z.

Patrick DM, Zhang CC, Tao Y, Yao H, Qi X, Schwartz RJ, Jun-Shen Huang L, & Olson EN. (2010). Defective erythroid differentiation in miR-451 mutant mice mediated by 14-3-3zeta. *Genes & Development*, 24:1614. https://doi.org/10.1101/gad.1942810.

Pattanshetty S, Kotrashetti VS, Nayak R, Bhat K, Somannavar P, & Babji D. (2014). PCR based detection of HPV 16 and 18 genotypes in normal oral mucosa of tobacco users and non-users. *Biotechnic & Histochemistry: Official Publication of the Biological Stain Commission*, 89:433. https://doi.org/10.3109/10520295.2014.887143.

Peng QS, Cheng YN, Zhang WB, Fan H, Mao QH, & Xu P. (2020). circRNA_0000140 suppresses oral squamous cell carcinoma growth and metastasis by targeting miR-31 to inhibit

Hippo signaling pathway. *Cell Death & Disease*, 11:112. https://doi.org/10.1038/s41419-020-2273-y.

Peng SY, Tu HF, Yang CC, Wu CH, Liu CJ, Chang KW, & Lin SC. (2018). miR-134 targets PDCD7 to reduce E-cadherin expression and enhance oral cancer progression. *International Journal of Cancer*, 143:2892. https://doi.org/10.1002/ijc.31638.

Perkins TM, & Shklar G. (1982). Delay in hamster buccal pouch carcinogenesis by aspirin and indomethacin. *Oral Surgery, Oral Medicine, Oral Pathology*, 53:170. https://doi.org/10.1016/0030-4220(82)90283-3.

Petti S. (2009). Lifestyle risk factors for oral cancer. *Oral Oncology*, 45:340. https://doi.org/10.1016/j.oraloncology.2008.05.018.

Piao L, Zhang M, Datta J, Xie X, Su T, Li H, Teknos TN, & Pan Q. (2012). Lipid-based nanoparticle delivery of pre-miR-107 inhibits the tumorigenicity of head and neck squamous cell carcinoma. *Molecular Therapy: The Journal of the American Society of Gene Therapy*, 20:1261. https://doi.org/10.1038/mt.2012.67.

Piao Y, Jung SN, Lim MA, Oh C, Jin YL, Kim HJ, Nguyen QK, Chang JW, Won HR, & Koo BS. (2023). A circulating microRNA panel as a novel dynamic monitor for oral squamous cell carcinoma. *Scientific Reports*, 13:2000. https://doi.org/10.1038/s41598-023-28550-y.

Piemonte ED, Lazos JP, & Brunotto M. (2010). Relationship between chronic trauma of the oral mucosa, oral potentially malignant disorders and oral cancer. *Journal of Oral Pathology & Medicine: Official Publication of the International Association of Oral Pathologists and the American Academy of Oral Pathology*, 39:513. https://doi.org/10.1111/j.1600-0714.2010.00901.x.

Piyathilake CJ, Bell WC, Jones J, Henao OL, Heimburger DC, Niveleau A, & Grizzle WE. (2005). Patterns of global DNA and histone methylation appear to be similar in normal, dysplastic and neoplastic oral epithelium of humans. *Disease Markers*, 21:147. https://doi.org/10.1155/2005/285134.

Place RF, Li LC, Pookot D, Noonan EJ, & Dahiya R. (2008). MicroRNA-373 induces expression of genes with complementary promoter sequences. *Proceedings of the National Academy of Sciences of the United States of America*, 105:1608. https://doi.org/10.1073/pnas.0707594105.

Poliseno L, Salmena L, Zhang J, Carver B, Haveman WJ, & Pandolfi PP. (2010). A coding-independent function of gene and pseudogene mRNAs regulates tumour biology. *Nature*, 465:1033. https://doi.org/10.1038/nature09144.

Prabhu SR, & Wilson DF. (2013). Human papillomavirus and oral disease - emerging evidence: a review. *Australian Dental Journal*, 58:2. https://doi.org/10.1111/adj.12020.

Prime SS, Thakker NS, Pring M, Guest PG, & Paterson IC. (2001). A review of inherited cancer syndromes and their relevance to oral squamous cell carcinoma. *Oral Oncology*, 37:1. https://doi.org/10.1016/s1368-8375(00)00055-5.

Ramos-Garcia P, Roca-Rodriguez MDM, Aguilar-Diosdado M, & Gonzalez-Moles MA. (2021). Diabetes mellitus and oral cancer/oral potentially malignant disorders: a systematic review and meta-analysis. *Oral Diseases*, 27:404. https://doi.org/10.1111/odi.13289.

Rasmussen KD, Simmini S, Abreu-Goodger C, Bartonicek N, Giacomo MD, Bilbao-Cortes D, Horos R, Lindern MV, Enright AJ, & O'Carroll D. (2010). The miR-144/451 locus is required for erythroid homeostasis. *Journal of Experimental Medicine*, 207:1351. https://doi.org/10.1084/jem.20100458.

Rather MI, Nagashri MN, Swamy SS, Gopinath KS, & Kumar A. (2013). Oncogenic microRNA-155 down-regulates tumor suppressor CDC73 and promotes oral squamous cell carcinoma cell proliferation: implications for cancer therapeutics. *The Journal of Biological Chemistry*, 288:608. https://doi.org/10.1074/jbc.M112.425736.

Raveche ES, Salerno E, Scaglione BJ, Manohar V, Abbasi F, Lin YC, Fredrickson T, Landgraf P, Ramachandra S, Huppi K, Toro JR, Zenger VE, Metcalf RA, & Marti GE. (2007). Abnormal microRNA-16 locus with synteny to human 13q14 linked to CLL in NZB mice. *Blood*, 109:5079. https://doi.org/10.1182/blood-2007-02-071225.

Ren W, Wang X, Gao L, Li S, Yan X, Zhang J, Huang C, Zhang Y, & Zhi K. (2014). MiR-21 modulates chemosensitivity of tongue squamous cell carcinoma cells to cisplatin by targeting PDCD4. *Molecular and Cellular Biochemistry*, 390:253. https://doi.org/10.1007/s11010-014-1976-8.

Rentoft M, Coates PJ, Laurell G, & Nylander K. (2012). Transcriptional profiling of formalin fixed paraffin embedded tissue: pitfalls and recommendations for identifying biologically relevant changes. *PloS One*, 7:e35276. https://doi.org/10.1371/journal.pone.0035276.

Reuschenbach M, Kansy K, Garbe K, Vinokurova S, Flechtenmacher C, Toth C, Prigge ES, Thiele OC, Reinert S, Hoffmann J, von Knebel Doeberitz M, & Freier K. (2013). Lack of evidence of human papillomavirus-induced squamous cell carcinomas of the oral cavity in southern Germany. *Oral Oncology*, 49:937. https://doi.org/10.1016/j.oraloncology.2013.03.451.

Rivera C. (2015). Essentials of oral cancer. *International Journal of Clinical and Experimental Pathology*, 8:11884. PMID: 26617944.

Rodríguez-Molinero J, Migueláñez-Medrán BDC, Puente-Gutiérrez C, Delgado-Somolinos E, Martín Carreras-Presas C, Fernández-Farhall J, & López-Sánchez AF. (2021). Association between oral cancer and diet: an update. *Nutrients*, 13:1299. https://doi.org/10.3390/nu13041299.

Roesler JM, Livingston EH, Srivatsan E, Chang P, & Wang MB. (1998). Deletion of P15 (MTS2) in head andneck squamous cell carcinomas. *The Journal of Surgical Research, 77*:50. https://doi.org/10.1006/jsre.1998.5337.

Ruby JG, Jan CH, & Bartel DP. (2007). Intronic microRNA precursors that bypass Drosha processing. *Nature*, 448:83. https://doi.org/10.1038/nature05983.

Rushatamukayanunt P, Morita K, Matsukawa S, Harada H, Shimamoto H, Tomioka H, & Omura K. (2014). Lack of association between high-risk human papillomaviruses and oral squamous cell carcinoma in young Japanese patients. *Asian Pacific Journal of Cancer Prevention: APJCP*, 15:4135. https://doi.org/10.7314/apjcp.2014.15.10.4135.

Saito Y, Liang G, Egger G, Friedman JM, Chuang JC, Coetzee GA, & Jones PA. (2006). Specific activation of microRNA-127 with downregulation of the proto-oncogene BCL6 by chromatin-modifying drugs in human cancer cells. *Cancer Cell*, 9:435. https://doi.org/10.1016/j.ccr.2006.04.020.

Sakuma T, Uzawa K, Onda T, Shiiba M, Yokoe H, Shibahara T, & Tanzawa H. (2006). Aberrant expression of histone deacetylase 6 in oral squamous cell carcinoma. *International Journal of Oncology*, 29:117. PMID: 16773191.

Salahshourifar I, Vincent-Chong VK, Kallarakkal TG, & Zain RB. (2014). Genomic DNA copy number alterations from precursor oral lesions to oral squamous cell carcinoma. *Oral Oncology*, 50:404. https://doi.org/10.1016/j.oraloncology.2014.02.005.

Sambrook J, Maniatis RH, Fristsch EF. Molecular cloning: a laboratory manual. (1995). New York:ColdSpring Harbor Laboratory Press, 3 Vols.

Sandberg R, Neilson JR, Sarma A, Sharp PA, & Burge CB. (2008). Proliferating cells express mRNAs with shortened 3' untranslated regions and fewer microRNA target sites. *Science* ,320:1643. https://doi.org/10.1126/science.1155390.

Santhi WS, Prathibha R, Charles S, Anurup KG, Reshmi G, Ramachandran S, Jissa VT, Sebastian P, & Radhakrishna Pillai M. (2013). Oncogenic microRNAs as biomarkers of oral tumorigenesis and minimal residual disease. *Oral Oncology*, 49:567. https://doi.org/10.1016/j.oraloncology.2013.01.001.

Santosh ABR, & Jones TJ. (2014). The epithelial-mesenchymal interactions: insights into physiological and pathological aspects of oral tissues. *Oncology Reviews*, 8:239. https://doi.org/10.4081/oncol.2014.239.

Saranath D, Chang SE, Bhoite LT, Panchal RG, Kerr IB, Mehta AR, Johnson NW, & Deo MG. (1991). High frequency mutation in codons 12 and 61 of H-ras oncogene in chewing tobacco-related human oral carcinoma in India. *British Journal of Cancer*, 63:573. https://doi.org/10.1038/bjc.1991.133.

Sarkar N, & Kumar A. (2021). microRNAs: new-age panacea in cancer therapeutics. *Indian Journal of Surgical Oncology*, 12:52. https://doi.org/10.1007/s13193-020-01110-w.

Scully C, & Bagan J. (2009). Oral squamous cell carcinoma overview. *Oral Oncology*, 45:301. https://doi.org/10.1016/j.oraloncology.2009.01.004.

Seitz H. (2009). Redefining microRNA targets. *Current Biology: CB*, 19:870. https://doi.org/10.1016/j.cub.2009.03.059.

Seiwert TY, Burtness B, Mehra R, Weiss J, Berger R, Eder JP, Heath K, McClanahan T, Lunceford J, Gause C, Cheng JD, & Chow LQ. (2016). Safety and clinical activity of pembrolizumab for treatment of recurrent or metastatic squamous cell carcinoma of the head and neck (KEYNOTE-012): an open-label, multicentre, phase 1b trial. *The Lancet-Onco*logy, 17:956. https://doi.org/10.1016/S1470-2045(16)30066-3.

Seoane Lestón J, & Diz Dios P. (2010). Diagnostic clinical aids in oral cancer. *Oral Oncology*, 46:418. https://doi.org/10.1016/j.oraloncology.2010.03.006.

Shah MY, Ferrajoli A, Sood AK, Lopez-Berestein G, & Calin GA. (2016). microRNA therapeutics in cancer- an emerging concept. *EBioMedicine*, 12:34. https://doi.org/10.1016/j.ebiom.2016.09.017.

Shah NM, Rushworth SA, Murray MY, Bowles KM, & MacEwan DJ. (2013). Understanding the role of NRF2-regulated miRNAs in human malignancies. *Oncotarget*, 4:1130. https://doi.org/10.18632/oncotarget.1181.

Shakunthala GK, Annigeri RG, & Arunkumar S. (2015). Role of oxidative stress in the pathogenesis of oral submucous fibrosis: a preliminary prospective study. *Contemporary Clinical Dentistry*, 6:S172. https://doi.org/10.4103/0976-237X.166823.

Sharbati-Tehrani S, Kutz-Lohroff B, Bergbauer R, Scholven J, & Einspanier R. (2008). miR-Q: a novel quantitative RT-PCR approach for the expression profiling of small RNA molecules such as miRNAs in a complex sample. *BMC Molecular Biology*, 9:34. https://doi.org/10.1186/1471-2199-9-34.

Shen YW, Shih YH, Fuh LJ, & Shieh TM. (2020). Oral submucous fibrosis: a review on biomarkers, pathogenic mechanisms, and treatments. *International Journal of Molecular Sciences*, 21:7231. https://doi.org/10.3390/ijms21197231.

Shi W, Yang J, Li S, Shan X, Liu X, Hua H, Zhao C, Feng Z, Cai Z, Zhang L, & Zhou D. (2015). Potential involvement of miR-375 in the premalignant progression of oral squamous cell carcinoma mediated via transcription factor KLF5. *Oncotarget*, 6:40172. https://doi.org/10.18632/oncotarget.5502.

Shi Z, Johnson JJ, Jiang R, Liu Y, & Stack MS. (2015). Decrease of miR-146a is associated with the aggressiveness of human oral squamous cell carcinoma. *Archives of Oral Biology*, 60:1416. https://doi.org/10.1016/j.archoralbio.2015.06.007.

Shibata T, Kokubu A, Saito S, Narisawa-Saito M, Sasaki H, Aoyagi K, Yoshimatsu Y, Tachimori, Y, Kushima R, Kiyono T, & Yamamoto M. (2011). NRF2 mutation confers malignant potential and resistance to chemoradiation therapy in advanced esophageal squamous cancer. *Neoplasia,*13:864. https://doi.org/10.1593/neo.11750.

Shin DM, Lee JS, Lippman SM, Lee JJ, Tu ZN, Choi G, Heyne K, Shin HJ, Ro JY, Goepfert H, Hong WK, & Hittelman WN. (1996). p53 expressions: Predicting recurrence and second primary tumors in head and neck squamous cell carcinoma. *Journal of the National Cancer*

Institute, 88:519. https://doi.org/10.1093/jnci/88.8.519.

Shiotani H, Denda A, Yamamoto K, Kitayama W, Endoh T, Sasaki Y, Tsutsumi N, Sugimura M, & Konishi Y. (2001). Increased expression of cyclooxygenase-2 protein in 4-nitroquinoline-1-oxide-induced rat tongue carcinomas and chemopreventive efficacy of a specific inhibitor, nimesulide. *Cancer Research*, 61:1451. PMID: 11245450.

Singh P, Srivastava AN, Sharma R, Mateen S, Shukla B, Singh A, & Chandel S. (2018). Circulating microRNA-21 expression as a novel serum biomarker for oral sub-mucous fibrosis and oral squamous cell carcinoma. *Asian Pacific Journal of Cancer Prevention: APJCP*, 19:1053. https://doi.org/10.22034/APJCP.2018.19.4.1053.

Slaughter DP, Southwick HW, & Smejkal W. (1953). Field cancerization in oral stratified squamous epithelium; clinical implications of multicentric origin. *Cancer*, 6:963.https://doi.org/10.1002/1097-0142(195309)6:5<963:aid cncr2820060515>3.0.co;2-q.

Slaughter DP. (1944). The multiplicity of origin of malignant tumors. *Surgery Gynecology & Obstetrics*, 79:89.

Snow AN, & Laudadio J. (2010). Human papillomavirus detection in head and neck squamous cell carcinomas. *Advances in Anatomic Pathology*, 17:394. https://doi.org/10.1097/PAP.0b013e3181f895c1.

Sobin LH, & Fleming ID. (1997). TNM classification of malignant tumors, fifth edition (1997). Union Internationale Contre le Cancer and the American Joint Committee on Cancer. *Cancer*, 80:1803. https://doi.org/10.1002/(sici)1097-0142(19971101)80:9<1803::aid-cncr16>3.0.co;2-9.

Song CM, Kwon TK, Park BL, Ji YB, & Tae K. (2015). Single nucleotide polymorphisms of ataxia telangiectasia mutated and the risk of papillary thyroid carcinoma. *Environmental and Molecular Mutagenesis*, 56:70. https://doi.org/10.1002/em.21898.

Spencer SA, Harris J, Wheeler RH, Machtay M, Schultz C, Spanos W, Rotman M, Meredith R, & Ang KK. (2008). Final report of RTOG 9610, a multi-institutional trial of reirradiation and chemotherapy for unresectable recurrent squamous cell carcinoma of the head and neck. *Head and Neck*, 30:281. https://doi.org/10.1002/hed.20697.

Starega-Roslan J, Krol J, Koscianska E, Kozlowski P, Szlachcic WJ, Sobczak K, & Krzyzosiak WJ. (2011). Structural basis of microRNA length variety. *Nucleic Acids Research*, 39:257. https://doi.org/10.1093/nar/gkq727.

Stavast CJ, & Erkeland SJ. (2019). The non-canonical aspects of microRNAs: many roads to gene regulation. *Cells*, 8:1465. https://doi.org/10.3390/cells8111465.

Steiman-Shimony A, Shtrikman O, & Margalit H. (2018). Assessing the functional association of intronic miRNAs with their host genes. *RNA*, 24:991. https://doi.org/10.1261/rna.064386.117.

Su CY, Shigeishi H, Nishimura R, Ohta K, & Sugiyama M. (2019). Detection of oral bacteria on the tongue dorsum using PCR amplification of 16S ribosomal RNA and its association with systemic disease in middle-aged and elderly patients. *Biomedical Reports*, 10:70. https://doi.org/10.3892/br.2018.1175.

Sun X, & Zhang L. (2017). MicroRNA-143 suppresses oral squamous cell carcinoma cell growth, invasion and glucose metabolism through targeting hexokinase 2. *Bioscience Reports*, 37:BSR20160404. https://doi.org/10.1042/BSR20160404.

Sung H, Ferlay J, Siegel RL, Laversanne M, Soerjomataram I, Jemal A, & Bray F. (2021). Global Cancer Statistics 2020: GLOBOCAN Estimates of Incidence and Mortality Worldwide for 36 Cancers in 185 Countries. *CA: A Cancer Journal for Clinicians*, 71:209. https://doi.org/10.3322/caac.21660.

Suzuki HI, Yamagata K, Sugimoto K, Iwamoto T, Kato S, & Miyazono K. (2009). Modulation of microRNA processing by p53. *Nature*, 460:529. https://doi.org/10.1038/nature08199.

Suzuki MM, & Bird A. (2008). DNA methylation landscapes: provocative insights from epigenomics. *Nature Reviews Genetics*, 9:465. https://doi.org/10.1038/nrg2341.

Taganov KD, Boldin MP, Chang KJ, & Baltimore D. (2006). NF-kappaB-dependent induction of microRNA miR-146, an inhibitor targeted to signaling proteins of innate immune responses. *Proceedings of the National Academy of Sciences of the United States of America*, 103:12481. https://doi.org/10.1073/pnas.0605298103.

Tan H, Huang S, Zhang Z, Qian X, Sun P, & Zhou X. (2019). Pan-cancer analysis on microRNA-associated gene activation. *EBioMedicine*, 43:82. https://doi.org/10.1016/j.ebiom.2019.03.082.

Tanaka T, Nishikawa A, Mori Y, Morishita Y, & Mori H. (1989). Inhibitory effects of non-steroidal anti-inflammatory drugs, piroxicam and indomethacin on 4-nitroquinoline 1-oxide-induced tongue carcinogenesis in male ACI/N rats. *Cancer Letters*, 48:177. https://doi.org/10.1016/0304-3835(89)90115-8.

Tang J, Chen H, Wong CC, Liu D, Li T, Wang X, Ji J, Sung JJ, Fang JY, & Yu J. (2018). DEAD-box helicase 27 promotes colorectal cancer growth and metastasis and predicts poor survival in CRC patients. *Oncogene*, 37:3006. https://doi.org/10.1038/s41388-018-0196-1.

Tay Y, Kats L, Salmena L, Weiss D, Tan SM, Ala U, Karreth F, Poliseno L, Provero P, Di Cunto F, Lieberman J, Rigoutsos I, & Pandolfi PP. (2011). Coding-independent regulation of the tumor suppressor PTEN by competing endogenous mRNAs. *Cell*, 147:344. https://doi.org/10.1016/j.cell.2011.09.029.

Tenore G, Nuvoli A, Mohsen A, Cassoni A, Battisti A, Terenzi V, Monaca MD, Raponi I, Brauner E, Felice FD, Musio D, Gioia CRTD, Messineo D, Mezi S, Carlo SD, Botticelli A, Valentini V, Marchetti P, Tombolini V, Vincentiis MD, Polimeni A, & Romeo U. (2020). Tobacco, alcohol and family history of cancer as risk factors of oral squamous cell carcinoma: case-control retrospective study. *Applied Sciences,* 10:3896. doi.org/10.3390/app10113896.

Thomas S, Balan A, & Balaram P. (2015). The expression of retinoblastoma tumor suppressor protein in oral cancers and precancers: a clinicopathological study. *Dental Research Journal*, 12:307. https://doi.org/10.4103/1735-3327.161427.

Thomas V, Rema Devi S, Jeyaseelan V, & Jeyseelan L. (2012). Mucosal disorders with oral epithelial dysplasia risk-development of a simple screening tool for general health care setting. *Oral Oncology*, 48:671. https://doi.org/10.1016/j.oraloncology.2012.02.011.

Thomson JM, Newman M, Parker JS, Morin-Kensicki, EM, Wright T, & Hammond SM. (2006). Extensive post-transcriptional regulation of microRNAs and its implications for cancer. *Genes & Development*, 20:2202. https://doi.org/10.1101/gad.1444406.

Thornton JE, & Gregory RI. (2012). How does Lin28 let-7 control development and disease?. *Trends in Cell Biology*, 22:474. https://doi.org/10.1016/j.tcb.2012.06.001.

Todd R, Donoff RB, & Wong DT. (1997). The molecular biology of oral carcinogenesis: toward a tumor progression model. *Journal of Oral and Maxillofacial Surgery: Official Journal of the*

American Association of Oral and Maxillofacial Surgeons, 55:613. https://doi.org/10.1016/s0278-2391(97)90495-x.

Troiano G, Mastrangelo F, Caponio VCA, Laino L, Cirillo N, & Lo Muzio L. (2018). Predictive prognostic value of tissue-based microRNA expression in oral squamous cell carcinoma: a systematic review and meta-analysis. *Journal of Dental Research*, 97:759. https://doi.org/10.1177/0022034518762090.

Tsukamoto Y, Fumoto S, Noguchi T, Yanagihara K, Hirashita Y, Nakada C, Hijiya N, Uchida T, Matsuura K, Hamanaka R, Murakami K, Seto M, Inomata M, & Moriyama M. (2015). Expression of DDX27 contributes to colony-forming ability of gastric cancer cells and correlates with poor prognosis in gastric cancer. *American Journal of Cancer Research*, 5:2998. PMID: 26693055.

Tu HF, Chang KW, Cheng HW, & Liu CJ. (2015). Upregulation of miR-372 and -373 associates with lymph node metastasis and poor prognosis of oral carcinomas. *The Laryngoscope*, 125:E365. https://doi.org/10.1002/lary.25464.

Usman S, Jamal A, Teh MT, & Waseem A. (2021). Major molecular signaling pathways in oral cancer associated with therapeutic resistance. *Frontiers in Oral Health*, 1:603160. https://doi.org/10.3389/froh.2020.603160.

Vader P, Mol EA, Pasterkamp G, & Schiffelers RM. (2016). Extracellular vesicles for drug delivery. *Advanced Drug Delivery Reviews*, 106:148. https://doi.org/10.1016/j.addr.2016.02.006.

van der Schroeff MP, & Baatenburg de Jong RJ. (2009). Staging and prognosis in head and neck cancer. *Oral Oncology*, 45:356. https://doi.org/10.1016/j.oraloncology.2008.05.022.

van der Waal I. (2009). Potentially malignant disorders of the oral and oropharyngeal mucosa; terminology, classification and present concepts of management. *Oral Oncology*, 45:317. https://doi.org/10.1016/j.oraloncology.2008.05.016.

van der Waal I. (2010). Potentially malignant disorders of the oral and oropharyngeal mucosa; present concepts of management. *Oral Oncology*, 46:423. https://doi.org/10.1016/j.oraloncology.2010.02.016.

van Rooij E, & Kauppinen S. (2014). Development of microRNA therapeutics is coming of age. *EMBO Molecular Medicine*, 6:851. https://doi.org/10.15252/emmm.201100899.

van Zandwijk N, Pavlakis N, Kao SC, Linton A, Boyer MJ, Clarke S, Huynh Y, Chrzanowska A, Fulham MJ, Bailey DL, Cooper WA, Kritharides L, Ridley L, Pattison ST, MacDiarmid J, Brahmbhatt H, & Reid G. (2017). Safety and activity of microRNA-loaded minicells in patients with recurrent malignant pleural mesothelioma: a first-in-man, phase 1, open-label, dose-escalation study. *The Lancet-Oncology*, 18:1386. https://doi.org/10.1016/S1470-2045(17)30621-6.

Varambally S, Cao Q, Mani RS, Shankar S, Wang X, Ateeq B, Laxman B, Cao X, Jing X, Ramnarayanan K, Brenner JC, Yu J, Kim JH, Han B, Tan P, Kumar-Sinha C, Lonigro RJ, Palanisamy N, Maher CA, & Chinnaiyan AM. (2008). Genomic loss of microRNA-101 leads to overexpression of histone methyltransferase EZH2 in cancer. *Science*, 322:1695. https://doi.org/10.1126/science.1165395.

Vasudevan S, Tong Y, & Steitz JA. (2007). Switching from repression to activation: microRNAs can up-regulate translation. *Science*, 318:1931. https://doi.org/10.1126/science.1149460.

Vecchione A, Belletti B, Lovat F, Volinia S, Chiappetta G, Giglio S, Sonego M, Cirombella R, Onesti EC, Pellegrini P, Califano D, Pignata S, Losito S, Canzonieri V, Sorio R, Alder H, Wernicke D, Stoppacciaro A, Baldassarre G, & Croce CM. (2013). A microRNA signature defines chemoresistance in ovarian cancer through modulation of angiogenesis. *Proceedings of the National Academy of Sciences of the United States of America*, 110:9845. https://doi.org/10.1073/pnas.1305472110.

Veluthattil AC, Sudha SP, Kandasamy S, & Chakkalakkoombil SV. (2019). Effect of hypofractionated, palliative radiotherapy on quality of life in late-stage oral cavity cancer: a prospective clinical trial. *Indian Journal of Palliative Care*, 25:383. https://doi.org/10.4103/IJPC.IJPC_115_18.

Venkatesh T, Nagashri MN, Swamy SS, Mohiyuddin SM, Gopinath KS, & Kumar A. (2013). Primarymicrocephaly gene MCPH1 shows signatures of tumor suppressors and is regulated by miR-27a in oral squamous cell carcinoma. *PLoS One*. 8:e54643. https://doi.org/10.1371/journal.pone.0054643.

Venturelli S, Sinnberg TW, Berger A, Noor S, Levesque MP, Böcker A, Niessner H, Lauer UM, Bitzer M, Garbe C, & Busch C. (2014). Epigenetic impacts of ascorbate on human metastatic melanoma cells. *Frontiers in Oncology*, 4:227.

https://doi.org/10.3389/fonc.2014.00227.

Vermorken JB, Mesia R, Rivera F, Remenar E, Kawecki A, Rottey S, Erfan J, Zabolotnyy D, Kienzer HR, Cupissol D, Peyrade F, Benasso M, Vynnychenko I, De Raucourt D, Bokemeyer C, Schueler A, Amellal N, & Hitt R. (2008). Platinum-based chemotherapy plus cetuximab in head and neck cancer. *The New England Journal of Medicine*, 359:1116. https://doi.org/10.1056/NEJMoa0802656.

Volinia S, Calin GA, Liu CG, Ambs S, Cimmino A, Petrocca F, Visone R, Iorio M, Roldo C, Ferracin M, Prueitt RL, Yanaihara N, Lanza G, Scarpa A, Vecchione A, Negrini M, Harris CC, & Croce CM. (2006). A microRNA expression signature of human solid tumors defines cancer gene targets. *Proceedings of the National Academy of Sciences of the United States of America*, 103:2257. https://doi.org/10.1073/pnas.0510565103.

Wang C, Chen Z, Ge Q, Hu J, Li F, Hu J, Xu H, Ye Z, & Li LC. (2014). Up-regulation of p21(WAF1/CIP1) by miRNAs and its implications in bladder cancer cells. *FEBS Letters*, 588:4654. https://doi.org/10.1016/j.febslet.2014.10.037.

Wang CH, Wu KH, Yang YL, Peng CT, Tsai FJ, Lin DT, Chiu CF, Lin CC, & Bau DT. (2011). Association between ataxia telangiectasia mutated gene polymorphisms and childhood leukemia in Taiwan. *The Chinese Journal of Physiology*, 54:413. https://doi.org/10.4077/CJP.2011.AMM106.

Wang L, & Ganly I. (2014). The oral microbiome and oral cancer. *Clinics in Laboratory Medicine*, 34:711. https://doi.org/10.1016/j.cll.2014.08.004.

Wang M, Qiu Y, Zhang R, Gao L, Wang X, Bi L, & Wang Y. (2019). MEHP promotes the proliferation of oral cancer cells via down regulation of miR-27b-5p and miR-372-5p. *Toxicology in vitro: An International Journal Published in Association with BIBRA*, 58:35. https://doi.org/10.1016/j.tiv.2019.03.014.

Wang Y, Wang S, Wu Y, Ren Y, Li Z, Yao X, Zhang C, Ye N, Jing C, Dong J, Zhang K, Sun S, Zhao M, Guo W, Qu X, Qiao Y, Chen H, Kong L, Jin R, Wang X, … & Zhou X. (2017). Suppression of the growth and invasion of human head and neck squamous cell carcinomas via regulating STAT3 signaling and the miR-21/β-catenin axis with HJC0152. *Molecular Cancer Therapeutics*, 16:578. https://doi.org/10.1158/1535-7163.MCT-16-0606.

Wang Y, Zhu Y, Lv P, & Li L. (2015). Targeting miR-21 with AS-miR-21 suppresses aggressive growth of human tongue squamous cell carcinoma *in vivo*. *International Journal of Clinical and Experimental Pathology*, 8:4773. PMID: 26191167.

Wang Z. (2011). The principles of miRNA-masking antisense oligonucleotides technology. *Methods in Molecular Biology,* 676:43. https://doi.org/10.1007/978-1-60761-863-8_3.

Warnakulasuriya S, Johnson NW, & van der Waal I. (2007). Nomenclature and classification of potentially malignant disorders of the oral mucosa. *Journal of Oral Pathology & Medicine: Official Publication of the International Association of Oral Pathologists and the American Academy of Oral Pathology*, 36:575. https://doi.org/10.1111/j.1600-0714.2007.00582.x.

Warnakulasuriya S, Trivedy C, & Peters TJ. (2002). Areca nut use: an independent risk factor for oral cancer. *The British Medical Journal*, 324:799. https://doi.org/10.1136/bmj.324.7341.799.

Warnakulasuriya S. (2018). Clinical features and presentation of oral potentially malignant disorders. *Oral Surgery, Oral Medicine, Oral Pathology and Oral Radiology*, 125:582. https://doi.org/10.1016/j.oooo.2018.03.011.

Warnakulasuriya S. (2020). Oral potentially malignant disorders: A comprehensive review on clinical aspects and management. *Oral Oncology*, 102:104550. https://doi.org/10.1016/j.oraloncology.2019.104550.

Weng J, Zhang H, Wang C, Liang J, Chen G, Li W, Tang H, & Hou J. (2017). miR-373-3p Targets DKK1 to Promote EMT-Induced Metastasis via the Wnt/β-Catenin Pathway in Tongue Squamous Cell Carcinoma. *BioMed Research International*, 2017:6010926. https://doi.org/10.1155/2017/6010926.

Wetzel SL, & Wollenberg J. (2020). Oral Potentially Malignant Disorders. *Dental Clinics of North America*, 64:25. https://doi.org/10.1016/j.cden.2019.08.004.

White JS, Weissfeld JL, Ragin CC, Rossie KM, Martin CL, Shuster M, Ishwad CS, Law JC, MyersEN, Johnson JT, & Gollin SM. (2007). The influence of clinical and demographic risk factors on the establishment of head and neck squamous cell carcinoma cell lines. *Oral Oncology*, 43:701. https://doi.org/10.1016/j.oraloncology.2006.09.001.

Wickens M, & Takayama K. (1994). Deviants or emissaries. *Nature*, 367:17. https://doi.org/10.1038/367017a0.

Wiggins JF, Ruffino L, Kelnar K, Omotola M, Patrawala L, Brown D, & Bader AG. (2010). Development of a lung cancer therapeutic based on the tumor suppressor microRNA-34. *Cancer Research*, 70:5923. https://doi.org/10.1158/0008-5472.CAN-10-0655.

Wightman B, Ha I, & Ruvkun G. (1993). Posttranscriptional regulation of the heterochronic gene lin-14 by lin-4 mediates temporal pattern formation in C. elegans. *Cell*, 75:855. https://doi.org/10.1016/0092-8674(93)90530-4.

Wiklund ED, Gao S, Hulf T, Sibbritt T, Nair S, Costea DE, Villadsen SB, Bakholdt V, Bramsen JB, Sørensen JA, Krogdahl A, Clark SJ, & Kjems J. (2011). MicroRNA alterations and associated aberrant DNA methylation patterns across multiple sample types in oral squamous cell carcinoma. *PloS One*, 6:e27840. https://doi.org/10.1371/journal.pone.0027840.

Williams HK. (2000). Molecular pathogenesis of oral squamous carcinoma. *Molecular Pathology: MP*, 53:165. https://doi.org/10.1136/mp.53.4.165.

Williams PM, Poh CF, Hovan AJ, Ng S, & Rosin MP. (2008). Evaluation of a suspicious oral mucosal lesion. *Journal (Canadian Dental Association)*, 74:275. PMID: 18387268.

Wong TS, Ho WK, Chan JY, Ng RW, & Wei WI. (2009). Mature miR-184 and squamous cell carcinoma of the tongue. *The Scientific World Journal*, 9:130. https://doi.org/10.1100/tsw.2009.12.

Wu L, & Belasco JG. (2005). Micro-RNA regulation of the mammalian lin-28 gene during neuronal differentiation of embryonal carcinoma cells. *Molecular and Cellular Biology,* 25:9198. https://doi.org/10.1128/MCB.25.21.9198-9208.2005.

Wu M, Duan Q, Liu X, Zhang P, Fu Y, Zhang Z, Liu L, Cheng J, & Jiang H. (2020). MiR-155-5p promotes oral cancer progression by targeting chromatin remodeling gene ARID2. *Biomedicine & Pharmacotherapy = Biomedecine & Pharmacotherapie*, 122:109696. https://doi.org/10.1016/j.biopha.2019.109696.

Xia L, Tan S, Zhou Y, Lin J, Wang H, Oyang L, Tian Y, Liu L, Su M, Wang H, Cao D, & Liao Q. (2018). Role of the NFκB-signaling pathway in cancer. *OncoTargets and Therapy*, 11:2063. https://doi.org/10.2147/OTT.S161109.

Xiaoqian W, Bing Z, Yangwei L, Yafei Z, Tingting Z, Yi W, Qingjun L, Suxia L, Ling Z, Bo W, & Peng Z. (2021). DEAD-box Helicase 27 promotes hepatocellular carcinoma progression through ERK Signaling. *Technology in Cancer Research & Treatment*, 20:15330338211055953. https://doi.org/10.1177/15330338211055953.

Xie M, Li M, Vilborg A, Lee N, Shu MD, Yartseva V, Šestan N, & Steitz JA. (2013). Mammalian 5'-capped microRNA precursors that generate a single microRNA. *Cell*, 155:1568. https://doi.org/10.1016/j.cell.2013.11.027.

Xu Z, Huang CM, Shao Z, Zhao XP, Wang M, Yan TL, Zhou XC, Jiang EH, Liu K, & Shang ZJ. (2017). Autophagy induced by areca nut extract contributes to decreasing cisplatin toxicity in oral squamous cell carcinoma cells: roles of reactive oxygen species/AMPK signaling. *International Journal of Molecular Sciences*, 18:524. https://doi.org/10.3390/ijms18030524.

Xue HY, Guo P, Wen WC, & Wong HL. (2015). Lipid-based nanocarriers for RNA delivery. *Current Pharmaceutical Design*, 21:3140. https://doi.org/10.2174/1381612821666150531164540.

Yan Z, Tong X, Ma Y, Liu S, Yang L, Yang X, Yang X, Bai M, & Fan H. (2017). Association between ATM gene polymorphisms, lung cancer susceptibility and radiation-induced pneumonitis: a meta-analysis. *BMC Pulmonary Medicine*, 17:205. https://doi.org/10.1186/s12890-017-0555-7.

Yan ZY, Luo ZQ, Zhang LJ, Li J, & Liu JQ. (2017). Integrated analysis and microRNA expression profiling identified seven miRNAs associated with progression of oral squamous cell carcinoma. *Journal of Cellular Physiology*, 232:2178. https://doi.org/10.1002/jcp.25728.

Yang C, Li D, Bai Y, Song S, Yan P, Wu R, Zhang Y, Hu G, Lin C, Li X, & Huang L. (2018). DEAD-box helicase 27 plays a tumor-promoter role by regulating the stem cell-like activity of human colorectal cancer cells. *OncoTargets and Therapy*, 12:233. https://doi.org/10.2147/OTT.S190814.

Yang H, Gu J, Wang KK, Zhang W, Xing J, Chen Z, Ajani JA, & Wu X. (2009). MicroRNA expression signatures in Barrett's esophagus and esophageal adenocarcinoma. *Clinical Cancer Research: An Official Journal of the American Association for Cancer Research*, 15:5744. https://doi.org/10.1158/1078-0432.CCR-09-0385.

Yang JS, Maurin T, Robine N, Rasmussen KD, Jeffrey KL, Chandwani R, Papapetrou EP, Sadelain M, O'Carroll D, & Lai EC. (2010). Conserved vertebrate mir-451 provides a platform for Dicer-independent, Ago2-mediated microRNA biogenesis. *Proceedings of the National Academy of Sciences of the United States of America*, 107:15163. https://doi.org/10.1073/pnas.1006432107.

Yang SW, Lee YS, Chang LC, Hsieh TY, & Chen TA. (2015). Outcome of excision of oral erythroplakia. *The British Journal of Oral & Maxillofacial Surgery*, 53:142. https://doi.org/10.1016/j.bjoms.2014.10.016.

Yang X, Ruan H, Hu X, Cao A, & Song L. (2017). miR-381-3p suppresses the proliferation of oral squamous cell carcinoma cells by directly targeting FGFR2. *American Journal of Cancer Research*, 7:913. PMID: 28469963.

Yeh LY, Yang CC, Wu HL, Kao SY, Liu CJ, Chen YF. Lin SC, & Chang KW. (2020). The *miR-372*-ZBTB7A oncogenic axis suppresses TRAIL-R2 associated drug sensitivity in oral carcinoma. *Frontiers in Oncology*, 10:47. https://doi.org/10.3389/fonc.2020.00047.

Yin H, Kanasty RL, Eltoukhy AA, Vegas AJ, Dorkin JR, & Anderson DG. (2014). Non-viral vectors for gene-based therapy. *Nature Reviews Genetics*, 15:541. https://doi.org/10.1038/nrg3763.

Yoda M, Kawamata T, Paroo Z, Ye X, Iwasaki S, Liu Q, & Tomari Y. (2010). ATP-dependent human RISC assembly pathways. *Nature Structural & Molecular Biology*, 17:17. https://doi.org/10.1038/nsmb.1733.

Yu T, Liu K, Wu Y, Fan J, Chen J, Li C, Yang Q, & Wang Z. (2014). MicroRNA-9 inhibits the proliferation of oral squamous cell carcinoma cells by suppressing expression of *CXCR4* via the Wnt/β-catenin signaling pathway. *Oncogene*, 33:5017. https://doi.org/10.1038/onc.2013.448.

Yue J, & Tigyi G. (2010). Conservation of miR-15a/16-1 and miR-15b/16-2 clusters. *Mammalian Genome: Official Journal of the International Mammalian Genome Society*, 21:88. https://doi.org/10.1007/s00335-009-9240-3.

Zanaruddin SN, Yee PS, Hor SY, Kong YH, Ghani WM, Mustafa WM, Zain RB, Prime SS, Rahman ZA, & Cheong SC. (2013). Common oncogenic mutations are infrequent in oral

squamous cell carcinoma of Asian origin. *PloS One*, 8:e80229. https://doi.org/10.1371/journal.pone.0080229.

Zeng B, Li Y, Jiang F, Wei C, Chen G, Zhang W, Zhao W, & Yu D. (2019). LncRNA GAS5 suppresses proliferation, migration, invasion, and epithelial-mesenchymal transition in oral squamous cell carcinoma by regulating the miR-21/PTEN axis. *Experimental Cell Research*, 374:365. https://doi.org/10.1016/j.yexcr.2018.12.014.

Zhang B, Li Y, Hou D, Shi Q, Yang S, & Li Q. (2017). MicroRNA-375 inhibits growth and enhances radiosensitivity in oral squamous cell carcinoma by targeting insulin like growth factor 1 receptor. *Cellular Physiology and Biochemistry: International Journal of Experimental Cellular Physiology, Biochemistry, and Pharmacology*, 42:2105. https://doi.org/10.1159/000479913.

Zhang H, Kolb FA, Jaskiewicz L, Westhof E, & Filipowicz W. (2004). Single processing center models for human Dicer and bacterial RNase III. *Cell*, 118:57. https://doi.org/10.1016/j.cell.2004.06.017.

Zhang Q, He Y, Nie M, & Cai W. (2017). Roles of miR-138 and ISG15 in oral squamous cell carcinoma. *Experimental and Therapeutic Medicine*, 14:2329. https://doi.org/10.3892/etm.2017.4720.

Zhang S, He Y, Liu C, Li G, Lu S, Jing Q, Chen X, Ma H, Zhang D, Wang Y, Huang D, Tan P, Chen J, Zhang X, Liu Y, & Qiu Y. (2020). miR-93-5p enhances migration and invasion by targeting RGMB in squamous cell carcinoma of the head and neck. *Journal of Cancer*, 11:3871. https://doi.org/10.7150/jca.43854.

Zhang S, Ma H, Zhang D, Xie S, Wang W, Li Q, Lin Z, & Wang Y. (2018). LncRNA KCNQ1OT1 regulates proliferation and cisplatin resistance in tongue cancer via miR-211-5p mediated Ezrin/Fak/Src signaling. *Cell Death & Disease*, 9:742. https://doi.org/10.1038/s41419-018-0793-5.

Zhang X, Lv J, Liu P, Xie X, Wang M, Liu D, Zhang H, & Jin J. (2021). Poly-IgA complexes and disease severity in IgA Nephropathy. *Clinical Journal of the American Society of Nephrology: CJASN*, 16:1652. https://doi.org/10.2215/CJN.01300121.

Zhang XJ, Jin Y, Song JL, & Deng F. (2019). MiR-373 promotes proliferation and metastasis of oral squamous cell carcinoma by targeting SPOP. *European Review for Medical and Pharmacological Sciences*, 23:5270. https://doi.org/10.26355/eurrev_201906_18193.

Zhang Y, Liu W, Chen Y, Liu J, Wu K, Su L, Zhang W, Jiang Y, Zhang X, Zhang Y, Liu C, Tao L, Liu B, & Zhang H. (2018). A cellular microRNA facilitates regulatory T lymphocyte development by targeting the *FOXP3* promoter TATA-Box motif. *Journal of Immunology* 200:1053. https://doi.org/10.4049/jimmunol.1700196.

Zhao C, & Liu Z. (2021). MicroRNA 617 targeting SERPINE1 inhibited the progression of oral squamous cell carcinoma. *Molecular and Cellular Biology*, 41:e0056520. https://doi.org/10.1128/MB.00565-20.

Zheng G, Li N, Jia X, Peng C, Luo L, Deng Y, Yin J, Song Y, Liu H, Lu M, Zhang Z, Gu Y, & He Z. (2016). MYCN-mediated miR-21 overexpression enhances chemo-resistance via targeting CADM1 in tongue cancer. *Journal of Molecular Medicine*,94:1129. https://doi.org/10.1007/s00109-016-1417-0.

Zhong X, Lu Q, Zhang Q, He Y, Wei W, & Wang Y. (2021). Oral microbiota alteration associated with oral cancer and areca chewing. *Oral Diseases*, 27: 226. https://doi.org/10.1111/odi.13545.

Zhou AD, Diao LT, Xu H, Xiao ZD, Li JH, Zhou H, & Qu LH. (2012). β-Catenin/LEF1 transactivates the microRNA-371-373 cluster that modulates the Wnt/β-catenin-signaling pathway. *Oncogene*, 31:2968. https://doi.org/10.1038/onc.2011.461.

Zhou J, Tao D, Tang D, & Gao Z. (2015). Correlation of human papilloma virus with oral squamous cell carcinoma in Chinese population. *International Journal of Clinical and Experimental Medicine*, 8:18172. PMID: 26770416.

Zhou X, Ren Y, Liu A, Han L, Zhang K, Li S, Li P, Li P, Kang C, Wang X, & Zhang L. (2014). STAT3 inhibitor WP1066 attenuates miRNA-21 to suppress human oral squamous cell carcinoma growth in vitro and *in vivo*. *Oncology Reports*, 31:2173. https://doi.org/10.3892/or.2014.3114.

Zhu X, Shao P, Tang Y, Shu M, Hu WW, & Zhang Y. (2019). hsa_circRNA_100533 regulates GNAS by sponging hsa_miR_933 to prevent oral squamous cell carcinoma. *Journal of Cellular Biochemistry*, 120:19159. https://doi.org/10.1002/jcb.29245.

Zhuang Z, Hu F, Hu J, Wang C, Hou J, Yu Z, Wang TT, Liu X, & Huang H. (2017). MicroRNA-218 promotes cisplatin resistance in oral cancer via the PPP2R5A/Wnt signaling pathway. *Oncology Reports*, 38:2051. https://doi.org/10.3892/or.2017.5899.

Zini A, Czerninski R, & Sgan-Cohen HD. (2010). Oral cancer over four decades: epidemiology, trends, histology, and survival by anatomical sites. *Journal of Oral Pathology & Medicine: Official Publication of the International Association of Oral Pathologists and the American Academy of Oral Pathology*, 39:299. https://doi.org/10.1111/j.1600-0714.2009.00845.x.

8. APPENDICES

Appendix-I: Equipment and other supplies

Item	Company/Supplier
Cell culture incubator (CO_2)	Thermo Scientific Forma, USA
Centrifuge (refrigerated)	Hettich, Germany
Centrifuge tubes (15 mL & 50 mL)	Tarson, India
ChemiDoc XRS+ System	Bio-Rad, USA
Cryovials	Tarson, India
Culture dishes	Nunc, Denmark
Culture flask	Nunc, Denmark
Electrophoresis system (Agarose)	Bangalore Genei, India
Electrophoresis system (Polyacrylamide)	Bangalore Genei, India
Elix water system	Millipore, USA
Filtration system, 0.2 µm Stericup	Tarson, India
Freezer (-20ºC)	Vestfrost, Denmark
Freezer (-80ºC)	New Brunswick, USA
Gel documentation system	UltraLum Inc., USA
Glassware	Borosil, India
Gloves (plastic)	Star, India
Incubator (37˚C)	Lab Companion, India
Laminar hood (Bacterial)	Labline Instruments, India
Laminar hood (Tissue culture)	Kirloskar, India
Leica Inverted Microscope DMi1	Leica Microsystems, Germany
Microfuge	Bangalore Genei, India/ Hettich, Germany
Microscopic Cover Glass	Blue Star, India
Microwave oven	Kenstar, India
NanoDrop™ 1000 spectrophotometer	Thermo Scientific, USA
Neubauer haemocytometer	HyClone, Logan, UT, USA
Olympus CKX4 inverted microscope	Olympus Optical Co., Japan

PCR tubes (0.5 mL)	Axygen, USA/ Tarson, India
Petridishes	Tarson, India
pH meter	Eutech Instruments, Thermo Scientific, USA
Pipettes	Gilson, USA/ Tarson, India
Power packs	Amersham, USA/Bangalore Genei, India
PVDF membrane	PALL, USA
StepOnePlus Real-time PCR machine	Applied Biosystems, US
QuantStudio3 Real-time PCR machine	Applied Biosystems, US
Thermal cycler (Mastercycler)	Eppendorf Corp., Hamburg,Germany
Tips (Filtered)	Tarson, India
Tips (normal)	Tarson, India
Trans-Blot electrophoretic transfer cell	Bio-Rad, USA
Tubes (1.5 mL)	Axygen, USA
Tubes (15 mL)	Tarson, India
Tubes (50 mL)	Tarson, India
Tubes (0.6 mL)	Tarson, India
UV-Transilluminator	Bangalore Genei, India
Vacuum pump	CKM Electricals, India
VICTOR™ *X* Multilabel Plate Readers	PerkinElmer, USA
Water bath	PolyScience, USA
Weighing balance	Orion, India

Appendix-II: Chemicals and media

Item	Company/Supplier	Catalog #
2-Mercaptoethanol	Sigma-Aldrich, USA	M-3148
Acetic acid, glacial	SDFCL, India	20001
Acrylamide	SRL, India	15657
Agar	Himedia, India	RM201
Agarose	Lonza, USA	50004
Ammonium acetate	Sigma-Aldrich, USA	A-1542

Ammonium persulphate	Sigma-Aldrich, USA	A-3678
Ampicillin	Sigma-Aldrich, USA	A-9518
Antibiotic/antimycotic solution (100X)	Sigma-Aldrich, USA	A-5955
Bovine serum albumin (BSA)	Sigma-Aldrich, USA	A-4503
Bromophenol blue	Sigma-Aldrich, USA	B-6131
Calcium chloride	Sigma-Aldrich, USA	C-3881
CellLytic™ M Cell Lysis Reagent	Sigma-Aldrich, USA	C2978
CellLytic™ MT Cell Lysis Reagent	Sigma-Aldrich, USA	C3228
Chloroform	SRL, India	84155
Coomassie brilliant blue G-250	Merck, Germany	1.15444.0025
Coomassie brilliant blue R-250	Sigma-Aldrich, USA	B-6131
Difco™ noble agar	BD Biosciences, USA	214220
Dimethyl sulphoxide (DMSO)	Sigma-Aldrich, USA	D-8418
dNTPs	Thermo Scientific, USA	R0181
Dulbecco's modified eagle medium (DMEM)	Sigma-Aldrich, USA	D-5648
Dulbecco's phosphate buffered saline (DPBS)	Sigma-Aldrich, USA	D-5652
Diethyl pyrocarbonate (DEPC)	Sigma-Aldrich, USA	D-5758
Ethidium bromide	Sigma-Aldrich, USA	E-8751
Ethylenediaminetetraacetic acid (EDTA)	Sigma-Aldrich, USA	EDS
Ethanol	Himedia, India	MB106
Formamide	Sigma-Aldrich, USA	F-7503
Formaldehyde	Sigma-Aldrich, USA	F-8775
Gibco™ Fetal bovine serum	Thermo Fisher Scientific™, USA	10270106
Glycerol	SDFCL, India	20118
Glycine	SRL, India	66327
Hydrochloric acid	SDFCL India	20125
Hydroquinone	Sigma-Aldrich, USA	H9003
IPTG (Isopropyl ß-D-	Fermentas, Canada	R0392

thiogalactopyranoside)		
Isopropanol	SDFCL, India	20224
Ladder (Lambda DNA/ *Eco*RI plus *Hind*III marker)	Thermo Fisher Scientific™, USA	SM0191
Ladder (GeneRuler 100 bp plus DNA)	Thermo Fisher Scientific™, USA	SM0321
LB broth	Himedia, India	M575
Matrigel	Corning Ltd.	354230
Methanol	SRL, India	65524
MOPS	Sigma-Aldrich, USA	M8899
N, N,-Methyl bis-Acrylamide	Sigma-Aldrich, USA	M-7526
Opti-MEM™	Thermo Fisher Scientific™, USA	31985070
Passive lysis Buffer	Promega, USA	E194A
PageRuler™ plus prestained protein ladder	Thermo Fisher Scientific™, USA	26619
PAGEmark™ Tricolour PLUS	GBIOSCIENCES, India	786-419
Phenol	SRL, India	1624132
Protease inhibitor cocktail	Sigma-Aldrich, USA	P-8340
RNALater	Sigma-Aldrich, USA	R-0901
Sodium bisulphite	Sigma-Aldrich, USA	S9000
Sodium bicarbonate	SDFCL, India	20241
Sodium dihydrogen phosphate 1-hydrate	SDFCL, India	20245
Sodium dodecyl sulphate	SDFCL, India	40175
di-Sodium hydrogen phosphate 2-hydrate	SDFCL, India	20249
Sodium hydroxide	SDFCL, India	68151
TEMED (N, N, N', N'-tetra-methylethylenediamine)	Sigma-Aldrich, USA	T-8133
Tri Reagent®	Sigma-Aldrich, USA	T9424
Triton X-100	Sigma-Aldrich, USA	X-100
Tris	SRL, India	79420
Trypsin (0.05%)	Sigma-Aldrich, USA	T4049
Trypan blue	Sigma-Aldrich, USA	T6146
Tween 20	Sigma-Aldrich, USA	T7949
X-gal	Thermo Fisher Scientific™, USA	R0401
Xylene cyanol	Sigma-Aldrich, USA	X-4126

Appendix-III: Kits

Kit	Company/Supplier	Catalog #
CaspGLOW™FlurosceinActive Caspase-3 staining kit	Biovision, USA	K183
Dual Luciferase® reporter assay	Promega, USA	E1910
DyNAmo ColorFlash SYBR Green qPCR Kit	Thermo Fisher Scientific™, USA	F-416L
GenEluteTM gel extraction kit	Sigma-Aldrich, USA	NA1111
GenEluteTM plasmid mini prep kit	Sigma-Aldrich, USA	PLN70
Immobilon Western chemiluminescent HRP Substrate	Merck, Germany	WBKLS0100
InsT/A clone PCR product	Thermo Fisher Scientific™, USA	K1214
Lipofectamine 2000® transfection reagent	Thermo Fisher Scientific™, USA	11668027
MirVana™ miRNA isolation kit	Ambion, USA	AM1561
Turbofect™ transfection reagent	Thermo Fisher Scientific™, USA	R0531
Verso cDNA synthesis kit	Thermo Fisher Scientific™, USA	AB1453A
Wizard®Genomic DNA Purification Kit	Promega, USA	A1620

Appendix-IV: Enzymes

Enzyme	Company/Supplier	Catalog #
Eco RV restriction endonuclease	Thermo Fisher Scientific™, USA	ER0301
Sac I restriction endonuclease	Thermo Fisher Scientific™, USA	ER1135
Eco RI restriction endonuclease	Thermo Fisher Scientific™, USA	ER0271
Hind III restriction endonuclease	Thermo Fisher Scientific™, USA	ER0501
Xho I restriction endonuclease	Thermo Fisher Scientific™, USA	ER0691
Dpn I restriction endonuclease	Thermo Fisher Scientific™, USA	ER1701
Pme I restriction endonuclease	Thermo Fisher Scientific™, USA	ER1341
Mlu I restriction endonuclease	Thermo Fisher Scientific™, USA	ER0561
Not I restriction endonuclease	Thermo Fisher Scientific™, USA	ER0591
RNaseA	Thermo Fisher Scientific™, USA	EN0531
T4 DNA Ligase	Thermo Fisher Scientific™, USA	EL0331
Taq DNA polymerase	3B BlackBio Biotech	3B014
Phusion High-Fidelity	Thermo Fisher Scientific™, USA	F549S

Appendix-V: Antibodies

Primary antibodies	Company	Catalog #
Anti-TOPORS antibody	Abcam, USA	ab86383
Anti-mouse β-actin antibody	Sigma-Aldrich, USA	A5441
Anti-mouse-p21 antibody	Cell Signaling technology, USA	2946
Anti-mouse-p53 antibody	Thermo Fisher Scientific™, USA	AH00152

Secondary antibodies	Company	Catalog #
Anti-mouse IgG HRP-conjugated	Bangalore Genei, India	105502
Anti-rabbit IgG HRP-conjugated	Bangalore Genei, India	105499

Appendix-VI: Plasmid vectors

Vectors	Company/Supplier
pcDNA3.1(+)	Thermo Fisher Scientific™, USA
pTZ57R	Thermo Fisher Scientific™, USA
pMIR-REPORT™	Thermo Fisher Scientific™, USA
pGL3-Basic	Promega, USA
pGL3-Control	Promega, USA
pRL-TK	Promega, USA
pBluescript II KS (+)	Agilent Technologies, USA

9. Publications

1. Sarkar N, Kumar A. microRNAs: New-Age Panacea in Cancer Therapeutics. Indian J Surg Oncol. 2021 Apr;12(Suppl 1):52-56. doi: 10.1007/s13193-020-01110-w. Epub 2020 Jun 6. PMID: 33994728; PMCID: PMC8119568.

2. Sarkar N, Champaka G, Kumar A. A closer look into functional implications of the interaction between miR-617 and *DDX27* promoter in OSCC pathogenesis (manuscript under preparation).

10. Abstract submitted/ meeting attended

1. Sarkar N, Champaka G, Kumar A. A closer look into the enigma of RNA Activation by miR-617 in OSCC. Noncoding RNAs in Development and Cell Differentiation, Jan 30-Feb 2, 2023, Weizmann Institute of Science, Rehovot, Israel.

2. Attended the conference, Phenotypic Heterogeneity as a driver of Cancer Progression, Jan 5-7, 2020, Indian Institute of Science, Bengaluru, India.